NASA Contractor Report 3848

The Lateral-Directional Characteristics of a 74-Degree Delta Wing Employing Gothic Planform Vortex Flaps

Arthur C. Grantz

NASA

NASA Contractor Report 3848

The Lateral-Directional Characteristics of a 74-Degree Delta Wing Employing Gothic Planform Vortex Flaps

Arthur C. Grantz

Virginia Polytechnic Institute and State University
Blacksburg, Virginia

NASA

National Aeronautics
and Space Administration

Scientific and Technical
Information Branch

1984

INTRODUCTION

In recent years, considerable interest has been expressed in the tactical supercruiser.[1] This next generation fighter is intended to cruise efficiently at supersonic speeds and yet maintain or better the transonic maneuver performance of today's lightweight fighters. Efficient cruise performance dictates a thin, highly swept, slender wing in order to minimize wave drag penalties. This can conflict with the maneuver requirement. The modern lightweight fighter illustrates the excellent transonic maneuverability of a moderately swept wing and leading edge vortex strakes. Consequently, designing a slender wing with the desired maneuver and supersonic characteristics presents a major challenge in the development of the tactical supercruiser.

There are two approaches to designing a slender wing for this multiple role. The traditional method[2-5] optimizes wing camber and twist for attached flow at the supersonic design point. The desired attached flow wing shape for maneuver is approximated through deployment of leading and trailing edge flaps. Unfortunately, it is very difficult to maintain attached flow along the highly swept leading edges. Flow separation generally reduces the available leading edge thrust and results in increased drag. The alternative method treats the maneuver point differently. It is well known that flow separation around a highly swept leading edge may take the form of a vortex. If the flow separation can be controlled such that the low surface pressures due to the vortex act upon a deflected leading edge flap, the resultant suction may cause an effective thrust to be recovered. Several studies have indicated that the proper choice of leading edge camber can provide a favorable balance between vortex lift and vortex induced thrust recovery.[6]

Designing a slender wing for attached flow at moderate to high angles of attack leads to severe wing warp and complicated leading-edge flap systems. The optimal camber and twist distribution typically is determined with inviscid flow models due to the difficulty associated with modeling the highly three-dimensional boundary layers characteristic of these wings. Unfortunately, this inviscid approximation is rarely satisfactory, and adverse flow separation occurs at this design condition. Wings optimized for vortex flow also require substantial wing warp. In contrast to the attached flow case however, vortex flow will respond to flat plate approximations of the optimum leading-edge shape with only minimal losses.[7] Flow separation is exploited rather than suppressed. The appropriate leading edge profile for these leading edge vortex flaps (LEVF), however, has yet to be defined.

As with any aerodynamic system, there are tradeoffs to be made. The ideal flap geometry[8] would fix the separation point at the leading edge, trap the vortex on the flap for its entire length, promote flow reattachment along the flap hinge-line, and not adversely affect the stability characteristics of the wing (figure 1). These requirements are not easily met. By restricting the flap to be planar (simple) and with a sharp leading edge (fixed separation line), the design parameter space can be reduced to two variables: leading edge profile and flap deflection angle. The leading edge profile determines the flap area distribution. The profile is usually chosen to concentrate the vortex induced loads on the flap and manipulate the vortex strength distribution. Flap deflection influences the overall vortex strength by changing the flow incidence or upwash angle at the leading edge. For example, deflecting the leading edge downwards will reduce the vortex strength by reducing the upwash angle at the leading edge. Flap deflection allows a given flap geometry to be used for several different flow environments.

Numerous configurations have been proposed with varying degrees of success (figure 2).[9-11] A constant chord, full span LEVF is one of the simplest choices, shows significant improvements in L/D, but suffers pitchup at moderate to high angles of attack. An inversely tapered, full span LEVF alleviates the pitchup, but in turn sacrifices L/D. Part span and segmented LEVF can be tailored to maintain acceptable longitudinal characteristics, but have not shown the L/D potential of the constant chord, full span LEVF. As experience with the vortex flap was gained, a design optimization code was developed at the NASA Langley Research Center to specify a LEVF geometry. As a result, the latest generation of vortex flaps, constrained in the design procedure to provide flow reattachment along the flap hinge line, utilizes a "gothic" planform.

The experimental LEVF research to date has strived to develop a data base appropriate for performance calculations. Wind tunnel tests have attempted to optimize L/D at moderate to high lift coefficients without incurring a pitching moment penalty. Theoretical methods have also focused on longitudinal problems, but from the analysis and design standpoint. Consequently, the experimental and analytical expertise concerning the lateral-directional characteristics of slender wings employing LEVF is extremely limited.

With regard to lateral-directional characteristics, numerous slender wing/body configurations were investigated during the supersonic cruise transport studies of the 1970's.[12-15] These designs promoted attached flow and typically inhibited leading edge vortex flows when possible. Concepts included delta, arrow, and cranked arrow wing planforms with wing leading edge sweep angles of between 65 and 80 degrees. The wind tunnel models used were not of the generic type, but represented complete aircraft; they included

horizontal and vertical tails, leading and trailing edge flaps, a high fineness ratio fuselage, and engine nacelles. Several lateral-directional deficiencies were noted in these tests which may impact the design of slender wings employing LEVF. Insufficient C_{n_β}, excessive C_{ℓ_β}, and limited roll power were frequently encountered. Directional instabilities were usually due to long, slender fuselage noses extending far forward of the moment reference center. Wing alone, the slender planform typically realized increasingly stable values of C_{n_β} with angle of attack. Attached flow leading edge flaps may produce either favorable or unfavorable increments in C_{n_β} depending on their geometry. Large negative values of the effective dihedral parameter are characteristic of slender wing configurations. Because of the low moment of inertia about the roll axis relative to the pitch and yaw axes, excessive $-C_{\ell_\beta}$ may aggravate a dutch roll tendency. Leading edge flap deflections and wing anhedral have been shown to be effective in reducing the magnitude of $-C_{\ell_\beta}$.

Slender wing aircraft often are unable to provide the roll power necessary to counter their high effective dihedral during crosswind landings. Small wing spans severely bound the aileron span, area, and moment arms and as a result limit the available roll power. Consequently, high landing speeds at low lift coefficients are dictated. Trailing edge flaps mixed with ailerons as elevons are generally used during low-speed flight in order to increase the lift coeficient for a given pitch angle. As a result, the deflection angle available for aileron use is significantly reduced. An alternative approach to providing roll control might depend on asymmetrical LEVF deflections. It has been postulated that by directing the flap produced forces in the proper direction, rolling and yawing moments and possibly side force may be generated. Whether the magnitudes of these forces and moments

would be comparable to those produced by conventional control surfaces has yet to be investigated.

From a theoretical standpoint, there are relatively few methods available which predict separation induced vortex flow effects as compared to attached flow methodology, even fewer methods which predict lateral-directional as compared to longitudinal characteristics, and fewer still which will predict both. For vortex flow, longitudinal force and moment properties are often estimated with linear methods by coupling the suction analogy of Polhamus[16] to either a Vortex Lattice Method (Lamar[17]) or a Quasi-Vortex Lattice Method (Lan[18]). For detailed surface pressure distributions, additional real flow effects, and as a consequence, increased accuracy, non-linear methods must be used. Examples of such methods include the Free Vortex Sheet Method (Johnson et al.[19]), free vortex filament methods (Kandil et al.[20] or Mehrotra[21]), and the Euler methods (Jameson[22]). However, for lateral-directional properties, the available methods are limited to an extension of the Quasi-Vortex Lattice Method called VORSTAB[23] and to the Free Vortex Sheet Method.

Linear methods continue to be attractive for their relative simplicity and low computer cost. For vortex flow estimates, these intrinsic qualities are typified in Lamar's Vortex Lattice Method coupled with the Polhamus Suction Analogy (VLM-SA).[17] Although it does not predict details of the surface load distributions, this method is extremely useful for estimating longitudinal forces and, to a lesser degree, moments. In addition, VLM-SA has been validated for a very wide variety of configurations. An alternative linear method was developed by Lan who coupled the suction analogy with his Quasi-Vortex Lattice Method (QVLM). In its original form, this method was limited to longitudinal forces and moments. However, Lan and Hsu[23] recently developed VORSTAB, an extension of QVLM, to provide lateral-directional

results. This relatively new method has yet to be validated however, against a sufficiently broad range of experimental data.

The non-linear vortex flow methods are primarily used to obtain detailed three-dimensional surface pressures. In addition to the pressures themselves, they offer better estimates of pitching moments, root bending moments, and distributed loads than do the linear methods. Much as would be expected though, the non-linear methods are more expensive in both human and computer resources than the linear methods. Possibly the cheif non-linear method in use to date is the Free Vortex Sheet Method (FVS). Based on higher order panel technology, the FVS method has been shown to provide good estimates of wing surface pressures, forces, and moments. Additionally, this method is not limited to longitudinal configurations. Although the FVS method is comparable to other 3-D non-linear methods in terms of resource expenditures, this method is too expensive to use for initial force and moment estimates during preliminary design.

Early in the design process, simple, low cost, linear methods which can be quickly applied to a wide variety of configurations are typically favored. For longitudinal results, VLM-SA does very well. There is a need however, for a lateral-directional method. For the present investigation, it was decided to concentrate the theoretical studies on VORSTAB. This program is attractive for several reasons. It is a simple, inexpensive code to apply. VORSTAB is sufficiently general that it permits multiple lifting surfaces of arbitrary planform, leading and trailing edge flaps, vertical surfaces, and a body of revolution fuselage. Vortex breakdown effects are accounted for by utilizing a correlation parameter derived from the predicted leading edge suction distribution for attached flow. Empirical formulae, derived from a least square analysis of the delta wing data of Wentz,[24] are used to predict the

angle for vortex breakdown at the trailing edge, the progression rate of vortex breakdown, and the vortex lift recovered in the breakdown region. The theoretical predictions provided by VORSTAB have yet to be evaluated against a sufficiently diverse range of experimental data. In particular, camber and vertical tail effects have yet to be documented. Some theory-experiment correlations have been made by Lan and Hsu,[23] but these are limited to planar wings of delta, cropped delta, and cranked arrow planforms. In addition, Lan questions the validity of some of the wind tunnel data used in the comparisons. Until the theory's utility has been substantiated, the program's usefulness will be extremely limited.

As the vortex flap concept for generating maneuver lift has matured, the lateral-directional properties of these slender wing-flap configurations have become increasingly important. Consequently, both the experimental data base and the analytical techniques for predicting these characteristics need improvement. As a result, the purpose of this investigation is to determine the low-speed lateral-directional characteristics of a generic 74 degree delta wing-body configuration employing the latest generation, gothic planform, vortex flaps. In addition, the experimental data is to be compared against VORSTAB predictions to aid in documenting this new method.

LIST OF SYMBOLS

b	Wingspan 1.838 ft.
c	Mean aerodynamic chord
C_D	Drag coefficient
C_{D_0}	Zero lift drag coefficient
C_ℓ	Rolling moment coefficient
C_{ℓ_β}	Rolling moment due to sideslip stability parameter
C_L	Lift coefficient
C_{L_α}	Lift curve slope
$C_{L_{max}}$	Maximum lift coefficient

C_m	Pitching moment coefficient
C_{m_0}	Zero lift pitching moment coefficient
C_n	Yawing moment coefficient
C_{n_β}	Yawing moment due to sideslip stability parameter
C_Y	Side force coefficient
C_{Y_β}	Side force due to sideslip stability parameter
LEVF	Leading edge vortex flap
L/D	Lift to drag ratio
L/D_{max}	Maximum lift to drag ratio
S	Wing area 3.81067 ft.^{2}
S_f	Flap area (each) 0.4327 ft.^{2}
S_t	Vertical tail area 0.3125 ft.^{2}
α, deg	Angle of attack
α_0, deg	Angle of attack for zero lift
β, deg	Angle of sideslip
δ_{LE}, deg	Leading edge deflection angle
δ_A, deg	Differential aileron deflection angle

DESCRIPTION OF EXPERIMENT

The generic wind-tunnel model illustrated in figure 3 includes an uncambered wing with sharp edges, leading and trailing edge flaps, a body of revolution fuselage, and a centerline mounted vertical tail. The "canopy like" appendage to the fuselage was necessary to house pressure instrumentation and was faired into the fuselage for a minimum of flow interference. Leading-edge flap deflection angles of -30, 0, 30, 35, 40, and 45 degrees, measured normal to the flap hingeline, were obtained through the use of flush mounted brackets. Trailing edge flap deflections of 0, ±10, and ±20 degrees were set with adjustable pinch hinges. Gaps between the leading or trailing edge flaps and the wing were sealed along the lower surface with thin mylar tape.

The NASA Langley Research Center 7- by 10-Foot High-Speed Wind Tunnel was utilized for this experiment. Force and moment measurements were made with

two six-component strain-gauge balances. The forward balance measured loads on the ogive nose only with a metric break just forward of the canopy while the main balance measured loads for the entire model. Wing surface pressures were not recorded during this particular test. Figure 4 shows the model on the high angle of attack stability rig and the HS-15 sting. Sideslip and angle of attack were obtained through a combination of pitch and roll. Angle of attack was varied between 0 and 40 degrees with sideslip angles ranging between -16 and +16 degrees. A detailed run schedule is presented in Table A1. The test Mach number was 0.20 for a Reynolds number of 7.05 million based on the mean aerodynamic chord.

The wind-tunnel data have been corrected for blockage and jet boundary effects as per references 26 and 27 respectively. Balance chamber pressures were measured and the axial force measurements were adjusted to correspond to free-stream static pressure acting in the model chamber. Sting and balance bending were accounted for in the determination of sideslip and angle of attack. Boundary layer transition was fixed by the method of reference 28; 0.10 inch wide transition strips of No. 90 carborundum grains were placed 1.0 inch streamwise from the flap and vertical tail leading edges. A similar 0.10 inch wide ring of No. 80 carborundum grains was placed 1.5 inches aft of the nose.

The longitudinal data are presented in the stability system of axes and the lateral-directional data are given in the body system of axes as shown in figure 5. The reference wing area is based on the planform area of the 74 degree delta wing extended into the centerline plus the area of the undeflected LEVF. The reference mean aerodynamic chord is assumed to be that of the reference wing exclusive of the LEVF. The lateral-directional stability derivatives were determined for $\beta = 0$ by differencing data obtained

at $\beta = \pm 4$ degrees. In assembling the test matrix and in analyzing the data, the following perspective was maintained. The 0 degree deflection was considered to be the baseline case. This planar configuration retains full vortex flow effects and permits the comparison of one vortex flow to another. Force and moment increments due to vortex flap deflection would compare very differently to an attached flow wing, however. The 40 degree deflection was designed for 14 degrees angle of attack where it was to generate a vortex that remained on the flap for the length of the flap and promote flow reattachment along the flap hinge line. The 30 degree deflection was representative of an off-design condition which was to illustrate the vortex flow sensitivity or insensitivity to flap deflection angle. The -30 degree deflection was to simulate a landing configuration where the maximum lift coefficient for a given angle of attack is desired.

EXPERIMENTAL RESULTS AND DISCUSSION

Longitudinal Aerodynamic Characteristics

Although this investigation is primarily concerned with the lateral directional characteristics of vortex flaps, an understanding of their longitudinal characteristics will prove helpful. Figure 6a illustrates lift as a function of angle of attack. As is typical of planar, slender wings employing vortex flow, the curves can be split into three regions. At very low angles of attack, the vortex lift effects are small. The lift curve is locally characterized by a nearly linear region with a relatively shallow slope. This is the low angle of attack region. Increasing the angle of attack leads to the formation of leading-edge vortices and vortex lift. The lift curve transitions to and maintains a steeper slope for the angle-of-attack range in which the vortex lift dominates. This is the vortex flow region. Eventually, the angle of attack is increased to the point where the vortex becomes unstable

and bursts. Coincident with this deterioration of the vortex is a gradual loss of vortex lift. Consequently, the lift curve slope tapers off until $C_{L_{max}}$ is attained. This is the vortex burst region. It should be emphasized that vortex burst may occur at a much lower angle of attack than the angle for $C_{L_{max}}$. These same trends are seen when the LEVF are deflected. As would be expected, positive, downward deflections show an extended linear range. They also show the normal shift with the increased wing camber. As the angle of attack is increased, a vortex eventually forms on the deflected flap. Since the local angle of attack at the leading edge has been reduced through flap deflection, the vortex that forms is substantially weaker than that for the baseline case at the same wing angle of attack. In addition, the deflected flap trades a portion of the vortex lift for thrust. Consequently, for angles of attack below 40 degrees, there is a significant reduction in lift as a result of postive flap deflection. Reducing the local angle of attack however, allows the deflected flap cases to carry the vortex to higher angles of attack before bursting occurs. Notice that there is a significant change in C_{L_α} at 25 degrees angle of attack for the baseline case while C_{L_α} for the 30 and 40 degree cases does not decay until 36 degrees.

The inverted -30 degree deflection is a special case. Specifically considered for landing configurations, it is intended to produce high lift at low angles of attack. The upward deflection initiates the vortex lift increment at slightly negative angles of attack and for angles below 15 degrees, it yields a roughly constant increase in C_L of 0.04 over the undeflected case. This represents a 6- to 9-percent improvement between 10 and 15 degrees over baseline performance. As the angle of attack is increased above 20 degrees, there is no lift advantage to the inverted flap.

The configuration pitching moment characteristics are shown in figure 6b as a function of angle of attack and lift coefficient. For the 0 and -30 degree cases, C_m varies almost linearly with angle of attack for angles below vortex breakdown. Note the slight pitchup for the 0 degree case beginning at 25 degrees angle of attack. For the -30 degree case, pitchup occurs at 28 degrees and is more pronounced. For the 0 and -30 degree cases the vortex forms at a very low angle of attack and does not change significantly until bursting occurs. For the 30 and 40 degree deflections however, the vortex forms later and grows in stages. The very slight nonlinearities in the pitching moment curve indicate when the vortex begins to take effect, when it begins to spill off the flap, and when it begins to burst. Both the 30 and 40 degree cases indicate pitchup beginning at 36 degrees angle of attack. Note that the angles mentioned in reference to pitchup and vortex burst correspond to the angles mentioned earlier while discussing the lift curve slopes of the various flap cases.

Figure 6c and 6d illustrate the fundamental effects of vortex flaps: reducing drag and improving L/D. For lift coefficients below 0.8, deflecting the LEVF downward significantly improves the configuration L/D. The maximum L/D is improved by 18 and 22 percent over the baseline by deflecting the 30 and 40 degree flaps. L/D_{max} for the 40 degree case also occurs at an 85 percent higher lift coefficient than the baseline. At the design angle of attack of 14 degrees, the 40 degree flaps yield a lift coefficient of 0.42. Pressure data and limited oil flow photographs (figure 6e) from a concurrent test indicated that the 40 degree flap was operating as designed: the vortex was contained on the flap for the majority of its length with only a slight amount of spillage near the wing trailing edge. Flow reattachment occurred on or very near the flap hinge line. Although the 30 degree case represents an

off-design case, note the good L/D performance relative to the design and baseline cases. The 30 degree case represents a 10 degree perturbation in flow incidence at the leading edge with only minimal losses. As would be expected, the -30 degree flaps incur a substantial penalty in L/D. However, during an approach and landing, reduced L/D implies improved glideslope control. The increased drag eliminates the need for other forms of speed brakes and allows for higher power settings on landing which minimizes engine spool-up time during go-around attempts.

Lateral-Directional Aerodynamic Characteristics

<u>Effect of LEVF Deflection</u>.- The basic lateral-directional stability derivatives C_{y_β}, C_{n_β}, and C_{ℓ_β} of the complete wing-body-vertical-tail configuration are shown in figure 7a and 7b as functions of angle of attack and lift coefficient. For the remaining figures, if the vertical tail is not specifically mentioned, assume a tail-on configuration. Consider the 0 degree baseline case. It shows a relatively constant level of directional stability up to 25 degrees angle of attack with a rapid deterioration for higher angles. C_{y_β} and C_{ℓ_β} also show deterioration for angles above 25 degrees. The -30 degree case follows similar trends. Note that C_{y_β} and C_{ℓ_β} are considerabley increased in magnitude by deflecting the flap upwards. The 30 and 40 degree deflections have destabilizing tendencies. Increasing flap deflection yields magnitude reductions in both C_{y_β} and C_{ℓ_β} and reduced values of C_{n_β} at moderate to high angles of attack. Note however that the unstable crossing for C_{n_β} is much more gradual for the downward flap deflections. The unstable breaks in C_{y_β} and C_{ℓ_β} have also been softened. As discussed earlier, a reduced level of effective dihedral may be desirable. Comparable trends are also shown for these stability parameters against lift coefficient.

Effect of vertical tail and forebody.- The vertical tail and forebody

effects on the lateral directional stability parameters are presented in

figures 8a and 8b for the 0 and 40 degree flap cases. The wing-body-vertical

tail case represents the complete configuration, the wing-body case excludes

the effects of the tail, and the forebody case includes only forebody effects.

Note that, for this particular configuration, the forebody has only a small

effect on the high angle of attack characteristics. For the 0 degree case,

tail effectiveness deteriorates above 25 degrees. Note the adverse effect on

C_{y_β} and C_{ℓ_β} for these angles. In comparison, the tail remains effective for

the 40 degree case for the entire angle attack range tested. However, the 40

degree wing-body configuration has reduced levels of C_{n_β} at moderate to high

angles of attack relative to the 0 degree case.

A flow model which might produce these characteristics is illustrated in

figure 9. For a wing designed for attached flow, the vertical tail often is

blanketed in separated, turbulent flow at moderate to high angles of attack.

In the case of vortex flow, the circulation induced flow reattachment along

the flap hingeline helps to keep the vertical tail effective up to moderate

angles of attack. At high angles of attack however, the windward vortex has

the tendency to spill off the flap and migrate in towards the tail. As the

low pressure vortex core moves inboard, it may reverse the direction of the

vertical tail sidewash field and induce adverse yawing and rolling moments.

In addition, the stronger windward vortex is forced down onto the wing surface

and slightly inboard while the weaker leeward vortex tends to lift off and

drift outboard. Consequently, this asymmetric vortex structure has the

potential to produce undesirable forces and moments.

Compare the characteristics of the 0 degree baseline and the 40 degree

flaps. Ignoring fuselage area, the 0 degree case does not have any

significant lateral area other than the vertical tail. In contrast, the 40

degree case has 64 percent of its lateral area in the LEVF. For the 0 degree

case, the vortex maintains the tail effectiveness through freestream flow

entrainment up to 25 degrees angle of attack. Above 25 degrees, the windward

vortex moves inboard and begins to more directly affect the tail. As the low

pressure core of the windward vortex nears the tail, adverse yawing and

rolling moments are generated in addition to adverse side force. In contrast,

the 40 degree flap case will support a much weaker vortex system for a given

angle of attack. In addition, the windward vortex will tend to stay trapped

on the windward flap and resist migration inboard. Note that for the entire

angle of attack range tested, the 40 degree case tail remains effective and

and there is no indication of the vortex migrating inward. The decaying

directional stability at moderate angles of attack is a wing-body vortex flap

phenomena and does not imply a loss of vertical tail effectiveness.

The basic lateral-directional forces and moments are illustrated in the

following group of figures as a function of sideslip for specific angles of

attack. Figures 10 through 12 provide a component buildup for the 0 degree

baseline while figures 13 through 15 correspond to a similar buildup for the

40 degree design case. Figure 16 through 18 compare the characteristics of

the complete configuration for each flap deflection. These figures provide

more information than the standard stability derivative comparisons and will

be used to improve the current flow model.

Figure 10 illustrates the yawing moment characteristics of the

undeflected baseline configuration. For the entire sideslip range tested, it

is readily apparent that the vertical tail is the only source of directional

stabilty for angles of attack up to 25 degrees. It is interesting to note

that the nose accounts for the majority of the wing-body yawing moment for

this angle of attack range. Also note the reduced tail effectiveness for small sideslip angles at 5 and 15 degrees angle of attack. At 25 degrees, the windward vortex begins to reduce the vertical tail effectiveness at large sideslip angles. By 35 degrees angle of attack, the tail has begun to produce adverse yawing moments. Note that the nose no longer dominates the wing-body yawing moments.

The rolling moments for the 0 degree case as a function of sideslip and angle of attack are shown in figure 11. For angles of attack of up to 25 degrees, the rolling moments generated are produced by the wing-body with only slight vertical tail effects. As the windward vortex approaches the tail, the low pressure core induces a destabilizing rolling moment which opposes the stable wing-body properties. As would be expected, the nose has virtually no effect on the configuration rolling moment characteristics.

The side force characteristics are presented in figure 12. As was shown for the yawing moment characteristics at low to moderate angles of attack, the vertical tail shows reduced effectiveness for small sideslip angles. At 30 degrees, the vertical tail looses its effectiveness entirely, while at 35 degrees, the tail produces undesirable increments in side force.

Figures 13 through 15 illustrate the characteristics of the 40 degree case. Although the trends are basically similar to the baseline case just discussed, there is an additional point to be made. For the baseline case, the lateral area resides in the fuselage and in the vertical tail. The 40-degree case however, has considerable lateral area in the LEVF. Consequently, it would not be surprising to see the wing-body characteristics dominating the configuration yawing moment properties. Figure 13c and 13d in particular emphasize this point. Despite acceptable tail effectiveness, the unstable

nature of the wing-body is sufficient to drive the configuration directionally unstable for small sideslip angles.

The yawing moment characteristics of the various flap deflections are compared in figure 16. The trends are similar for 5 and 15 degrees angle of attack. At 25 degrees, the 30 and 40 degree flap deflections eliminate the unstable break at large sideslip angles. This is due to the downward deflected flap's ability to hold the windward vortex away from the vertical tail. Controlling the windward vortex also helps to extend the usable sideslip range at high angles of attack. Figures 17 and 18 illustrate this tendency relative to the configuration rolling moment and side force properties.

Effect of Asymmetrical LEVF Deflection.- The objective of this portion of the experimental program was to determine if asymmetrical LEVF deflections could produce rolling moments comparable to those of conventional ailerons. The baseline case in this instance is represented by the symmetric 30 degree LEVF deflection. The differential aileron deflections of ±10 and ±20 degrees are superimposed onto this symmetric 30 degree case for comparison purposes. All cases include a vertical tail. As presented in figure 19, the asymmetric LEVF deflections are not suitable for producing rolling moments. The rolling moment increments that can be produced in this fashion vary considerably in magnitude with angle of attack, are accompanied by adverse yawing moments, and are small relative to those generated through aileron deflections. Note that the conventional differential ailerons produce relatively constant rolling moment increments which are accompanied by favorable yawing moments. Figure 20 illustrates that the asymmmetric LEVF are capable of producing large side forces at moderate to high angles of attack. The small rolling and yawing moments can most probably be trimmed out leaving a net side force. Direct

side force control might be useful in maneuvering and crosswind landing situations.

Extending the flow model to describe these characteristics is straight forward. Consider the 0:45 case. This configuration has the left leading edge at 0 degrees and the right leading edge at 45 degrees. At low to moderate angles of attack, there is a relatively strong vortex on the left-hand side and a relatively weak vortex on the right-hand side. Stronger vortex lift on the left-hand side is enough to account for the postive rolling moments. As in the case of the 40 degree symmetric LEVF, the weaker vortex on the 45 degree flap has enough strength and area to generate adverse yawing moments and large side forces. The yawing moments and side forces are generated because the left-hand flap does not have any lateral area with which to oppose them. Note that the trends are similar for the 35:45 degree case, but they are smaller in magnitude: there is less of an imbalance in lateral area. As the angle of attack is increased above 20 degrees, the 0 degree vortex has moved inboard while the 45 degree vortex has spilled off the flap but remains near the flap hingeline. The 0 degree vortex begins to influence the tail producing rolling and yawing moments which counter and eventually overpower the moments generated by the wing. Above 28 degrees, the 0 degree vortex has probably begun to burst while the 45 degree vortex has moved inboard into the vicinity of the vertical tail. As a result, there is an increasingly positive rolling moment and negative yawing moment. At this stage, the flap and vertical tail are both producing positive side force.

The stability derivatives for the asymmetric cases are presented in figure 21. The characteristics for the 30 degree baseline have been presented previously in figure 7. By differentially deflecting the leading edges ±5 degrees to 35:45, there is a substantial increase in both C_{Y_β} and C_{n_β} between

15 and 30 degrees angle of attack. The 0:45 deflection shows little change in C_{Y_β} , but does present a slight reduction in C_{n_β} at 25 degrees angle of attack. The 0:45 deflections also reduce C_{ℓ_β} slightly relative to the symmetric 30 degree case.

Figures 22 through 24 present the yawing moment, rolling moment, and side-force characteristics of the asymmetric LEVF as functions of sideslip. These figures are included because it is important to note that the lateral-directional characteristics of the 0:45 and 35:45 LEVF deflections do not differ significantly from the characteristics of the symmetric 30 degree case. The asymmetric LEVF do not show any unusual characteristics other than an expected offset in yawing moment, rolling moment, and side force at zero sideslip.

THEORETICAL ANALYSIS
Longitudinal Estimates

Although this study is primarily concerned with lateral-directional characteristics, VORSTAB has longitudinal features of interest not available in other linear methods to empirically account for vortex breakdown effects. The longitudinal predictions from VORSTAB, with and without vortex burst effects, are compared in figures 25 through 28 against experimental data. Additionally, theoretical predictions from the widely used VLM-SA of Lamar, which does not account for vortex breakdown effects, are also presented.

The longitudinal predictions for the 0 degree baseline are presented in figures 25a and 25b. Relative to VLM-SA, the lift and drag estimates from VORSTAB are surprisingly poor. Relative to the experimental data, the VORSTAB burst-off case (vortex burst features disabled) shows the proper trends, but the lift, drag, and pitching moment estimates are too low, too high, and too high, respectively. With the vortex burst-on case (vortex burst features

enabled), the lift and drag estimates worsen, while the pitching moment estimates improve. The combination of low lift and reasonable pitching moment characteristics imply that the VORSTAB burst-on longitudinal load centroid was calculated to be too far aft. Although the impact of the vortex burst-on features on the longitudinal characteristics was too severe, the angle of attack for which the vortex lift effects begin to deteriorate was correctly predicted. These vortex burst features began to influence VORSTAB's estimates at 25 degrees angle of attack, the angle which was identified earlier during the analysis of the experimental data.

Figure 26 illustrates the performance of VORSTAB and VLM-SA relative to the 40 degree case. For this cambered configuration, the VLM-SA and VORSTAB lift estimates are very good. While VLM-SA slightly under predicts the high angle-of-attack lift characteristics, VORSTAB is slightly low for the low to moderate angle of attack range. Also, in contrast to the baseline case, the VORSTAB burst-on calculations correctly predict the break in the lift curve. Although the drag estimates are slightly high, the vortex burst effects are correctly accounted for. As for the baseline case, the pitching moments are over-estimated in magnitude. Since the longitudinal loads are correctly predicted for the 40 degree case, yet the pitching moments remain over-estimated, this is further evidence of a load centroid located too far aft.

The VORSTAB estimates for the 30 and -30 degree cases, figure 27 and 28 respectively, are similar to the estimates calculated for the 40 and 0 degree cases, respectively. Although the vortex burst effects are not correctly predicted for the 30 degree case, the basic lift and drag comparisons are good. The pitching moments are over predicted. The VORSTAB -30 degree estimates of the lift and drag characteristics are poor relative to those available from VLM-SA. The pitching moment estimates for the burst-on case

are fortuitous. Note that the vortex burst effects are predicted by VORSTAB to occur at 25 and 20 degrees angle of attack for the 30 and -30 degree flap deflections, respectively. However, the longitudinal analysis of the experimental data indicated that these angles were 36 and 28 degrees respectively.

It is not surprising that the method used in VORSTAB to account for vortex burst effects does not accurately estimate the data. The angle of attack for vortex breakdown at the wing trailing edge, the upstream progression of the breakdown point, and the amount of vortex lift remaining in the breakdown region are each empirically determined from least square approximations of data assembled by Wentz. The Wentz study presents wind and water tunnel data for several planar, sharp edged delta wings of varying leading edge sweep angles. It does not include data which can be used to determine how the vortex breakdown effects of a planar delta wing compare with those of a cambered delta wing or with other than straight leading edges. The angle of attack corresponding to vortex breakdown was well predicted for the 0 degree case. The amount of vortex lift remaining in the breakdown region however, was significantly under-estimated. Considering that the baseline case is the only configuration without wing camber, one would have expected the theory to experiment correlation to be relatively good. Although the effects of vortex burst on the longitudinal characteristics of the 40 degree case were well predicted, these would seem to be chance results. Remember that the burst-on estimates for the 30 degree case, a 10 degree difference in flap deflection, were relatively poor.

Lateral-Directional Estimates

VORTSTAB stability derivative estimates for the 0 degree baseline, in tail-off and tail-on configurations, are compared to experimental results in

figures 29a and 29b. For the tail-off case, all three stability derivatives are over-estimated for angles of attack above 5 degrees. At 5 degrees however, the theoretical estimates correspond very well to experiment. Since the wing does not contribute any lateral area from a theoretical standpoint, the over-estimated values for C_{Y_β} and C_{n_β} must be due to fuselage effects. C_{ℓ_β} is greatly over-estimated. For the tail-on configuration, it is surprising to see under predicted values for C_{Y_β} and C_{n_β} at 5 and 15 degrees. This indicates that the theoretical increments associated with adding the vertical tail are too small. It is interesting to note that the C_{Y_β} curves for the tail-off and tail-on case are identical except for an offset and a slope change. This implies that the effect of the vertical tail on C_{Y_β} is accounted for by an increment in C_{Y_β} at zero angle of attack which deteriorates with angle of attack to simulate tail blanketing. Although the trends are correct, the vortex burst features are insufficient to describe the rapid deterioration of C_{Y_β} and C_{n_β} at angles of attack above 25 degrees. For these angles of attack, the windward vortex has migrated into the vicinity of the tail and produces adverse rolling and yawing moments. This characteristic of the flow is not accounted for by VORSTAB.

Figures 30a and 30b present the VORSTAB estimates for the 40 degree LEVF deflection. For the tail-off configuration, note that despite under-estimated C_{Y_β} values, the C_{n_β} estimates tend to be accurate or high. This indicates a lateral load centroid which is located too far forward. Note that the theory does not predict the gradual deterioration of C_{n_β} with angle of attack. C_{ℓ_β} remains over-estimated. For the tail-on configuration, the vertical tail effects on C_{Y_β} and C_{n_β} are under-estimated as for the 0 degree case. Note that C_{Y_β} is too low for the entire angle-of-attack range.

Figure 31 illustrates the theory to experiment comparisons for the 30 degree LEVF deflection. As before, the Cy_β and Cn_β estimates are too low and indicate that the vertical tail effects have not been properly accounted for. C_{ℓ_β} compares more favorably to experiment for this flap deflection as opposed to the 0 and 40 degree cases. Figure 32 presents the VORSTAB lateral-directional estimates for the -30 degree flap deflection. As with the tail-off configurations for the 0 and 40 degree LEVF, the stability derivatives are correctly estimated at 5 degrees angle of attack. In contrast to the previous cases, VORSTAB Cy_β estimates are too large. Consequently, the Cn_β estimates are also high. The break in the Cy_β and Cn_β curves is due to the windward vortex affecting the vertical tail, a characteristic of the vortex flow not accounted for by VORSTAB.

CONCLUSIONS

An investigation to determine the low-speed lateral-directional characteristics of a generic 74 degree delta wing-body configuration employing the latest generation, gothic planform vortex flaps has been conducted. In addition, the theoretical estimates from VORSTAB were compared against the experimental data to aid in documenting this new method. The results may be summarized as follows:

1. LEVF deflections of 30 and 40 degrees significantly reduce the magnitude of C_{ℓ_β} relative to the baseline for a specified angle of attack or lift coefficient.

2. For angles of attack above 15 degrees, the downward LEVF deflections significantly reduce the configuration directional stability despite improved vertical tail effectiveness.

3. The inverted -30 degree deflection substantially increased the configuration $-C_{\ell_\beta}$. Considering that this flap deflection is

intended for approach and landing, there may be insufficient roll power to balance the large $-C_{\ell_\beta}$ values during a crosswind landing.

4. The inverted -30 degree deflection slightly improved the configuration directional stability.

5. Asymmetric LEVF deflections are not suitable for producing rolling moments.

6. Asymmetric LEVF deflections can produce significant side forces at moderate to high angles of attack. Accompanying rolling and yawing moments are small and could easily be trimmed out using conventional control surfaces. Direct side force control might be useful during maneuver or crosswind landing situations.

7. From a longitudinal standpoint, VORSTAB load estimates vary from very good for the 30 and 40 degree deflections to poor for the 0 and -30 degree deflections. The longitudinal load centroid is calculated too far aft resulting in pitching moments which were consistently over-estimated.

8. VORSTAB lateral-directional calculations provide ballpark estimates at low to moderate angles of attack. VORSTAB does not account for vortex interactions with the vertical tail.

9. VORSTAB consistently over-estimates wing effective dihedral.

10. VORSTAB tends to over-estimate wing-body C_{y_β} and C_{n_β}. The theory also under-estimates vertical tail contributions to C_{y_β} and C_{n_β}.

11. The empirical formulae for predicting vortex burst effects are not reliable in their present form. With the vortex burst features active, the predicted trends are generally correct.

However, the magnitude of the vortex burst effect is typically

over-estimated.

REFERENCES

1. "Design Conference Proceedings: Technology for Supersonic Cruise Military Aircraft," AFFDL-TR-77-85, Vol. I, U. S. Air Force, 1976.

2. Child, R. D., "Design and Analysis of a Supersonic Penetration Maneuvering Fighter," Rockwell International, NASA CR-132633, April, 1975.

3. Meyer, R. C., and Fields, W. D., "Configuration Development of a Supersonic Cruise Strike-fighter," AIAA Paper 78-148, Jan. 1978.

4. Miller, D. S., Schemensky, R. T., "Design Study Results of a Supersonic Cruise Fighter Wing," AIAA Paper 79-062, Jan. 1979.

5. Foss, W. E., Jr., and Sorrells, R. B., III, "Trade Studies Resulting to a Long Range Mach 2.6 Supercruiser," NASA TM-78811, Dec. 1978.

6. Campbell, J. F., "Vortex-Flow Aerodynamics - An Emerging Design Capability," Astronautics and Aeronautics, p55-57, AIAA, May 1981.

7. Lamar, J. E., Schemensky, R. T., and Reddy, C. S., "Development of a Vortex Lift Design Procedure and Application to a Slender Maneuver Wing Configuration," Journal of Aircraft, Vol. 18, No. 4, pp. 259-266, April 1981.

8. Rao, D. M., "Leading Edge 'Vortex Flaps' for Enhanced Subsonic Aerodynamics of Slender Wings," ICAS Paper 80-13.5, Oct. 1980.

9. Rao, D. M., "Leading Edge Vortex-Flap Experiments on a 74 Degree Delta Wing," NASA CR-159161, Nov. 1979.

10. Marchman, J. F., III, "Effectiveness of Leading Edge Vortex Flaps on 60 and 75 Degree Delta wings," Journal of Aircraft, Vol. 18, No. 4, pp. 280-286, April 1981.

11. Rao, D. M., "Segmented Vortex Flaps," AIAA Paper 83-0424, January 1983.

12. Lockwood, V. E., "Effect of Leading Edge Contour and Vertical Tail Configuration on the Low Speed Stability Characteristics of a Supersonic Transport Model Having a Highly Swept Arrow Wing," NASA TM-78683, LaRC, March 1978.

13. McLemore and Parlett, "Low Speed Wind Tunnel Tests of a 1/10 Scale Model of a Blended Arrow Supersonic Cruise Aircraft," NASA TN-D-8410, LaRC, June 1977.

14. Coe and Weston, "Effects of Wing Leading Edge Deflection on the Low Speed Characteristics of a Low Aspect Ratio Highly Swept Arrow Wing Configuration," NASA TP-1434, LaRC, June 1979.

15. Coe, Smith, and Parlett, "Low Speed Wind Tunnel Investigation of an Advanced Supersonic Cruise Arrow Wing Configuration," NASA TM-74043, LaRC, July 1977.

16. Polhamus, Edward C., "Application of the Leading-Edge-Suction Analogy of Vortex Lift to the Drag due to Lift of Sharp-edge Delta Wings," NASA TN D-4739, August, 1968.

17. Lamar, John E., and Gloss, Blair B., "Subsonic Aerodynamic Characteristics of Interacting Lifting Surfaces with Separated Flow around Sharp Edges Predicted by a Vortex-Lattice Method," NASA TN D-7921, Sept., 1975.

18. Lan, Edward C., "A Quasi-Vortex-Lattice Method in Thin Wing Theory," Journal of Aircraft, Vol. 11, No. 9, Sept., 1974.

19. Johnson, F. T., Lu, P., Tinoco, E. N., and Epton, M. A., "An Improved Panel Method for the Solution of Three-Dimensional Leading-Edge Vortex Flows: Volume I - Theory Document," NASA CR-3278, July, 1980.

20. Kandil, O. A., Mook, D. T., and Nayfeh, A. H., "A Numerical Technique for Computing Subsonic Flow Past Three-Dimensional Canard Wing Configurations with Edge Separation," AIAA Paper 77-1, Jan., 1977.

21. Mehrotra, S. C. and Lan, C. E., "A Theoretical Investigation of the Aerodynamics of Low Aspect Ratio Wings with Partial Leading Edge Separation," NASA CR-145304, 1978.

22. Jameson, A., Schmidt, W., and Turkel E., "Numerical Solutions of the Euler Equations by Finite Volume Methods Using Runge-Kutta Time-Stepping Schemes," AIAA-81-1259, June, 1981.

23. Lan, C. E. and Hsu, C. H., "Effects of Vortex Breakdown on Longitudinal and Lateral-Directional Aerodynamics of Slender Wings by the Suction Analogy," AIAA-82-1385, August, 1982.

24. Wentz, W. H., "Wind Tunnel Investigation of Vortex Breakdown on Slender Sharp-Edged Wings," NASA CR-98737, 1969.

25. Fox, Charles H., and Huffman, Jarrett K., "Calibration and Test Capabilities of the Langley 7- by 10-foot High Speed Tunnel," NASA TN-74027, 1977.

26. Herriot, J. G., "Blockage Corrections for Three Dimensional Flow Closed Throat Wind Tunnels, With Consideration of the Effect of Compressibility," NACA Report 995, 1950.

27. Gillis, Polhamus, and Gray, "Charts for Determining Jet Boundary Corrections for Complete Models in 7- by 10- Foot Closed Rectangular Wind Tunnels," NACA WR L-123, 1945. (Formerly NASA ARR L5G31.)

28. Braslow, A. L., Hicks, R. M., and Harris, R. V., Jr.; "Use of Grit-Type Boundary-Layer-Transition Trips on Wind Tunnel Models." NASA TN D-3579, Sept. 1966.

APPENDIX A

Data Supplement

The symbols used in the data tabulation are defined as follows:

ALPHA   angle of attack, deg

BETA   angle of sideslip, deg

CD   drag-force coefficient; stability axis

CL   lift-force coefficient; stability axis

CM   pitching-moment coefficient; stability axis

CRM   rolling-moment coefficient; stability axis

CY   side-force coefficient; body axis

CYM   yawing-moment coefficient; body axis

APPENDIX A

TABLE A1.- WIND-TUNNEL RUN SCHEDULE

Run	Date	α (deg)	β (deg)	δ_{LE} (deg)	δ_A (deg)	Tail
5	1/12/84	0-40	0	0	0	ON
6	1/12/84	5	*	0	0	ON
7	1/12/84	15	*	0	0	ON
8	1/12/84	25	*	0	0	ON
9	1/12/84	30	*	0	0	ON
10	1/12/84	35	*	0	0	ON
11	1/13/84	5	*	0	0	OFF
12	1/13/84	15	*	0	0	OFF
13	1/13/84	25	*	0	0	OFF
14	1/13/84	30	*	0	0	OFF
15	1/13/84	35	*	0	0	OFF
16	1/16/84	0-40	0	40	0	ON
17	1/16/84	5	*	40	0	ON
18	1/16/84	15	*	40	0	ON
19	1/16/84	25	*	40	0	ON
20	1/16/84	30	*	40	0	ON
21	1/16/84	35	*	40	0	ON
22	1/17/84	5	*	40	0	OFF
23	1/17/84	15	*	40	0	OFF
24	1/17/84	25	*	40	0	OFF
25	1/17/84	30	*	40	0	OFF
26	1/17/84	35	*	40	0	OFF

* β = 0, 2, 4, 6, 8, 12, 16, -2, -4, -6, -8, -12, -16

APPENDIX A

TABLE A1.- CONCLUDED

Run	Date	α (deg)	β (deg)	δ_{LE} (deg)	δ_A (deg)	Tail
27	1/18/84	0-40	0	0:45	0	ON
28	1/18/84	5	*	0:45	0	ON
29	1/18/84	15	*	0:45	0	ON
30	1/18/84	25	*	0:45	0	ON
31	1/18/84	30	*	0:45	0	ON
32	1/18/84	35	*	0:45	0	ON
33	1/20/84	0-40	0	35:45	0	ON
34	1/20/84	5	*	35:45	0	ON
35	1/20/84	15	*	35:45	0	ON
36	1/20/84	25	*	35:45	0	ON
37	1/20/84	30	*	35:45	0	ON
38	1/20/84	35	*	35:45	0	ON
39	1/20/84	0-40	0	30	0	ON
40	1/23/84	5	*	30	0	ON
41	1/23/84	15	*	30	0	ON
42	1/23/84	25	*	30	0	ON
43	1/23/84	30	*	30	0	ON
44	1/23/84	35	*	30	0	ON
46	1/23/84	0-40	0	30	±10	ON
47	1/23/84	0-40	0	30	±20	ON
48	1/24/84	0-40	0	-30	0	ON
49	1/24/84	5	*	-30	0	ON
50	1/24/84	15	*	-30	0	ON
51	1/24/84	25	*	-30	0	ON
52	1/24/84	30	*	-30	0	ON
53	1/24/84	35	*	-30	0	ON

* β = 0, 2, 4, 6, 8, 12, 16, -2, -4, -6, -8, -12, -16

APPENDIX A

TABLE A2.- TABULATED DATA

TEST NUM 121. RUN NUM 5.

BETA DEG	ALPHA	CL	CD	CM	CRM	CYM	CY
.02	-1.17	-.0226	.0133	.0042	.0002	-.0015	.0054
-.07	3.60	.1466	.0251	-.0169	.0007	-.0012	.3056
-.14	7.80	.3196	.0594	-.0352	.0004	-.0010	.0059
-.21	12.04	.5082	.1221	-.0538	.0006	-.0007	.0047
-.29	16.41	.7298	.2267	-.0743	.0002	-.0007	.0053
-.36	20.74	.9653	.3748	-.0990	.0005	-.0004	.0053
-.44	25.14	1.1871	.5592	-.1171	-.0008	.0008	.0077
-.51	29.42	1.3299	.7481	-.1254	-.0067	.0021	.0071
-.56	33.75	1.4382	.9549	-.1430	.0001	-.0037	.0051
-.62	37.97	1.4650	1.1361	-.1613	.0011	-.0029	.0054
-.75	40.72	1.3889	1.1897	-.1744	.0004	-.0045	.0016
.01	-1.17	-.0203	.0072	.0060	.0004	-.0021	.0133

TEST NUM 121. RUN NUM 6.

BETA DEG	ALPHA	CL	CD	CM	CRM	CYM	CY
-.09	5.11	.2062	.0299	-.0217	.0005	-.0016	.0076
2.14	5.08	.2000	.0257	-.0209	-.0027	.0008	-.0003
3.79	4.99	.2115	.0280	-.0225	-.0060	.0042	-.0107
5.86	5.18	.2202	.0289	-.0237	-.0095	.0093	-.0275
7.31	4.84	.1963	.0210	-.0204	-.0101	.0128	-.0370
12.20	5.20	.2176	.0258	-.0233	-.0176	.0263	-.3715
16.56	5.17	.2116	.0231	-.0238	-.0217	.0374	-.1062
-2.00	5.02	.1960	.0290	-.0208	.0035	-.0033	.0085
-3.70	4.95	.1942	.0294	-.0212	.0067	-.0067	.0162
-6.04	5.10	.2050	.0314	-.0229	.0107	-.0118	.0254
-8.37	5.02	.1992	.0303	-.0222	.0132	-.0173	.0371
-12.04	4.77	.1932	.0284	-.0227	.0183	-.0273	.3627
-15.83	5.23	.2124	.0307	-.0258	.0241	-.0361	.0886
-.28	5.18	.2024	.0286	-.0213	.0010	-.0018	.0064

TEST NUM 121. RUN NUM 7.

BETA DEG	ALPHA	CL	CD	CM	CRM	CYM	CY
-.12	14.99	.6284	.1747	-.0656	.0001	.0002	-.0039
1.91	14.86	.6244	.1719	-.0655	-.0076	.0024	-.0105
4.15	15.57	.6752	.1954	-.0717	-.0164	.0064	-.0236
5.96	15.58	.6754	.1947	-.0712	-.0237	.0103	-.0327
7.94	15.09	.6323	.1736	-.0666	-.0293	.0155	-.0430
11.93	15.21	.6309	.1771	-.0639	-.0407	.0273	-.0763
16.47	15.52	.6215	.1772	-.0623	-.0515	.0371	-.1068
-2.05	15.55	.6650	.1926	-.0695	.0080	-.0025	.3031
-4.18	15.10	.6466	.1831	-.0681	.0155	-.0058	.0103
-6.08	15.06	.6499	.1847	-.0688	.0229	-.0098	.0178
-8.15	15.19	.6585	.1894	-.0691	.0307	-.0156	.0339
-12.18	15.19	.6397	.1850	-.0661	.0423	-.0268	.0606
-15.98	14.98	.6102	.1745	-.0629	.0511	-.0347	.0818
-.23	16.06	.6830	.2005	-.0702	.0002	-.0003	-.0025

TEST NUM 121. RUN NUM 8.

BETA DEG	ALPHA	CL	CD	CM	CRM	CYM	CY
-.22	25.21	1.1713	.5522	-.1142	-.0004	.0030	-.0057
1.90	25.18	1.1447	.5379	-.1085	-.0097	.0050	-.0121
4.12	25.26	1.1349	.5346	-.1100	-.0223	.0075	-.0199
5.73	25.25	1.1125	.5247	-.1108	-.0296	.0087	-.0255
7.97	25.60	1.0967	.5269	-.1083	-.0351	.0082	-.0319
11.86	25.46	1.0711	.4895	-.0966	-.0455	.0072	-.0349
15.82	25.29	.8341	.4045	-.0675	-.0292	-.0129	-.0124
-1.95	24.98	1.1347	.5269	-.1112	.0069	-.0008	.0039
-4.11	24.89	1.1279	.5249	-.1079	.0166	-.0030	.0118
-6.14	24.83	1.1092	.5150	-.1089	.0281	-.0051	.0187
-8.03	24.79	1.0876	.5047	-.1102	.0352	-.0063	.3229
-12.06	24.79	1.0297	.4804	-.1018	.0457	-.0060	.0321
-16.19	25.31	.8763	.4227	-.0727	.0313	.0184	-.0021
-.31	25.60	1.1510	.5325	-.1134	-.0030	.0015	-.0030

APPENDIX A

TABLE A2.- CONTINUED

TEST NUM 121.   RUN NUM 9.

BETA DEG	ALPHA	CL	CD	CM	CRM	CYM	CY
.00	30.34	1.3478	.7837	-.1291	-.0036	.0022	-.0044
1.89	30.26	1.3272	.7678	-.1284	-.0102	.0009	-.0066
3.98	30.03	1.3009	.7459	-.1294	-.0159	.0014	-.0103
5.81	30.01	1.2515	.7205	-.1238	-.0186	-.0016	-.0110
7.83	30.06	1.1863	.6877	-.1126	-.0187	-.0063	-.0069
11.92	29.89	.9719	.5659	-.1035	-.0100	-.0282	-.0028
15.78	30.12	.9107	.5341	-.1169	-.0196	-.0278	-.0253
-2.24	30.21	1.3477	.7768	-.1288	.0078	.0038	.0005
-4.30	30.15	1.3251	.7637	-.1284	.0153	.0046	.0047
-6.15	29.95	1.2924	.7404	-.1286	.0188	.0058	.0077
-7.96	29.68	1.2333	.7009	-.1220	.0224	.0068	.0051
-12.17	29.70	.9975	.5728	-.1126	.0036	.0360	-.0065
-16.09	29.56	.9308	.5319	-.1176	.0155	.0376	.0117
-.07	30.10	1.3452	.7735	-.1277	-.0027	.0022	-.0043

TEST NUM 121.   RUN NUM 10.

BETA DEG	ALPHA	CL	CD	CM	CRM	CYM	CY
-.08	35.27	1.4423	1.0118	-.1477	.0003	-.0016	-.0022
-.08	35.37	1.4409	1.0129	-.1482	-.0001	-.0014	-.0018
2.03	35.41	1.3835	.9745	-.1434	-.0003	-.0043	.0105
3.93	35.44	1.3156	.9334	-.1382	.0025	-.0145	.0140
5.97	35.28	1.1448	.8127	-.1167	.0067	-.0271	.0063
7.92	35.25	1.0942	.7769	-.1132	.0019	-.0318	-.0028
11.57	35.41	1.0315	.7376	-.1192	-.0108	-.0383	-.0109
15.45	35.56	1.0145	.7279	-.1443	-.0213	-.0391	-.0272
-2.13	35.30	1.4374	1.0077	-.1491	.0018	.0053	-.0070
-4.02	35.14	1.3760	.9610	-.1469	-.0002	.0112	-.0112
-6.07	34.90	1.3421	.9306	-.1454	.0040	.0175	-.0186
-8.27	34.60	1.2191	.8400	-.1414	-.0050	.0396	-.0214
-12.27	34.77	1.1208.	.7762	-.1548	.0062	.0577	-.0201
-15.84	34.58	1.0817	.743A	-.1652	.0222	.0532	-.0060
-.20	35.06	1.4354	.9937	-.1464	-.0002	-.0011	-.0029

TEST NUM 121.   RUN NUM 11.

BETA DEG	ALPHA	CL	CD	CM	CRM	CYM	CY
.04	5.22	.2044	.0312	-.0216	.0005	.0001	.0010
1.93	5.26	.2045	.0292	-.0211	-.0025	-.0008	-.0011
3.87	5.54	.2217	.0319	-.0225	-.0060	-.0017	-.0033
5.91	5.74	.2153	.030C	-.0217	-.0089	-.0021	-.0082
8.11	5.55	.2239	.0308	-.0223	-.0124	-.0029	-.0120
11.68	5.29	.2104	.0277	-.0206	-.0157	-.0042	-.0189
15.98	5.21	.1970	.0254	-.0188	-.0185	-.0063	-.0287
-1.93	4.97	.1902	.0283	-.0197	.0034	.0012	-.0023
-4.13	5.11	.1969	.0303	-.0207	.0069	.0023	-.0015
-6.13	5.11	.1936	.030C	-.0211	.0102	.0032	-.0043
-8.09	5.15	.1991	.0297	-.0210	.0126	.0041	-.0032
-11.65	4.89	.1874	.0269	-.0202	.0163	.0057	.0003
-16.41	5.10	.1926	.0267	-.0204	.0214	.0086	.0075
.02	4.89	.1879	.0269	-.0192	.0006	-.0004	.0031

TEST NUM 121.   RUN NUM 12.

BETA DEG	ALPHA	CL	CD	CM	CRM	CYM	CY
-.11	15.13	.6555	.1837	-.0655	-.0004	.0001	.0004
1.96	15.18	.6407	.1773	-.0640	-.0082	-.0012	-.0015
3.97	15.19	.6554	.1829	-.0664	-.0153	-.0024	-.0039
6.33	15.50	.6716	.1909	-.0679	-.0242	-.0038	-.0044
8.06	15.64	.6559	.1858	-.0649	-.0292	-.0043	-.0072
12.13	15.20	.6026	.1663	-.0562	-.0365	-.0057	-.0148
16.06	15.12	.5905	.1641	-.0525	-.0461	-.0072	-.0246
-2.13	15.53	.6708	.1915	-.0672	.0085	.0017	-.0022
-4.09	15.10	.6465	.1797	-.0655	.0152	.0029	-.0035
-6.19	14.82	.6340	.1732	-.0648	.0228	.0042	-.0035
-7.89	14.90	.6356	.1748	-.0643	.0282	.0051	-.0024
-11.86	14.87	.6072	.1680	-.0570	.0368	.0066	.0022
-15.95	14.78	.5780	.1591	-.0520	.0459	.0085	.0045
-.19	15.02	.6275	.1699	-.0625	-.0001	-.0002	.0002

APPENDIX A

TABLE A2.- CONTINUED

TEST NUM	121.				RUN NUM	13.		
BETA DEG	ALPHA	CL	CD	CM	CRM	CYM	CY
.02	25.27	1.1511	.5367	-.1092	-.C020	.0011	-.0015
1.77	25.17	1.1249	.5224	-.1037	-.0087	.0003	-.0028
3.90	25.06	1.1250	.5225	-.1052	-.0199	-.0016	-.0034
5.90	25.16	1.0954	.5118	-.1051	-.0267	-.0026	-.0072
7.86	25.21	1.0569	.4961	-.0984	-.0293	-.0044	-.0104
11.95	25.43	.9971	.4753	-.0867	-.0402	-.0084	-.0116
15.7C	25.34	.9140	.4367	-.0740	-.0444	-.0118	-.0137
-2.19	25.10	1.1508	.5359	-.1080	.0066	.0027	-.0014
-4.06	25.07	1.1352	.5280	-.1349	.0152	.0042	.0007
-6.13	24.94	1.0970	.5077	-.1045	.0247	.0059	-.0002
-8.25	25.09	1.0595	.4926	-.1006	.0279	.0068	.0030
-12.09	25.20	1.0136	.4777	-.0912	.0384	.0109	.0040
-16.08	25.02	.9362	.4397	-.0784	.0445	.0157	.0063
-.46	25.50	1.1669	.5483	-.1109	-.0012	.0009	-.0000

TEST NUM	121.				RUN NUM	14.		
BETA DEG	ALPHA	CL	CD	CM	CRM	CYM	CY
.01	30.36	1.3465	.7794	-.1232	-.0041	.0018	.0020
1.97	30.49	1.3312	.7752	-.1242	-.0102	.0002	-.0020
3.79	30.49	1.3072	.7623	-.1256	-.0129	-.0020	-.0034
6.12	30.48	1.2375	.7230	-.1193	-.0152	-.0051	-.0070
8.09	30.11	1.1825	.6827	-.1115	-.0202	-.0081	-.0080
11.83	30.09	1.0299	.6000	-.1140	-.0168	-.0157	-.0133
15.92	30.23	.9492	.5566	-.1215	-.0270	-.0167	-.0366
-2.22	30.12	1.3240	.7571	-.1218	.0068	.0049	.0025
-4.08	29.87	1.3013	.7369	-.1220	.0137	.0069	.0047
-6.11	29.81	1.2817	.7273	-.1219	.0157	.0097	.0072
-7.98	29.89	1.2227	.6983	-.1159	.0179	.0120	.0071
-11.96	30.26	1.0964	.6402	-.1065	.0183	.0196	.0110
-15.97	29.85	1.0211	.5884	-.1146	.0277	.0267	.0170
.09	30.09	1.3231	.7552	-.1210	-.0042	.0018	.0004

TEST NUM	121.				RUN NUM	15.		
BETA DEG	ALPHA	CL	CD	CM	CRM	CYM	CY
.02	35.28	1.4205	.9914	-.1392	-.0028	.0045	.0079
2.05	35.30	1.3980	.9799	-.1405	-.0038	.0005	.0066
3.89	35.31	1.3620	.9564	-.1388	-.0065	-.0034	.0053
5.85	35.23	1.3091	.9193	-.1368	-.0086	-.0082	.0045
8.00	35.17	1.1444	.8063	-.1231	-.0043	-.0139	-.0151
11.75	35.23	1.0689	.7693	-.1356	-.0146	-.0211	-.0401
15.91	35.45	1.0420	.7429	-.1592	-.0267	-.0196	-.0477
-2.02	35.09	1.4124	.9773	-.1383	.0023	.0085	.0084
-4.30	34.82	1.3733	.9418	-.1351	.0050	.0124	.0130
-6.39	35.26	1.3537	.9451	-.1378	.0082	.0155	.0115
-9.18	35.05	1.3417	.9331	-.1426	.0151	.0182	.0070
-12.07	35.01	1.2529	.8728	-.1524	.0222	.0322	.0071
-16.03	34.89	1.1331	.7873	-.1646	.0283	.0360	.0442
-.12	35.39	1.4235	.9957	-.1395	-.0020	.0046	.0081

TEST NUM	121.				RUN NUM	16.		
BETA DEG	ALPHA	CL	CD	CM	CRM	CYM	CY
.02	-1.32	-.0922	.0246	.0114	.0004	-.0021	.0070
-.06	2.39	.0383	.0176	-.0036	.0005	-.0019	.0081
-.15	6.50	.1587	.0232	-.0196	.0006	-.0015	.0071
-.23	10.37	.2777	.0390	-.0321	.0003	-.0012	.0064
-.33	14.74	.4351	.0779	-.0521	-.0003	-.0015	.0073
-.42	19.17	.6279	.1581	-.0757	.0003	-.0011	.0070
-.52	23.47	.8203	.2766	-.0993	-.0020	.0006	.0099
-.60	27.34	1.0065	.4280	-.1223	-.0024	.0031	.0127
-.70	32.07	1.2231	.6547	-.1519	-.0020	.0059	.0125
-.78	36.23	1.3499	.8579	-.1637	-.0012	.0057	.0229
-.77	40.12	1.3705	1.0179	-.1604	.0122	.0010	.0267
.02	-1.33	-.0917	.0202	.0132	.0001	-.0029	.0142

APPENDIX A

TABLE A2.- CONTINUED

TEST NUM	121.				RUN NUM	17.		
BETA DEG	ALPHA	CL	CD	CM	CRM	CYM	CY
-.08	5.01	.1172	.0154	-.0128	.0003	-.0024	.0130
1.90	5.04	.1254	.0151	-.0135	-.0010	.0006	.0034
3.94	5.21	.1350	.0145	-.0145	-.0026	.0048	-.0082
5.95	5.36	.1406	.0141	-.0153	-.0038	.0106	-.0264
7.84	5.10	.1275	.0104	-.0135	-.0039	.0167	-.0434
12.06	5.20	.1377	.0133	-.0161	-.0046	.0303	-.0923
15.77	5.32	.1437	.0135	-.0183	-.0037	.0408	-.1178
-2.04	5.18	.1164	.0154	-.0130	.0018	-.0049	.0140
-3.94	5.15	.1166	.0158	-.0138	.0032	-.0084	.0221
-6.11	5.35	.1252	.0168	-.0153	.0048	-.0146	.0342
-8.04	5.11	.1163	.0163	-.0147	.0050	-.0203	.0474
-11.93	4.80	.1091	.0160	-.0154	.0050	-.0316	.0791
-15.78	5.18	.1260	.0135	-.0185	.0053	-.0406	.1078
.03	5.07	.1165	.0148	-.0126	.0003	-.0023	.0104

TEST NUM	121.				RUN NUM	18.		
BETA DEG	ALPHA	CL	CD	CM	CRM	CYM	CY
-.18	15.15	.4549	.0863	-.0536	-.0004	-.0019	.0092
2.08	15.26	.4606	.0819	-.0544	-.0035	.0008	-.0036
3.97	15.24	.4591	.0811	-.0538	-.0059	.0040	-.0130
5.86	15.52	.4694	.0851	-.0551	-.0087	.0082	-.0254
8.04	15.56	.4783	.0882	-.0562	-.0123	.0131	-.0361
12.11	14.88	.4655	.0849	-.0552	-.0186	.0242	-.0678
16.14	15.26	.4963	.0963	-.0600	-.0257	.0350	-.0984
-2.04	15.13	.4472	.0780	-.0530	.0025	-.0028	.0142
-3.89	14.90	.4393	.0761	-.0516	.0050	-.0055	.0222
-5.98	14.76	.4362	.0753	-.0514	.0081	-.0097	.0299
-8.42	14.92	.4479	.0789	-.0538	.0120	-.0154	.0446
-12.25	14.67	.4563	.0836	-.0559	.0192	-.0241	.0668
-15.89	15.48	.5030	.1007	-.0626	.0266	-.0332	.0882
-.04	14.92	.4382	.0736	-.0510	-.0004	-.0018	.0066

TEST NUM	121.				RUN NUM	19.		
BETA DEG	ALPHA	CL	CD	CM	CRM	CYM	CY
-.13	24.82	.8646	.3103	-.1034	-.0030	-.0003	.0087
1.99	24.87	.8854	.3225	-.1061	-.0108	.0005	.0051
3.84	24.78	.8828	.3204	-.1062	-.0160	.0029	-.0026
5.92	25.40	.9091	.3423	-.1098	-.0241	.0061	-.0106
7.80	25.28	.9041	.3397	-.1082	-.0292	.0113	-.0233
12.15	25.25	.8964	.3368	-.1086	-.0391	.0234	-.0544
15.79	24.89	.9075	.3420	-.1102	-.0480	.0321	-.0726
-1.95	25.05	.8902	.3270	-.1058	.0035	.0017	.0097
-4.09	25.27	.9025	.3371	-.1085	.0112	.0011	.0139
-6.06	25.00	.8914	.3279	-.1081	.0183	-.0005	.0193
-7.87	24.97	.8900	.3279	-.1082	.0244	-.0038	.0269
-12.00	24.91	.8936	.3320	-.1089	.0365	-.0156	.0564
-16.12	25.17	.9135	.3444	-.1142	.0439	-.0292	.0855
-.16	25.00	.8724	.3141	-.1036	-.0031	-.0005	.0088

TEST NUM	121.				RUN NUM	20.		
BETA DEG	ALPHA	CL	CD	CM	CRM	CYM	CY
-.28	30.20	1.1454	.5583	-.1407	-.0034	.0050	.0094
1.89	30.25	1.1368	.5539	-.1377	-.0122	.0034	.0064
3.71	30.27	1.1381	.5546	-.1379	-.0191	.0027	.0025
5.82	30.24	1.1221	.5454	-.1354	-.0265	.0031	-.0058
7.90	30.47	1.1252	.5542	-.1342	-.0333	.0053	-.0132
11.70	30.35	1.0779	.5287	-.1236	-.0392	.0078	-.0257
15.83	29.92	.9714	.4826	-.0914	-.0242	-.0151	.0107
-1.89	29.85	1.1359	.5430	-.1410	.0021	.0066	.0126
-4.09	30.20	1.1315	.5469	-.1397	.0089	.0085	.0176
-6.14	29.88	1.1030	.5243	-.1346	.0181	.0068	.0231
-8.15	30.39	1.1322	.5540	-.1386	.0252	.0076	.0298
-12.09	30.20	1.1019	.5353	-.1337	.0377	.0051	.0452
-16.07	29.98	1.0559	.5136	-.1193	.0381	.0113	.0417
-.10	30.10	1.1309	.5444	-.1389	-.0045	.0044	.0085

APPENDIX A

TABLE A2.- CONTINUED

TEST NUM 121.   RUN NUM 21.

BETA DEG	ALPHA	CL	CD	CM	CRM	CYM	CY
-.22	35.26	1.3314	.8101	-.1618	-.0032	.0040	.0161
1.95	35.29	1.3120	.7984	-.1568	-.0096	-.0001	.3087
3.91	35.26	1.2837	.7817	-.1486	-.0125	-.0029	.3064
6.02	35.47	1.2342	.7609	-.1365	-.01CC	-.0099	-.0001
7.90	35.26	1.1766	.7227	-.1244	-.0084	-.0174	.0019
11.92	35.42	1.1013	.6860	-.1143	-.0087	-.0335	.3041
15.87	35.48	1.0764	.6776	-.1107	-.0196	-.0350	.0074
-1.87	34.84	1.3192	.7863	-.1605	.0018	.0077	.0183
-3.99	35.01	1.3141	.7889	-.1587	.0092	.0110	.0237
-5.96	35.18	1.3093	.7914	-.1581	.0153	.0141	.0288
-8.05	35.17	1.2843	.7772	-.1532	.0209	.0180	.0308
-11.99	34.93	1.1406	.6924	-.1231	.0090	.0461	.0259
-16.16	35.02	1.0544	.6476	-.1229	.0100	.0580	.0227
-.12	35.39	1.3167	.8000	-.1601	-.0035	.0049	.0125

TEST NUM 121.   RUN NUM 22.

BETA DEG	ALPHA	CL	CD	CM	CRM	CYM	CY
.20	5.12	.1178	.0181	-.0134	.0004	.0007	-.0019
2.07	5.29	.1223	.0173	-.0140	-.0007	.0001	-.0025
4.15	4.89	.1105	.0152	-.0129	-.0019	-.0066	-.0007
6.19	4.83	.1121	.0144	-.0135	-.0026	-.0008	-.0041
8.39	4.89	.1173	.0140	-.0141	-.0033	-.0009	-.0066
12.36	4.88	.1248	.0144	-.0150	-.0037	-.0016	-.0130
16.23	4.65	.1197	.0120	-.0150	-.0023	-.0031	-.0215
-1.64	4.82	.1062	.0157	-.0110	.0012	.0014	-.0028
-3.69	5.44	.1345	.0206	-.0144	.0024	.0017	.0024
-5.77	5.53	.1389	.0222	-.0148	.0027	.0018	.0084
-8.00	5.74	.1393	.0227	-.0150	.0026	.0016	.0179
-11.94	5.94	.1363	.0221	-.0150	.0018	.0020	.0348
-15.96	5.97	.1303	.0233	-.0153	-.0004	.0041	.0490
.21	5.00	.1152	.0179	-.0130	.0006	.0009	-.0028

TEST NUM 121.   RUN NUM 23.

BETA DEG	ALPHA	CL	CD	CM	CRM	CYM	CY
.73	15.33	.4522	.0830	-.0538	.0000	.0001	-.0032
2.58	15.14	.4438	.0788	-.0518	-.0025	-.0004	-.0070
4.81	14.92	.4407	.0771	-.0507	-.0049	-.0016	-.0077
6.66	14.97	.4422	.0778	-.0508	-.0070	-.0031	-.0095
8.70	14.92	.4448	.0786	-.0507	-.0099	-.0056	-.0073
12.72	14.64	.4496	.0819	-.0515	-.0166	-.0117	-.0031
16.79	14.65	.4692	.0893	-.0541	-.0224	-.0155	-.0073
-1.36	15.20	.4398	.0785	-.0512	.0015	.0067	.0043
-3.03	15.04	.4350	.0776	-.0496	.0037	.0015	.0058
-5.21	15.33	.4477	.0829	-.0513	.0069	.0032	.0059
-7.39	15.35	.4468	.0839	-.0509	.0095	.0057	.0048
-11.19	16.11	.4835	.1004	-.0552	.0170	.0130	-.0006
-15.11	16.21	.4922	.1073	-.0565	.0233	.0179	-.0019
.80	15.28	.4452	.0788	-.0519	-.0001	-.0001	-.0020

TEST NUM 121.   RUN NUM 24.

BETA DEG	ALPHA	CL	CD	CM	CRM	CYM	CY
1.35	25.38	.8921	.3354	-.1059	-.0035	-.0011	.0046
3.19	25.40	.8865	.3315	-.1064	-.0093	-.0041	.0064
5.27	25.02	.8670	.3172	-.1034	-.0148	-.0071	.0095
7.07	24.62	.8633	.3119	-.1023	-.0202	-.0089	.0094
9.24	24.62	.8644	.3151	-.1007	-.0253	-.0106	.0094
13.10	24.70	.8737	.3246	-.0996	-.0337	-.0126	.0107
17.14	24.97	.8921	.3422	-.0984	-.0418	-.0170	.0105
-.80	25.44	.8706	.3239	-.1033	.0033	.0039	.0014
-2.81	25.30	.8671	.3213	-.1037	.0097	.0075	-.0015
-4.73	25.22	.8759	.3268	-.1051	.0160	.0107	-.0046
-6.83	25.55	.8855	.3367	-.1053	.0221	.0135	-.0049
-10.75	25.98	.8886	.3510	-.1030	.0308	.0177	-.0020
-14.85	25.80	.8794	.3465	-.1005	.0376	.0210	.0049
1.35	24.83	.8633	.3118	-.1013	-.0032	-.0016	.0032

APPENDIX A

TABLE A2.- CONTINUED

TEST NUM 121. RUN NUM 25.

BETA DEG	ALPHA	CL	CD	CM	CRM	CYM	CY
1.44	30.12	1.1232	.5458	-.1372	-.0040	.0018	.0098
3.58	30.10	1.1154	.5402	-.1349	-.0111	-.0034	.0118
5.48	29.94	1.1076	.5327	-.1333	-.0176	-.0073	.0111
7.51	30.09	1.1053	.5361	-.1312	-.0233	-.0097	.0101
9.68	29.75	1.0761	.5156	-.1239	-.0277	-.0114	.0099
13.53	29.66	1.0498	.5059	-.1126	-.0331	-.0133	.0132
17.28	29.02	1.0016	.4756	-.1012	-.0348	-.0168	.0210
-.46	30.18	1.1036	.5333	-.1355	.0021	.0064	.0081
-2.49	30.09	1.0938	.5257	-.1331	.0083	.0107	.0072
-4.41	30.25	1.1016	.5346	-.1332	.0149	.0155	.0062
-6.45	30.68	1.1069	.5488	-.1335	.0211	.0196	.0079
-10.47	30.61	1.0663	.5278	-.1251	.0307	.0262	.0088
-14.38	30.69	1.0340	.5163	-.1177	.0374	.0309	.0130
1.52	30.15	1.1088	.5356	-.1350	-.0038	.0014	.0098

TEST NUM 121. RUN NUM 26.

BETA DEG	ALPHA	CL	CD	CM	CRM	CYM	CY
1.73	35.32	1.3042	.7954	-.1566	-.0049	.0047	.0122
3.62	35.29	1.2967	.7898	-.1543	-.0047	-.0017	.0072
5.68	35.31	1.2802	.7809	-.1498	-.0132	-.0072	.0073
7.74	34.88	1.2237	.7347	-.1380	-.0143	-.0083	-.0005
9.69	34.37	1.1906	.7023	-.1306	-.0172	-.0111	-.0058
13.99	34.24	1.1286	.6697	-.1204	-.0185	-.0166	-.0108
17.75	34.16	1.1033	.6594	-.1274	-.0249	-.0249	-.0082
-.21	35.47	1.3049	.7983	-.1566	.0018	.0110	.0139
-2.26	35.42	1.2923	.7886	-.1546	.0071	.0160	.0176
-4.21	35.44	1.2781	.7866	-.1541	.0134	.0212	.0194
-6.34	35.47	1.2647	.7731	-.1501	.0183	.0268	.0202
-10.29	35.49	1.2096	.7417	-.1401	.0258	.0359	.0268
-14.26	35.74	1.1215	.6989	-.1262	.0246	.0408	.0340
1.87	35.08	1.2944	.7803	-.1549	-.0047	.0041	.0111

TEST NUM 121. RUN NUM 27.

BETA DEG	ALPHA	CL	CD	CM	CRM	CYM	CY
-.02	-1.23	-.0576	.0190	.0077	.0052	.0035	-.0162
.05	2.43	.0706	.0189	-.0077	.0069	.0012	-.0004
.13	6.38	.2041	.0329	-.0245	.0095	-.0022	.0171
.22	11.00	.3677	.0694	-.0410	.0111	-.0072	.0469
.28	15.27	.5451	.1307	-.0606	.0084	-.0102	.0815
.34	19.40	.7365	.2259	-.0837	.0040	-.0087	.1088
.38	23.75	.9436	.3659	-.1084	-.0016	-.0042	.1338
.45	27.98	1.1378	.5436	-.1284	-.0030	-.0000	.1483
.51	32.26	1.2884	.7442	-.1394	-.0047	-.0031	.1676
.63	36.34	1.3474	.9233	-.1450	.0068	-.0111	.1824
.75	39.96	1.2233	.9716	-.1334	.0167	-.0222	.1806
-.02	-1.22	-.0540	.0139	.0089	.0051	.0026	-.0098

TEST NUM 121. RUN NUM 28.

BETA DEG	ALPHA	CL	CD	CM	CRM	CYM	CY
.03	5.03	.1595	.0232	-.0174	.0089	-.0019	.0148
1.82	5.22	.1674	.0231	-.0148	.0068	.0001	.0090
3.82	5.43	.1787	.0240	-.0202	.0046	.0042	.0024
6.00	5.44	.1796	.0233	-.0205	.0024	.0104	-.0151
8.15	5.53	.1778	.0226	-.0239	.0002	.0171	-.0332
12.20	5.31	.1619	.0183	-.0202	-.0017	.0267	-.0658
16.22	5.35	.1625	.0209	-.0272	-.0031	.0406	-.1028
-1.94	4.67	.1349	.0183	-.0145	.0098	-.0036	.0141
-3.88	5.25	.1678	.0242	-.0189	.0135	-.0083	.0298
-5.86	5.31	.1757	.0249	-.0202	.0161	-.0130	.0402
-8.22	5.28	.1747	.0237	-.0198	.0180	-.0196	.0576
-12.08	5.14	.1712	.0215	-.0197	.0202	-.0299	.0862
-16.19	5.20	.1818	.0210	-.0217	.0221	-.0398	.1191
-1.93	5.04	.1555	.0220	-.0172	.0108	-.0046	.0168
.18	5.36	.1652	.0231	-.0185	.0088	-.0022	.0143

APPENDIX A

TABLE A2.- CONTINUED

TEST NUM 121. RUN NUM 29.

BETA DEG	ALPHA	CL	CD	CM	CRM	CYM	CY
-.00	15.01	.5329	.1239	-.C590	.0097	-.0113	.0813
1.83	14.88	.5230	.1193	-.0576	.0053	-.C074	.0695
3.83	15.04	.5285	.1213	-.0592	.0003	-.0031	.0583
5.79	15.03	.5263	.1198	-.0590	-.C044	.0018	.0428
7.95	15.23	.5287	.1218	-.0595	-.C099	.0070	.0304
11.99	15.37	.5363	.1261	-.0617	-.0200	.0182	-.0016
16.10	15.50	.5306	.1270	-.0623	-.0286	.0281	-.0348
-2.18	15.22	.5277	.1207	-.0585	.0149	-.0144	.3897
-3.97	15.33	.5486	.1290	-.0607	.0195	-.0166	.0972
-6.07	15.35	.5561	.1313	-.0618	.0262	-.0194	.1040
-8.00	15.29	.5627	.1321	-.0623	.0303	-.0233	.1151
-12.21	15.31	.5729	.1378	-.C623	.0463	-.0337	.1399
-15.99	14.93	.5389	.1253	-.0569	.0451	-.C434	.1526
.07	14.83	.5036	.1102	-.0552	.0107	-.0109	.0754

TEST NUM 121. RUN NUM 30.

BETA DEG	ALPHA	CL	CD	CM	CRM	CYM	CY
-.05	24.97	1.0010	.4162	-.1157	.0009	-.0017	.1313
2.00	24.94	.9966	.4130	-.1154	-.0068	.0020	.1200
3.98	24.87	.9837	.4053	-.1145	-.0146	.0052	.1067
5.90	25.02	.9857	.4098	-.1152	-.0218	.0081	.0967
7.77	24.99	.9735	.4045	-.1141	-.0293	.0106	.0853
11.84	25.11	.9622	.4034	-.1129	-.0445	.0150	.0642
15.95	25.27	.9317	.3966	-.1074	-.0528	.0160	.0451
-1.93	25.45	1.0158	.4292	-.1145	.0092	-.0051	.1463
-3.92	25.22	.9978	.4172	-.1102	.0182	-.0060	.1493
-6.08	24.91	.9944	.4142	-.1071	.0287	-.0087	.1519
-8.18	24.69	.9792	.4052	-.1046	.0363	-.0115	.1533
-12.28	24.96	.9797	.4136	-.1056	.0475	-.0141	.1638
-16.13	24.91	.9471	.4010	-.0984	.0492	-.0131	.1634
-.09	25.04	.9867	.4048	-.1136	.0002	-.0030	.1347

TEST NUM 121. RUN NUM 31.

BETA DEG	ALPHA	CL	CD	CM	CRM	CYM	CY
-.10	30.37	1.2289	.6553	-.1352	-.0017	-.0004	.1560
1.77	30.37	1.2293	.6552	-.1375	-.0074	-.0000	.1453
3.80	30.29	1.2130	.6443	-.1363	-.0161	.0015	.1343
5.73	30.10	1.1874	.6265	-.1339	-.0229	.0012	.1244
7.75	30.44	1.1732	.6303	-.1304	-.0286	-.0008	.1227
11.82	30.22	.9582	.5275	-.0944	-.0080	-.0328	.1187
15.42	30.34	.9297	.5134	-.1014	-.0243	-.0399	.1217
-2.12	30.44	1.2277	.6540	-.1341	.0085	.0003	.1619
-3.96	30.26	1.2178	.6440	-.1353	.0157	-.0004	.1640
-6.11	30.09	1.2165	.6421	-.1358	.0252	.0001	.1653
-8.17	29.89	1.1900	.6246	-.1344	.0338	.0006	.1638
-12.12	29.85	1.1150	.5874	-.1189	.0364	.0056	.1614
-16.24	29.83	1.0360	.5464	-.1017	.0339	.0213	.1453
-.06	30.56	1.2251	.6545	-.1351	-.0017	-.0003	.1543

TEST NUM 121. RUN NUM 32.

BETA DEG	ALPHA	CL	CD	CM	CRM	CYM	CY
-.22	35.36	1.3557	.8893	-.1483	.0044	-.0047	.1721
1.70	35.28	1.3246	.8885	-.1423	.0017	-.0106	.1666
3.79	35.05	1.2865	.8364	-.1351	-.0058	-.0150	.1595
6.11	35.16	1.1183	.7507	-.1155	.0111	-.0404	.1434
7.78	35.38	1.0806	.7308	-.1127	.0040	-.0455	.1430
11.89	35.13	1.0346	.6914	-.1090	-.0091	-.0502	.1302
15.72	35.39	1.0014	.6749	-.1095	-.0223	-.0527	.1246
-2.03	35.51	1.3827	.9106	-.1535	.0064	.0031	.1771
-4.25	35.29	1.3638	.8879	-.1543	.0107	.0098	.1744
-6.01	35.16	1.3156	.8520	-.1492	.0091	.0145	.1809
-7.99	35.22	1.2911	.8388	-.1456	.0143	.0187	.1817
-12.03	35.18	1.2278	.7985	-.1360	.0197	.0322	.1702
-16.06	34.77	1.0910	.7007	-.1272	.0185	.0419	.1487
-.06	35.07	1.3511	.8744	-.1472	.0033	-.0040	.1710

APPENDIX A

TABLE A2.- CONTINUED

TEST NUM 121.　　　　　　　　　　RUN NUM 33.

BETA DEG	ALPHA	CL	CD	CM	CRM	CYM	CY
-.02	-1.13	-.0866	.0246	.0106	.0065	-.0007	-.0007
.06	2.44	.0360	.0181	-.0037	.0017	-.0004	.0019
.15	6.59	.1595	.0242	-.0200	.002C	-.0008	.0052
.26	10.68	.2837	.0429	-.0331	.0035	-.0011	.0063
.31	14.99	.4351	.0822	-.0522	.0055	-.0030	.0140
.32	19.39	.6206	.1612	-.0751	.0028	-.0064	.0275
.16	23.70	.8171	.2813	-.1007	-.0002	-.0038	.0433
.17	27.92	1.0223	.4490	-.1266	-.0010	.0011	.0502
.2C	32.07	1.1965	.6398	-.1482	.0003	.0008	.0508
.20	36.40	1.3363	.8573	-.1638	.0029	.0002	.0589
.16	40.28	1.3416	1.0079	-.1568	.0203	-.0018	.0619
-.03	-1.14	-.0904	.0216	.0121	.0006	-.0014	.0065

TEST NUM 121.　　　　　　　　　　RUN NUM 34.

BETA DEG	ALPHA	CL	CD	CM	CRM	CYM	CY
-.06	4.81	.1079	.0177	-.0123	.0014	-.0017	.0096
1.94	4.90	.1127	.0127	-.0127	.0004	.0014	.0006
3.87	4.99	.1196	.0169	-.0139	-.0005	.0054	-.0081
6.15	5.20	.1268	.0167	-.0150	-.0019	.0122	-.0281
8.02	5.23	.1275	.0159	-.0159	-.0027	.0179	-.0424
11.97	5.41	.1387	.0171	-.0179	-.0037	.0296	-.0738
16.04	5.00	.1344	.0172	-.0191	-.0022	.0411	-.1095
-1.95	5.21	.1198	.0188	-.0140	.0031	-.0041	.0126
-3.86	5.09	.1187	.0196	-.0145	.0044	-.0083	.0225
-5.87	5.18	.1227	.0205	-.0150	.0055	-.0142	.0367
-7.93	5.32	.1249	.0204	-.0156	.0063	-.0203	.0524
-12.17	5.32	.1223	.0193	-.0162	.0063	-.0334	.0916
-15.87	5.06	.1176	.0194	-.0172	.0047	-.0429	.1243
-.07	5.35	.1122	.0142	-.0125	.0015	-.0023	.0097

TEST NUM 121.　　　　　　　　　　RUN NUM 35.

BETA DEG	ALPHA	CL	CD	CM	CRM	CYM	CY
-.12	15.12	.4418	.0816	-.0527	.0058	-.0038	.0183
1.84	15.00	.4342	.0795	-.0510	.0037	-.0013	.0070
3.88	15.44	.4609	.087C	-.0540	.0006	.0010	-.0023
5.99	15.04	.4498	.0828	-.0539	-.0027	.0057	-.0160
7.90	15.05	.4599	.0861	-.0548	-.0069	.0094	-.0247
12.02	15.32	.4889	.0981	-.0597	-.0153	.0203	-.0510
16.09	15.39	.5080	.1053	-.0630	-.0227	.0324	-.0822
-2.02	15.22	.4274	.0759	-.0513	.0082	-.0059	.0249
-3.86	14.88	.4262	.0760	-.0512	.0110	-.0087	.0311
-6.02	15.04	.4328	.0793	-.0519	.0135	-.0141	.0459
-8.15	15.10	.4394	.0819	-.0530	.0170	-.0188	.0592
-12.11	15.23	.4523	.0874	-.0548	.0227	-.0280	.0815
-16.14	15.38	.4665	.0951	-.0580	.0290	-.0370	.1059
-.12	15.09	.4214	.0726	-.0492	.0056	-.0041	.0172

TEST NUM 121.　　　　　　　　　　RUN NUM 36.

BETA DEG	ALPHA	CL	CD	CM	CRM	CYM	CY
-.12	25.38	.8918	.3376	-.1095	.0002	-.0026	.0474
1.76	25.37	.8953	.3393	-.1095	-.0056	-.0016	.0391
3.85	25.38	.8985	.3410	-.1099	-.0118	-.0007	.0290
5.75	25.08	.8850	.3305	-.1082	-.0169	.0023	.0173
7.94	25.31	.9026	.3435	-.1101	-.0236	.0066	.0056
11.83	25.36	.9148	.3521	-.1110	-.0342	.0169	-.0229
15.97	25.48	.9291	.3664	-.1117	-.0426	.0227	-.0383
-2.23	25.25	.8811	.3294	-.1062	.0084	-.0018	.0498
-4.17	25.15	.8740	.3261	-.1054	.0157	-.0008	.0520
-5.99	24.93	.8630	.3183	-.1055	.0223	-.0043	.0551
-8.06	25.25	.8749	.3301	-.1076	.0296	-.0097	.0654
-11.99	25.25	.8754	.3329	-.1082	.0410	-.0209	.0873
-16.16	25.17	.8797	.3366	-.1094	.0490	-.0320	.1199
-.08	25.11	.8694	.3191	-.1065	-.0000	-.0033	.0461

APPENDIX A

TABLE A2.- CONTINUED

| TEST NUM 121. | | | | RUN NUM 37. | | | |

BETA DEG	ALPHA	CL	CD	CM	CRM	CYM	CY
-.07	30.11	1.1011	.5324	-.1367	.0005	.3016	.0485
1.86	30.03	1.0942	.5253	-.1354	-.0064	-.0009	.0450
3.75	29.83	1.0621	.5141	-.1334	-.0124	-.0008	.0397
6.01	30.14	1.1069	.5371	-.1358	-.0202	.0000	.0255
7.80	30.04	1.1007	.5332	-.1338	-.0262	.0024	.0183
11.76	30.20	1.0900	.5365	-.1273	-.0343	.0043	.0057
15.87	30.34	.9968	.5060	-.0979	-.0192	-.0211	.0324
-2.18	30.19	1.1043	.5360	-.1378	.0079	.0026	.0538
-4.09	29.97	1.0904	.5226	-.1359	.0144	.0036	.0557
-6.01	29.94	1.0972	.5282	-.1363	.0233	.0026	.0607
-7.97	30.11	1.0919	.5300	-.1359	.0310	.0019	.0644
-12.23	30.17	1.0621	.5184	-.1307	.0423	-.0007	.0824
-16.13	30.45	1.0148	.5055	-.1162	.0422	.0086	.0748
-.01	30.26	1.1102	.5391	-.1375	.0001	.0008	.0498

| TEST NUM 121. | | | | RUN NUM 38. | | | |

BETA DEG	ALPHA	CL	CD	CM	CRM	CYM	CY
-.03	35.42	1.3100	.8058	-.1611	.0022	.0016	.0496
1.84	35.39	1.3030	.7997	-.1584	-.0027	-.0010	.0426
3.78	35.34	1.2833	.7873	-.1538	-.0068	-.0056	.0377
5.94	35.35	1.2432	.7660	-.1423	-.0068	-.0091	.0295
7.89	35.26	1.2033	.7421	-.1324	-.0071	-.0193	.0321
12.01	35.33	1.1067	.6933	-.1162	-.0025	-.0349	.0351
15.77	35.23	1.0785	.6760	-.1159	-.0115	-.0416	.0340
-2.26	35.49	1.2924	.7922	-.1606	.0099	.0061	.0554
-3.93	35.33	1.2795	.7791	-.1586	.0156	.0097	.0573
-6.00	35.06	1.2605	.7594	-.1564	.0220	.0123	.0622
-7.91	34.94	1.2466	.7503	-.1531	.0271	.0161	.0645
-12.14	34.94	1.1588	.7013	-.1324	.0276	.0304	.0630
-16.27	34.90	1.0160	.6245	-.1216	.0175	.0491	.0501
-.17	35.38	1.2936	.7899	-.1596	.0022	.0018	.0500

| TEST NUM 121. | | | | RUN NUM 39. | | | |

BETA DEG	ALPHA	CL	CD	CM	CRM	CYM	CY
-.03	-1.12	-.0757	.0210	.0098	.0005	-.0011	.0027
-.04	2.48	.0554	.0171	-.0059	.0005	-.0007	.0022
-.08	6.58	.1756	.0259	-.0211	.0006	-.0009	.0026
-.06	10.71	.3207	.0496	-.0378	.0008	-.0009	.0015
-.09	14.85	.4925	.1023	-.0584	.0005	-.0011	.0032
-.14	19.21	.6916	.2000	-.0775	.0012	-.0012	.0018
-.18	23.84	.9083	.3451	-.1013	.0010	.0008	.0051
-.21	28.18	1.1102	.5233	-.1238	.0016	.0037	.0042
-.24	32.29	1.2704	.7144	-.1432	.0012	.0053	.0056
-.29	36.61	1.4050	.9411	-.1608	.0005	.0083	.0172
.14	40.29	1.3769	1.0673	-.1619	.0188	.0050	.0214
-.03	-1.08	-.0692	.0184	.0108	.0004	-.0013	.0068
.02	-6.10	-.2570	.0523	.0306	.0008	-.0013	.0083
.02	-5.75	-.2300	.0499	.0277	.0007	-.0012	.0082
.00	-3.72	-.1532	.0342	.0192	.0005	-.0010	.0069
-.01	-1.63	-.0774	.0240	.0109	.0004	-.0012	.0069
-.03	.62	-.0008	.0176	.0021	.0003	-.0010	.0065
-.04	2.50	.0572	.0159	-.0054	.0004	-.0012	.0070
-.06	4.49	.1123	.0183	-.0122	.0006	-.0010	.0052
-.03	-1.10	-.0697	.0192	.0103	.0004	-.0016	.0080

| TEST NUM 121. | | | | RUN NUM 40. | | | |

BETA DEG	ALPHA	CL	CD	CM	CRM	CYM	CY
-.05	4.95	.1244	.0198	-.0150	.0005	-.0008	.0005
1.90	4.99	.1247	.0177	-.0151	-.0007	.0015	-.0058
3.94	5.21	.1375	.0178	-.0166	-.0022	.0052	-.0127
5.86	5.29	.1423	.0164	-.0176	-.0038	.0098	-.0259
7.95	5.45	.1534	.0164	-.0190	-.0058	.0158	-.0401
12.01	5.15	.1534	.0149	-.0198	-.0080	.0273	-.0685
16.06	5.20	.1618	.0150	-.0220	-.0088	.0377	-.1001
-1.89	4.80	.1117	.0161	-.0129	.0017	-.0034	.0051
-3.92	4.95	.1296	.0200	-.0158	.0031	-.0082	.0194
-5.89	5.03	.1345	.0211	-.0166	.0046	-.0134	.0299
-8.18	5.18	.1421	.0213	-.0184	.0062	-.0204	.0487
-12.04	5.03	.1359	.0206	-.0184	.0067	-.0314	.0804
-16.06	5.02	.1349	.0208	-.0196	.0064	-.0419	.1139
-.08	5.37	.1289	.0153	-.0146	.0003	-.0018	.0036

APPENDIX A

TABLE A2.- CONTINUED

TEST NUM 121. RUN NUM 41.

BETA DEG	ALPHA	CL	CD	CM	CRM	CYM	CY
-.03	15.18	.5085	.1066	-.0603	.0006	-.0013	.0008
1.87	15.08	.5033	.1037	-.0600	-.0033	.0008	-.0072
3.90	15.11	.5095	.1047	-.0613	-.0077	.0032	-.0122
6.07	15.45	.5285	.1120	-.0633	-.0130	.0070	-.0226
8.00	15.19	.5056	.1026	-.0606	-.0166	.0116	-.0313
11.84	15.04	.5072	.1019	-.0608	-.0243	.0219	-.0539
15.90	15.10	.5344	.1105	-.0654	-.0324	.0326	-.0790
-2.08	14.88	.4785	.0957	-.0580	.0047	-.0032	.0069
-4.07	15.06	.4999	.1045	-.0608	.0094	-.0060	.0117
-5.92	14.89	.4940	.1031	-.0606	.0139	-.0101	.0189
-8.19	14.91	.4948	.1047	-.0609	.0187	-.0155	.0335
-11.90	14.90	.4934	.1056	-.0598	.0254	-.0250	.0548
-16.13	15.02	.4978	.1088	-.0609	.0317	-.0352	.3829
-.10	14.97	.4794	.0942	-.0571	.0011	-.0016	.0019

TEST NUM 121. RUN NUM 42.

BETA DEG	ALPHA	CL	CD	CM	CRM	CYM	CY
-.16	25.38	.9769	.4000	-.1090	.0022	.0007	.0009
1.86	25.32	.9747	.3976	-.1077	-.0053	.0026	-.0061
3.82	25.08	.9685	.3896	-.1076	-.0139	.0032	-.0076
5.94	24.77	.9583	.3781	-.1072	-.0216	.0063	-.0157
8.49	25.07	.9728	.3897	-.1094	-.0305	.0104	-.0275
12.09	25.36	.9912	.4052	-.1133	-.0398	.0189	-.0443
15.75	25.42	.9836	.4075	-.1106	-.0485	.0208	-.0522
-2.23	25.22	.9493	.3621	-.1055	.0107	-.0009	.0054
-3.98	25.01	.9399	.3746	-.1041	.0168	-.0025	.0114
-5.94	25.21	.9600	.3884	-.1074	.0247	-.0056	.0174
-8.14	25.16	.9561	.3859	-.1092	.0310	-.0118	.0293
-12.07	25.18	.9529	.3880	-.1117	.0413	-.0207	.0531
-16.06	25.15	.9399	.3820	-.1084	.0498	-.0236	.0698
-.15	25.20	.9695	.3921	-.1080	.0020	.0007	.0014

TEST NUM 121. RUN NUM 43.

BETA DEG	ALPHA	CL	CD	CM	CRM	CYM	CY
-.17	29.94	1.1827	.6017	-.1323	.0013	.0033	.0026
1.80	30.04	1.1887	.6060	-.1326	-.0066	.0028	-.0028
3.96	29.89	1.1825	.5994	-.1317	-.0153	.0019	-.0057
5.75	30.13	1.1896	.6097	-.1320	-.0219	.0002	-.0071
8.08	30.42	1.1925	.6190	-.1312	-.0274	-.0002	-.0144
11.86	30.17	1.1332	.5861	-.1150	-.0299	-.0021	-.0135
15.92	29.99	.9967	.5209	-.0955	-.0143	-.0234	-.0072
-2.10	30.40	1.1799	.6079	-.1317	.0112	.0037	.0046
-4.13	30.21	1.1720	.5989	-.1308	.0187	.0043	.0093
-6.04	29.86	1.1497	.5784	-.1279	.0265	.0043	.0143
-8.08	30.06	1.1500	.5854	-.1284	.0314	.0060	.0198
-12.25	29.98	1.1128	.5671	-.1214	.0355	.0069	.0378
-15.99	29.87	1.0094	.5172	-.0988	.0270	.0261	.3141
-.15	30.26	1.1833	.6062	-.1322	.0008	.0026	.0039

TEST NUM 121. RUN NUM 44.

BETA DEG	ALPHA	CL	CD	CM	CRM	CYM	CY
-.16	35.22	1.3692	.8654	-.1554	.0001	.0071	.0068
1.73	35.29	1.3653	.8656	-.1540	-.0052	.0024	.0022
3.87	35.12	1.3449	.8493	-.1539	-.0095	-.0025	.0036
5.89	35.28	1.2876	.8224	-.1363	-.0061	-.0074	.0014
7.90	35.15	1.2083	.7727	-.1213	-.0001	-.0163	.0038
11.80	35.22	1.1035	.7144	-.1134	.0007	-.0327	.0085
15.84	34.97	1.0577	.6808	-.1083	-.0126	-.0373	.0042
-2.16	35.48	1.3517	.8596	-.1551	.0074	.0146	.0079
-3.98	35.32	1.3277	.8395	-.1511	.0126	.0196	.0098
-6.04	35.02	1.2937	.8094	-.1430	.0149	.0238	.0159
-8.39	35.02	1.2751	.8009	-.1377	.0207	.0274	.0133
-12.13	35.19	1.1198	.7187	-.1272	-.0005	.0572	.0106
-16.25	34.87	1.0487	.6667	-.1268	.0114	.0568	.0262
-.12	35.34	1.3594	.8598	-.1546	.0001	.0072	.0060

APPENDIX A

TABLE A2.- CONTINUED

TEST NUM 121. RUN NUM 46.

BETA DEG	ALPHA	CL	CD	CM	CRM	CYM	CY
-.03	-1.17	-.0631	.0212	.0059	.0092	.0044	-.0056
.48	2.54	.0621	.0173	-.0098	.0084	.0050	-.0087
.56	6.51	.1814	.0264	-.0247	.0089	.0062	-.0129
.11	10.69	.3267	.0521	-.0415	.0102	.0059	-.0110
.16	14.85	.4992	.1059	-.0623	.0115	.0072	-.0127
.21	19.05	.6868	.1984	-.0797	.0122	.0079	-.0160
.25	23.47	.9003	.3382	-.1042	.0127	.0100	-.0152
.28	27.73	1.0938	.5087	-.1243	.0113	.0104	-.0146
.33	32.00	1.2690	.7111	-.1445	.0106	.0119	-.0140
.36	36.14	1.3818	.9125	-.1585	.0107	.0124	-.0058
.43	39.80	1.3766	1.0517	-.1636	.0263	.0100	.0021
-.03	-1.18	-.0695	.0193	.0064	.0092	.0045	-.0068

TEST NUM 121. RUN NUM 47.

BETA DEG	ALPHA	CL	CD	CM	CRM	CYM	CY
-.03	-1.18	-.0800	.0289	.0122	.0159	.0086	-.0149
.06	2.37	.0414	.0232	-.0018	.0149	.0080	-.0135
.16	6.42	.1640	.0309	-.0173	.0152	.0092	-.0153
.27	10.62	.3030	.0540	-.0326	.0162	.0101	-.0193
.38	14.81	.4757	.1067	-.0526	.0181	.0115	-.0216
.49	18.86	.6554	.1945	-.0713	.0180	.0126	-.0256
.59	23.46	.8876	.3417	-.1020	.0183	.0147	-.0271
.68	27.63	1.0736	.5061	-.1221	.0169	.0148	-.0266
.78	32.00	1.2479	.7088	-.1405	.0162	.0160	-.0287
.87	36.09	1.3522	.9043	-.1544	.0193	.0174	-.0203
.98	39.78	1.3324	1.0297	-.1571	.0317	.0112	-.0057
-.03	-1.17	-.0792	.0270	.0131	.0156	.0082	-.0125

TEST NUM 121. RUN NUM 48.

BETA DEG	ALPHA	CL	CD	CM	CRM	CYM	CY
-.03	-1.11	.0154	.0151	-.0008	.0005	-.0012	.0032
-.04	2.60	.1603	.0341	-.0167	.0007	-.0008	.0033
-.06	6.76	.3239	.0728	-.0341	.0014	-.0006	.0010
-.09	10.88	.5019	.1369	-.0525	.0017	-.0009	.0030
-.11	15.01	.6903	.2311	-.0712	.0021	-.0004	-.0001
-.13	19.42	.8951	.3673	-.0902	.0036	-.0014	.0025
-.15	23.66	1.0766	.5286	-.1086	.0051	-.0009	.0034
-.18	28.26	1.2637	.7422	-.1268	.0056	.0012	.0057
-.21	32.23	1.2918	.8759	-.1242	.0039	.0041	.0126
-.25	36.38	1.2818	1.0035	-.1372	.0046	.0104	.0270
-.30	39.61	1.1750	1.0275	-.1419	.0049	.0110	.0421
-.02	-1.07	.0172	.0116	-.0001	.0006	-.0013	.0033

TEST NUM 121. RUN NUM 49.

BETA DEG	ALPHA	CL	CD	CM	CRM	CYM	CY
-.04	4.92	.2499	.0506	-.0256	.0010	-.0009	.0013
1.81	5.02	.2549	.0505	-.0261	-.0039	.0013	-.0093
3.91	5.09	.2616	.0509	-.0271	-.0086	.0046	-.0194
5.89	5.17	.2696	.0513	-.0284	-.0141	.0091	-.0343
7.93	5.32	.2769	.0520	-.0296	-.0197	.0142	-.0495
11.85	5.54	.2884	.0526	-.0316	-.0306	.0255	-.0831
15.94	5.29	.2791	.0479	-.0317	-.0396	.0357	-.1158
-1.98	4.88	.2375	.0468	-.0244	.0054	-.0024	.0070
-3.77	5.07	.2593	.0532	-.0271	.0102	-.0063	.0186
-6.00	5.13	.2648	.0544	-.0282	.0159	-.0120	.0355
-8.07	5.23	.2716	.0550	-.0294	.0215	-.0178	.0540
-12.04	5.17	.2630	.0525	-.0294	.0303	-.0283	.0868
-15.94	4.95	.2502	.0486	-.0288	.0374	-.0380	.1201
-.05	5.15	.2463	.0472	-.0251	.0009	-.0010	.0006

APPENDIX A

TABLE A2.- CONCLUDED.

TEST NUM	121.				RUN NUM	50.		
BETA DEG	ALPHA	CL	CD	CM	CRM	CYM	CY
-.12	15.27	.7026	.2372	-.0720	.0023	-.0008	.0005
1.85	15.19	.7021	.2346	-.0722	-.0070	.0024	-.0131
3.83	15.36	.7067	.2373	-.0725	-.0169	.0056	-.0272
5.95	15.48	.7155	.2409	-.0734	-.0274	.0098	-.0416
7.80	15.43	.7124	.2384	-.0735	-.0363	.0137	-.0554
11.96	15.50	.7132	.2379	-.0746	-.0572	.0243	-.0909
15.87	15.31	.6371	.2106	-.0589	-.0608	.0313	-.1190
-2.06	14.75	.6574	.2132	-.0676	.0120	-.0037	.0125
-3.90	15.07	.6822	.2278	-.0701	.0215	-.0075	.0231
-5.86	15.01	.6775	.2253	-.0703	.0310	-.0116	.0391
-7.95	14.97	.6735	.2231	-.0707	.0407	-.0171	.0576
-12.11	15.10	.6650	.2213	-.0707	.0607	-.0287	.0950
-16.17	15.17	.5894	.1972	-.0545	.0630	-.0358	.1224
-.07	15.22	.6841	.2254	-.0701	.0026	-.0014	.0031

TEST NUM	121.				RUN NUM	51.		
BETA DEG	ALPHA	CL	CD	CM	CRM	CYM	CY
-.09	25.22	1.1343	.5891	-.1145	.0052	-.0006	.0023
1.81	25.18	1.1380	.5890	-.1144	-.0090	.0024	-.0106
3.77	24.93	1.1249	.5758	-.1131	-.0230	.0051	-.0248
5.84	25.02	1.0826	.5576	-.1032	-.0308	.0073	-.0359
8.04	25.30	1.0450	.5450	-.0984	-.0387	.0087	-.0462
11.74	25.33	.9429	.4950	-.0860	-.0453	.0055	-.0493
15.90	25.36	.7315	.3871	-.0941	-.0284	-.0166	-.0375
-2.07	25.34	1.1257	.5862	-.1135	.0214	-.0038	.0197
-4.12	25.04	1.0789	.5564	-.1043	.0311	-.0069	.0310
-5.92	24.88	1.0512	.5405	-.1010	.0392	-.0083	.0395
-8.04	24.89	1.0054	.5171	-.0960	.0469	-.0103	.0494
-12.02	25.27	.7659	.4044	-.0670	.0239	.0172	.0130
-16.19	24.98	.7198	.3755	-.0783	.0398	.0142	.0332
-.08	25.46	1.1384	.5948	-.1146	.0042	-.0005	.0035

TEST NUM	121.				RUN NUM	52.		
BETA DEG	ALPHA	CL	CD	CM	CRM	CYM	CY
-.11	30.35	1.2689	.8025	-.1194	.0040	.0025	.0046
1.94	30.28	1.2619	.7950	-.1243	-.0031	.0028	-.0044
3.89	30.18	1.2178	.7650	-.1208	-.0126	.0030	-.0119
5.89	30.25	1.1375	.7183	-.1137	-.0173	.0022	-.0138
7.95	29.85	.9781	.6119	-.1215	-.0056	-.0204	-.0066
11.89	29.95	.9055	.5675	-.1349	-.0160	-.0281	-.0115
15.87	29.87	.8449	.5279	-.1335	-.0286	-.0225	-.0468
-2.04	30.10	1.2251	.7656	-.1188	.0122	.0024	.0123
-4.06	29.84	1.1689	.7251	-.1139	.0212	.0016	.0216
-6.26	30.43	1.0811	.6891	-.1062	.0210	.0089	.0153
-8.07	30.05	.9167	.5797	-.0908	.0131	.0214	.0039
-12.18	30.09	.8736	.5534	-.0931	.0289	.0295	.0209
-16.06	30.10	.8070	.5113	-.0949	.0401	.0303	.0471
-.11	30.32	1.2571	.7929	-.1188	.0038	.0026	.0036

TEST NUM	121.				RUN NUM	53.		
BETA DEG	ALPHA	CL	CD	CM	CRM	CYM	CY
-.09	35.40	1.2852	.9701	-.1329	.0041	.0096	.0196
1.83	35.25	1.2458	.9363	-.1375	.0031	.0040	.0252
3.87	34.97	1.1817	.8801	-.1380	.0008	-.0042	.0257
5.99	35.26	1.1176	.8444	-.1374	-.0046	-.0172	.0247
8.04	34.84	1.0726	.7999	-.1458	-.0095	-.0278	.0152
12.10	35.03	1.0071	.7545	-.1552	-.0237	-.0431	.0098
15.85	35.13	.9273	.6980	-.1471	-.0349	-.0370	-.0340
-1.91	35.18	1.2106	.9075	-.1216	.0034	.0126	.0189
-4.11	34.92	1.1586	.8624	-.1175	.0094	.0181	.0214
-5.99	35.04	1.0911	.8190	-.1156	.0163	.0291	.0200
-7.99	35.03	1.0163	.7633	-.1144	.0126	.0396	.0211
-12.02	35.10	.9505	.7146	-.1267	.0219	.0569	.0371
-16.15	35.20	.8626	.6508	-.1276	.0383	.0471	.0719
-.12	35.18	1.2866	.9635	-.1317	.0041	.0096	.0164

APPENDIX B

VLM-SA Input - 0 Degree LEVF Deflection

```
T119    74 DEG GOTHIC VF DESIGN  -   DEL(LE/TE)=0/0 DEGS
1.          1.         25.639     548.736    -28.358
10.
0.000       0.
-3.075      -0.75
-6.150      -1.5
-14.360     -1.500
-17.50      -3.200
-20.15      -4.420
-24.00      -5.900
-34.00      -9.400
-42.50      -12.16
-47.587     -13.657
-47.587     0.0
T119 DELF= 0/0 M=.2 20.  10.  .2   101.                      3.          1.
-1.5        -13.657
0.          0.
0.0         2.        21.
1.
-14.360     -1.5       -47.587    -11.0280  -47.587  -13.657  -17.50    -3.200
1.          1.        0.00001
/EOF
```

APPENDIX B

VLM-SA Input - 40 Degree LEVF Deflection

```
T119    74 DEG GOTHIC VF DESIGN  -   DEL(LE/TE)=40/0 DEGS
1.      1.        25.639    548.736   -28.358
10.
0.000    0.
-3.075   -0.75
-6.150   -1.5
-14.360  -1.500
-17.50   -2.980
-20.15   -4.070
-24.00   -5.480
-34.00   -8.870
-42.50   -11.55
-47.587  -13.120
-47.587  0.0
T119 DELF=40/0 M=.2 20.  10.  .2   101.                        3.           1.
-1.5     -13.120
0.       0.
0.0      2.       21.
1.
-14.360  -1.5      -47.587  -11.0280 -47.587  -13.120  -17.50  -2.980
1.       1.       40.0
/EOF
```

APPENDIX B

VORSTAB Input - 0 Degree LEVF, Tail Off, Vortex Burst On

```
A74 DEGREE DELTA WING WITH FUSELAGE AND 0 LEVF NO TAIL WITH VORTEX BURST
           1          0          0          1
           1          0          0          1
           1         15          0          1          0          0
           1          1          0          0
0.000
           8          0          3          1
1.5        13.68
14.360     1.5        0.0        14.36      1.5        0.0
47.587     13.68      0.0        47.587     11.028     0.0
           1
14.36      47.587     1.5        47.587     47.587     13.680     0.0        0.0
           7          2          1          0
0.0        3.64       8.64       14.64      20.64      27.64      33.227
0.0        1.95       4.00       6.18       8.21       10.48      12.18
0.0        0.0
0.0        12.18
0.2        274.3682   25.639     28.358     0.0
10.0       0.0        0.0        0.0
40.0       37.0       35.0       32.0       30.0       25.0       20.0       15.0
10.0       5.0
0.0
0.0
0.0
0.0
           1          3          6          6          1          6
0.0        47.587     1.0        7.0        1.0
0.0        2.0        3.5        5.5        7.0        9.0        47.587
0.0        0.61       0.78       1.25       1.43       1.5        1.5
```

APPENDIX B

VORSTAB Input - 40 Degree LEVF, Tail Off, Vortex Burst On

```
A74 DEGREE DELTA WING WITH FUSELAGE, 40 LEVF, BURST ON
                1         0         0         1
                1         0         0         1
                1         15        0         1         0         0
                1         1         0         0
0.000
                8         0         3         1
1.5             13.12
14.360          1.5       0.0       14.36     1.5       0.0
47.587          13.12     -1.6388   47.587    11.028    0.0
                1
14.36           47.587    1.5       47.587    47.587    13.120     0.0       0.0
                7         2         1         0
0.0             3.64      8.64      14.64     20.64     27.64      33.227
0.0             1.70      3.13      5.70      7.69      9.910      11.62
0.0             0.0
0.0             11.62
0.4             274.3682  25.639    28.358    0.0
10.0            0.0       0.0       0.0
50.0            45.0      40.0      35.0      30.0      25.0       20.0      15.0
10.0            5.0
0.0
0.0
0.0
0.0
                1         3         6         6         1          6
0.0             47.587    1.0       7.0       1.0
0.0             2.0       3.5       5.5       7.0       9.0        47.587
0.0             0.61      0.78      1.25      1.43      1.5        1.5
```

APPENDIX B

VORSTAB Input - 0 Degree LEVF, Tail On, Vortex Burst On

```
A74 DEGREE DELTA WING WITH FUSELAGE, 0 LEVF, VERTICAL TAIL, AND VORTEX BURST
           1          0          0          2
           1          0          0          1
           1         15          0          1          0          0
           1          1          0          0
0.000
           8          0          3          1
1.5       13.68
14.360     1.5        0.0       14.36      1.5        0.0
47.587    13.68       0.0       47.587    11.028      0.0
           1
14.36     47.587      1.5       47.587    47.587     13.680      0.0        0.0
           7          2          1          0
0.0        3.64       8.64      14.64      20.64      27.64      33.227
0.0        1.95       4.00       6.18       8.21      10.48      12.18
0.0        0.0
0.0       12.18
           1          4          0          1
           1          1          0          0          0          1
0.0
           5          0          0
           0
37.587    47.587      1.5       47.979     52.979     7.5        1.5       90.0
0.2      274.3682    25.639     28.358      0.0
10.0       0.0        0.0        0.0
40.0      37.0       35.0       32.0       30.0       25.0       20.0       15.0
10.0       5.0
0.0
0.0
0.0
0.0
0.0        0.0000                           0.0
           1          3          6          6          1          6
0.0       47.587      1.0        7.0        1.0
0.0        2.0        3.5        5.5        7.0        9.0       47.587
0.0        0.61       0.78       1.25       1.43       1.5        1.5
```

APPENDIX B

VORSTAB Input - 40 Degree LEVF, Tail On, Vortex Burst On

A74 DEGREE DELTA WING WITH FUSELAGE, 40 LEVF, VERTICAL TAIL, AND VORTEX BURST

```
          1         0         0         2
          1         0         0         1
          1        15         0         1         0         0
          1         1         0         0
0.000
          8         0         3         1
1.5      13.12
14.360    1.5       0.0      14.36      1.5       0.0
47.587   13.12     -1.6388  47.587    11.028     0.0
          1
14.36    47.587     1.5     47.587    47.587    13.120     0.0       0.0
          7         2         1         0
0.0       3.64      8.64     14.64     20.64     27.64     33.227
0.0       1.70      3.13      5.70      7.69      9.910     11.62
0.0       0.0
0.0      11.62
          1         4         0         1
          1         1         0         0         0         1
0.0
          5         0         0
          0
37.587   47.587     1.5     -47.979    52.979     7.5       1.5      90.0
0.2     274.3682   25.639    28.358     0.0
10.0      0.0       0.0       0.0
40.0     37.0      35.0      32.0      30.0      25.0      20.0      15.0
10.0      5.0
0.0
0.0
0.0
0.0
0.0
          1         3         6         6         1         6
0.0      47.587     1.0       7.0       1.0
0.0       2.0       3.5       5.5       7.0       9.0      47.587
0.0       0.61      0.78      1.25      1.43      1.5       1.5
```

APPENDIX B

VORSTAB Input - 40 Degree LEVF, Tail On, Vortex Burst Off

```
A 74 DEGREE DELTA WING WITH FUSELAGE, 40 LEVF, VERTICAL TAIL, NO VORTEX BURST
                1       0       0       2
                1       0       0       0
                1      15       0       1       0       0
                1       1       0       0
0.000
                8       0       3       1
1.5            13.12
14.360          1.5     0.0    14.36    1.5     0.0
47.587         13.12   -1.6388  47.587  11.028   0.0
                1
14.36          47.587   1.5    47.587   47.587  13.120   0.0     0.0
                7       2       1       0
0.0             3.64    8.64   14.64    20.64   27.64   33.227
0.0             1.70    3.13    5.70     7.69    9.910   11.62
0.0             0.0
0.0            11.62
                1       4       0       1
                1       1       0       0       0       1
0.0
                5       0       0
                0
37.587         47.587   1.5    47.979   52.979   7.5     1.5     90.0
0.2           274.3682  25.639  28.358   0.0
10.0            0.0     0.0     0.0
40.0           37.0    35.0    32.0     30.0    25.0    20.0    15.0
10.0            5.0
0.0
0.0
0.0
0.0
0.0
                1       3       6       6       1       6
0.0            47.587   1.0     7.0     1.0
0.0             2.0     3.5     5.5     7.0     9.0    47.587
0.0             0.61    0.78    1.25    1.43    1.5     1.5
```

Primary
Vortex

Flow
Reattachment

Leading Edge
Separation

Secondary
Vortex

Figure 1.- LEVF design philosophy.

Constant Chord	Inverse Tapered	Part Span Inverse Tapered	Segmented Inverse Tapered	Gothic
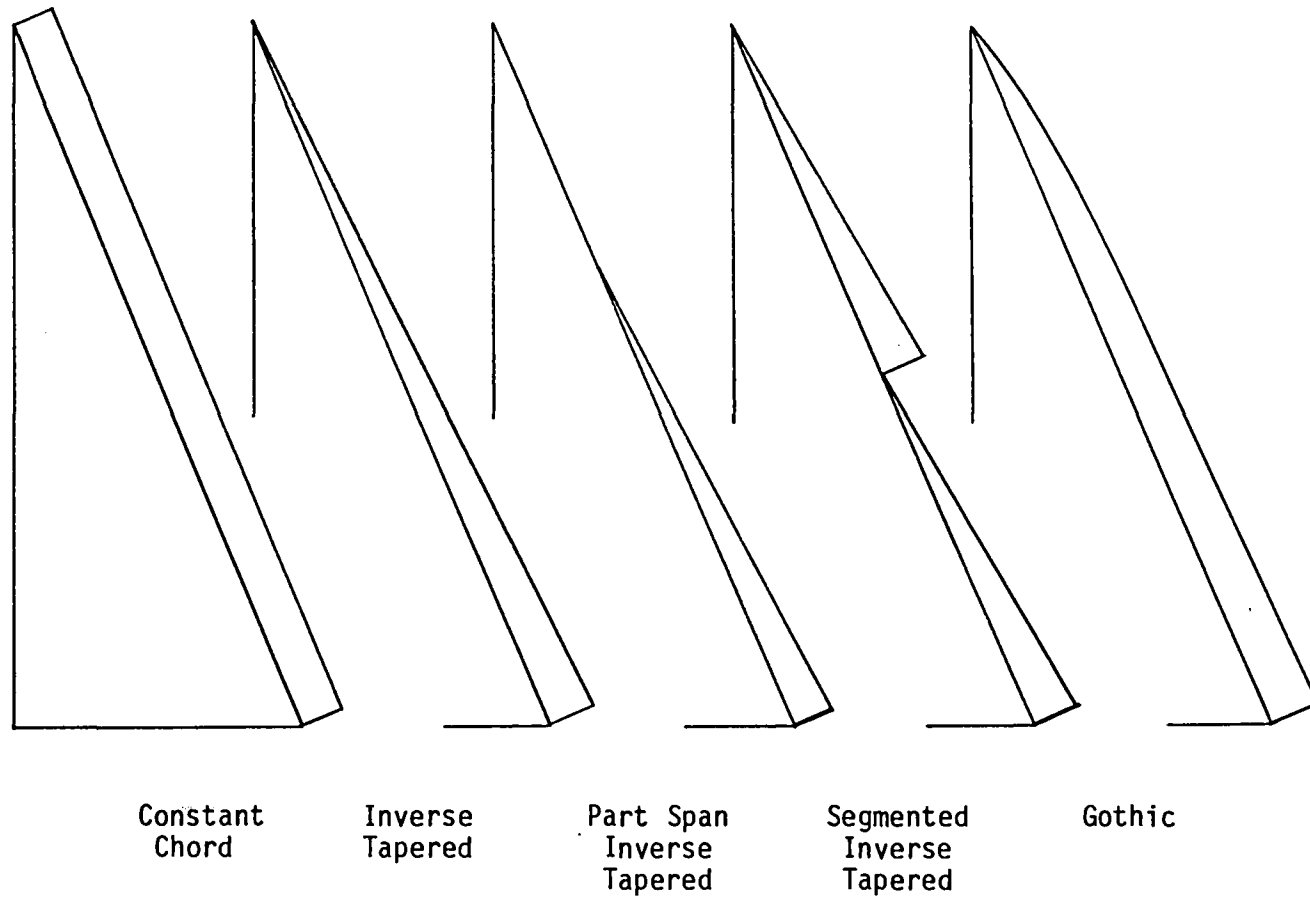
Figure 2.- Current LEVF leading-edge geometries.

Figure 3.- Wind-tunnel model geometry.

74°

9.128

2.65

3.40

3.65

2.00
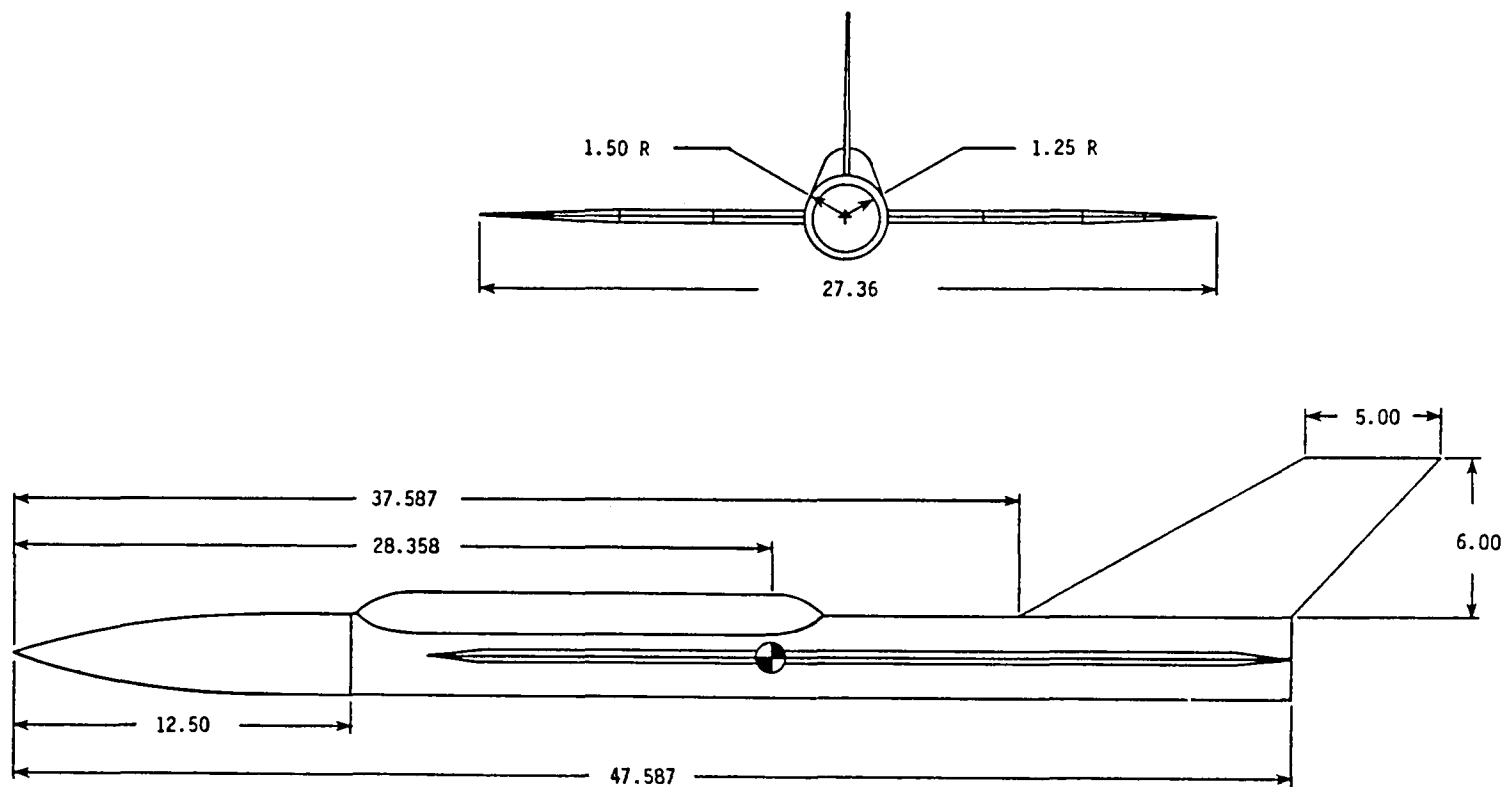
(All dimensions in inches)
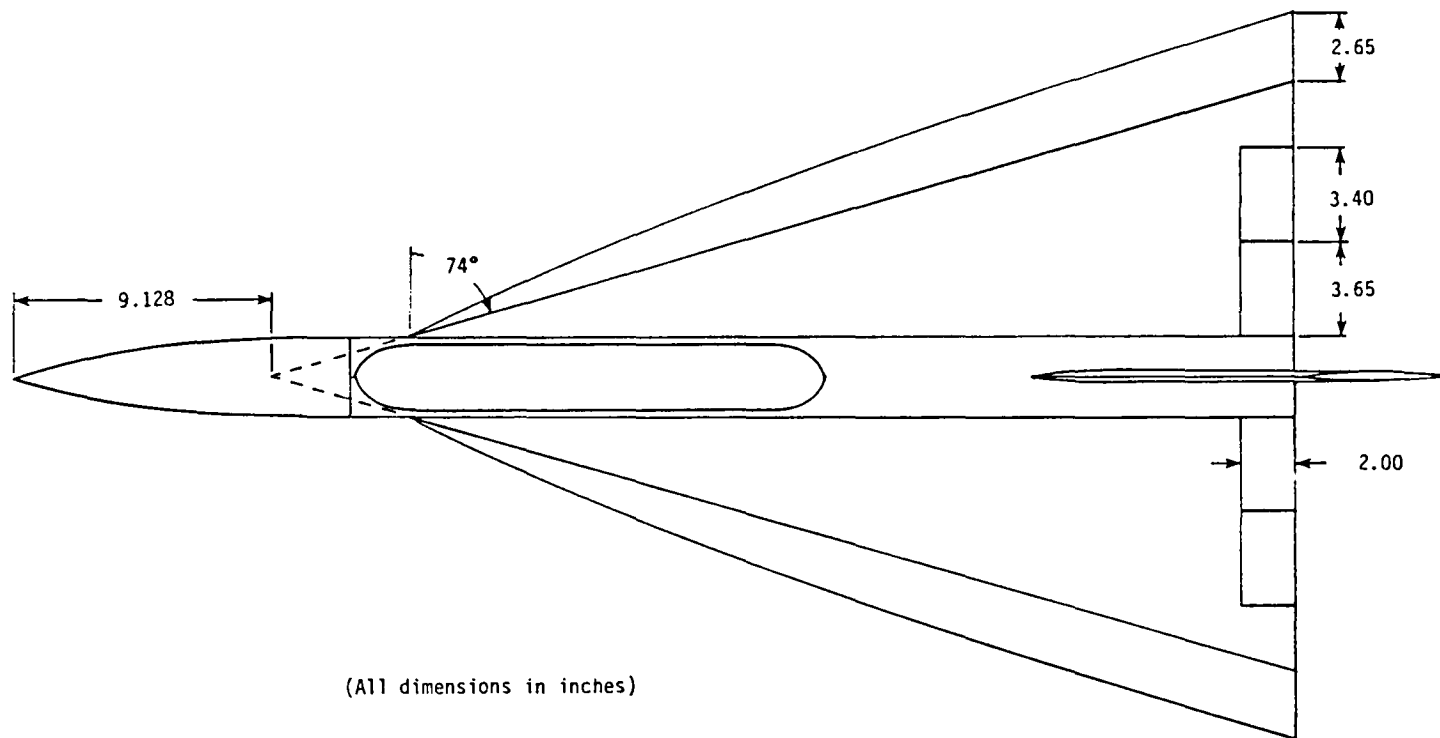
Figure 3.- Concluded.
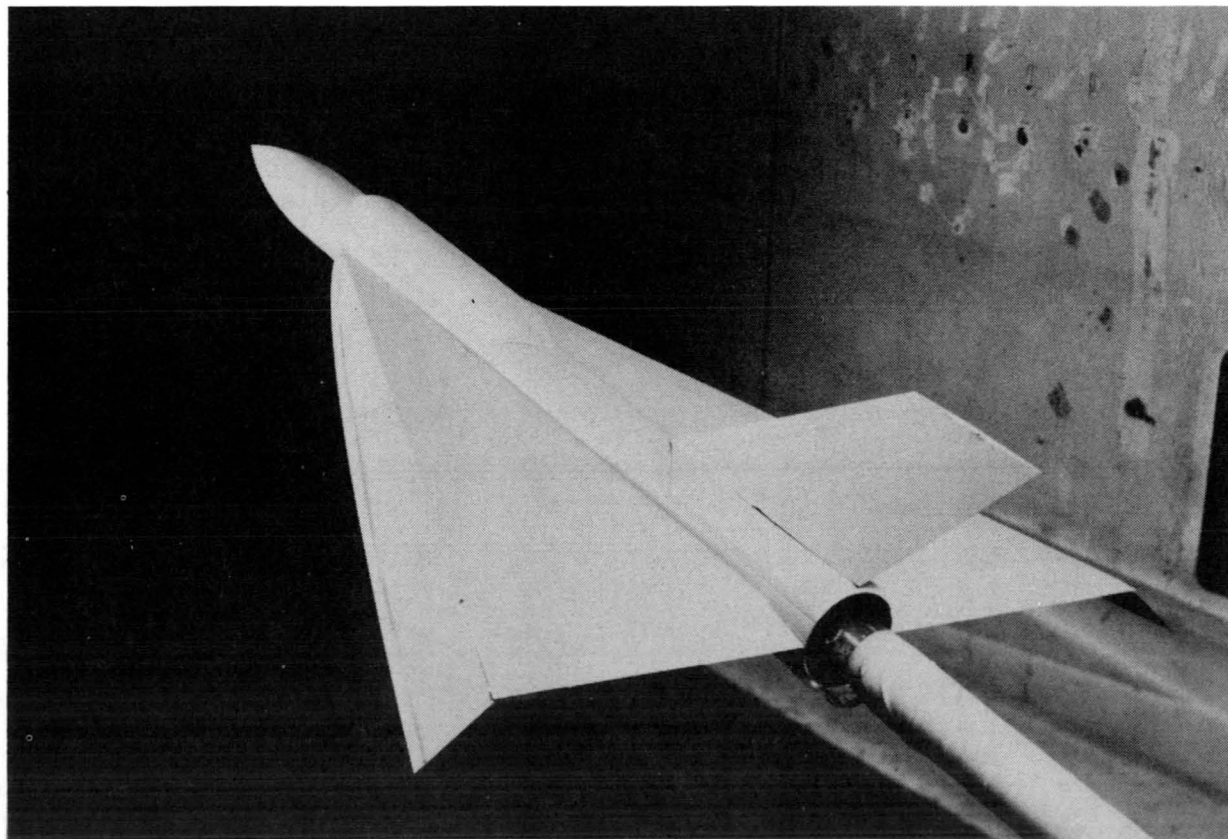
Figure 4.- Wind-tunnel model in the NASA Langley Research Center
7- by 10-Foot High-Speed Tunnel.
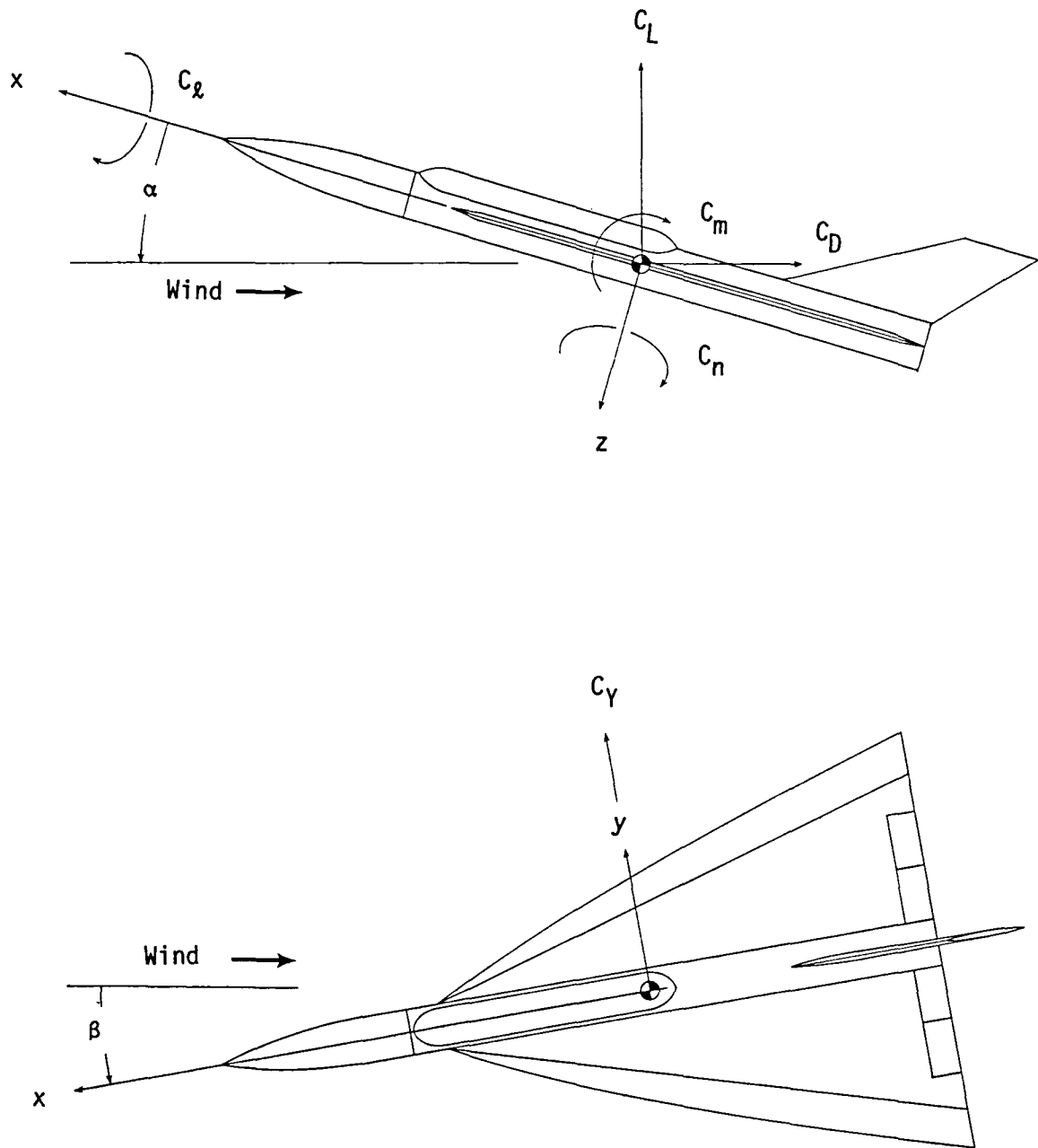
Figure 5.- System of axes.
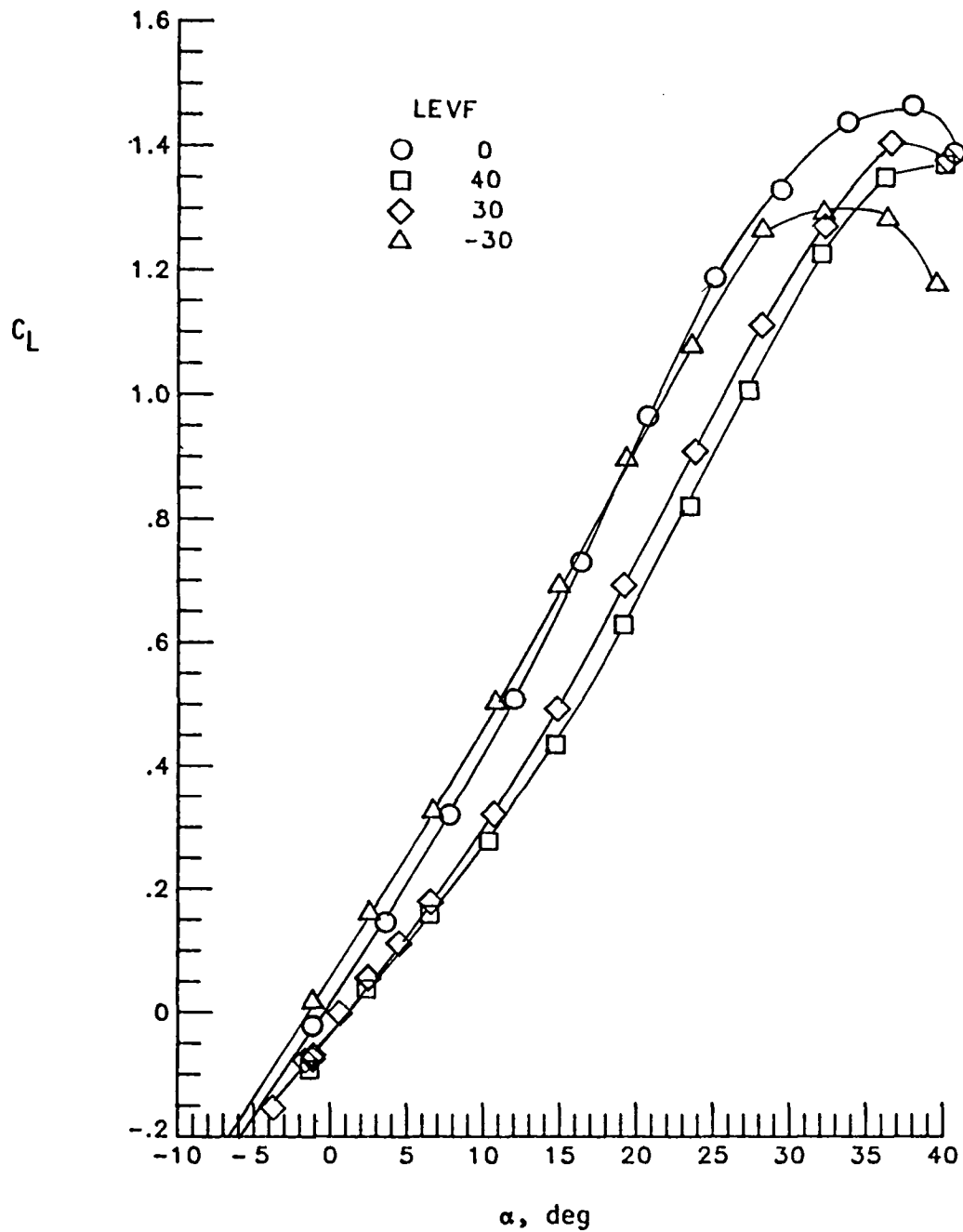
(a) Lift characteristics.

Figure 6.- Effect of LEVF deflection on longitudinal aerodynamic characteristics.
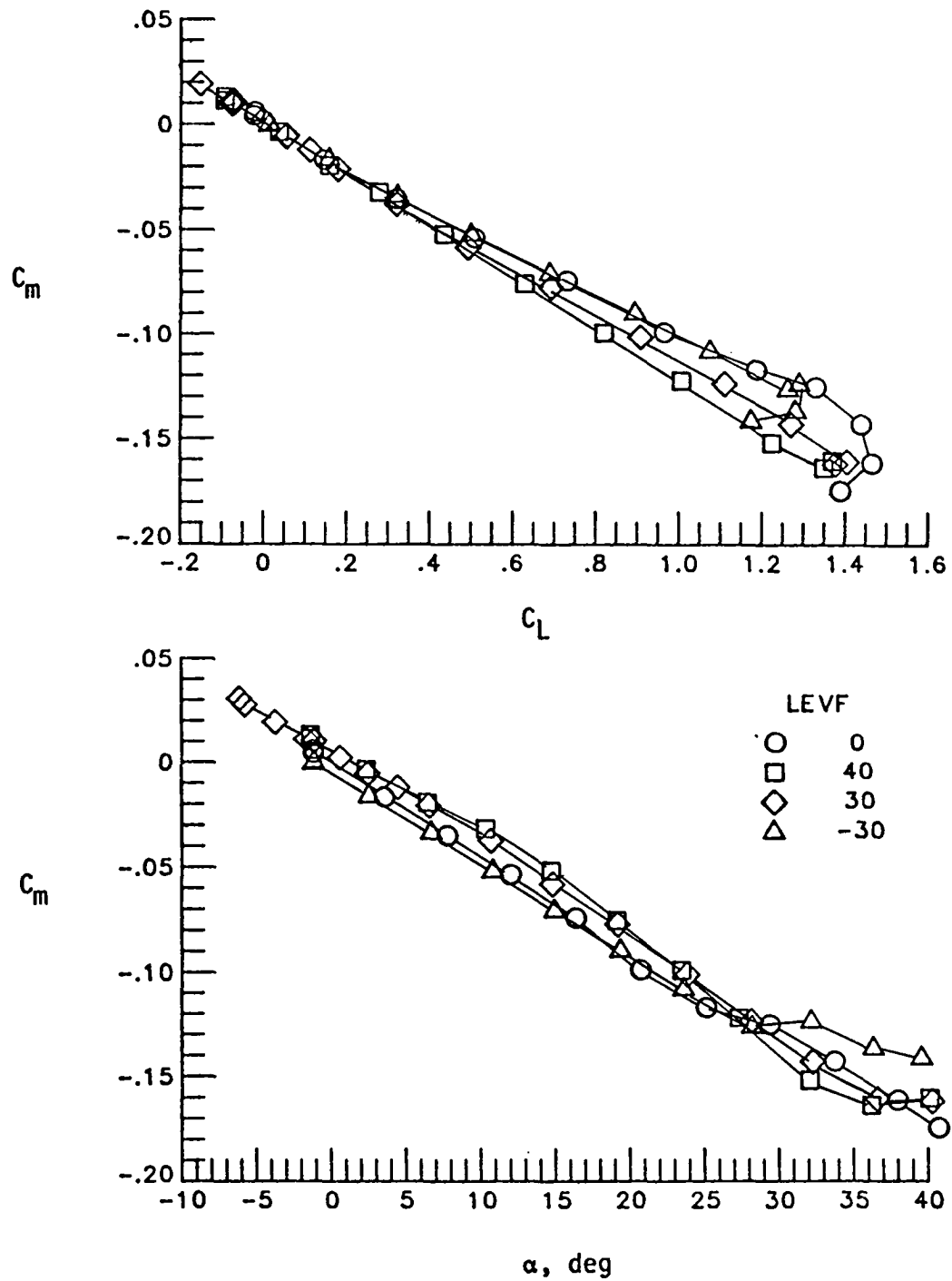
(b) Pitching moment characteristics.
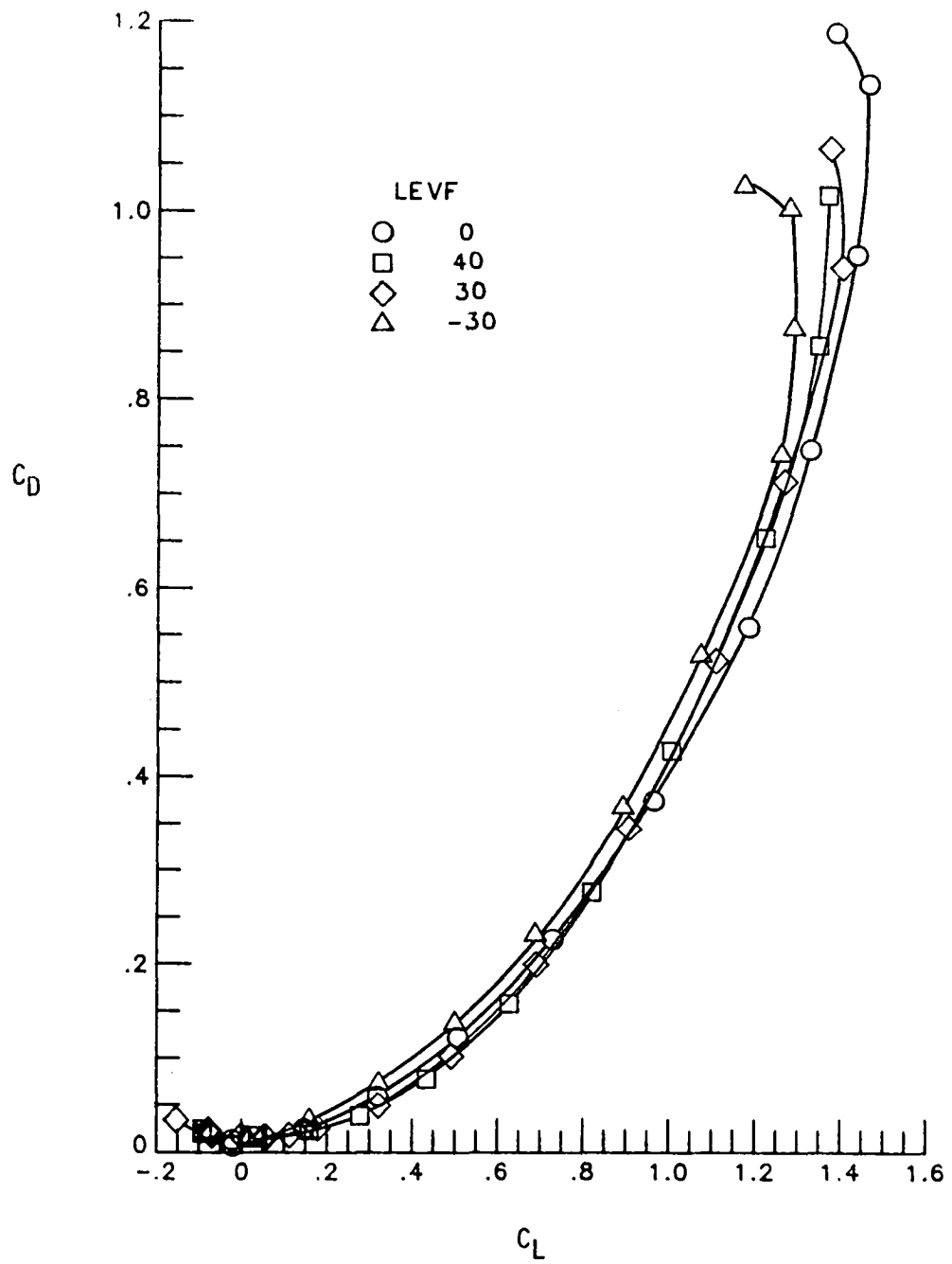
Figure 6.- Continued

(c) Drag characteristics.
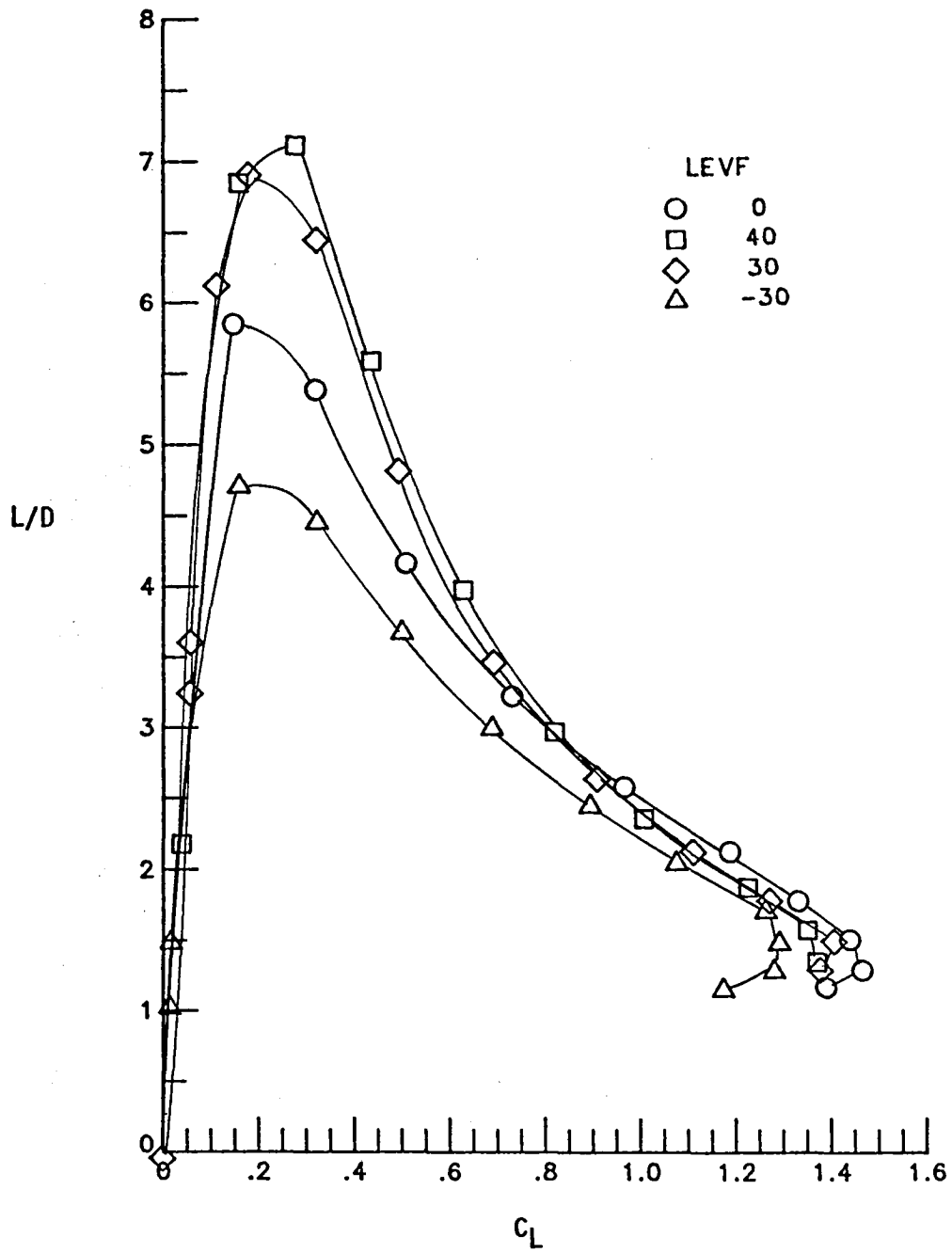
Figure 6.- Continued

Figure 6.- Continued.

(d) Lift-to-drag ratio.
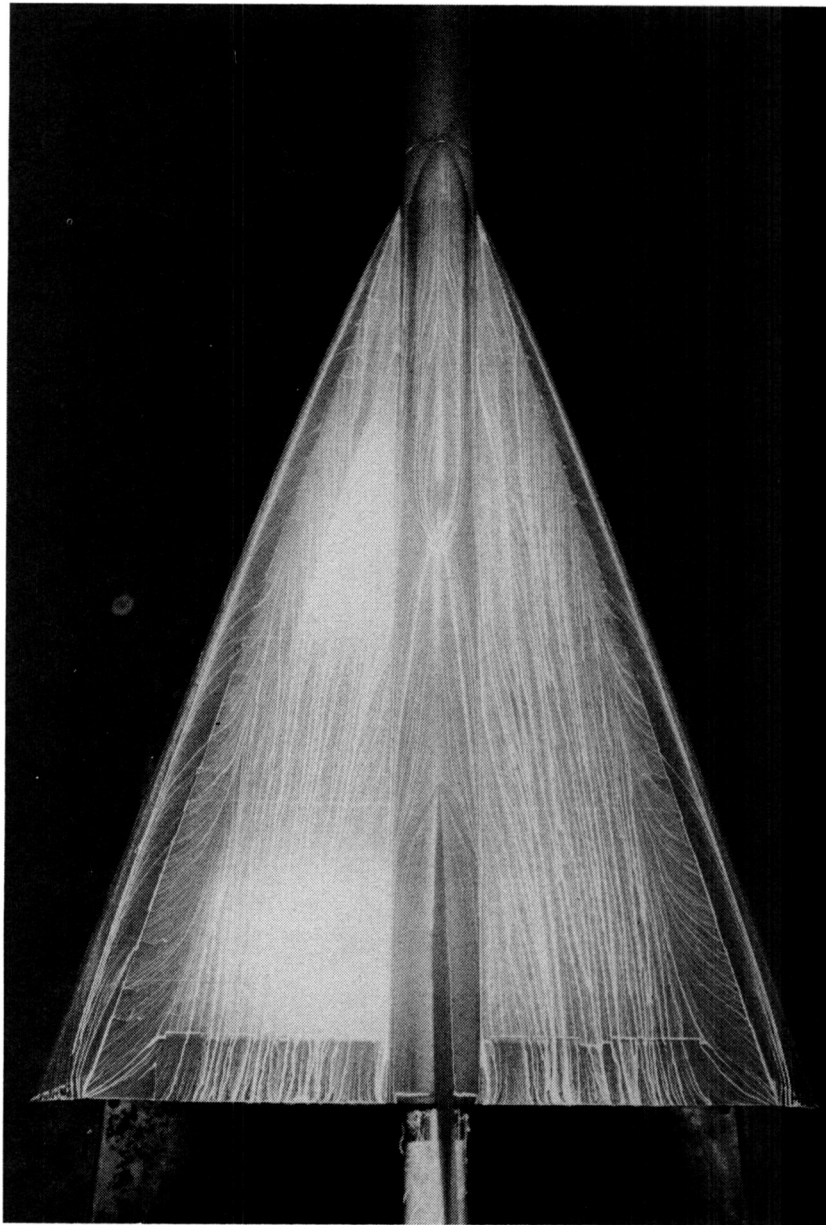
Figure 6.- Concluded.

(e) Oil flow photograph: $\delta_{LE} = 40$, $\alpha = 14^0$.
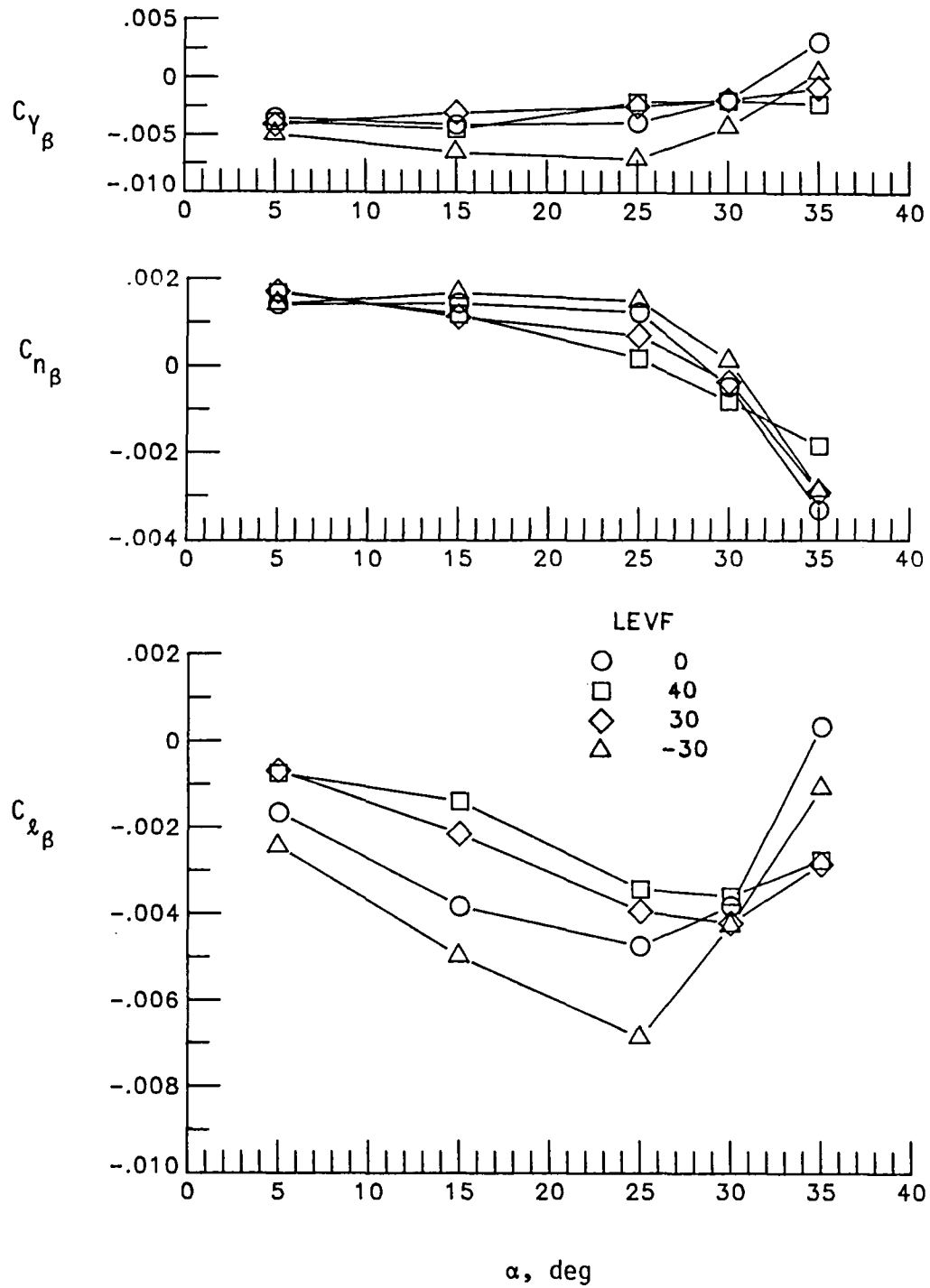
Figure 7a.- Effect of LEVF deflection on lateral-directional stability derivatives as a function of angle of attack.
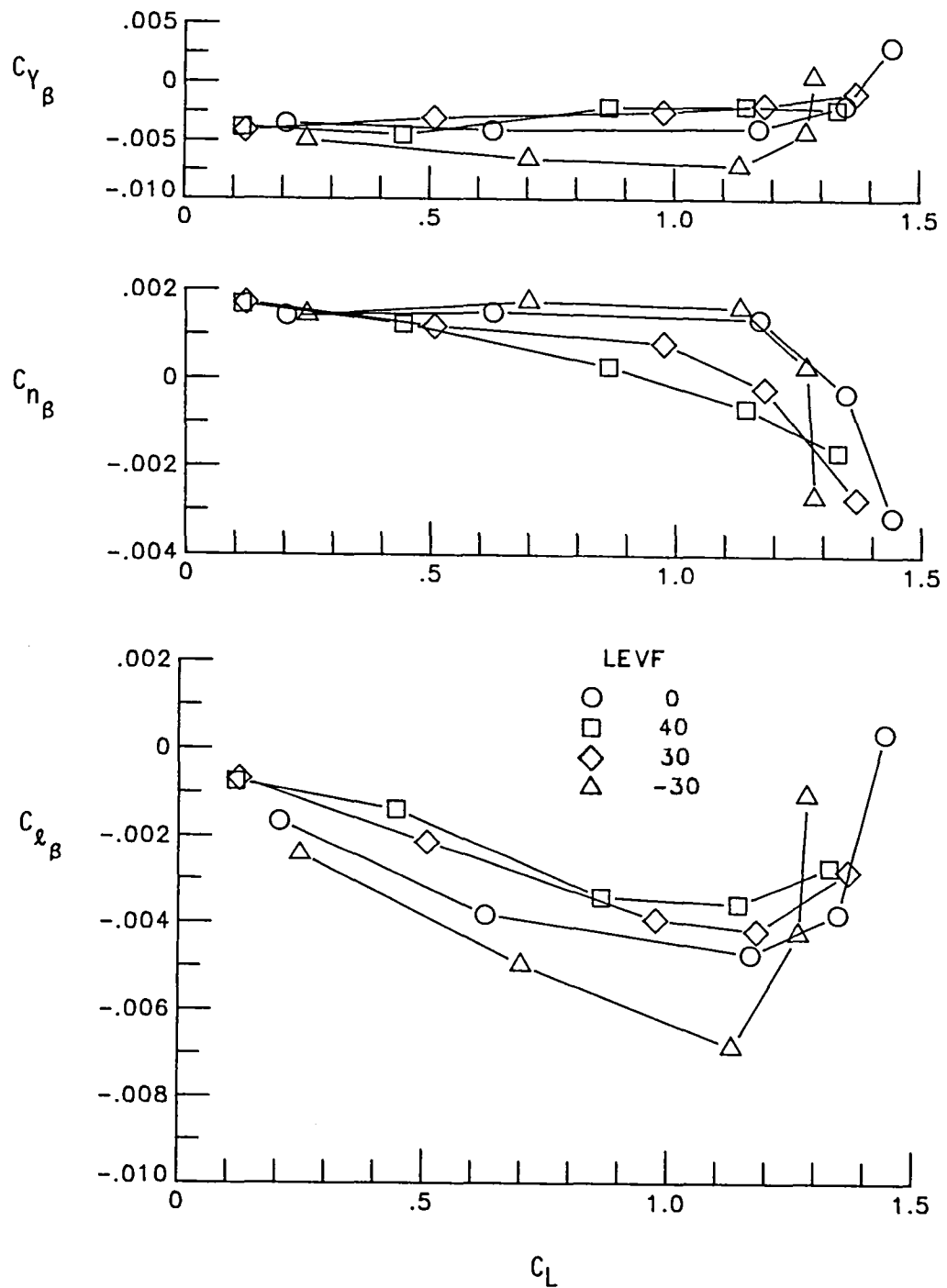
Figure 7b.- Effect of LEVF deflection on lateral-directional stability derivatives as a function of lift coefficient.
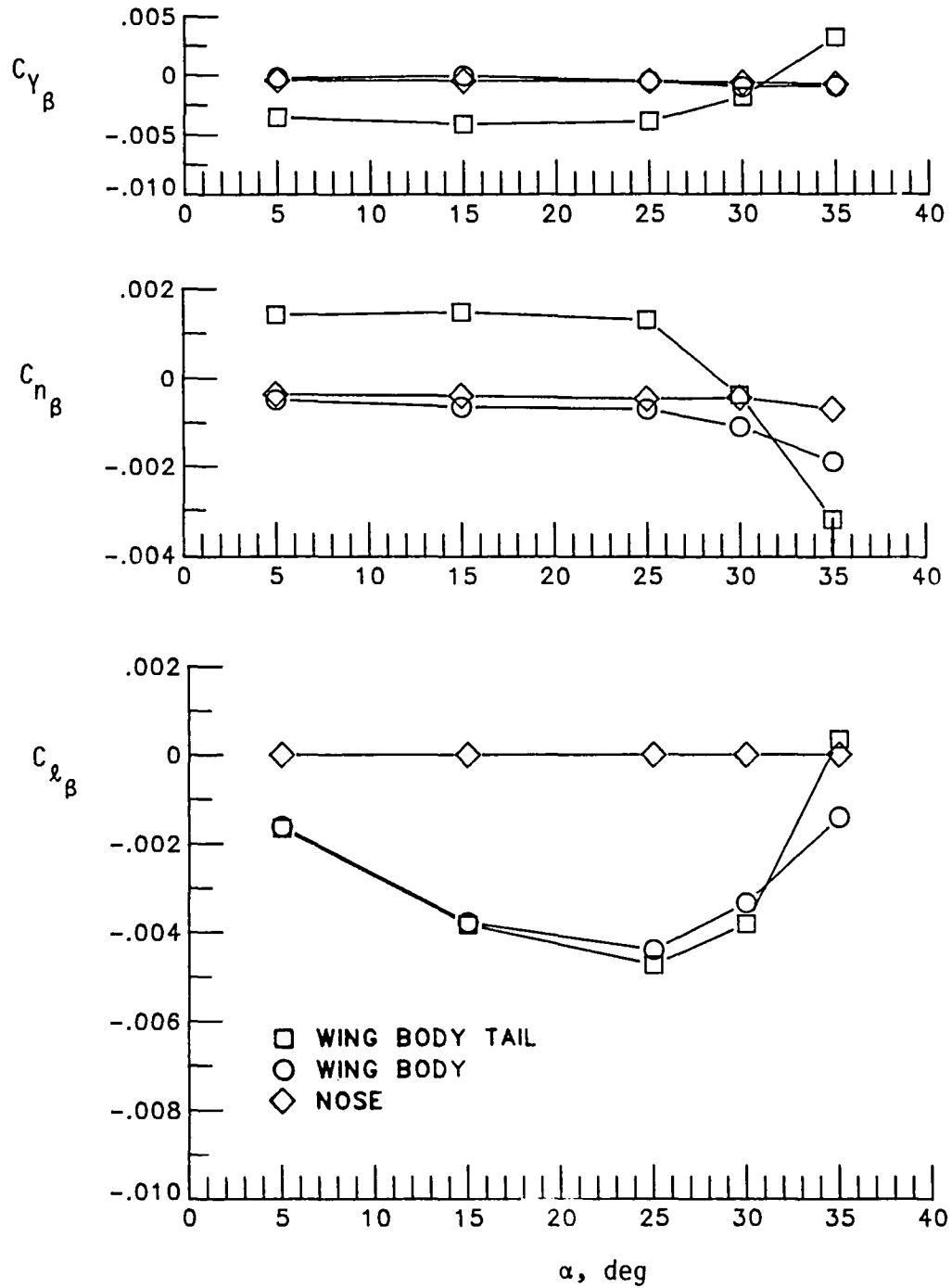
Figure 8a.- Effect of vertical tail and nose on the lateral-directional stability derivatives with $\delta_{LE} = 0°$.
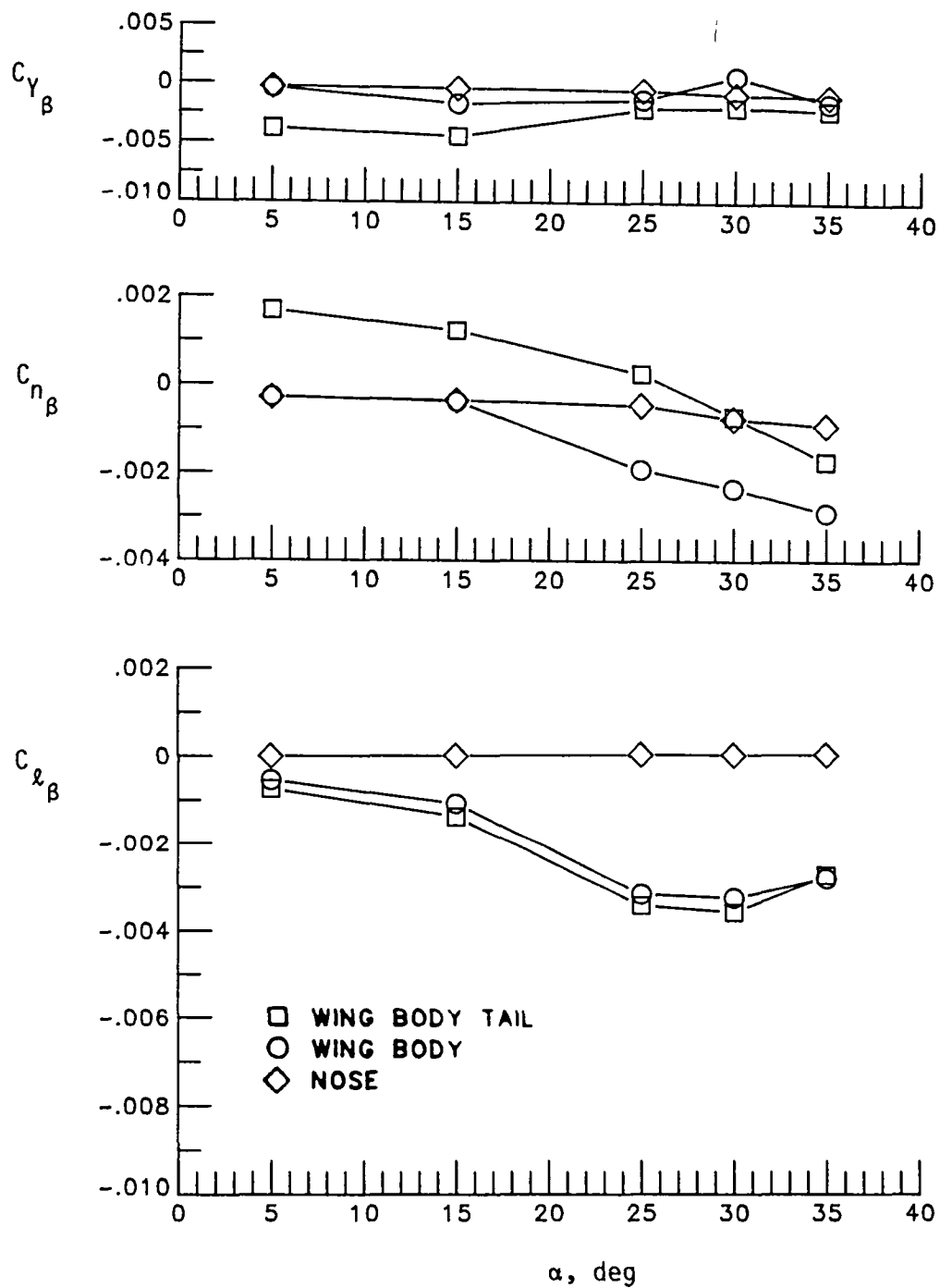
Figure 8b.- Effect of vertical tail and nose on the lateral-directional stability derivatives with $\delta_{LE} = 40°$.
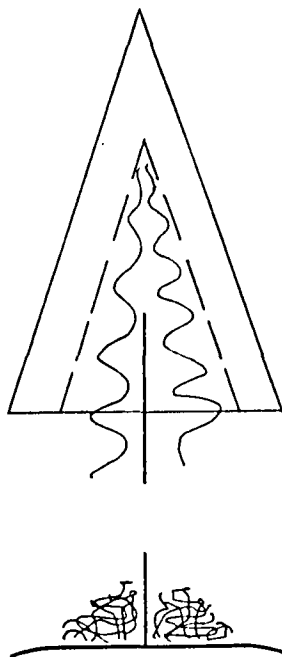
Attached flow vertical
tail blanketed in
turbulent flow region
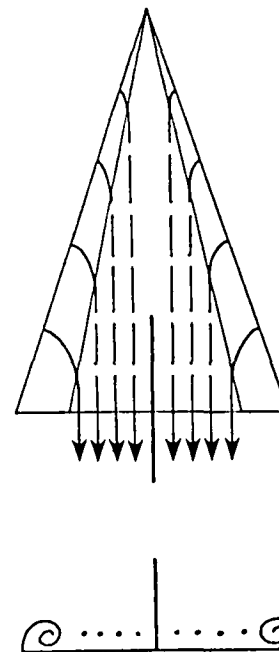
Vortical flow entrains
freestream flow to improve
vertical tail effectiveness

Figure 9.- Aerodynamic flow model of a slender wing employing LEVF.

high, weak   low, strong
leeward vortex   windward vortex

high, strong   low, bursting
leeward vortex   windward vortex

Low to moderate angles of attack   High angles of attack
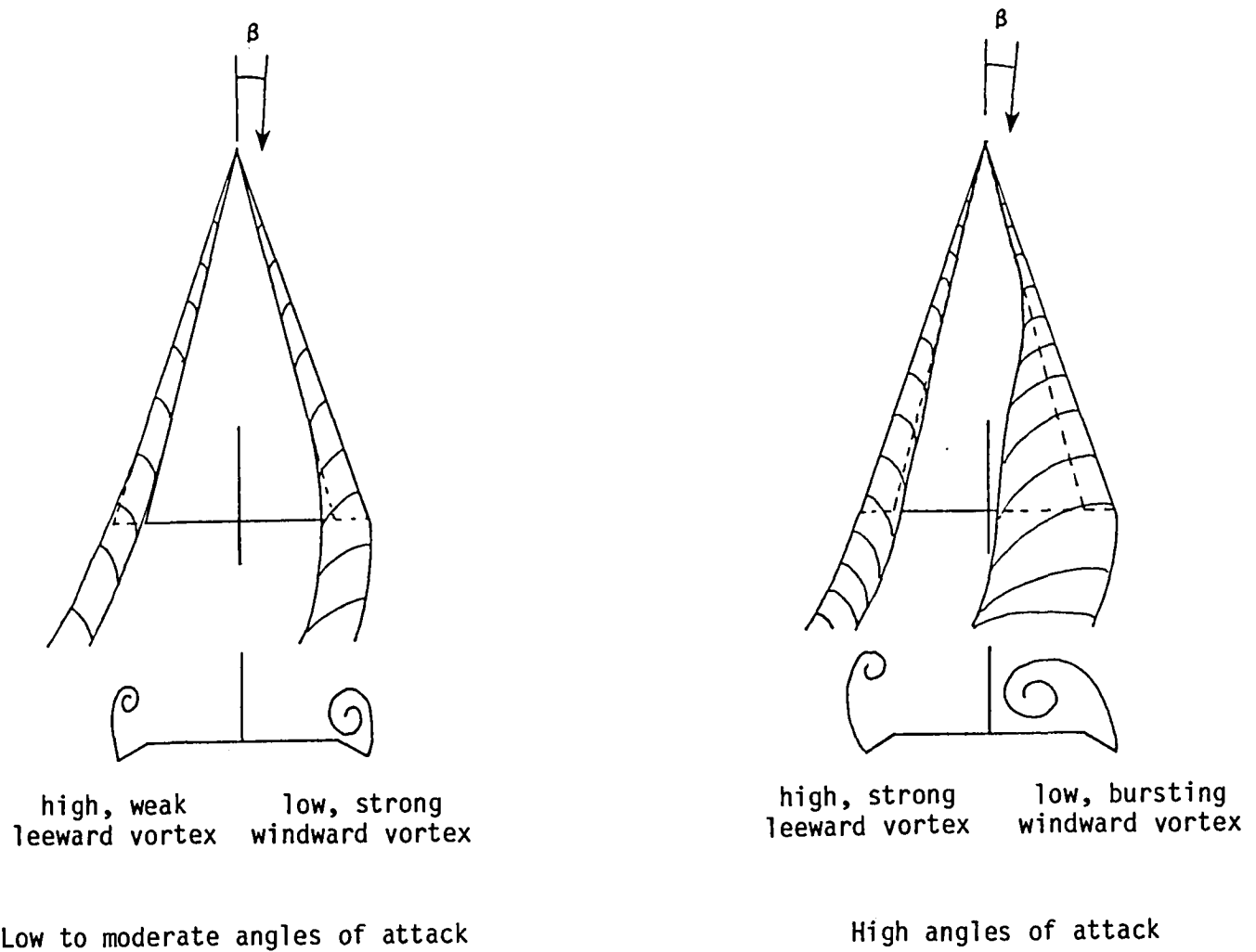
Figure 9.- Concluded.

(a) $\alpha = 5^0$
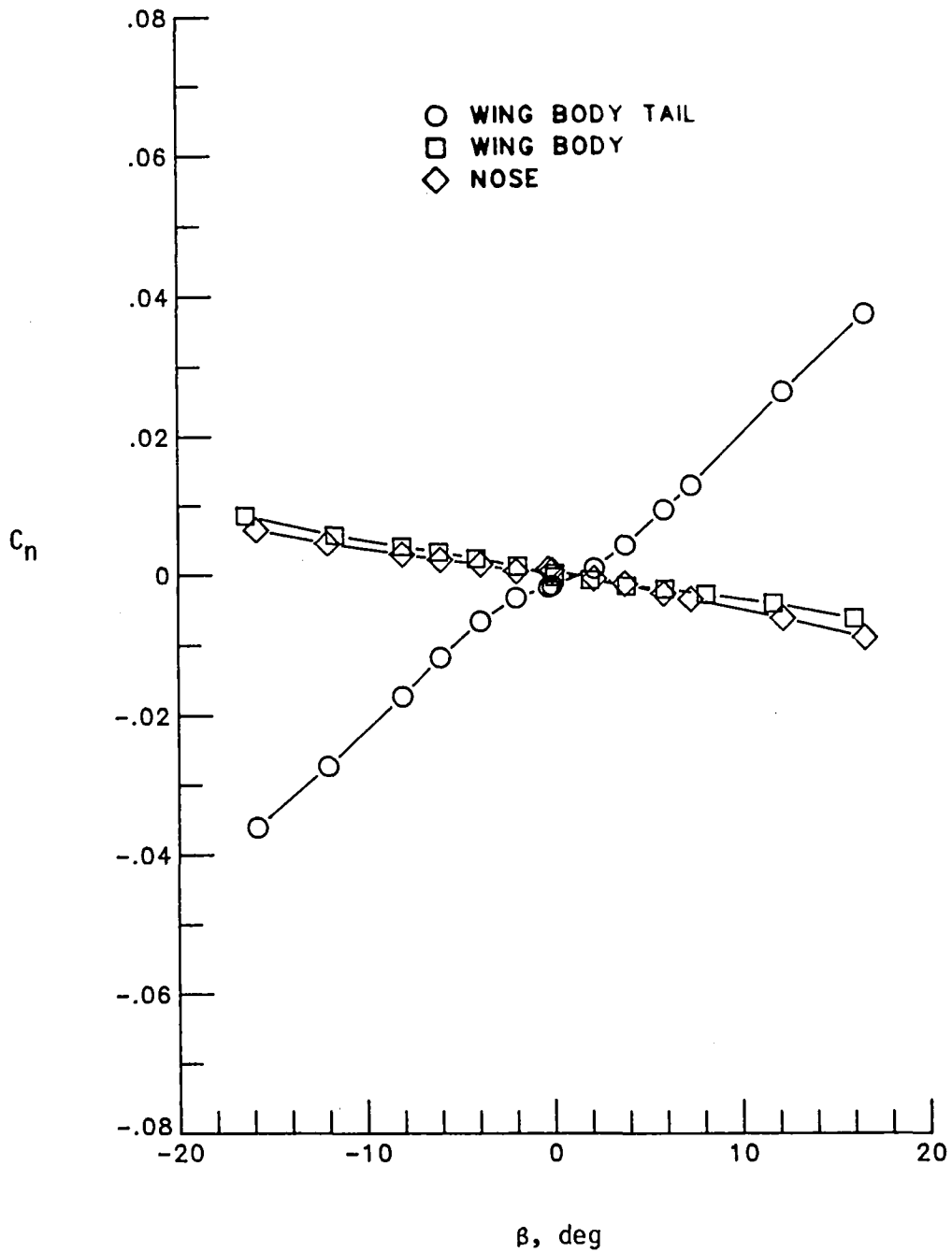
Figure 10.- Effect of vertical tail and nose on the yawing moment characteristics with $\delta_{LE} = 0°$.

(b) $\alpha = 15^0$
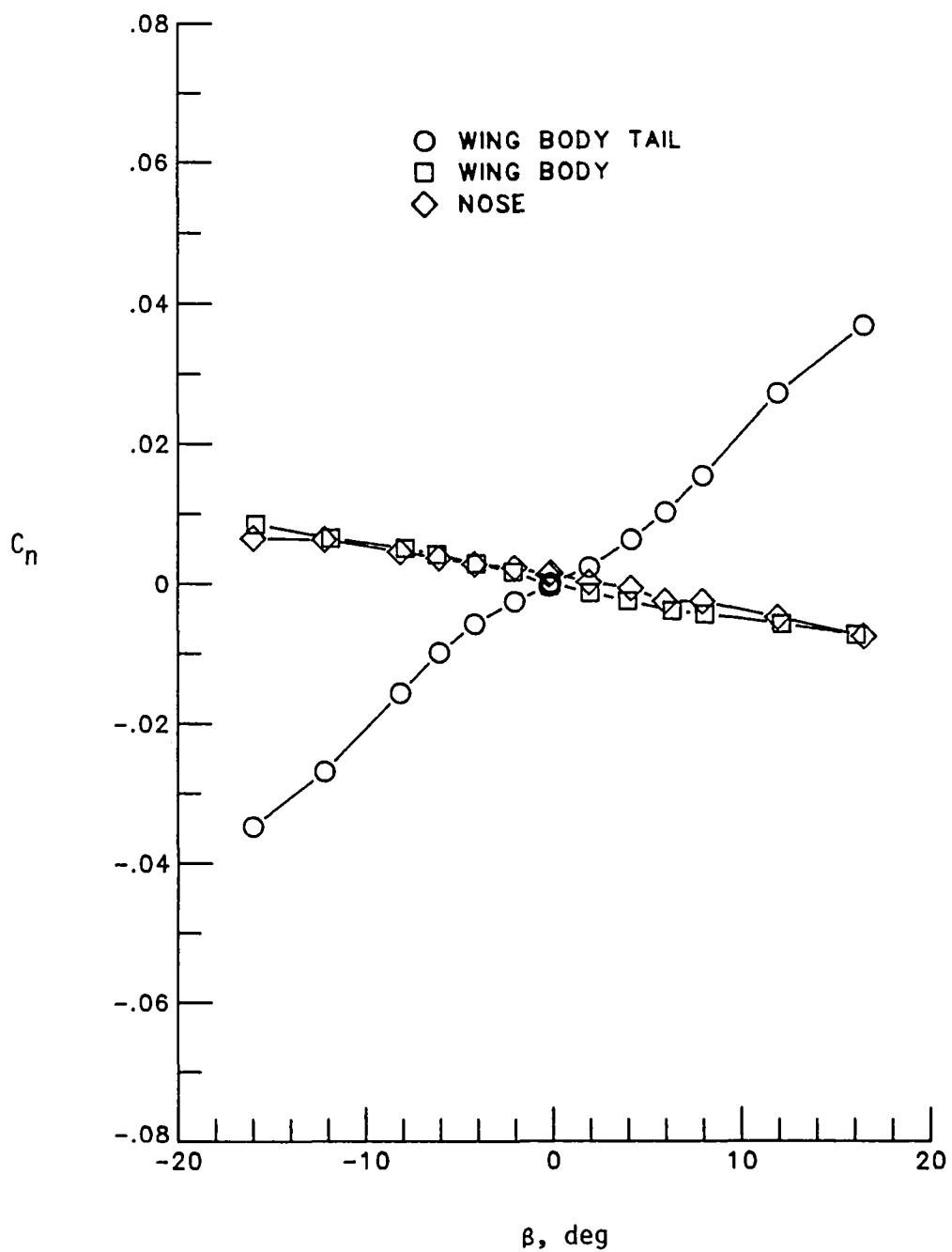
Figure 10.- Continued

(c) $\alpha = 25^0$
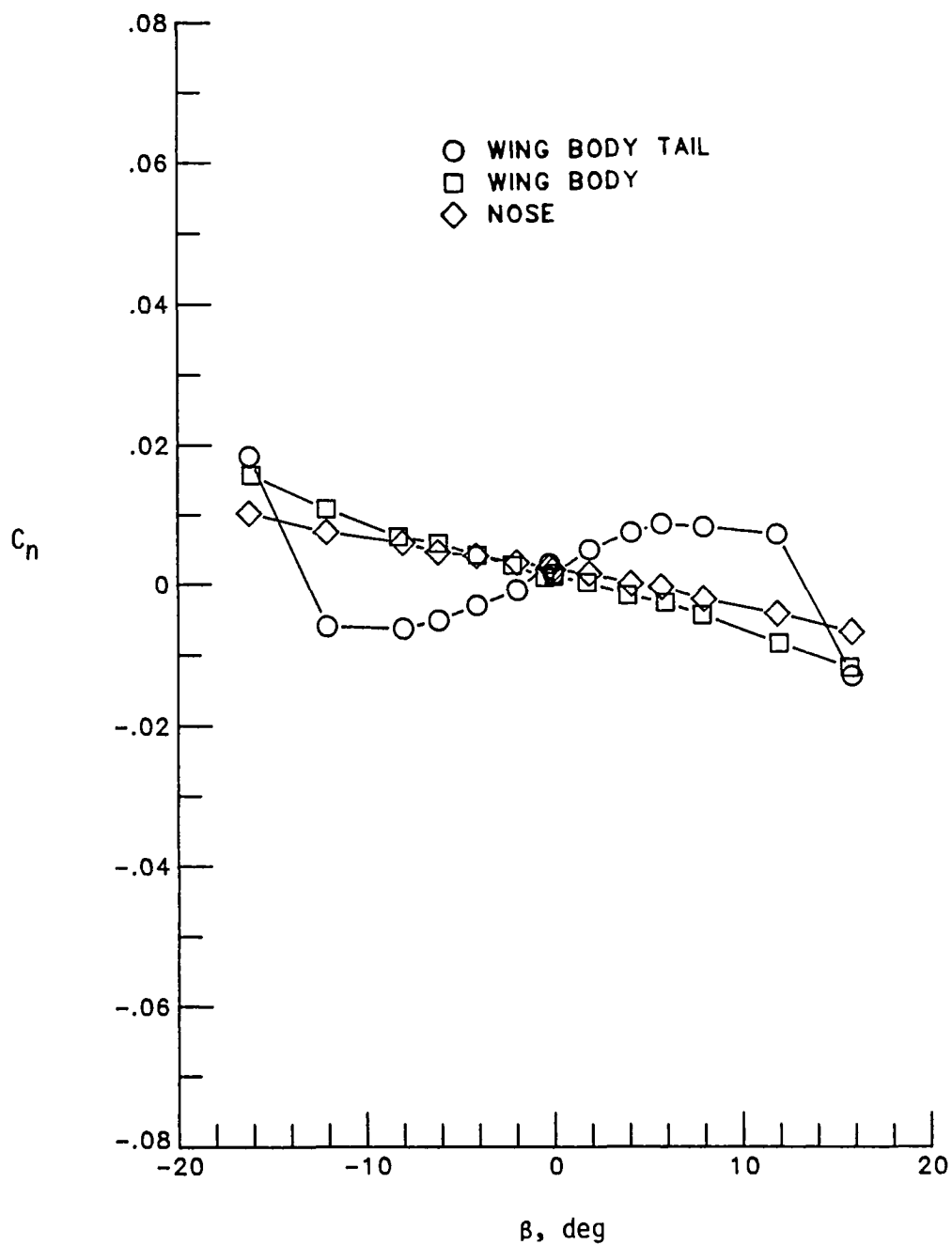
Figure 10.- Continued

(d) $\alpha = 30^0$
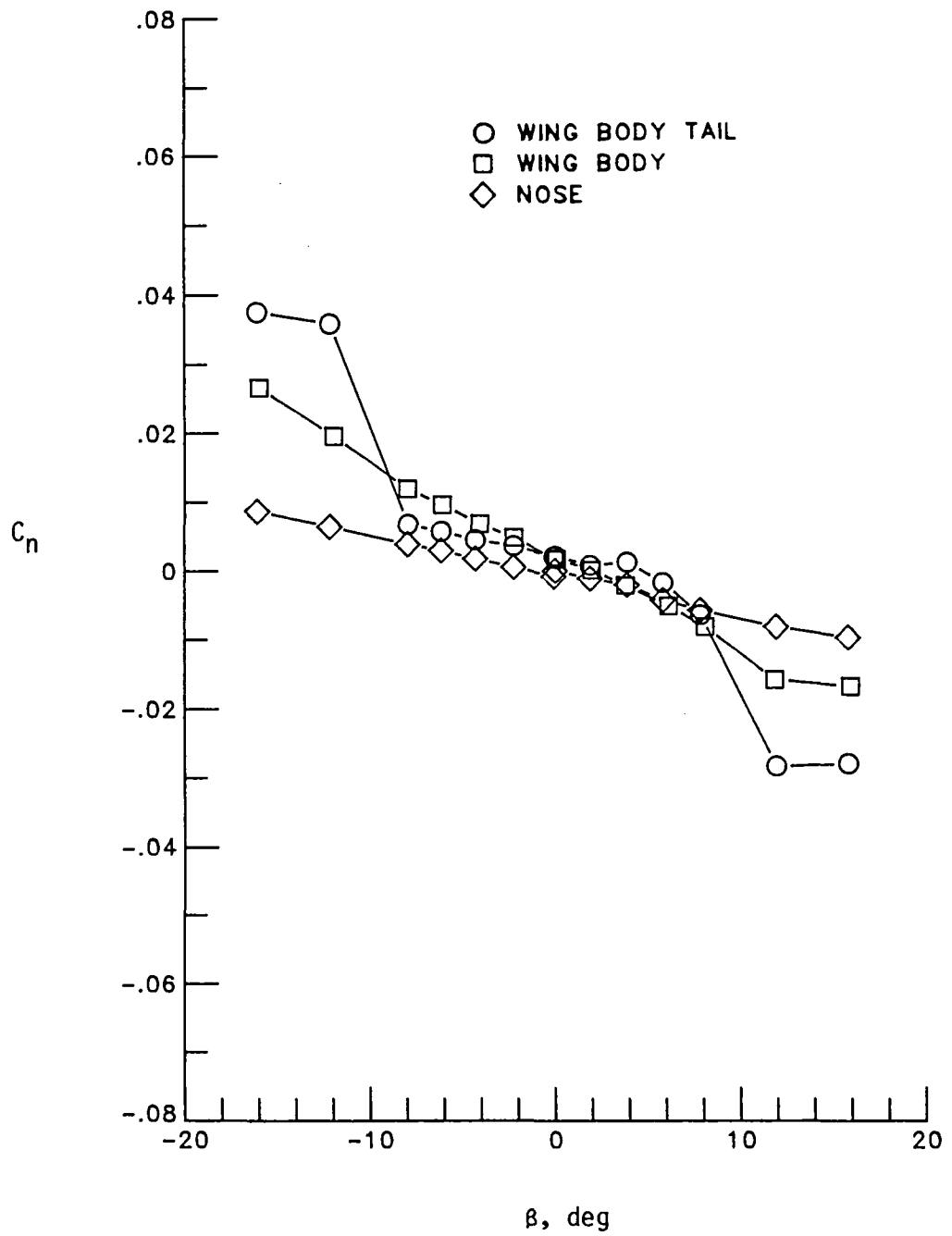
Figure 10.- Continued

(e) $\alpha = 35^0$
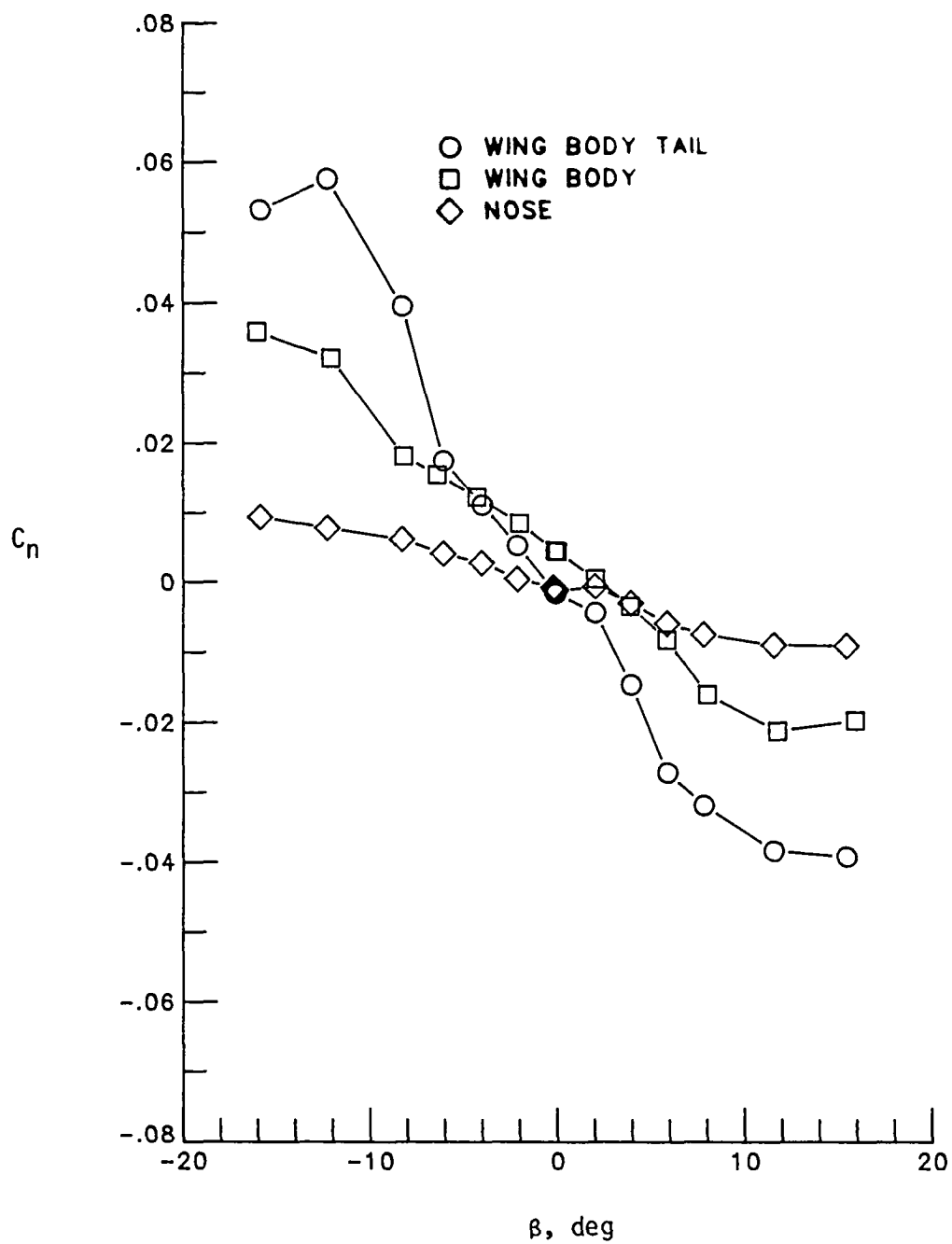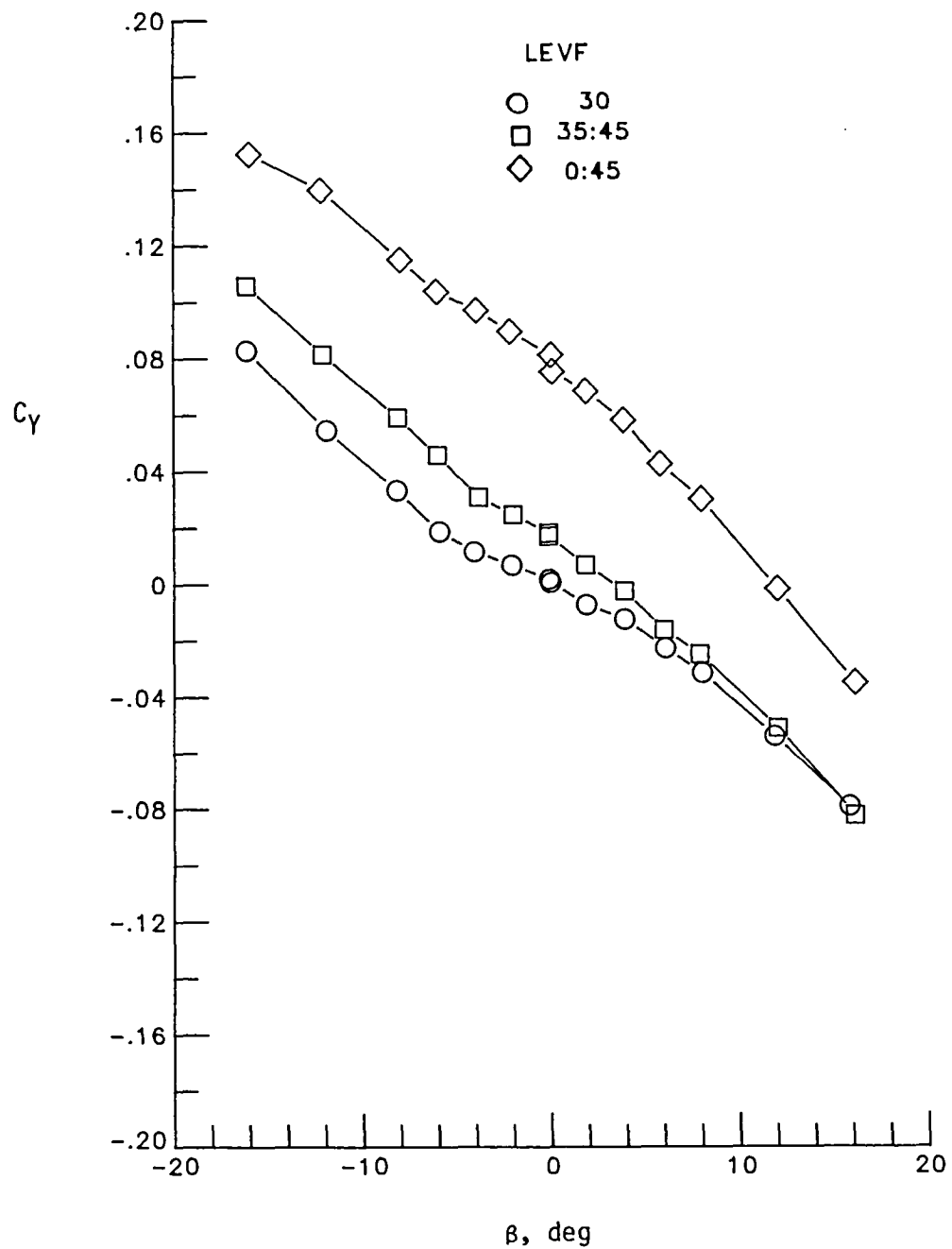
Figure 10.- Concluded.
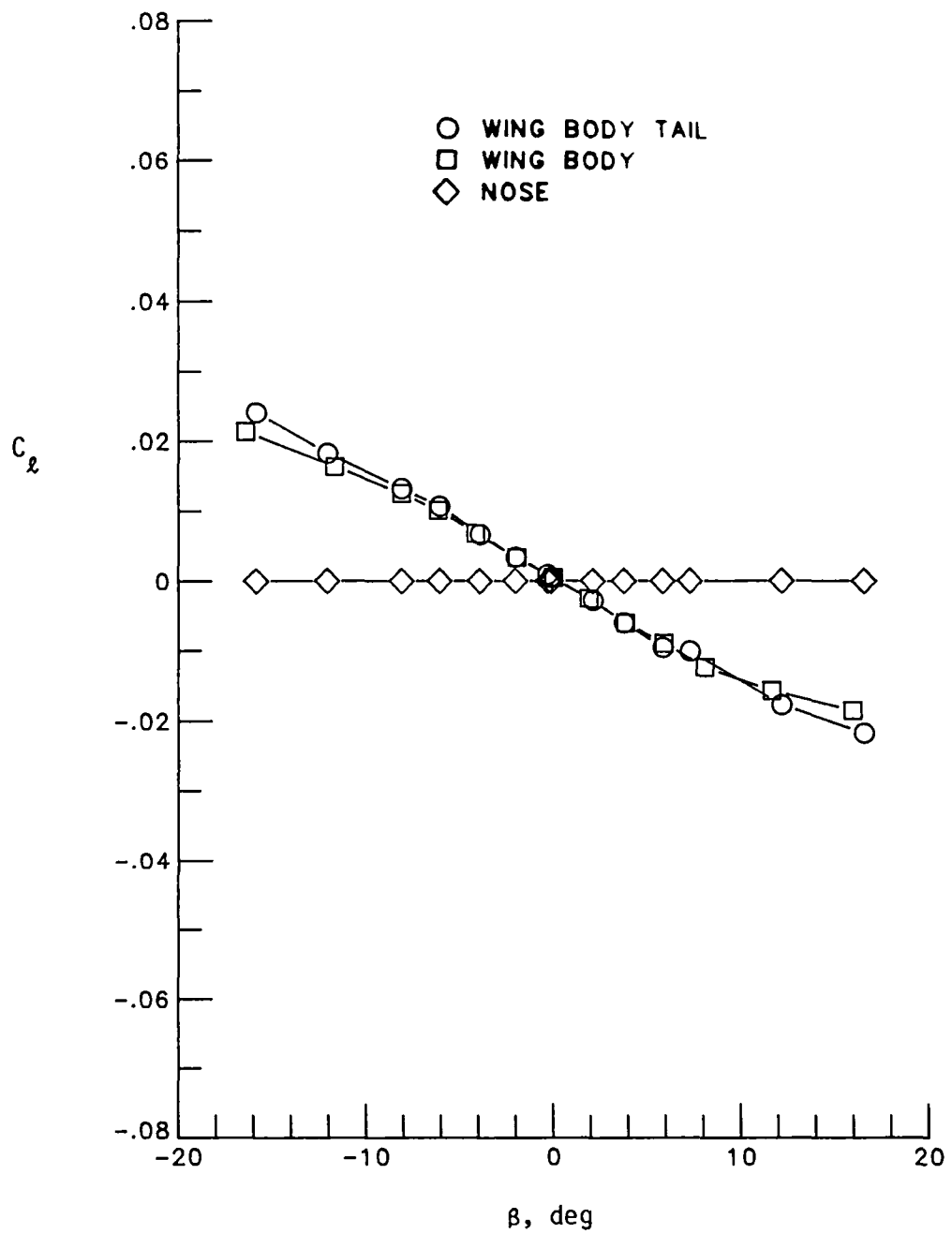
Figure 11.- Effect of vertical tail and nose on the rolling moment
characteristics with $\delta_{LE} = 0°$.

(b) $\alpha = 15^0$
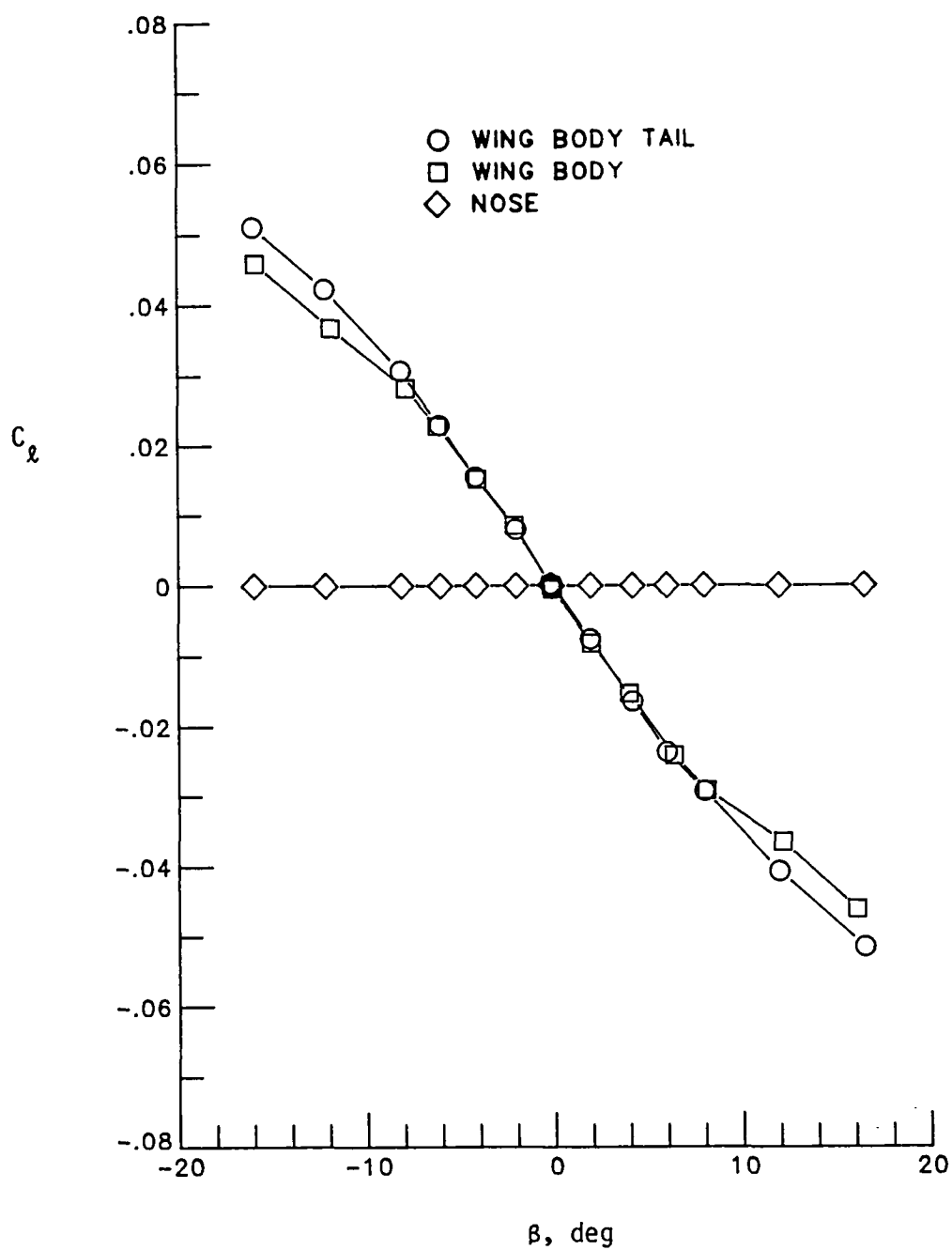
Figure 11.- Continued

(c) $\alpha = 25^0$
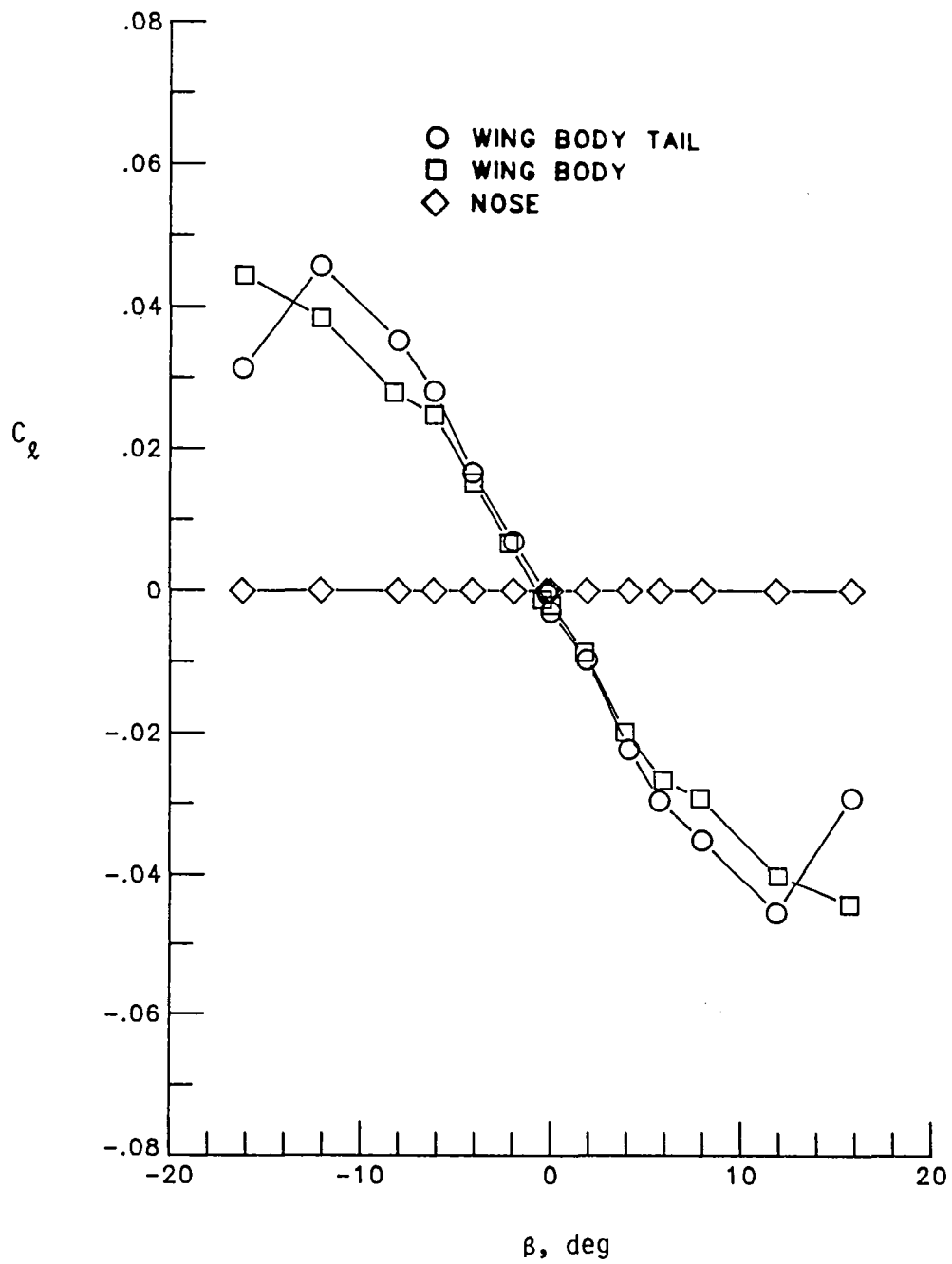
Figure 11.- Continued

(d) $\alpha = 30^0$
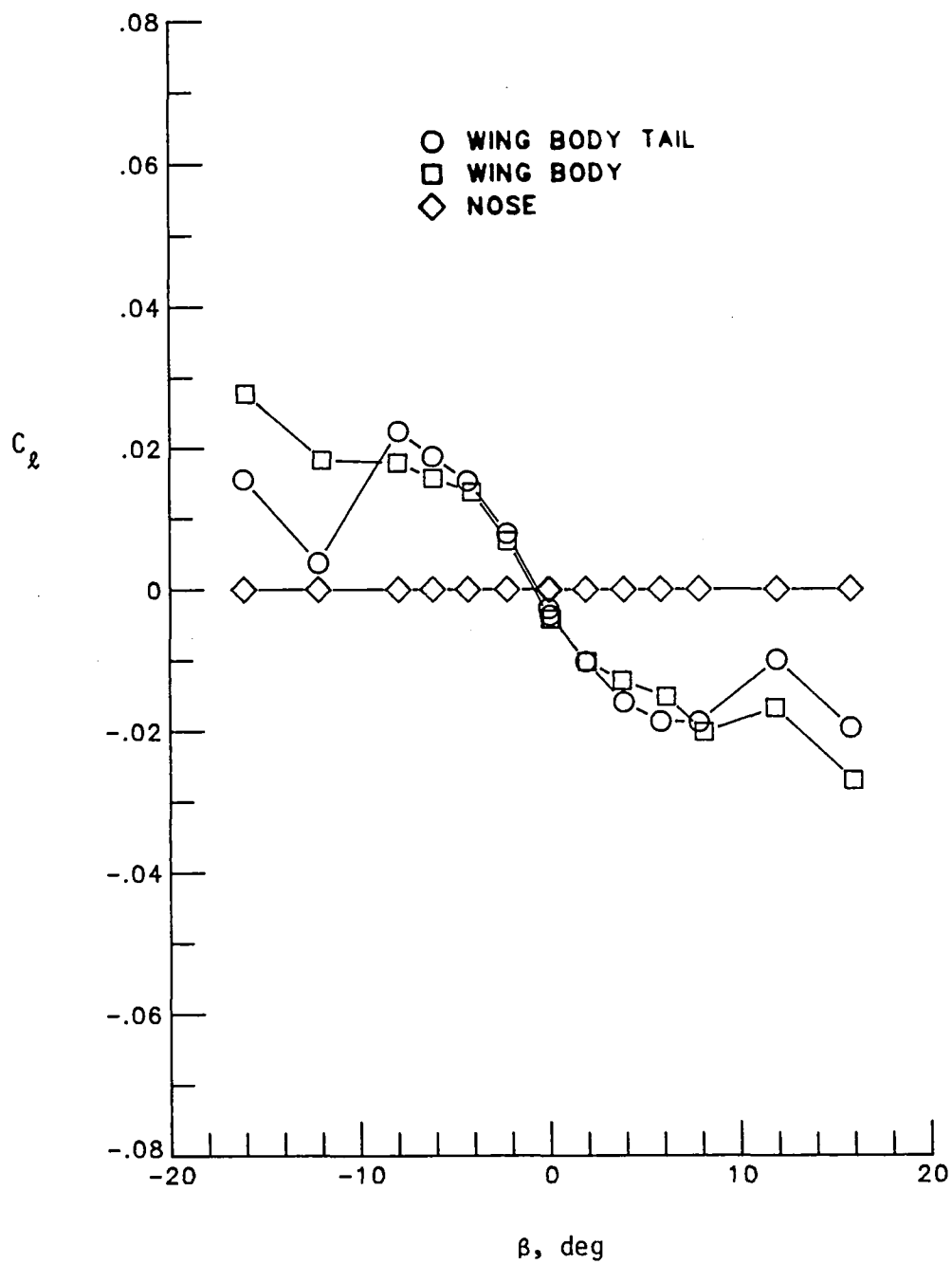
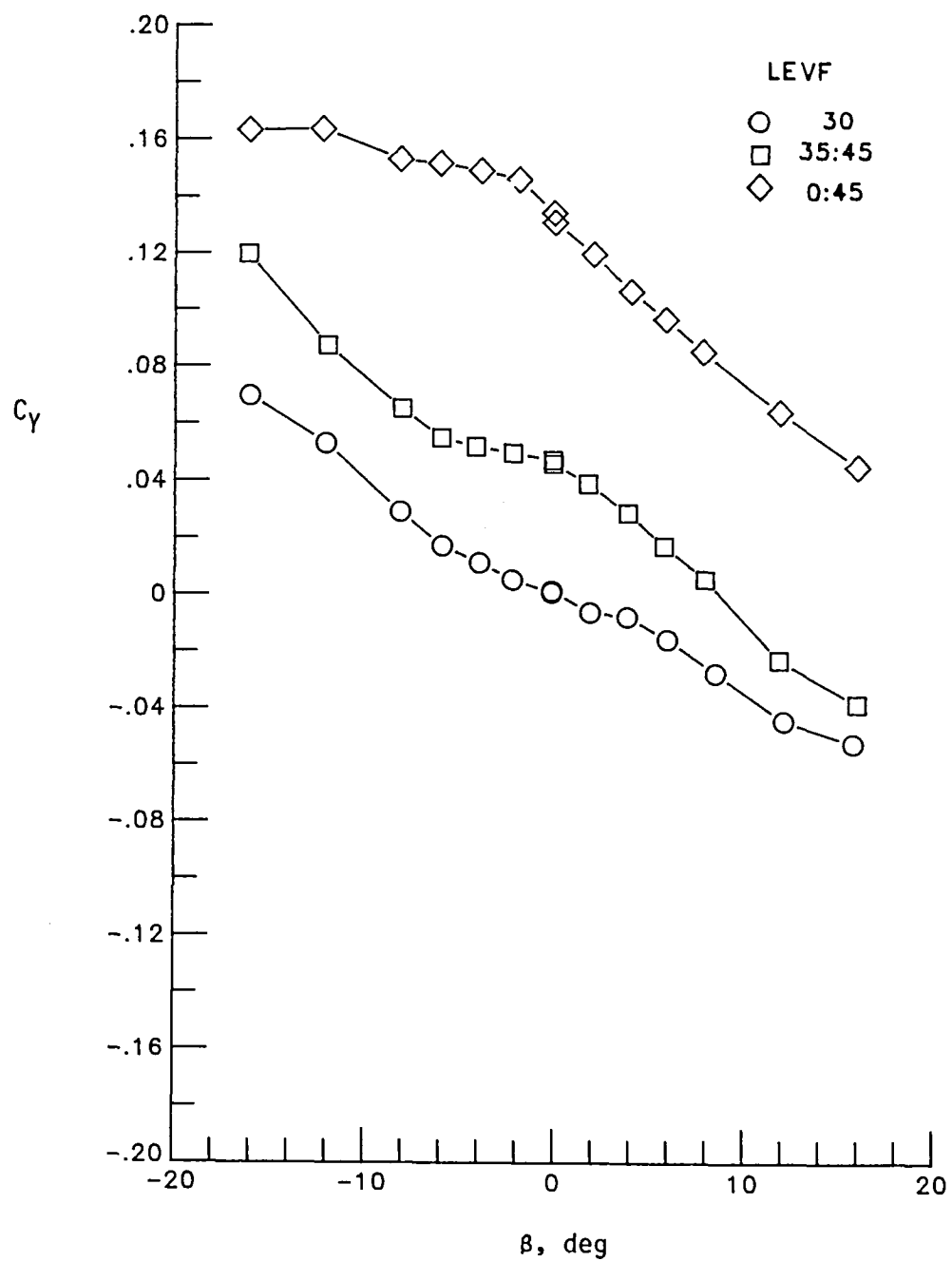Figure 11.- Continued

(e) $\alpha = 35^0$
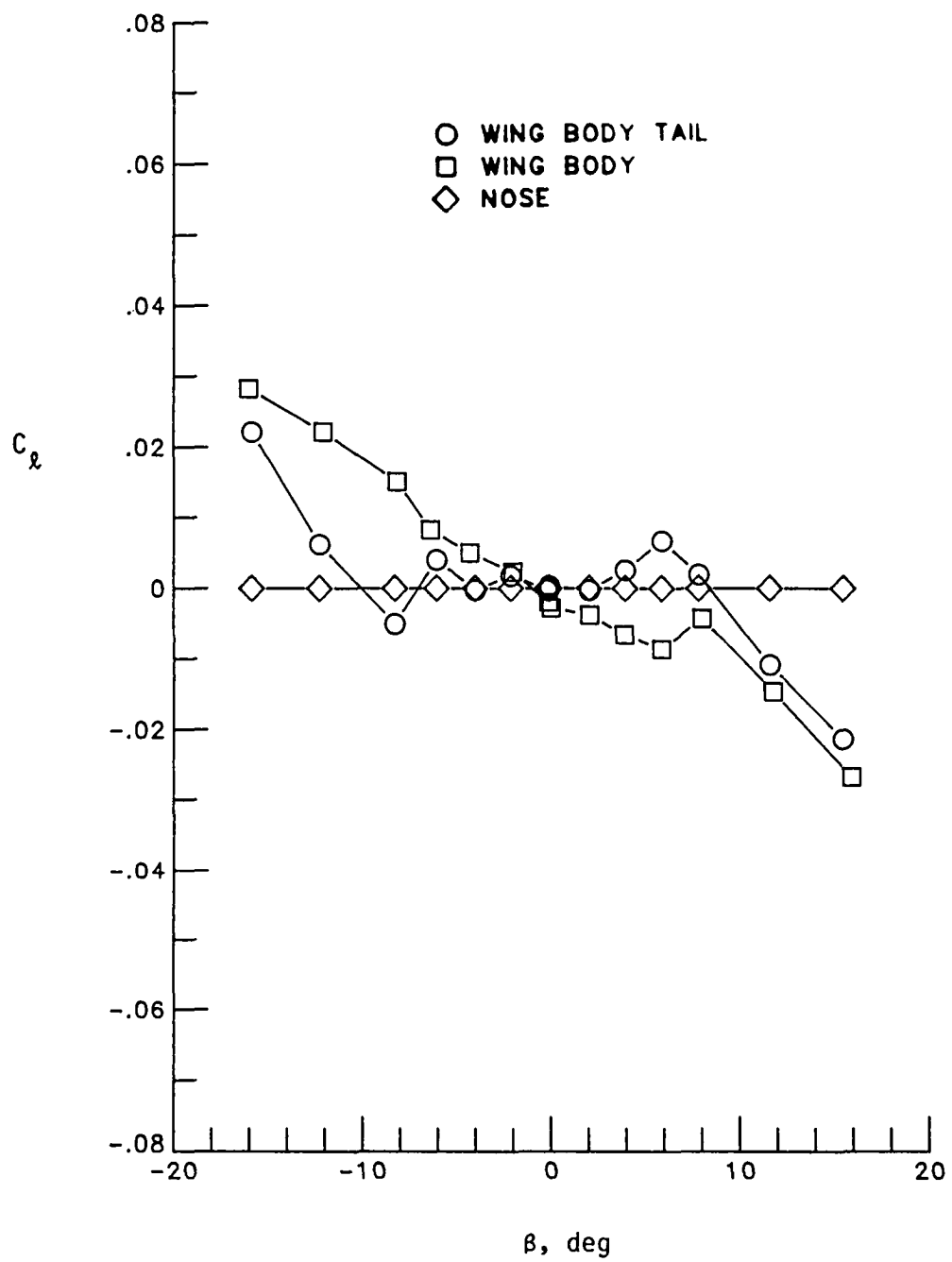
Figure 11.- Concluded.

(a) $\alpha = 5^0$
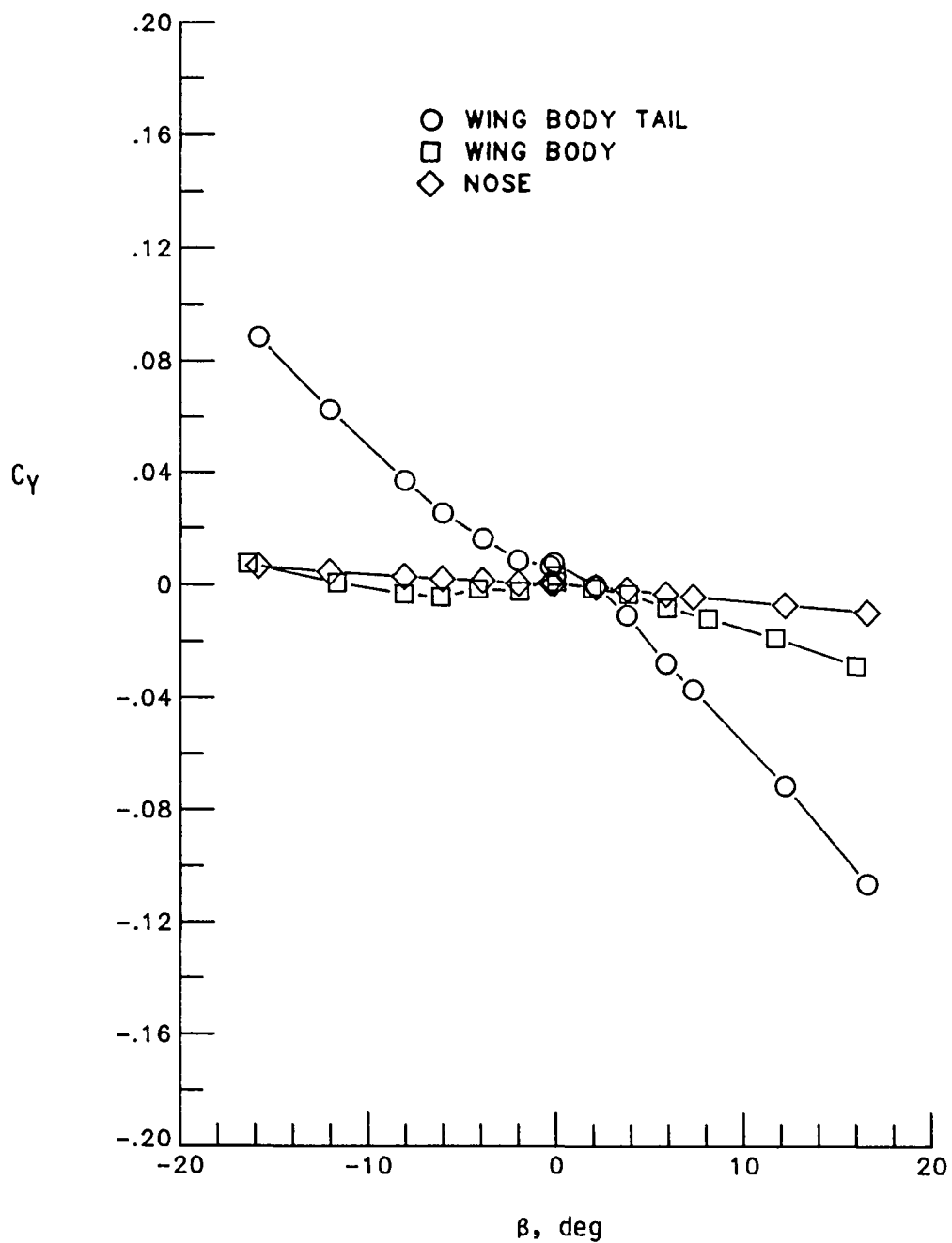
Figure 12.- Effect of vertical tail and nose on the side-force
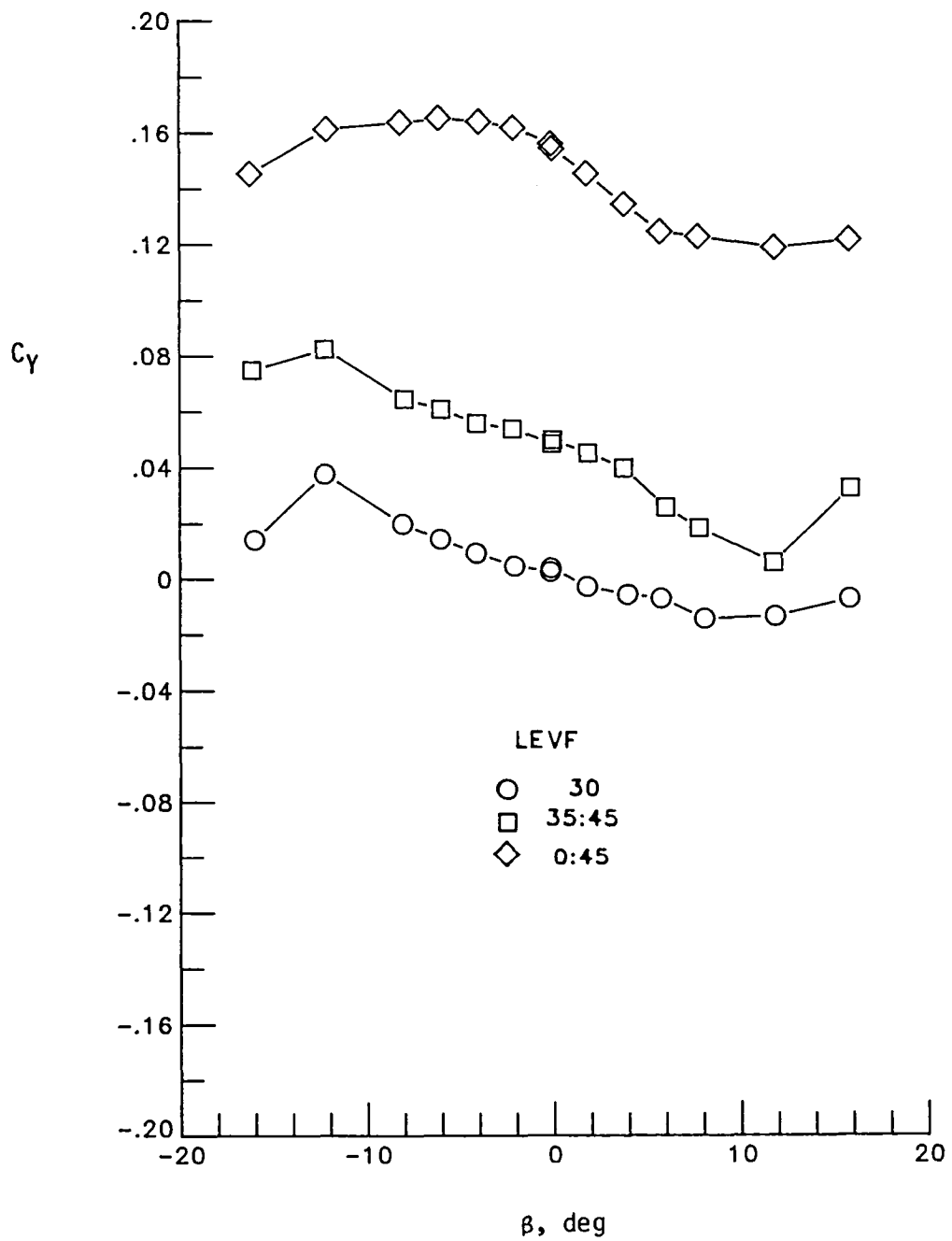characteristics with $\delta_{LE} = 0°$.

(b) $\alpha = 15^0$
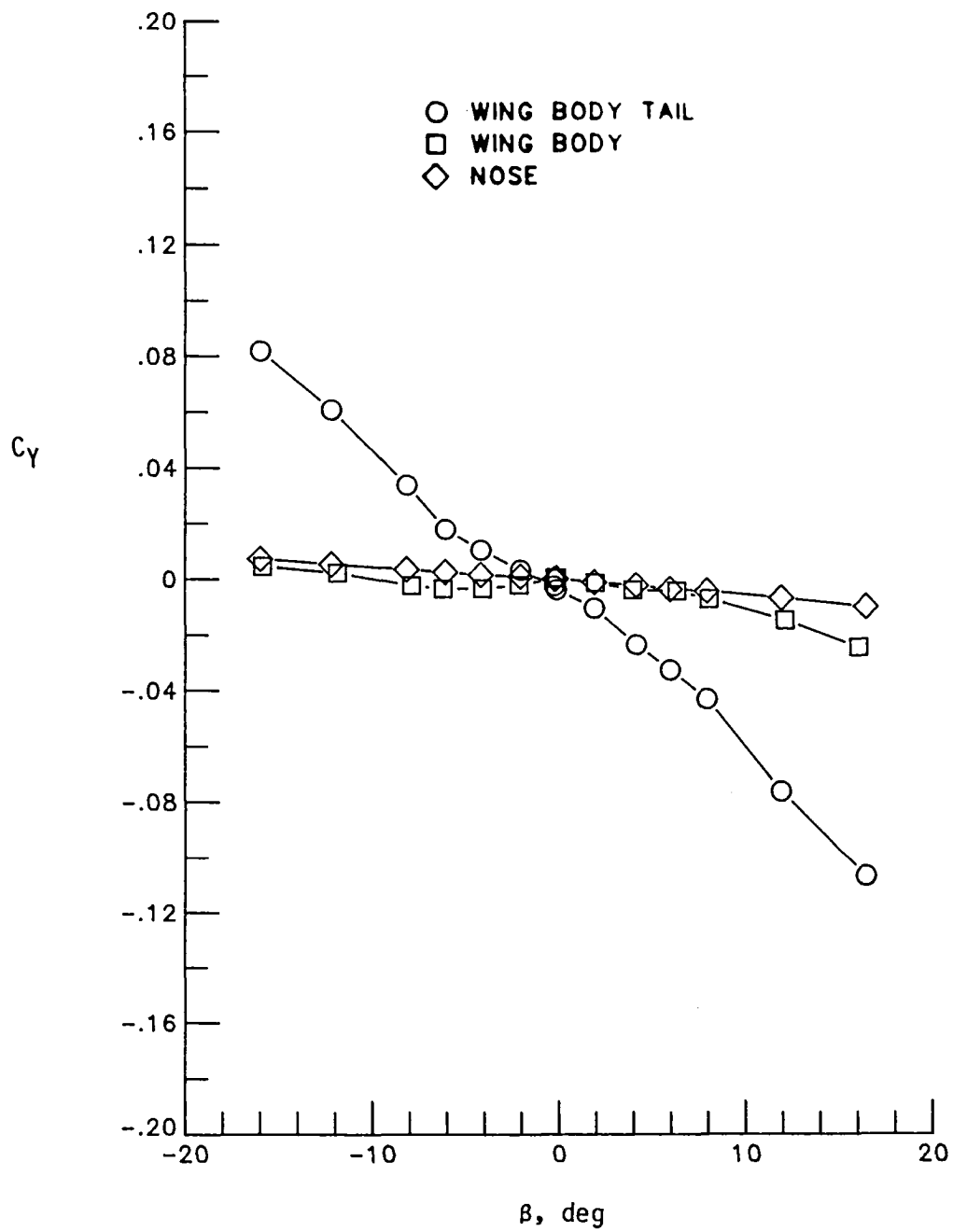
Figure 12.- Continued
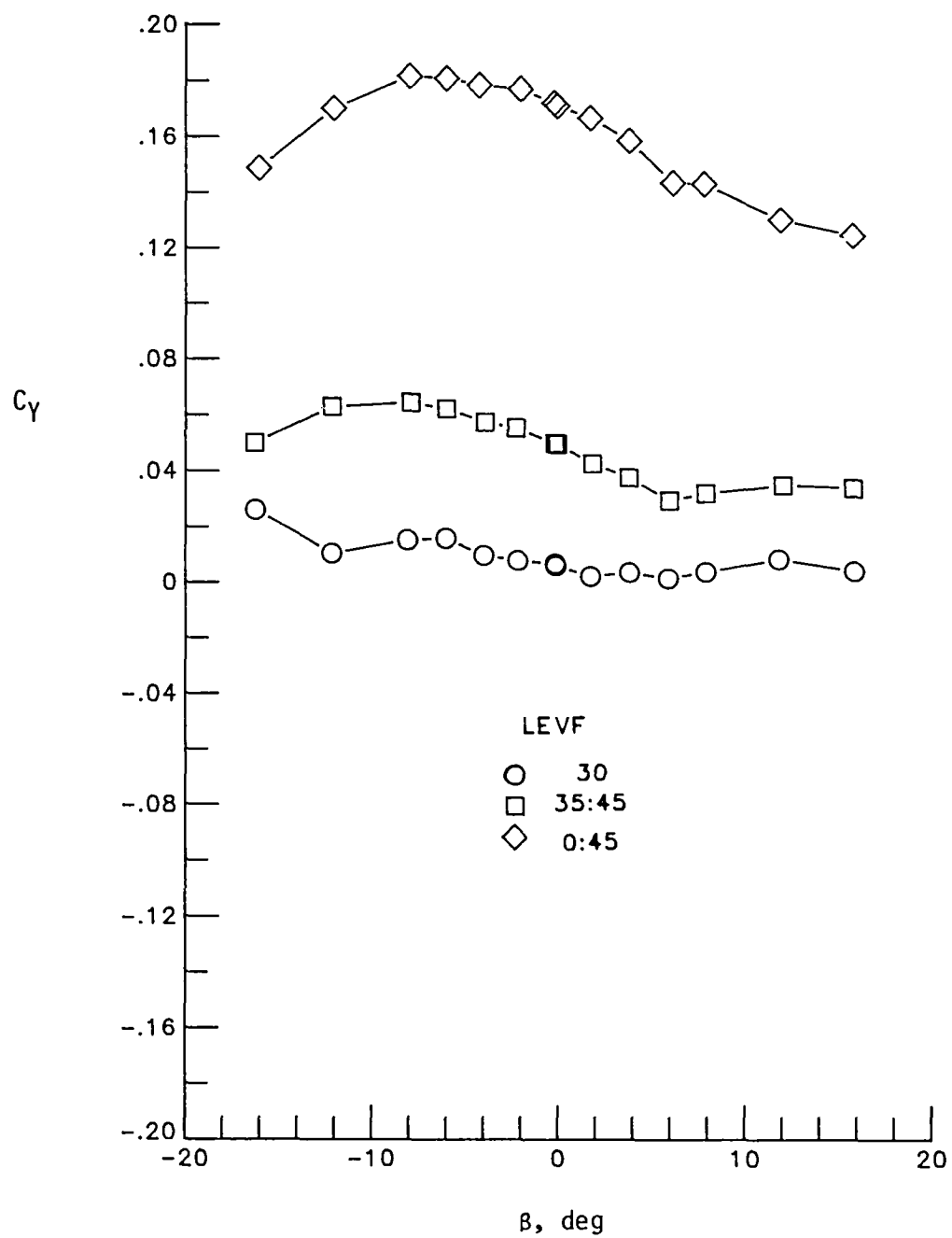
(c) $\alpha = 25^0$
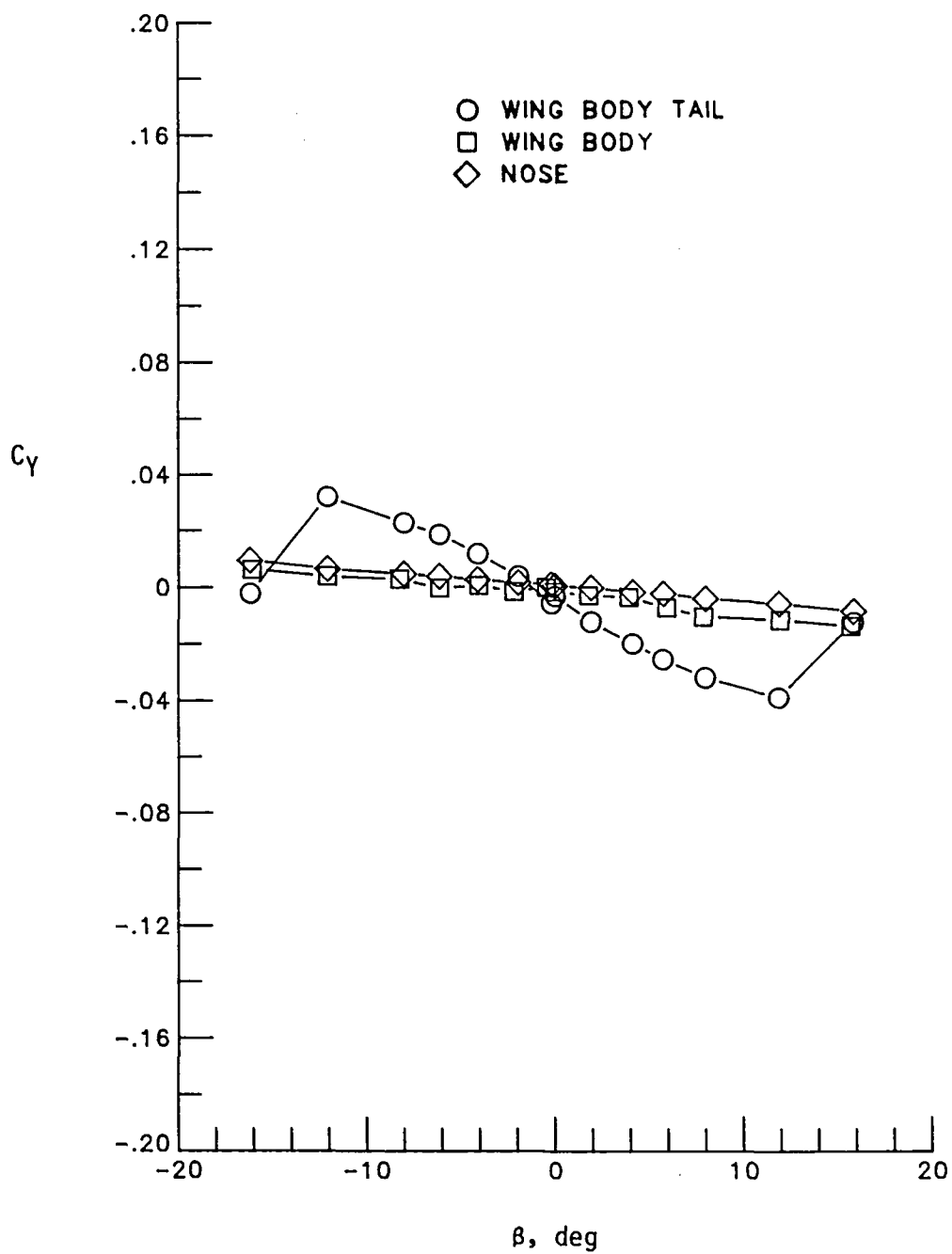
Figure 12.- Continued

(d) $\alpha = 30^0$
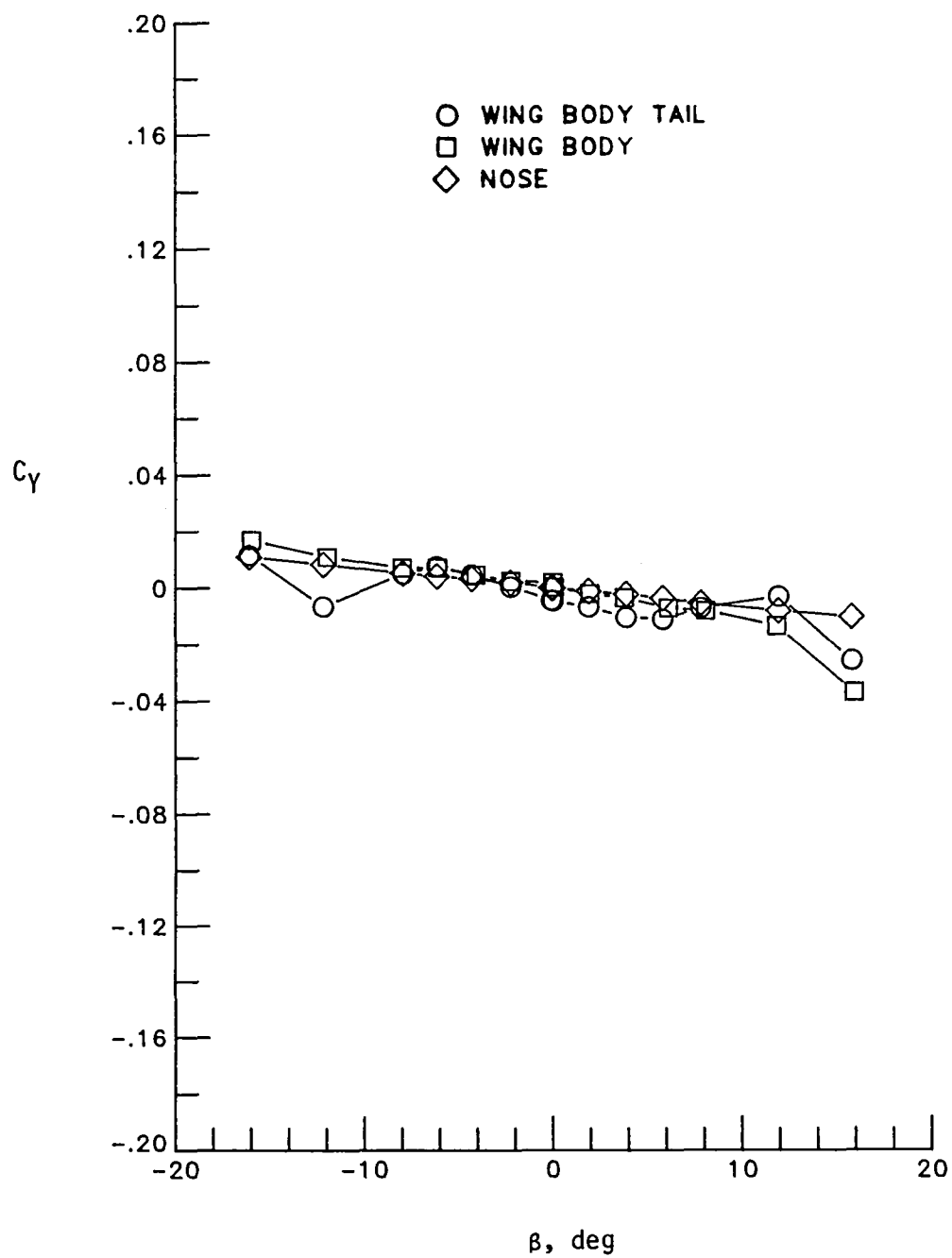
Figure 12.- Continued

(e) $\alpha = 35^0$
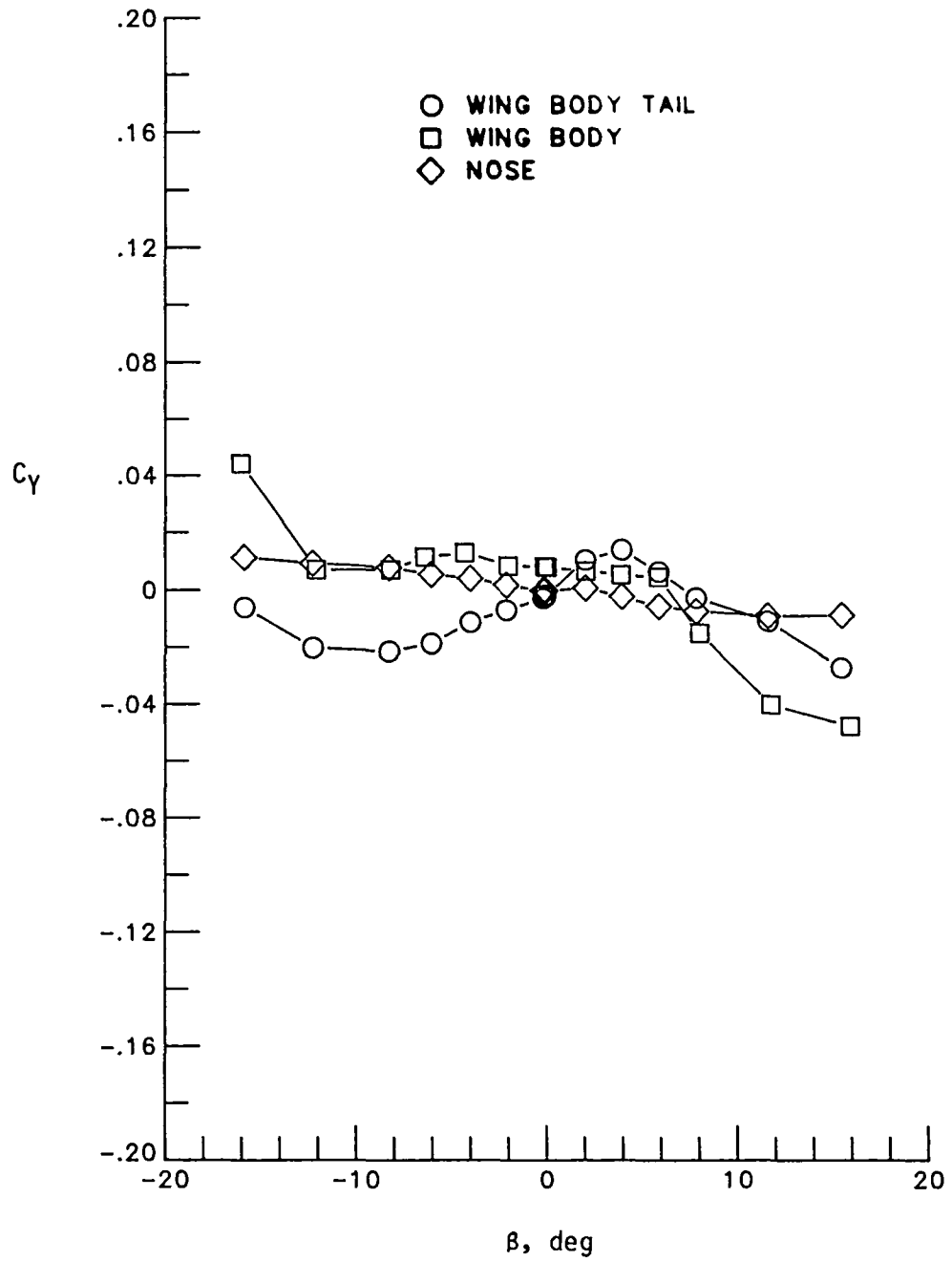
Figure 12.- Concluded.
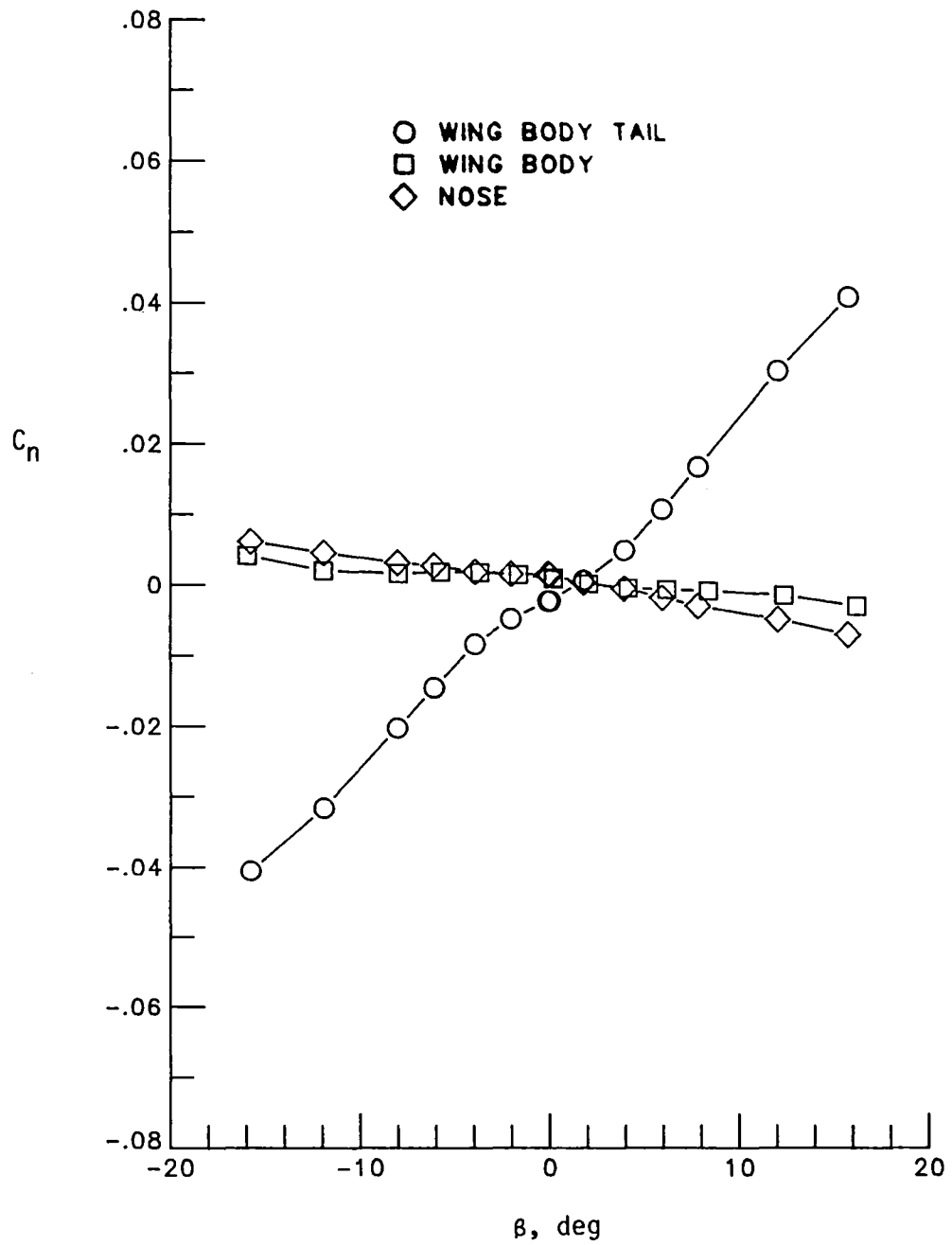
(a) $\alpha = 5^0$

Figure 13.- Effect of vertical tail and nose on the yawing moment characteristics with $\delta_{LE} = 40°$.

(b) $\alpha = 15^0$
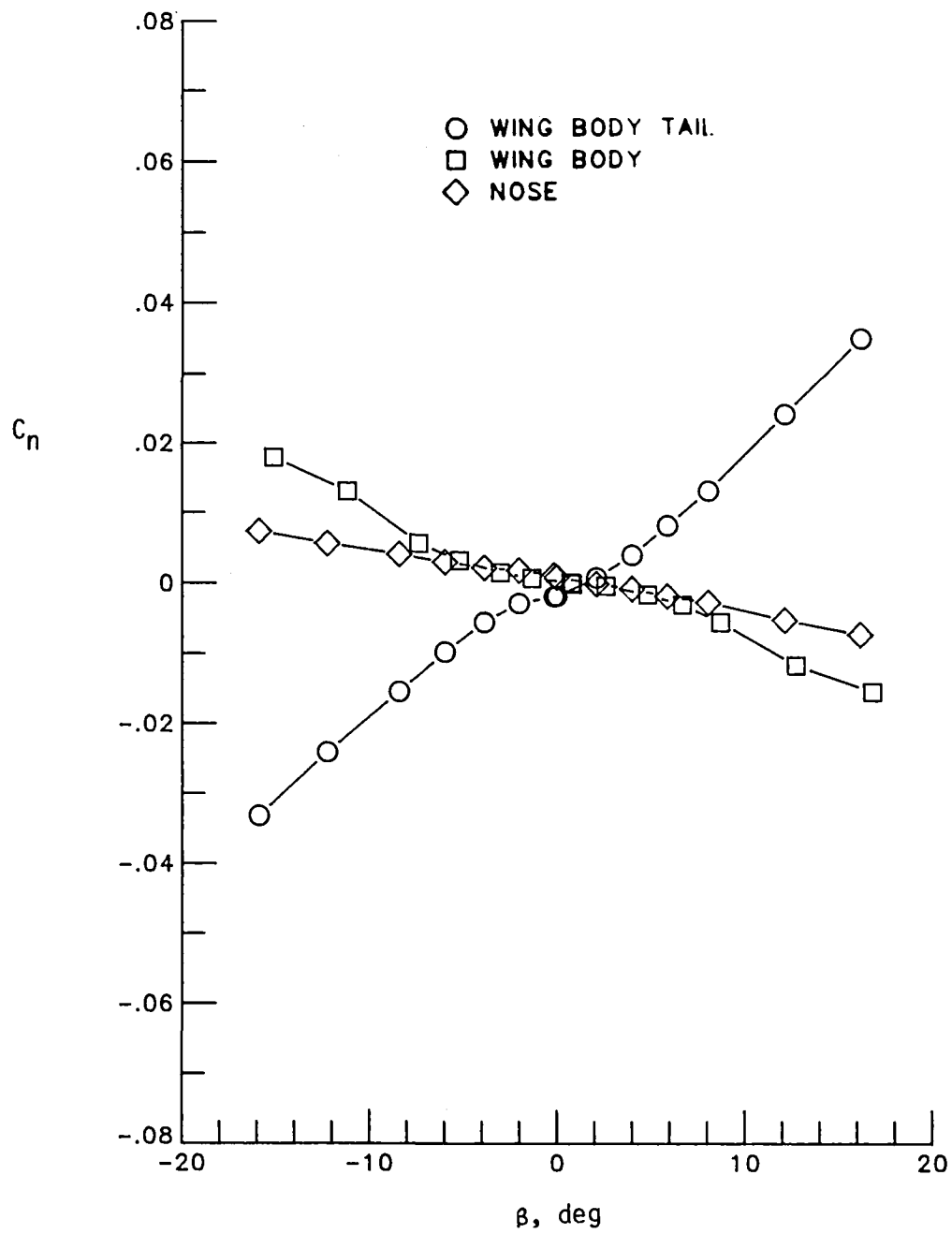
Figure 13.- Continued

(c) $\alpha = 25^0$
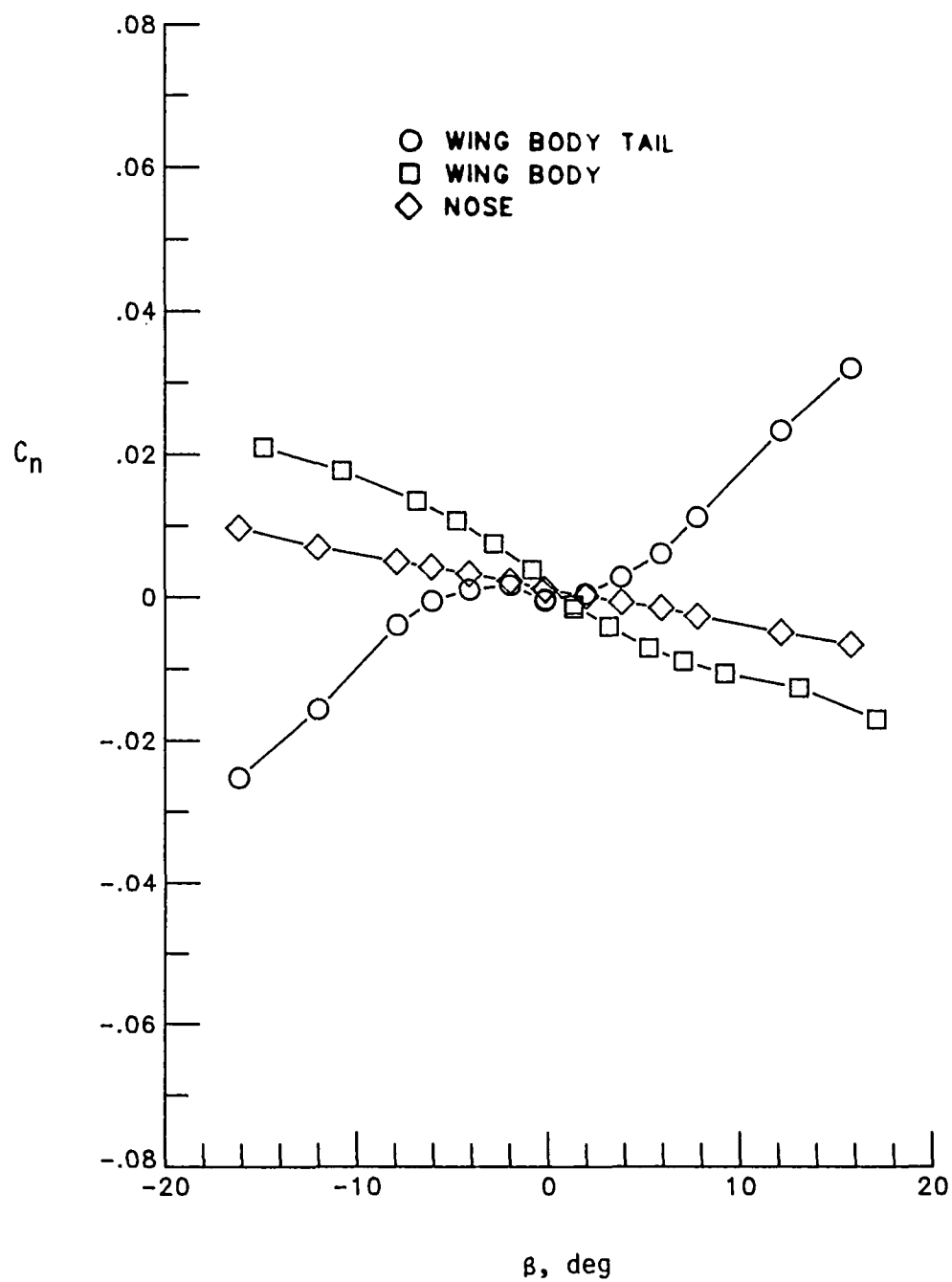
Figure 13.- Continued

(d) $\alpha = 30^0$
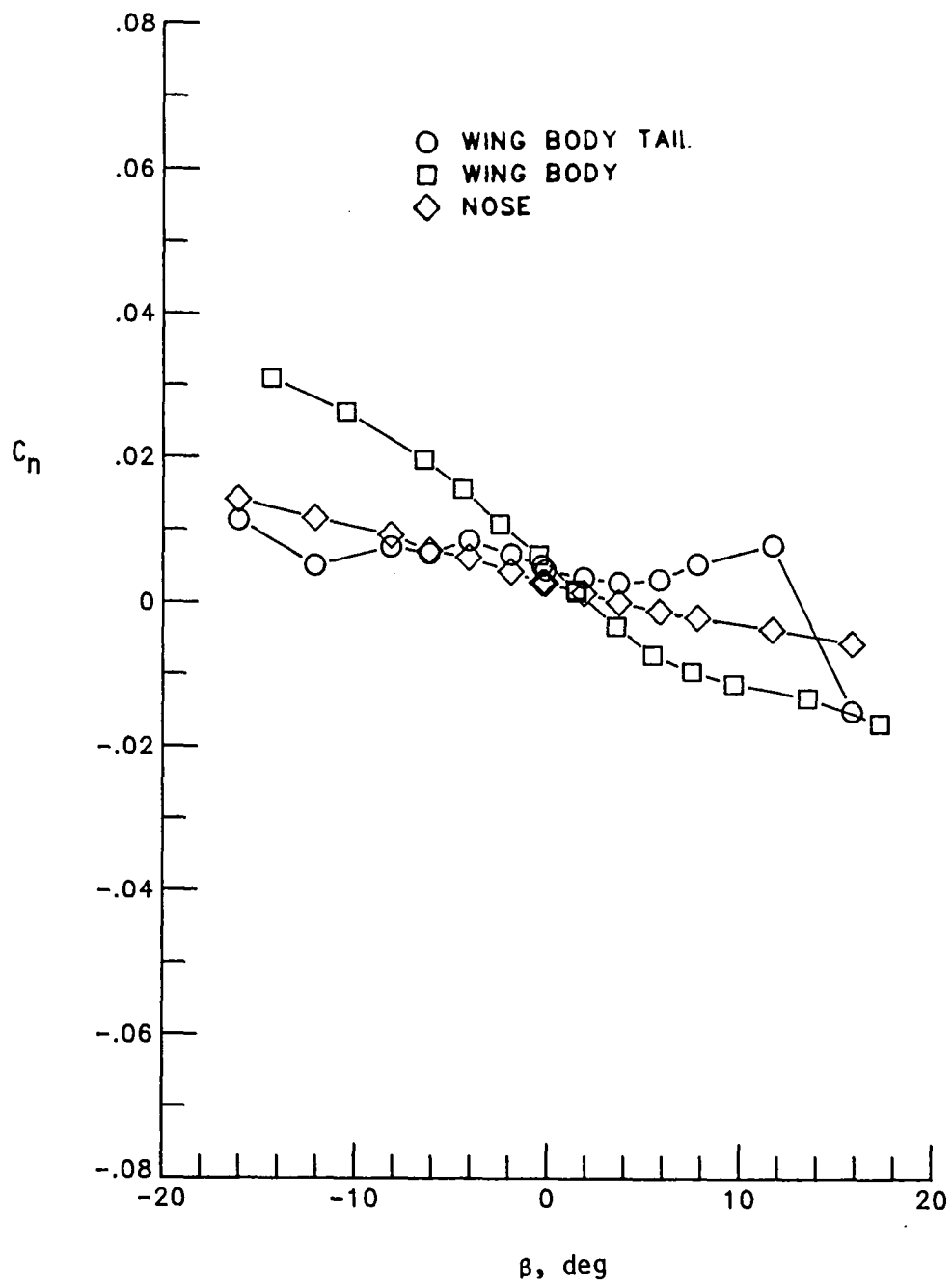
Figure 13.- Continued

(e) $\alpha = 35^0$
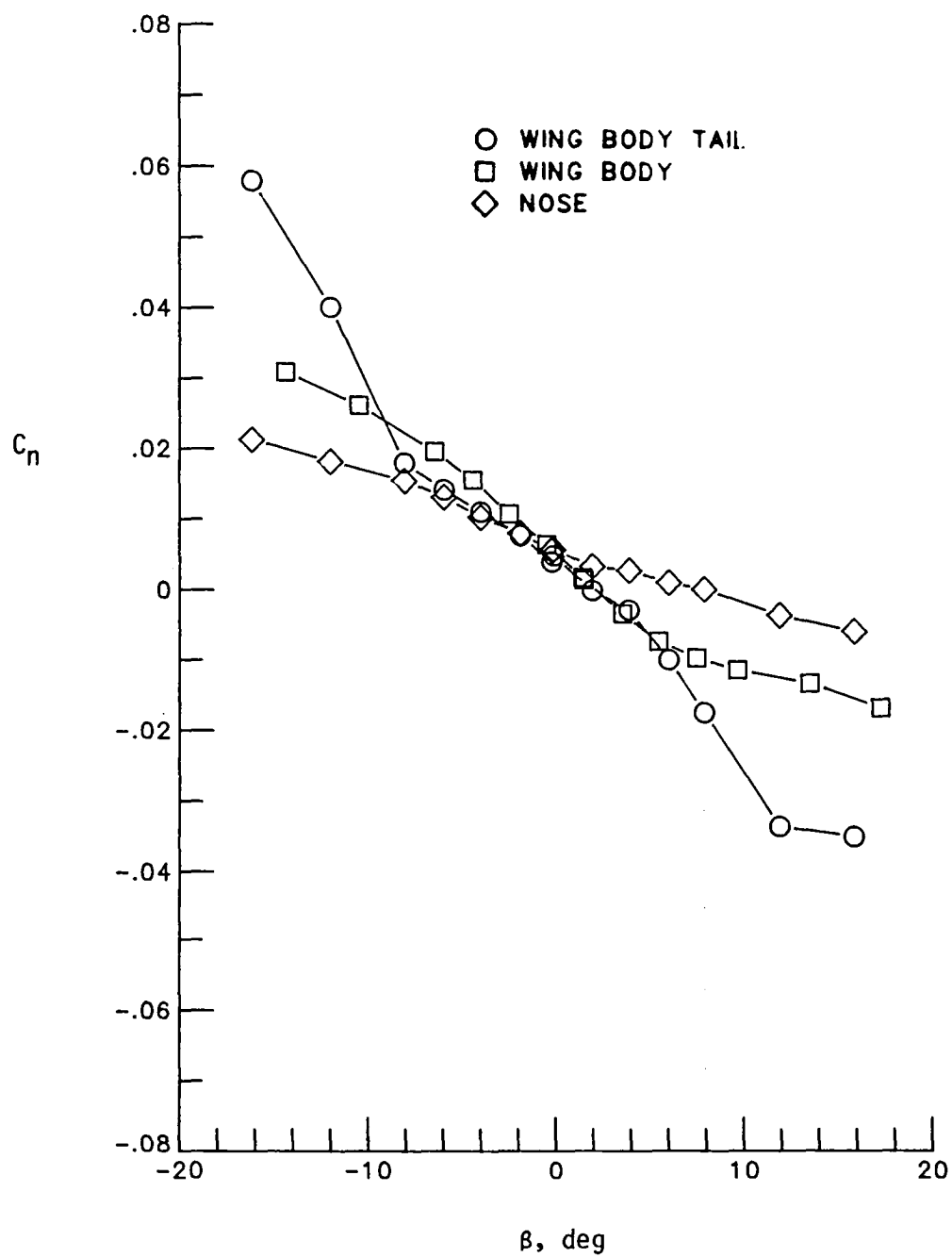
Figure 13.- Concluded.

(a) $\alpha = 5^0$
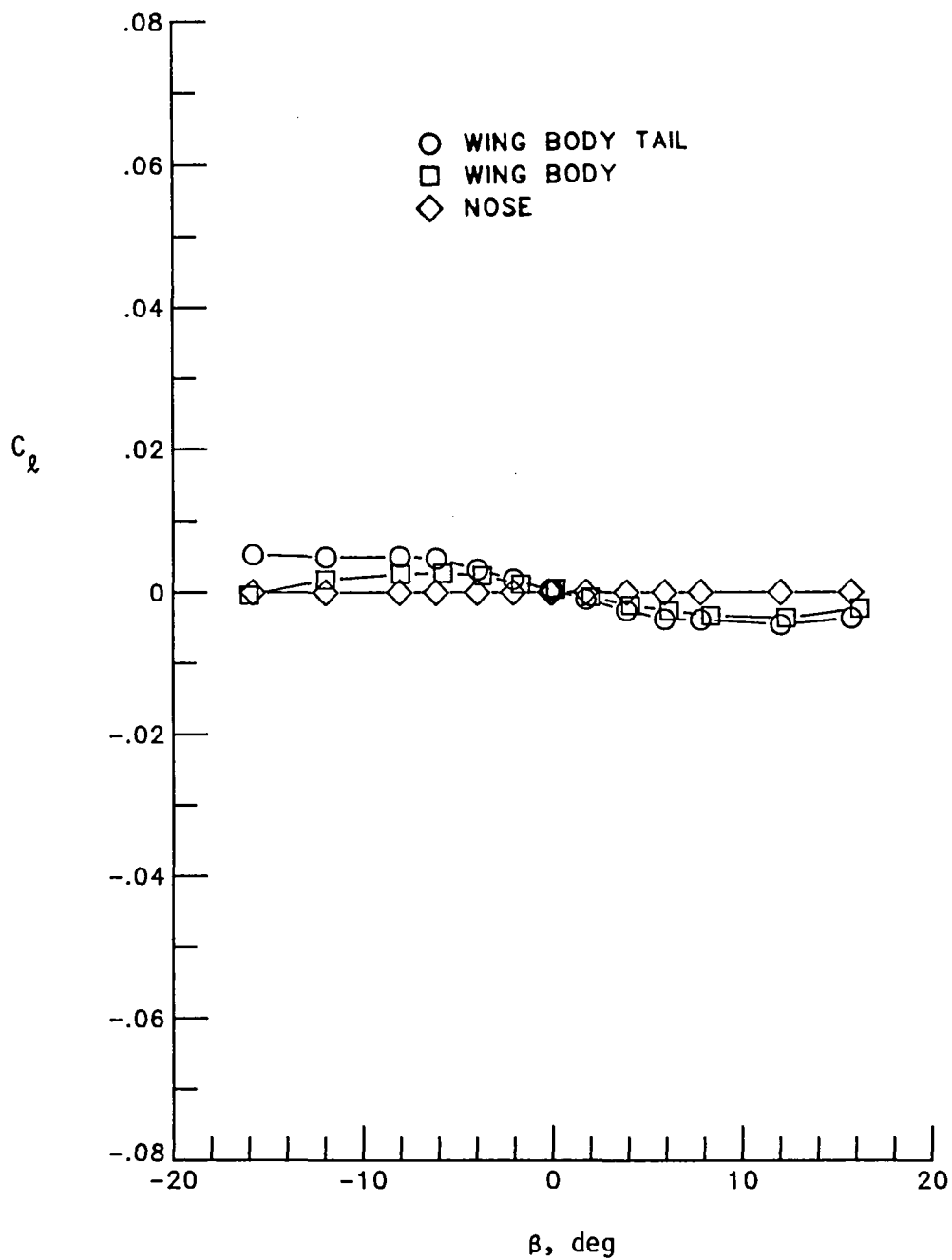
Figure 14.- Effect of vertical tail and nose on the rolling moment characteristics with $\delta_{LE} = 40°$.

(b) $\alpha = 15^0$
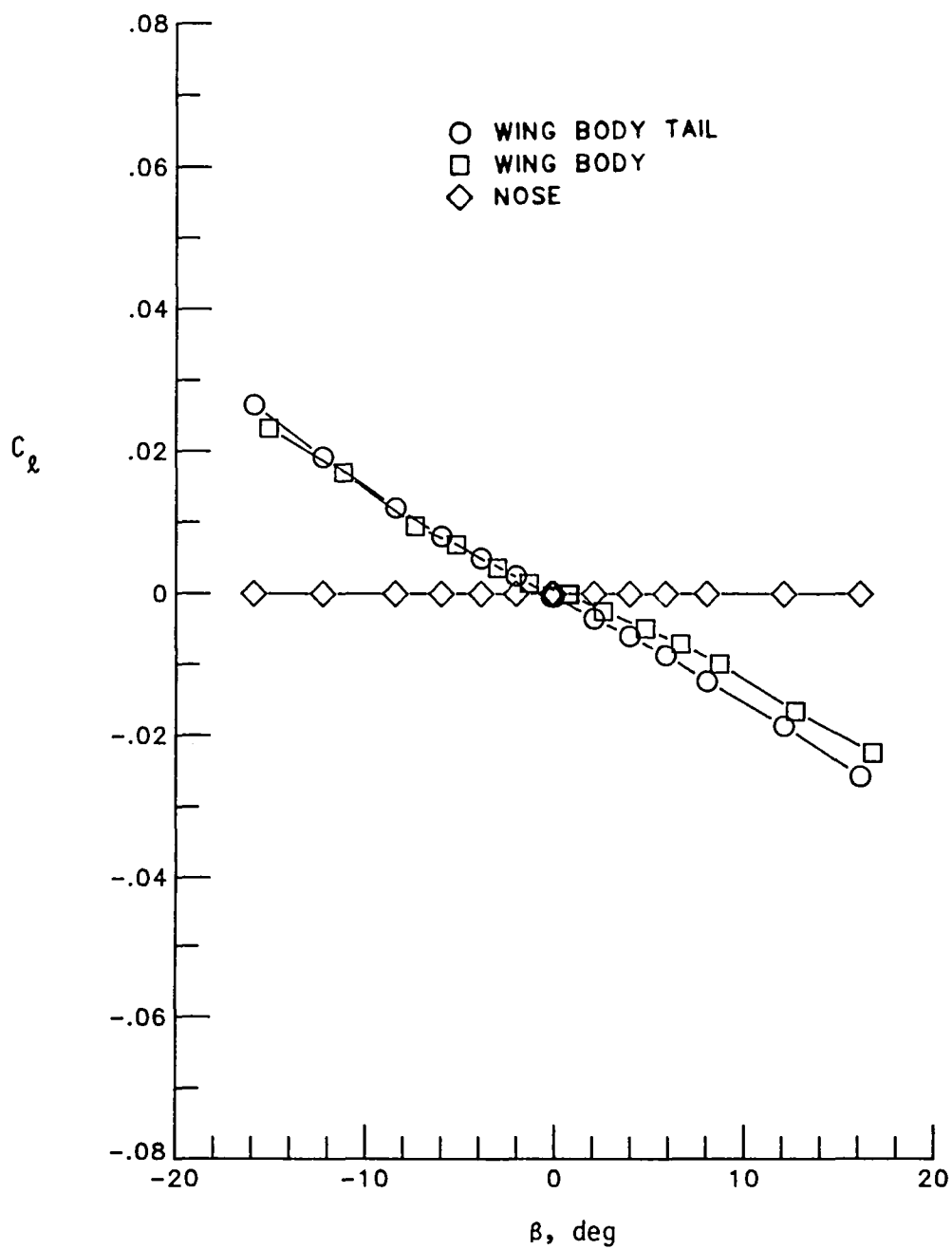
Figure 14.- Continued

(c) $\alpha = 25^0$
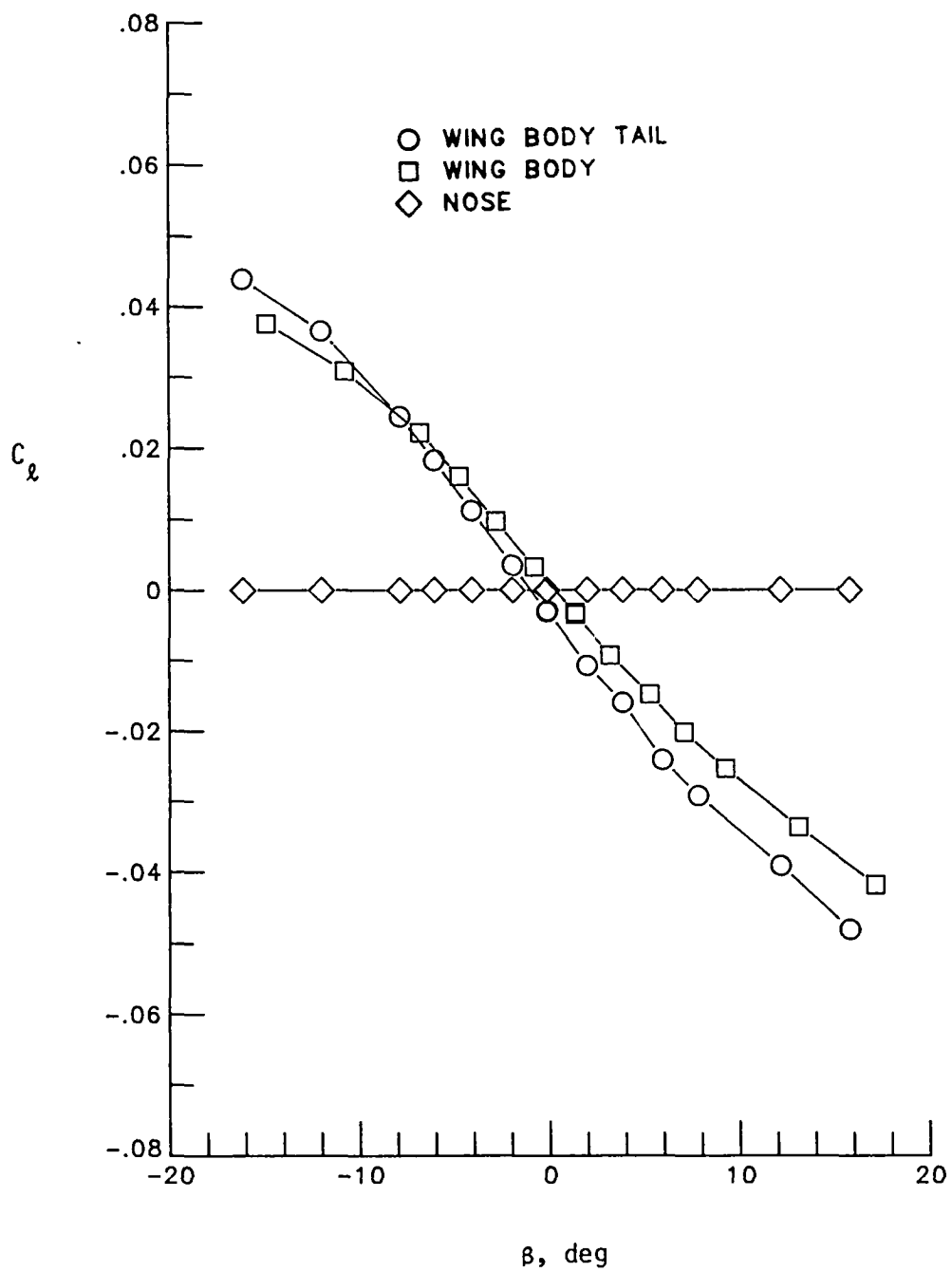
Figure 14.- Continued

(d) $\alpha = 30^0$
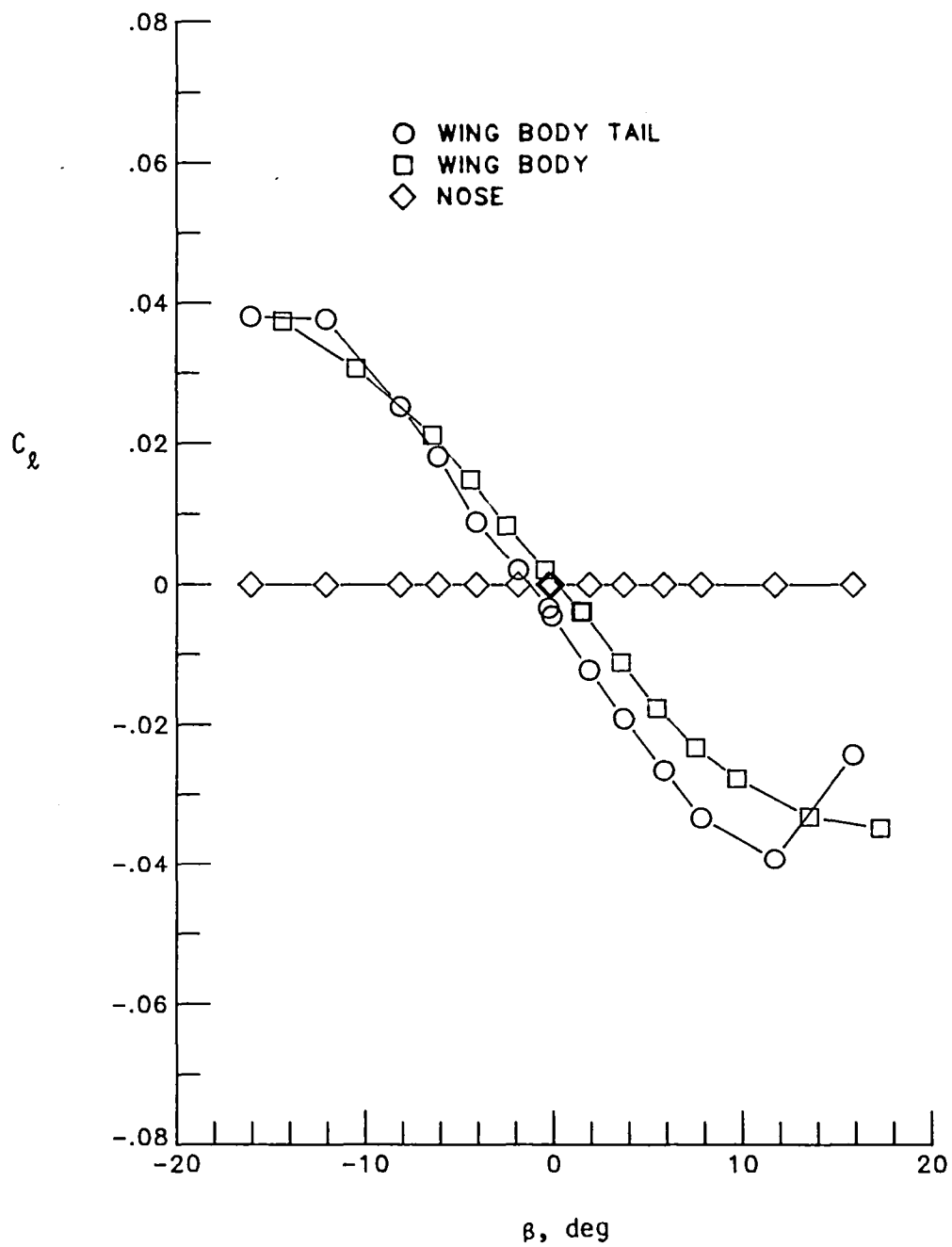
Figure 14.- Continued

(e) $\alpha = 35^0$
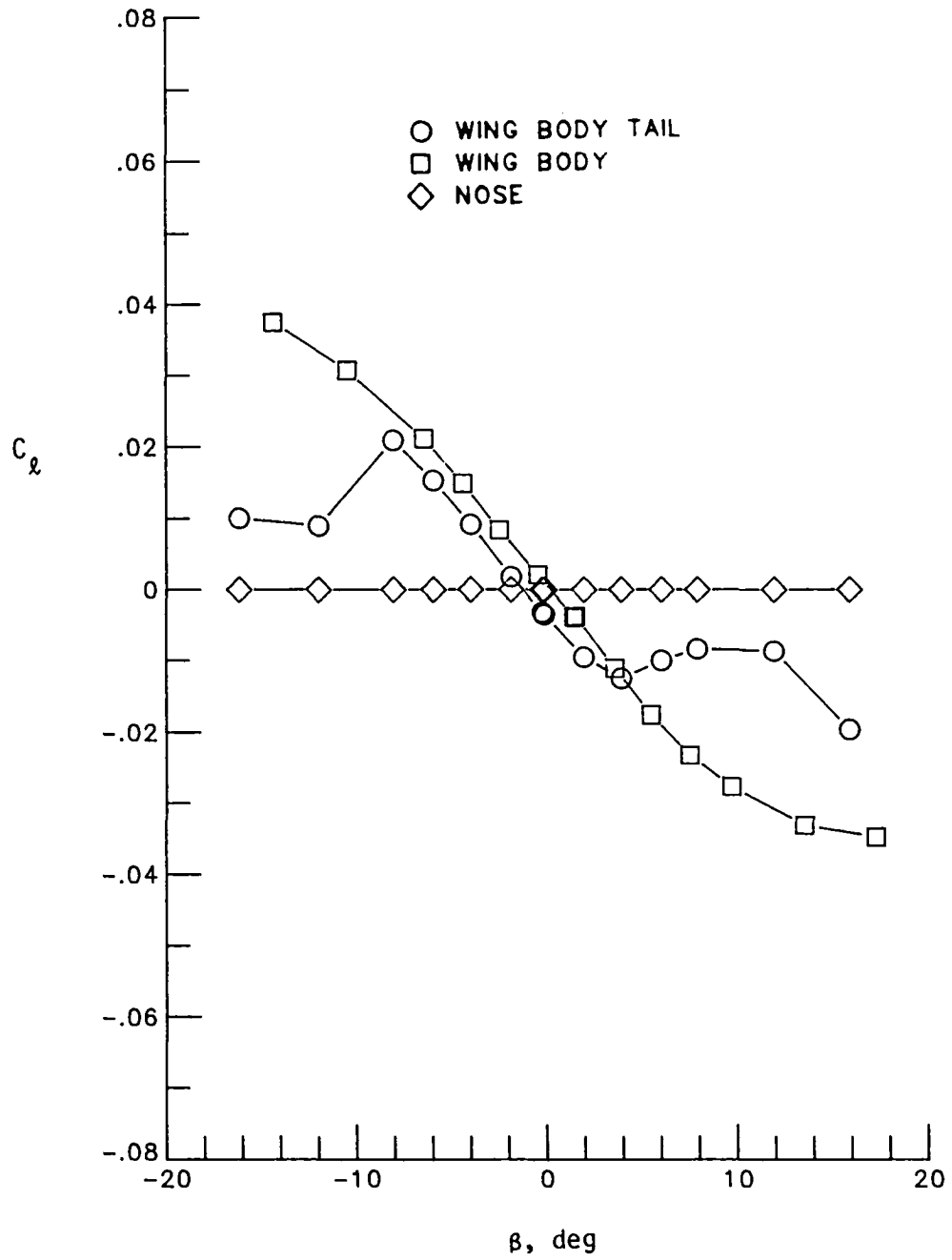
Figure 14.- Concluded.

(a) $\alpha = 5^0$
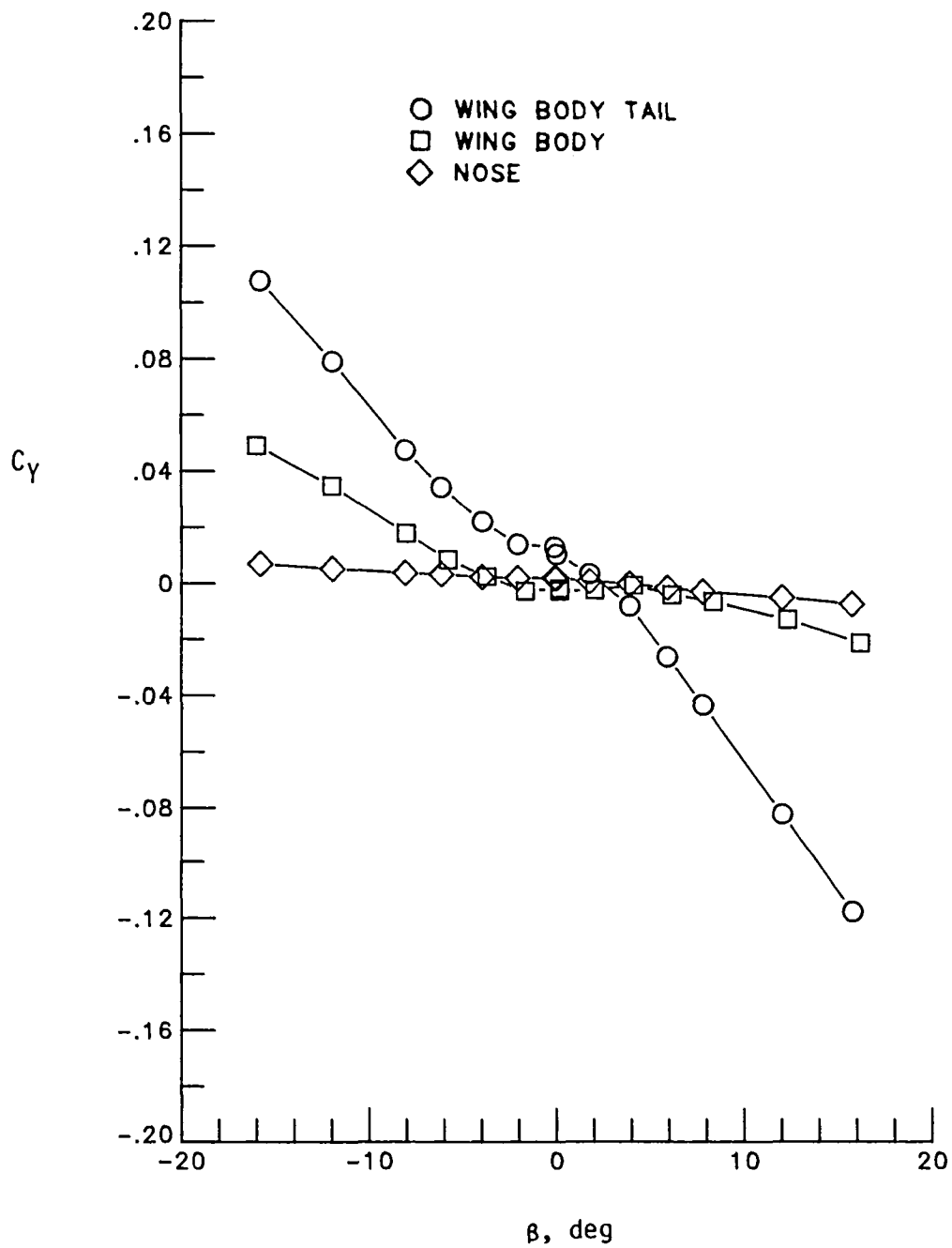
Figure 15.- Effect of vertical tail and nose on the side-force characteristics with $\delta_{LE} = 40°$.

(b) α = 15⁰
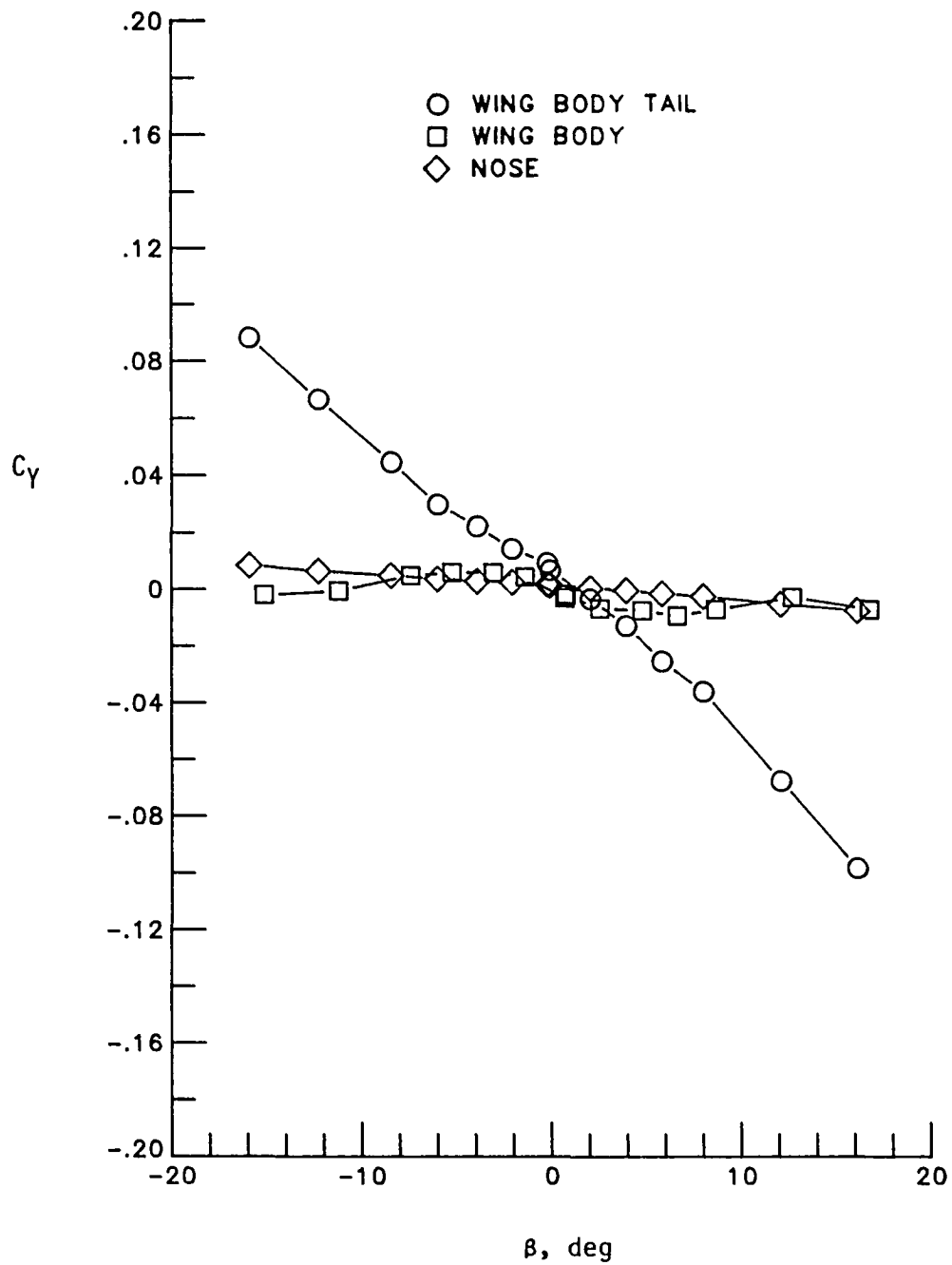
Figure 15.- Continued

(c) $\alpha = 25^0$
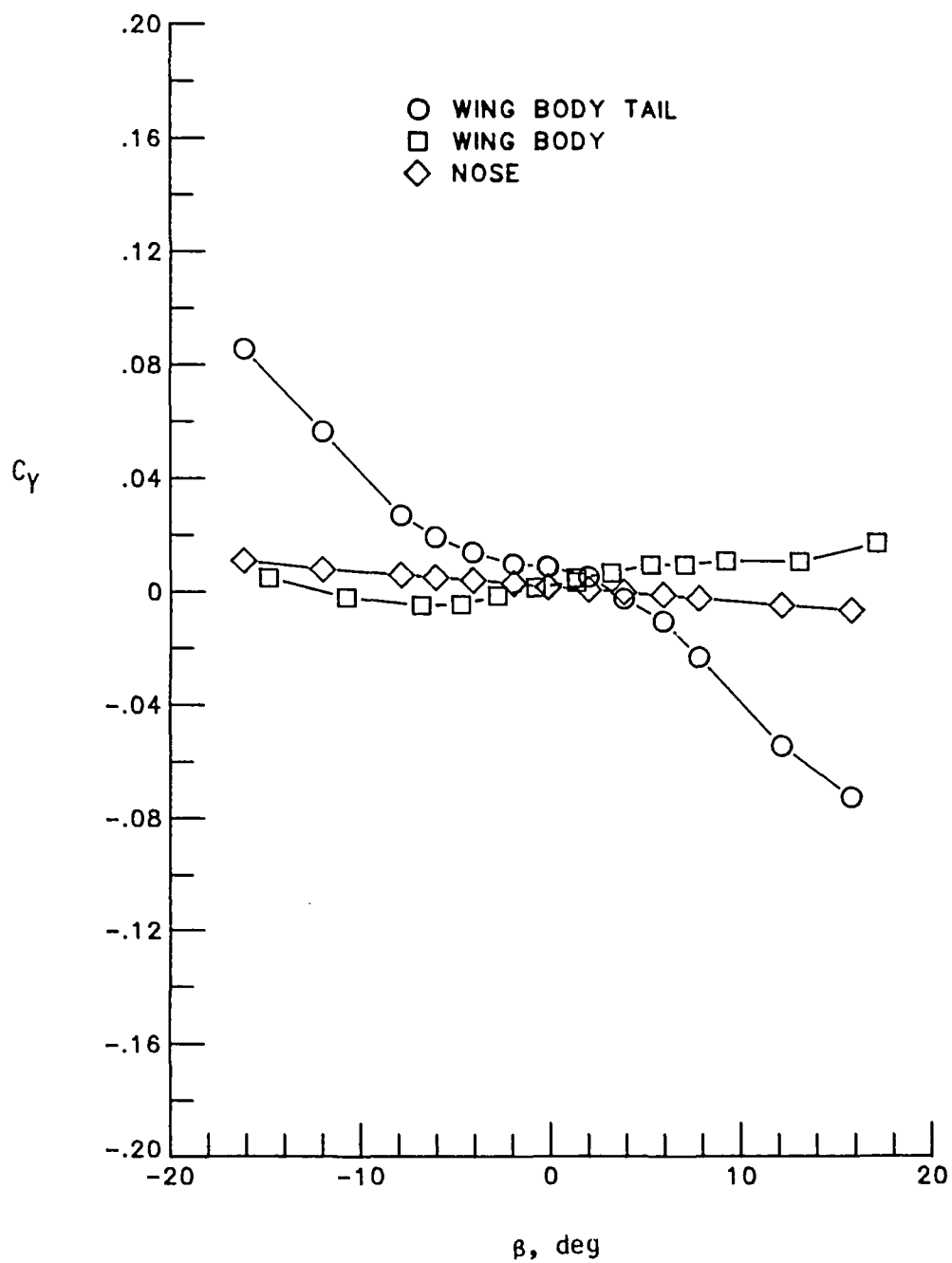
Figure 15.- Continued

(d) $\alpha = 30^0$
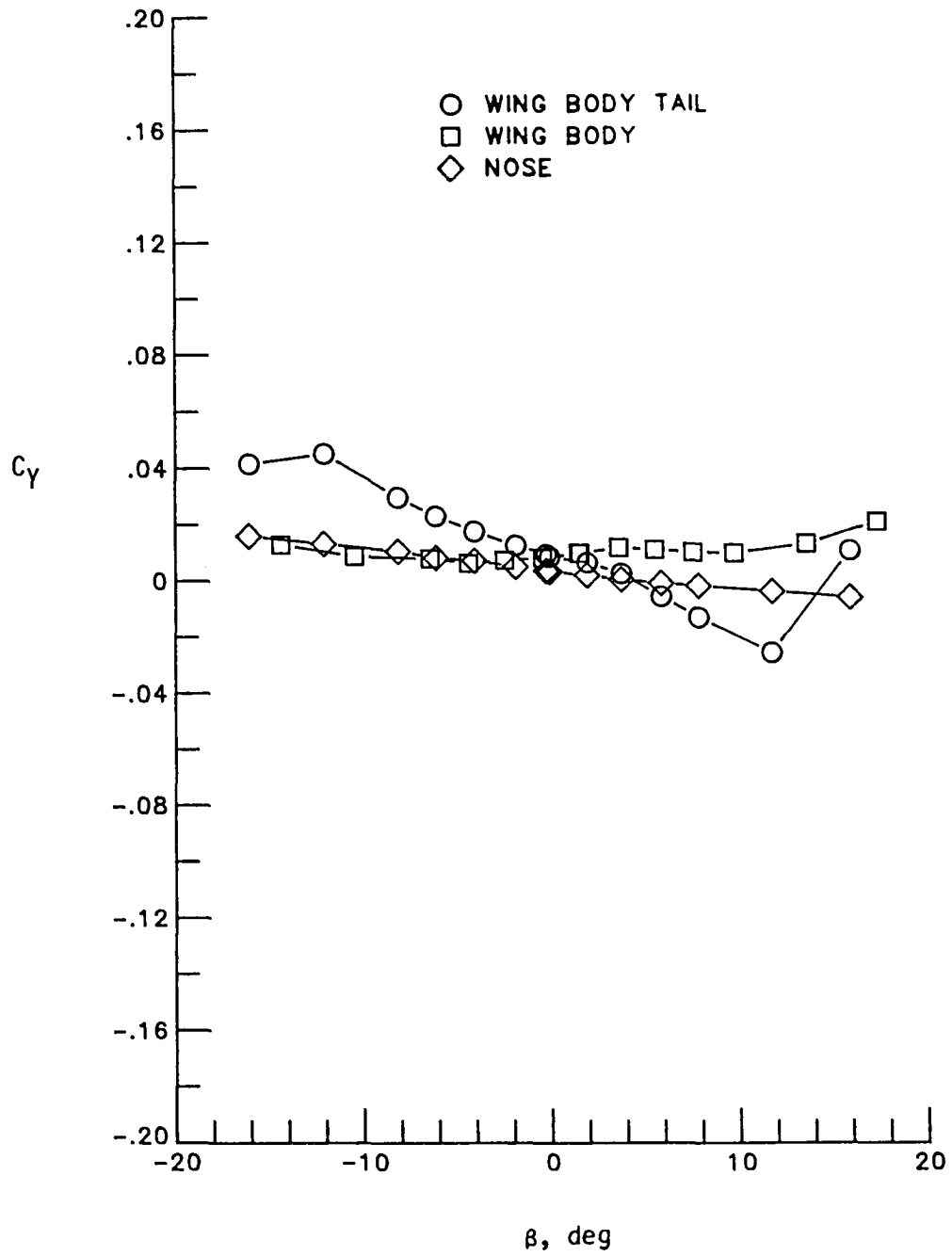
Figure 15.- Continued

(e) α = 35⁰
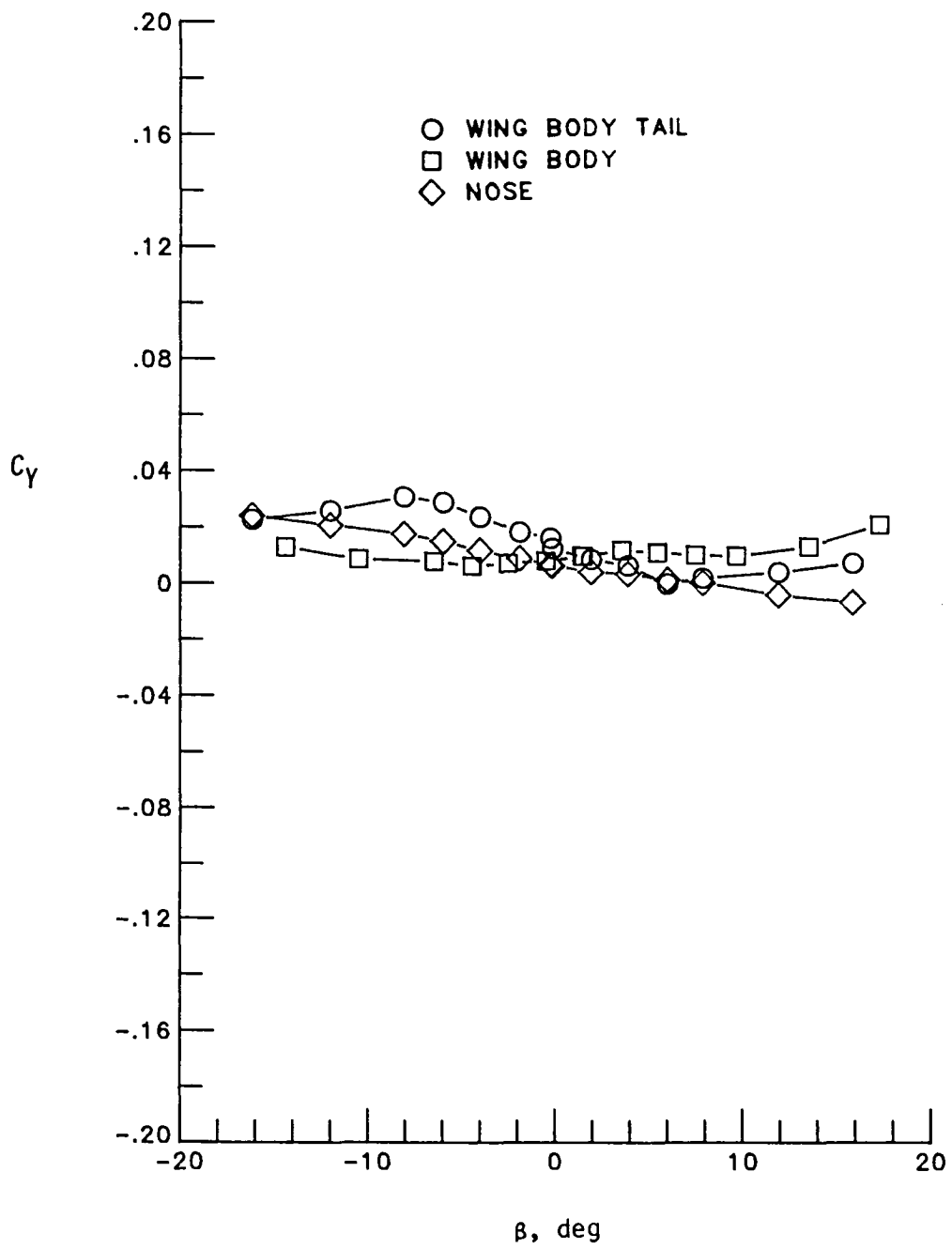
Figure 15.- Concluded.

(a) $\alpha = 5^0$
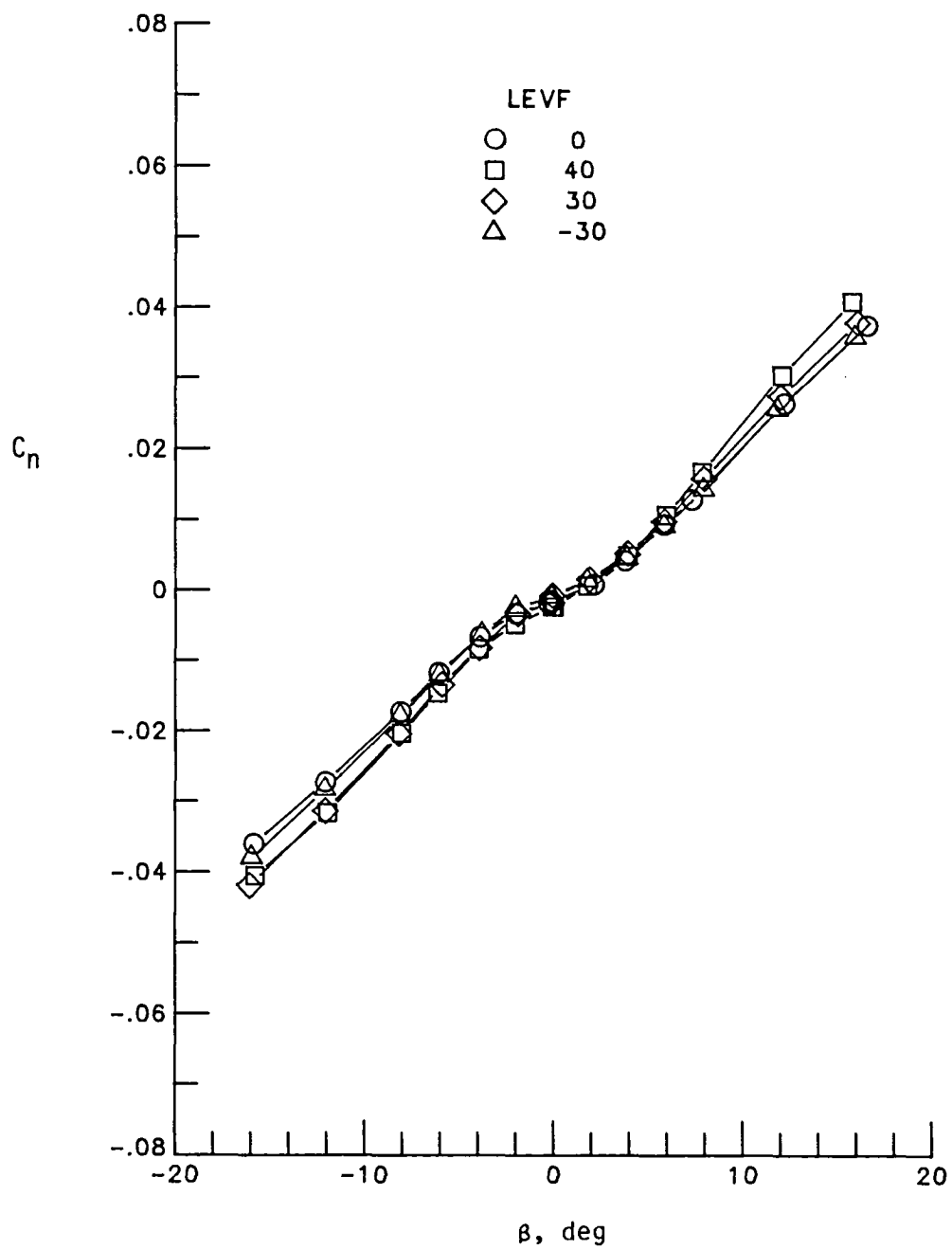
Figure 16.- Effect of LEVF deflection on yawing moment
characteristics.

(b) $\alpha = 15^0$
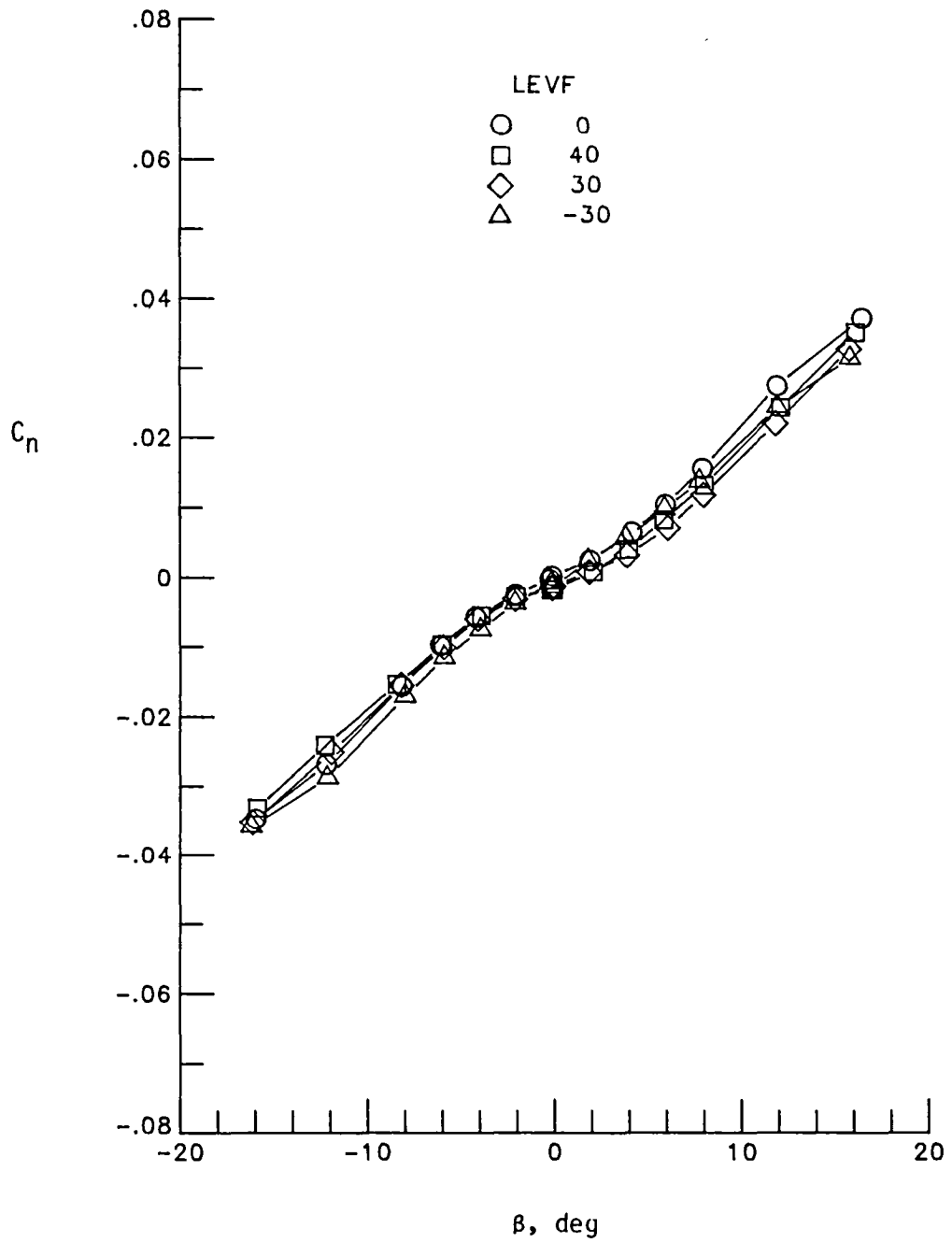
Figure 16.- Continued

(c) $\alpha = 25^0$
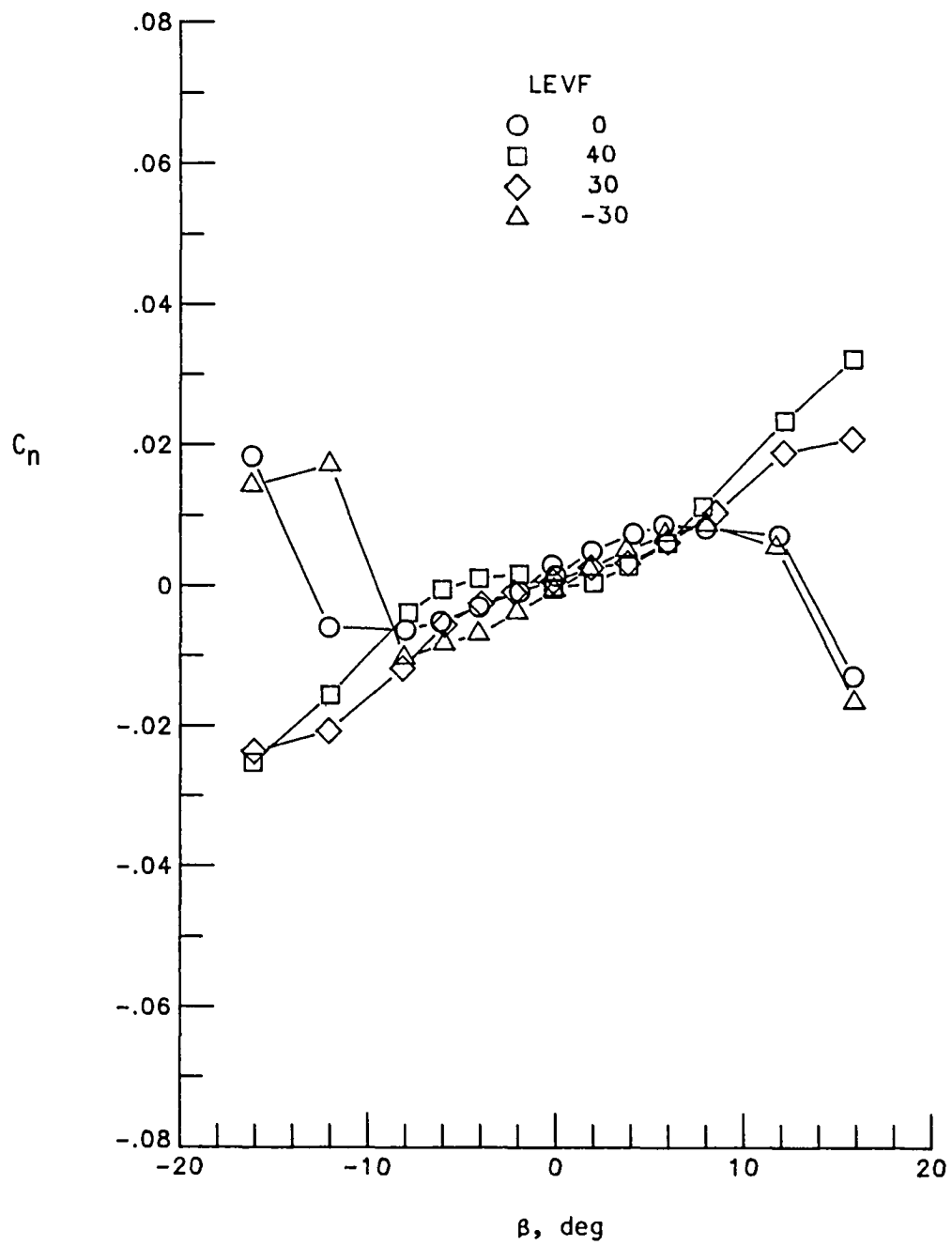
Figure 16.- Continued

(d) $\alpha = 30^0$
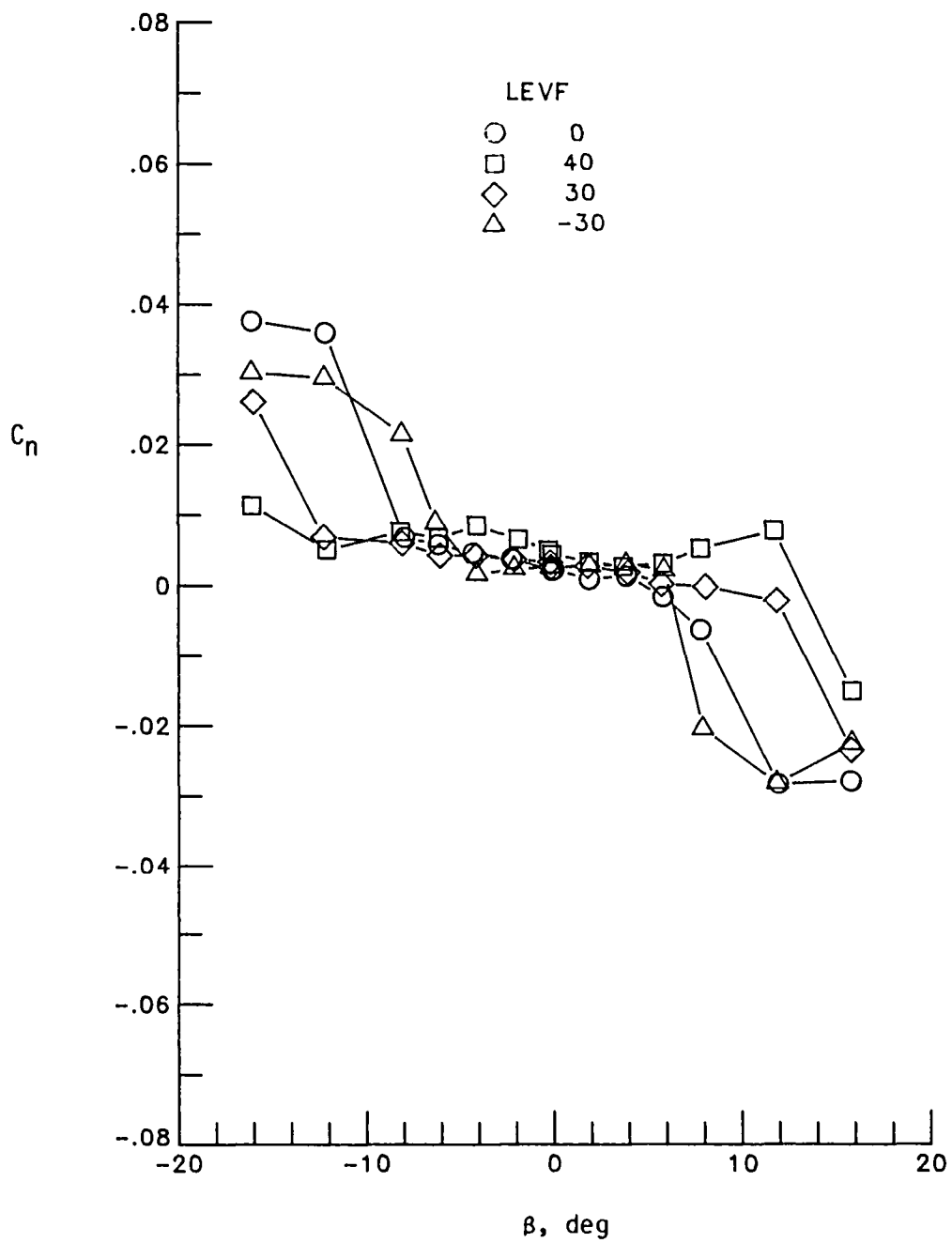
Figure 16.- Continued

(e) α = 35⁰
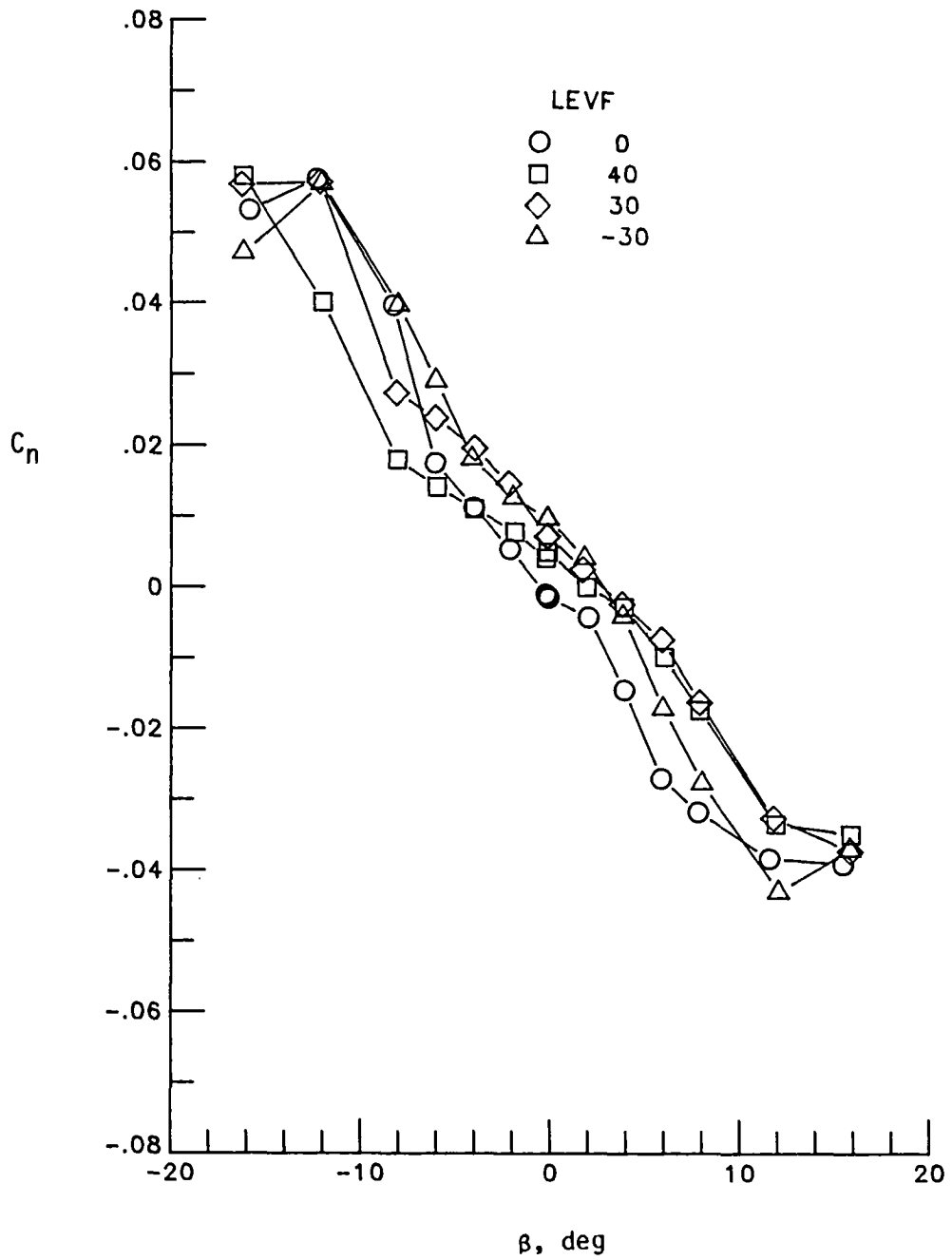
Figure 16.- Concluded.

(a) $\alpha = 5^0$
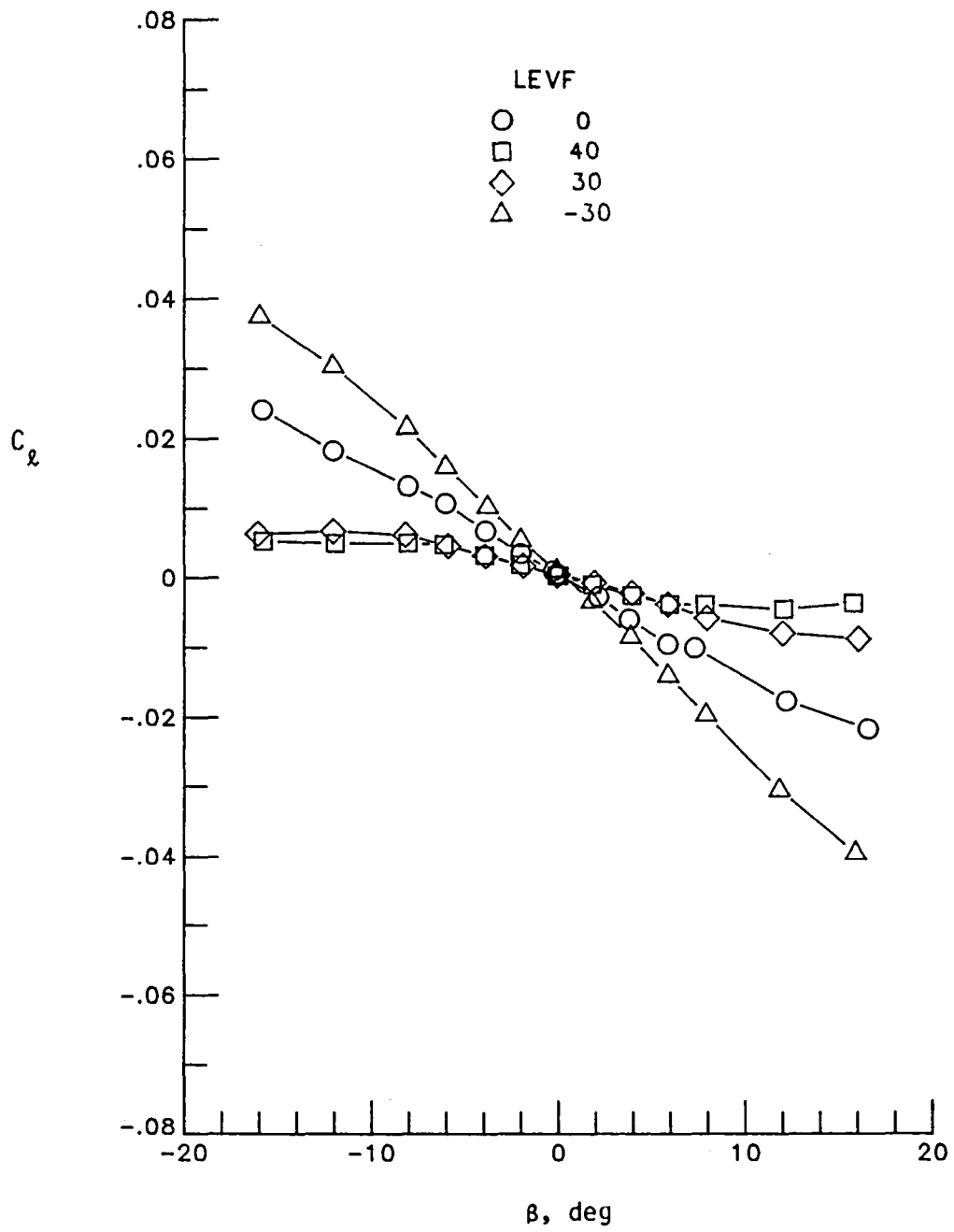
Figure 17.- Effect of LEVF deflection on rolling moment characteristics.

(b) $\alpha = 15^0$
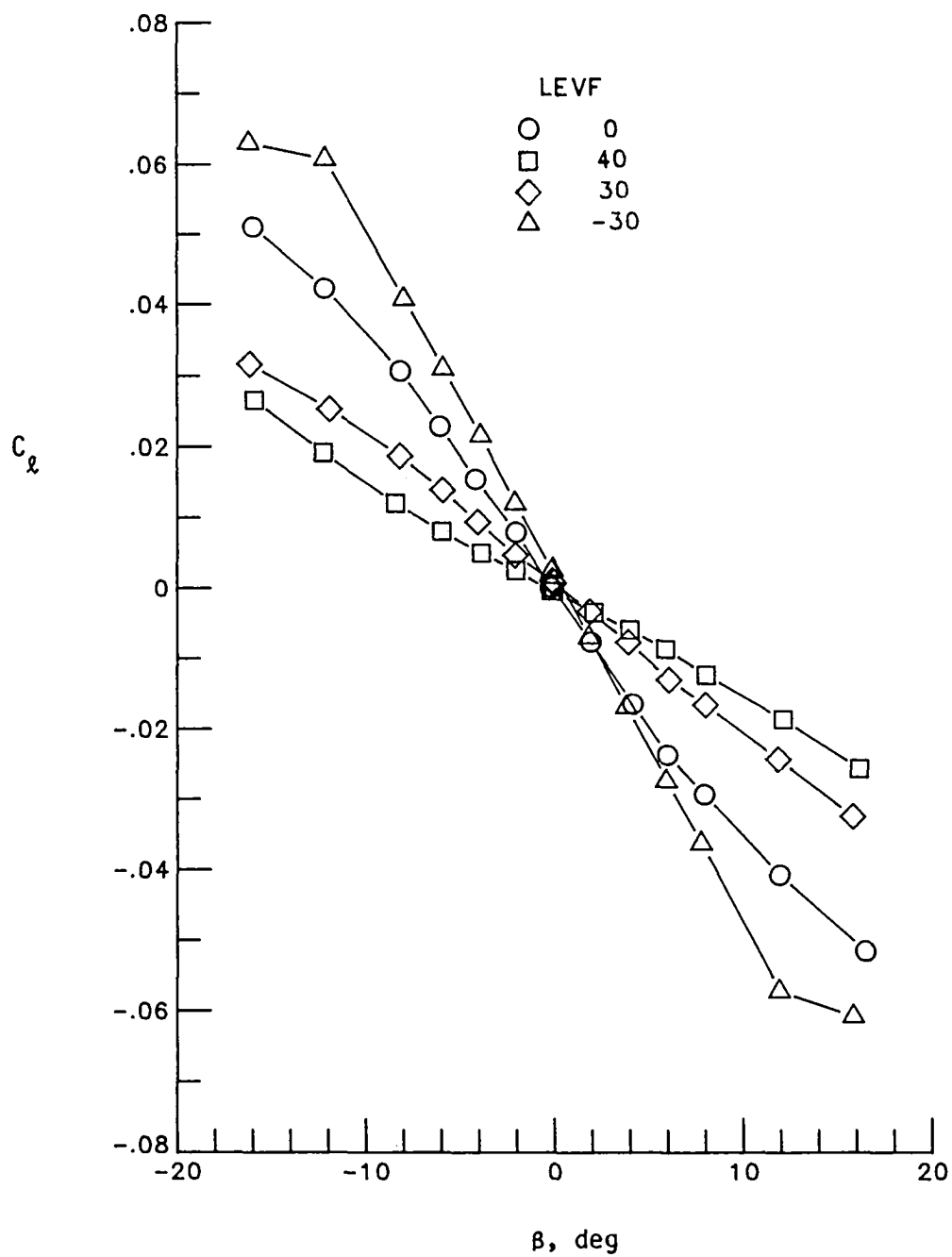
Figure 17.- Continued

(c) α = 25⁰
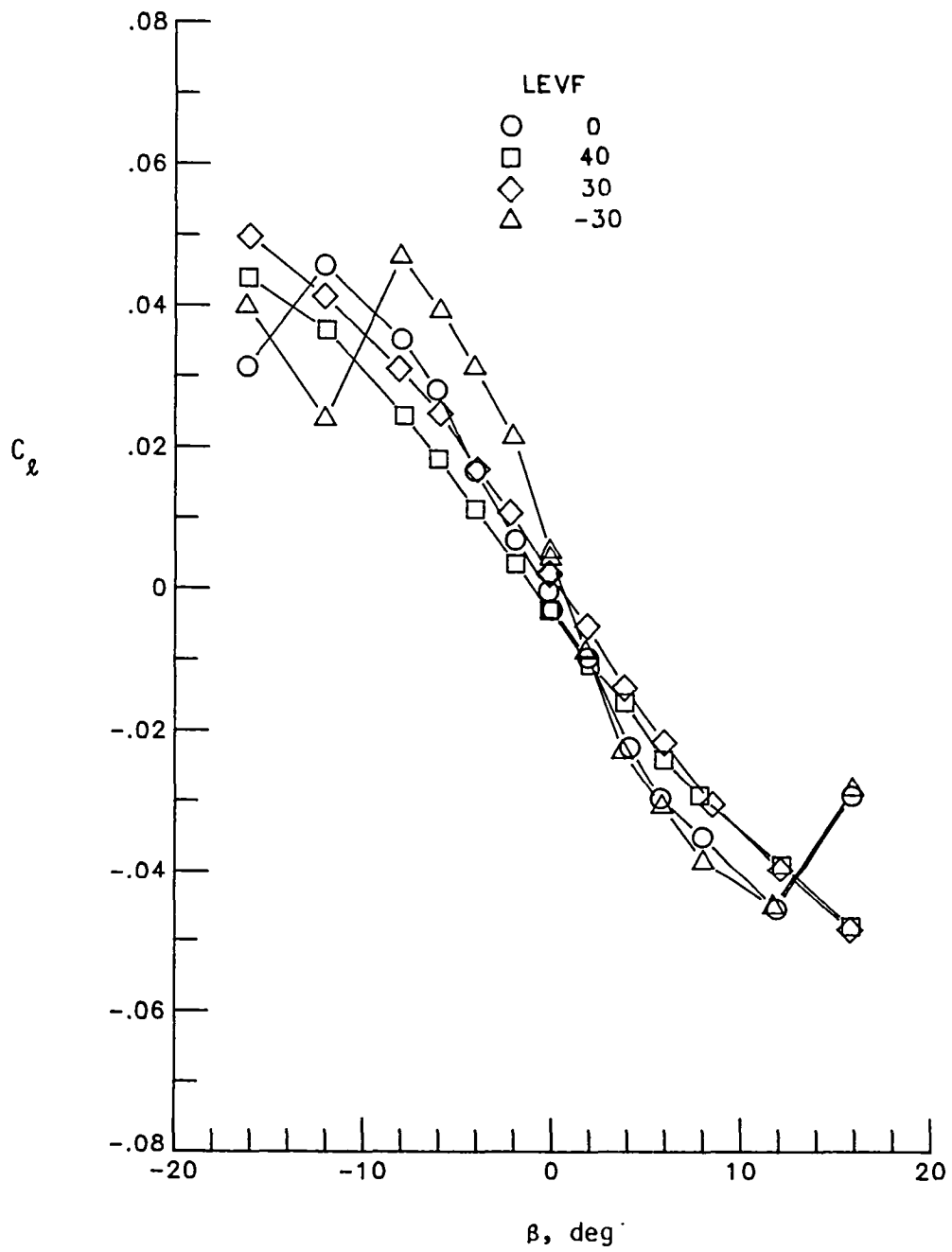
Figure 17.- Continued

(d) α = 30⁰
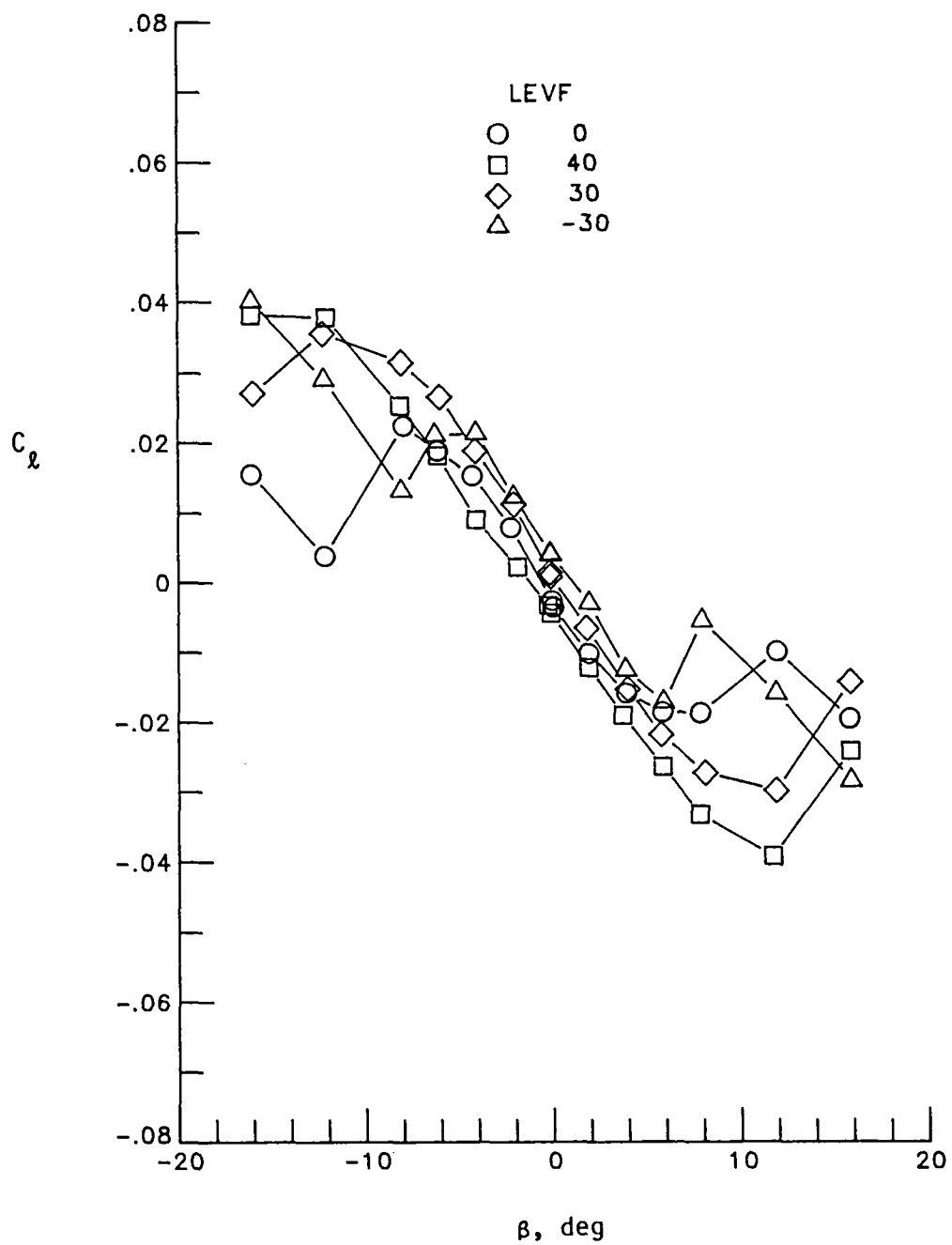
Figure 17.- Continued

(e) $\alpha = 35^0$
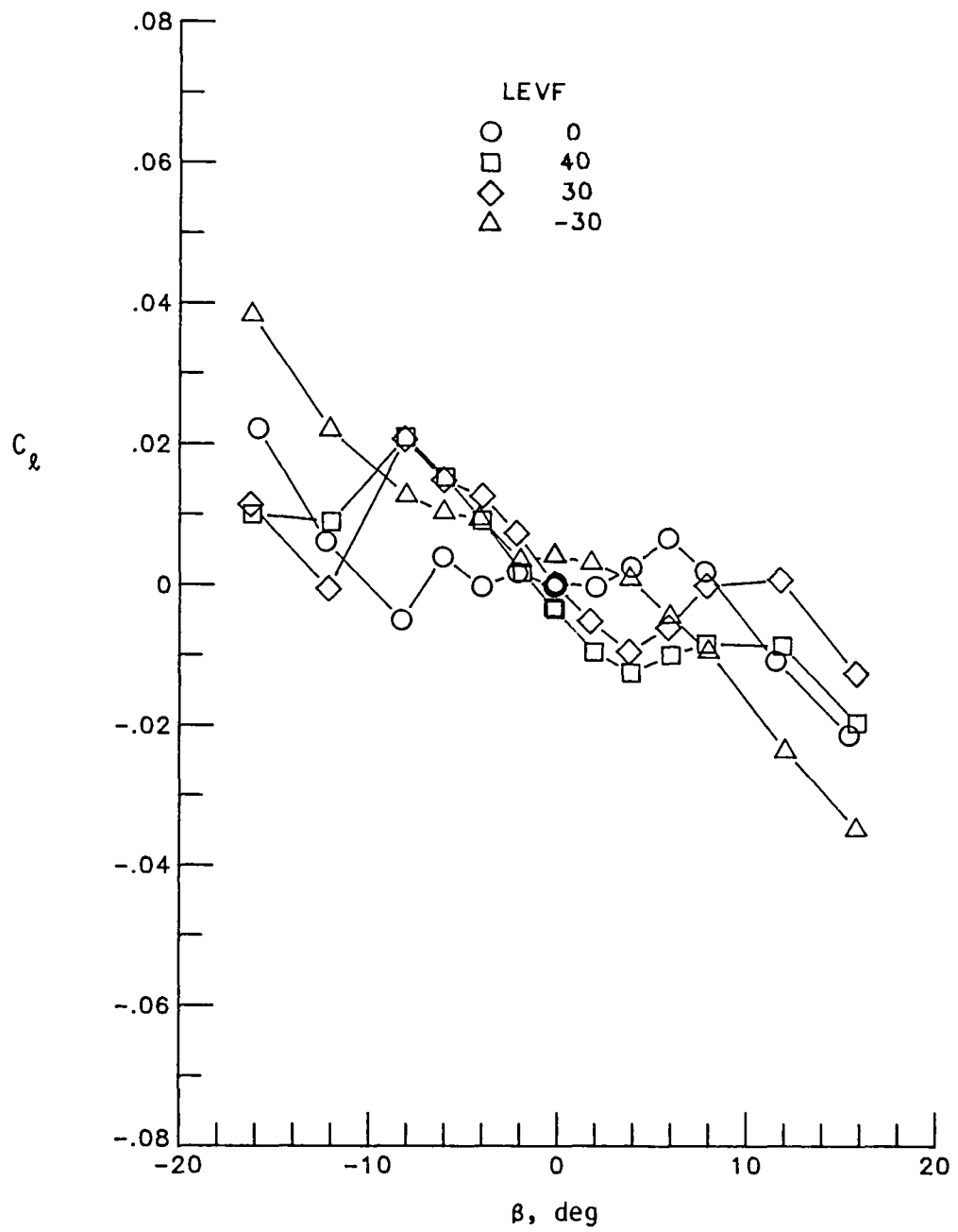
Figure 17.- Concluded.

(a) $\alpha = 5^0$
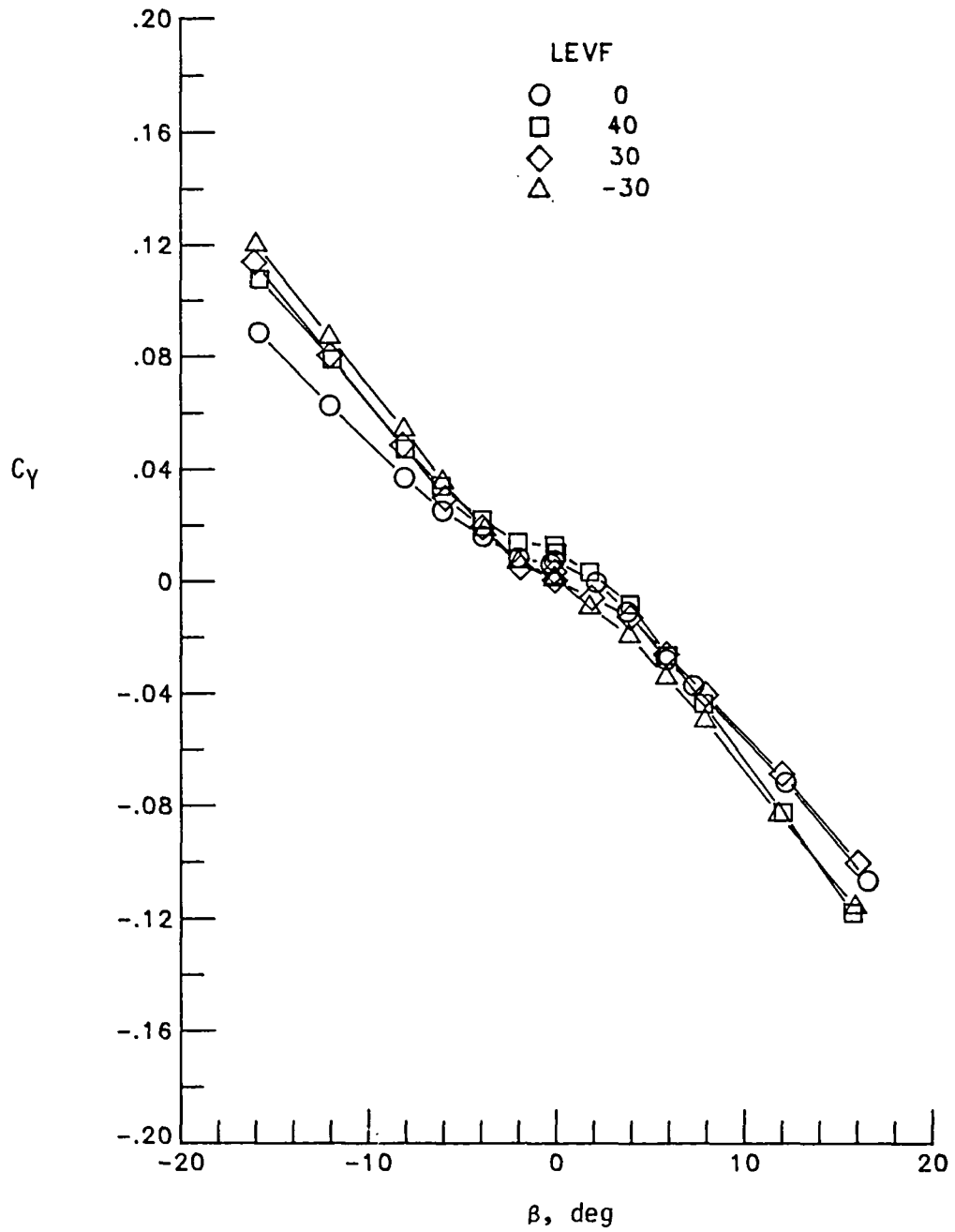
Figure 18.- Effect of LEVF deflection on side-force
characteristics.

(b) $\alpha = 15^0$
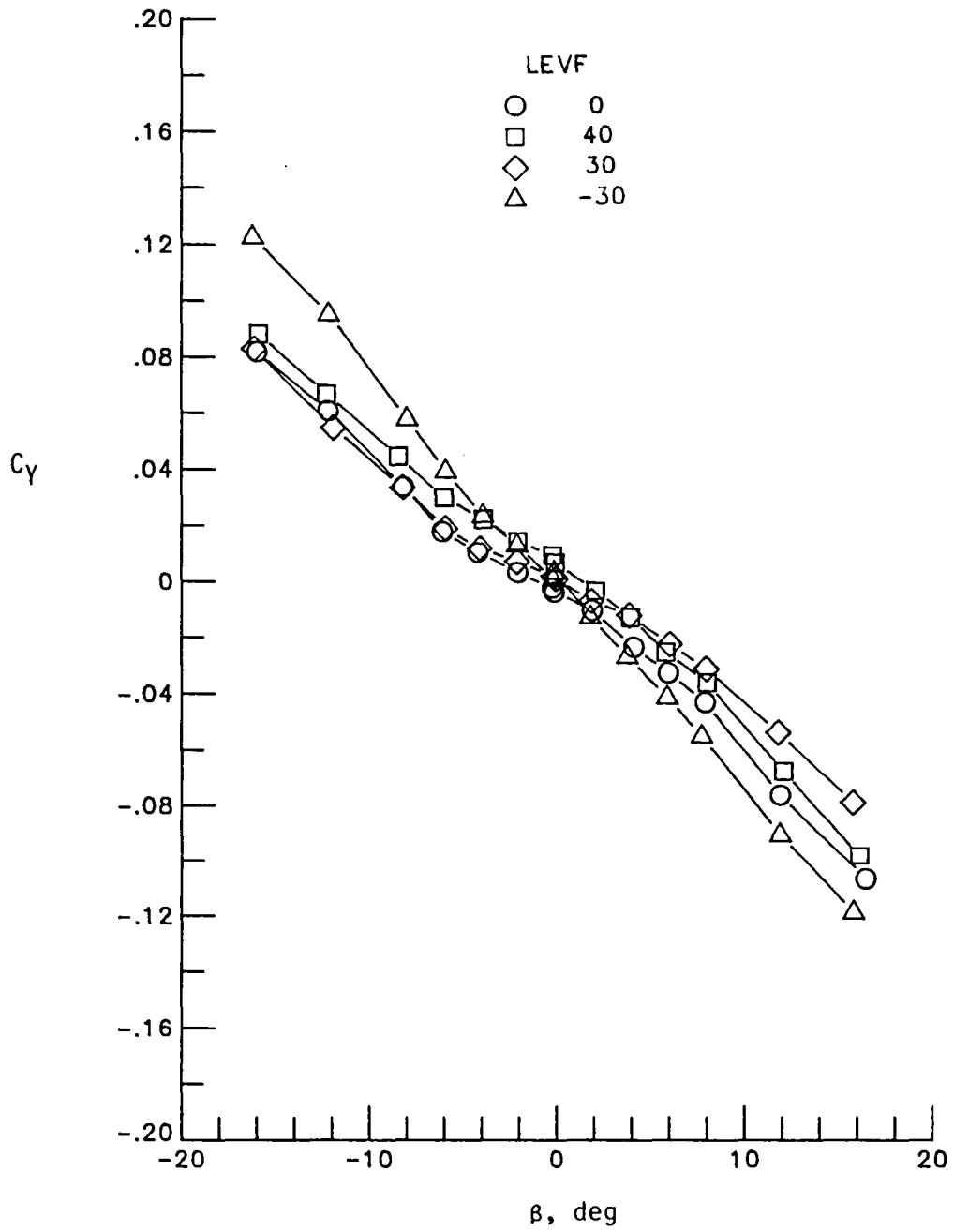
Figure 18.- Continued

(c) $\alpha = 25^0$
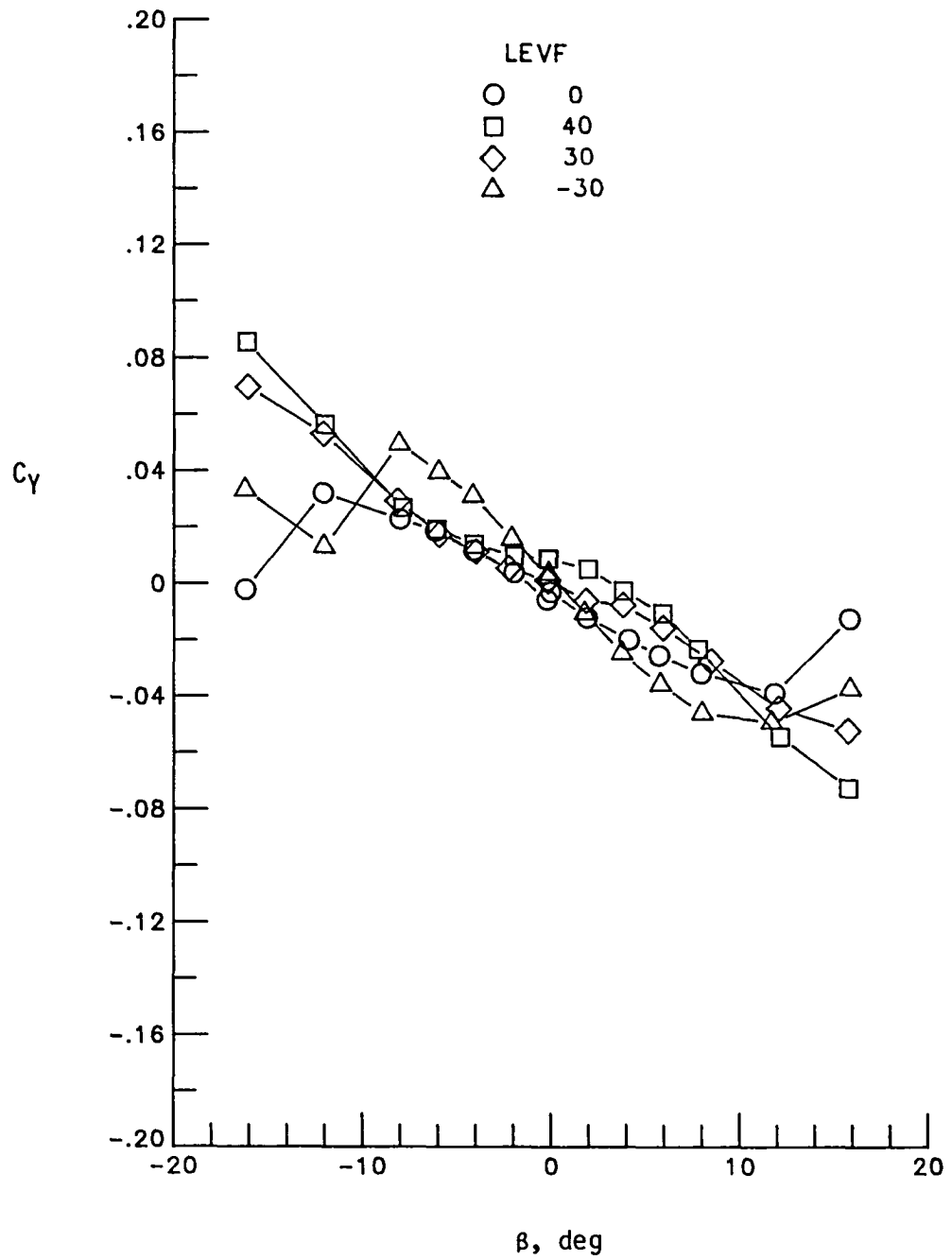
Figure 18.- Continued

(d) α = 30⁰
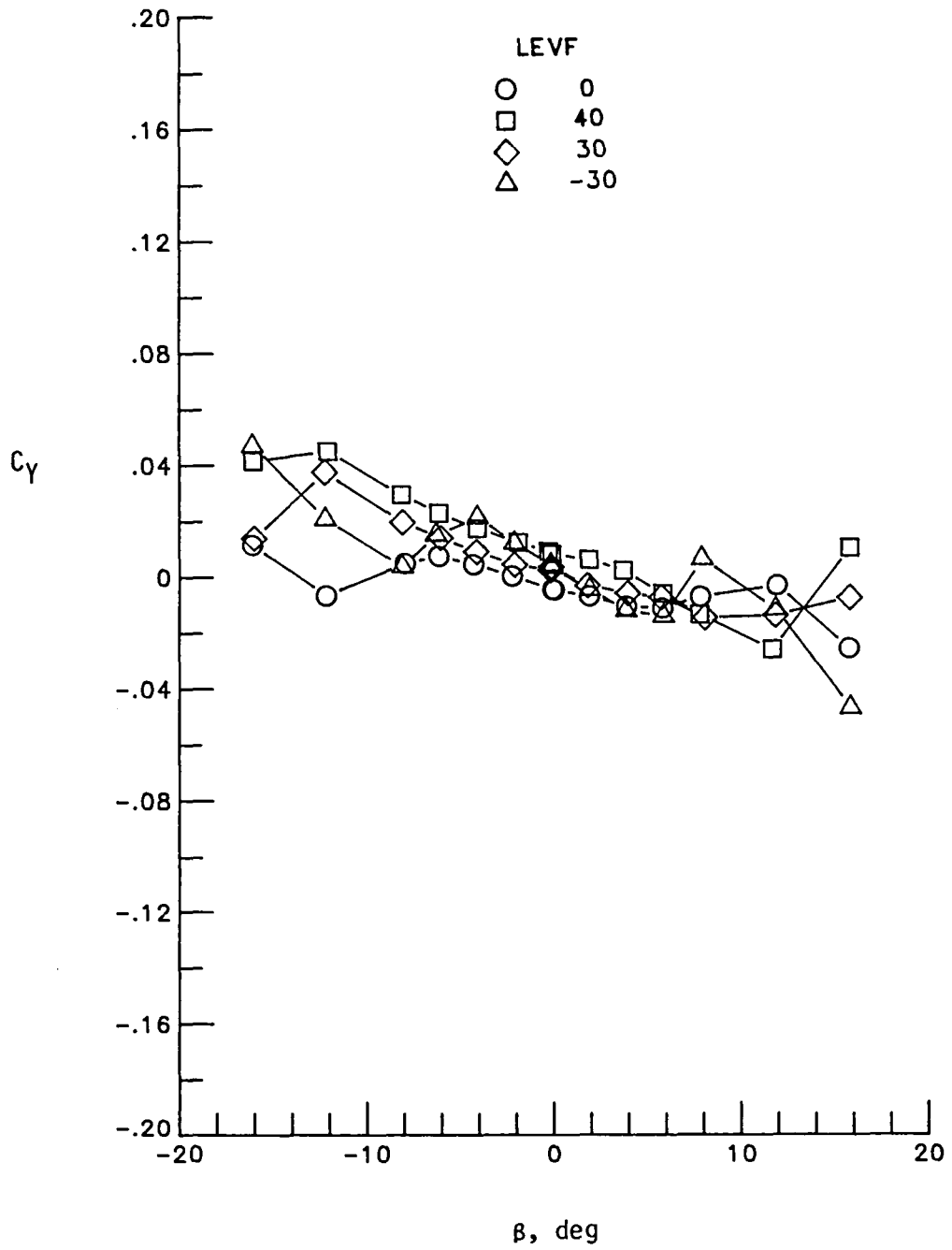
Figure 18.- Continued

(e) $\alpha = 35^0$
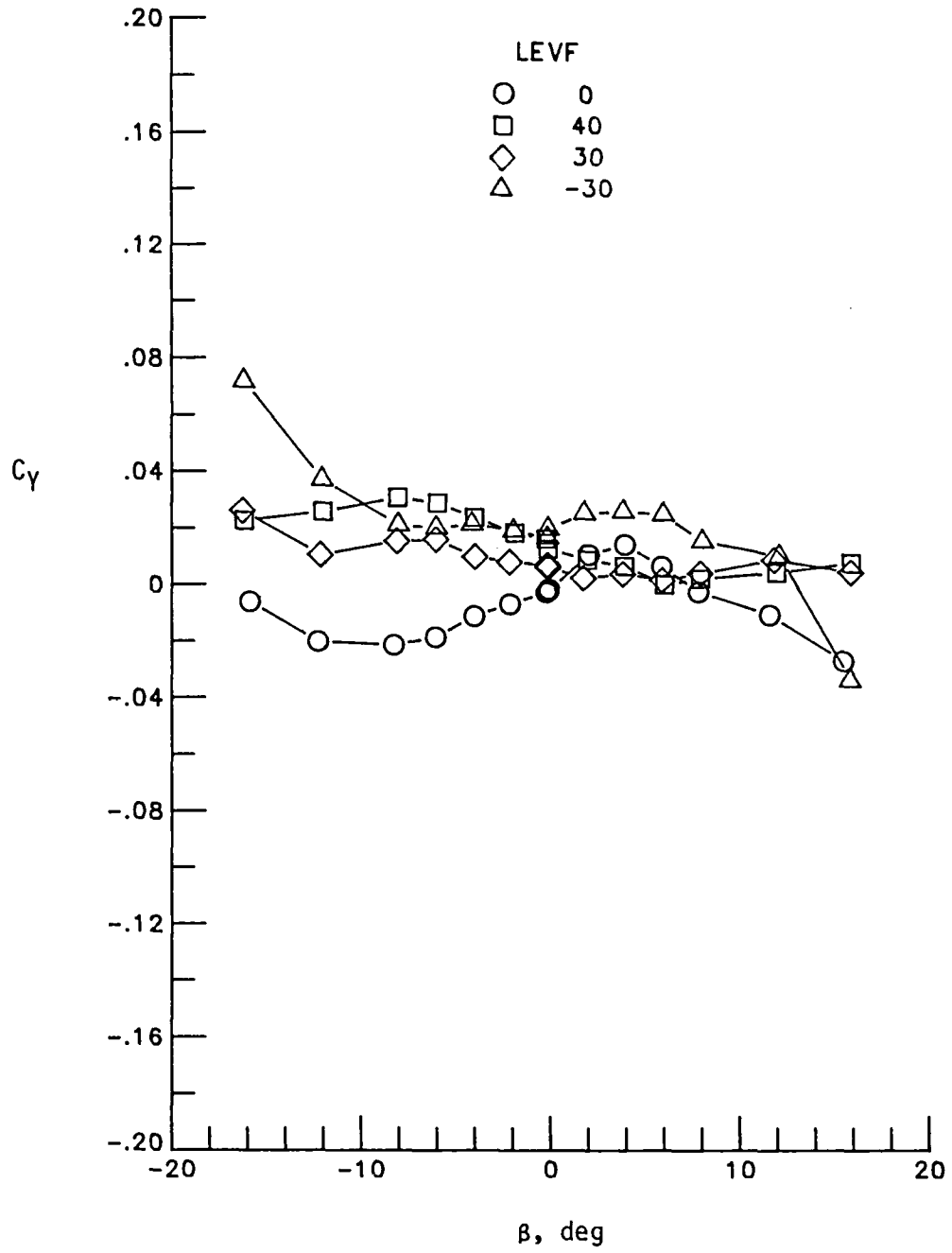
Figure 18.- Concluded.
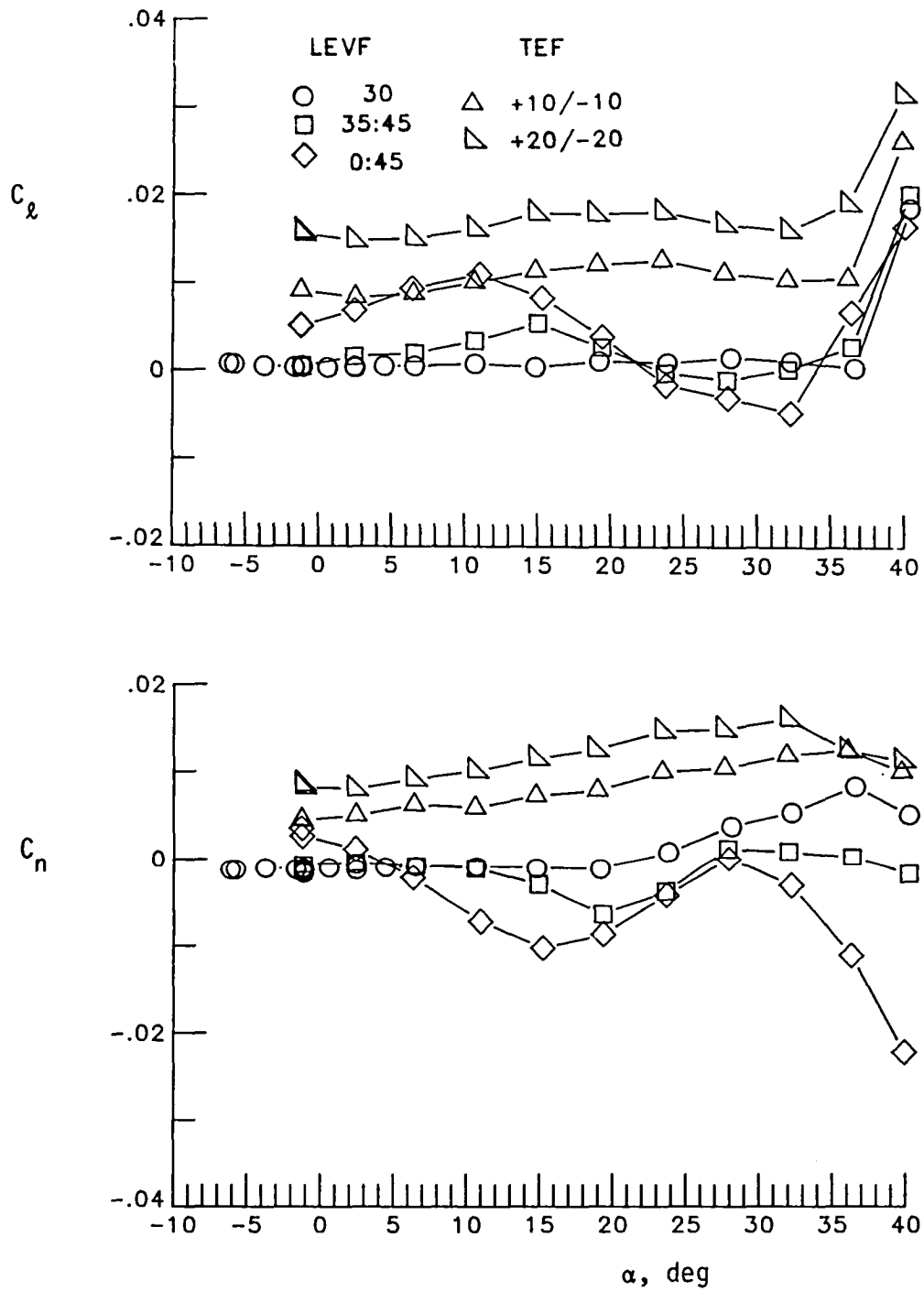
Figure 19.- Effect of asymmetrical LEVF and differential aileron deflection on rolling and yawing moments.
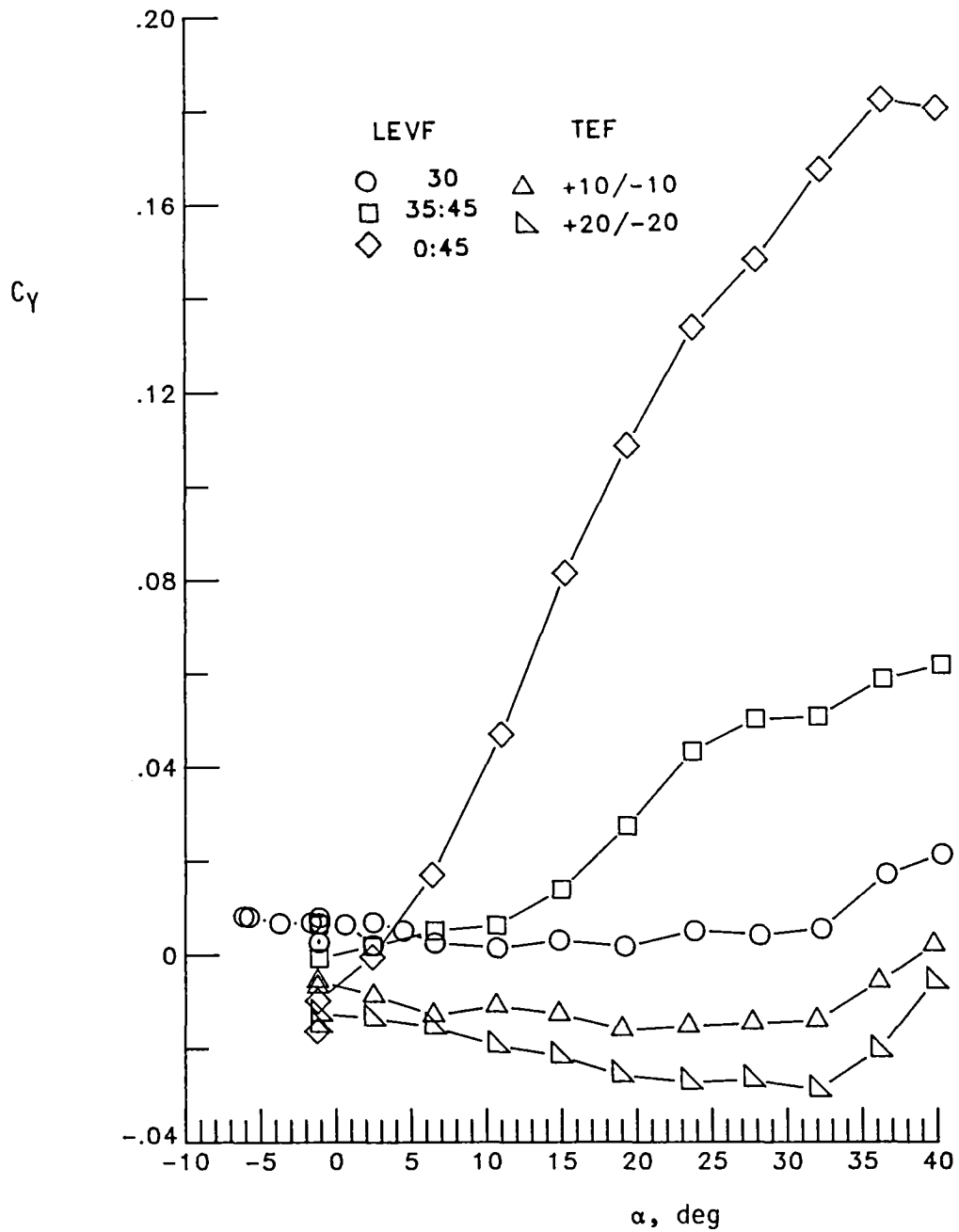
Figure 20.- Effect of asymmetrical LEVF and differential
aileron deflection on side force.
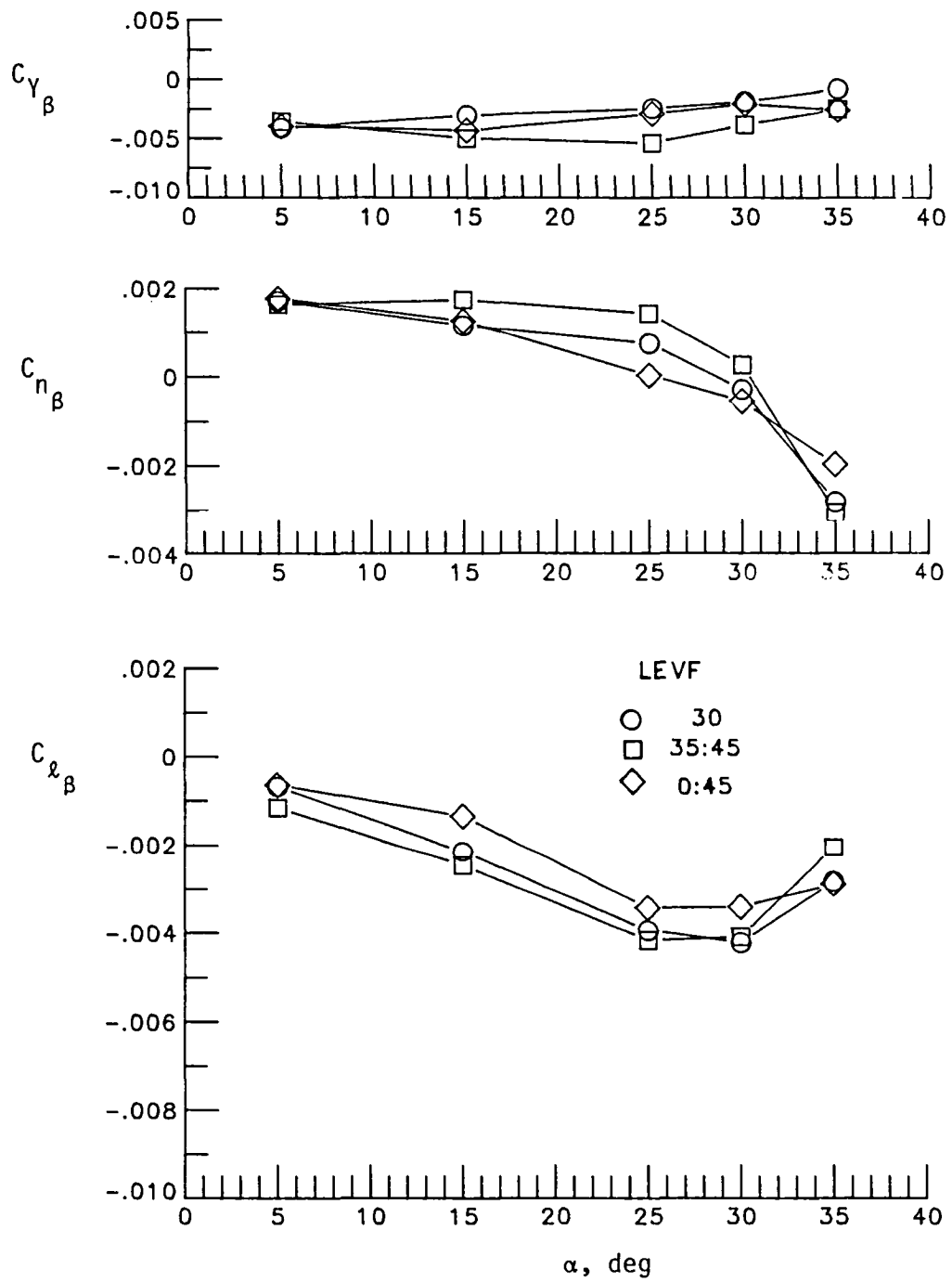
Figure 21.- Effect of asymmetrical LEVF deflection on lateral-directional stability derivatives.

(a) $\alpha = 5^0$
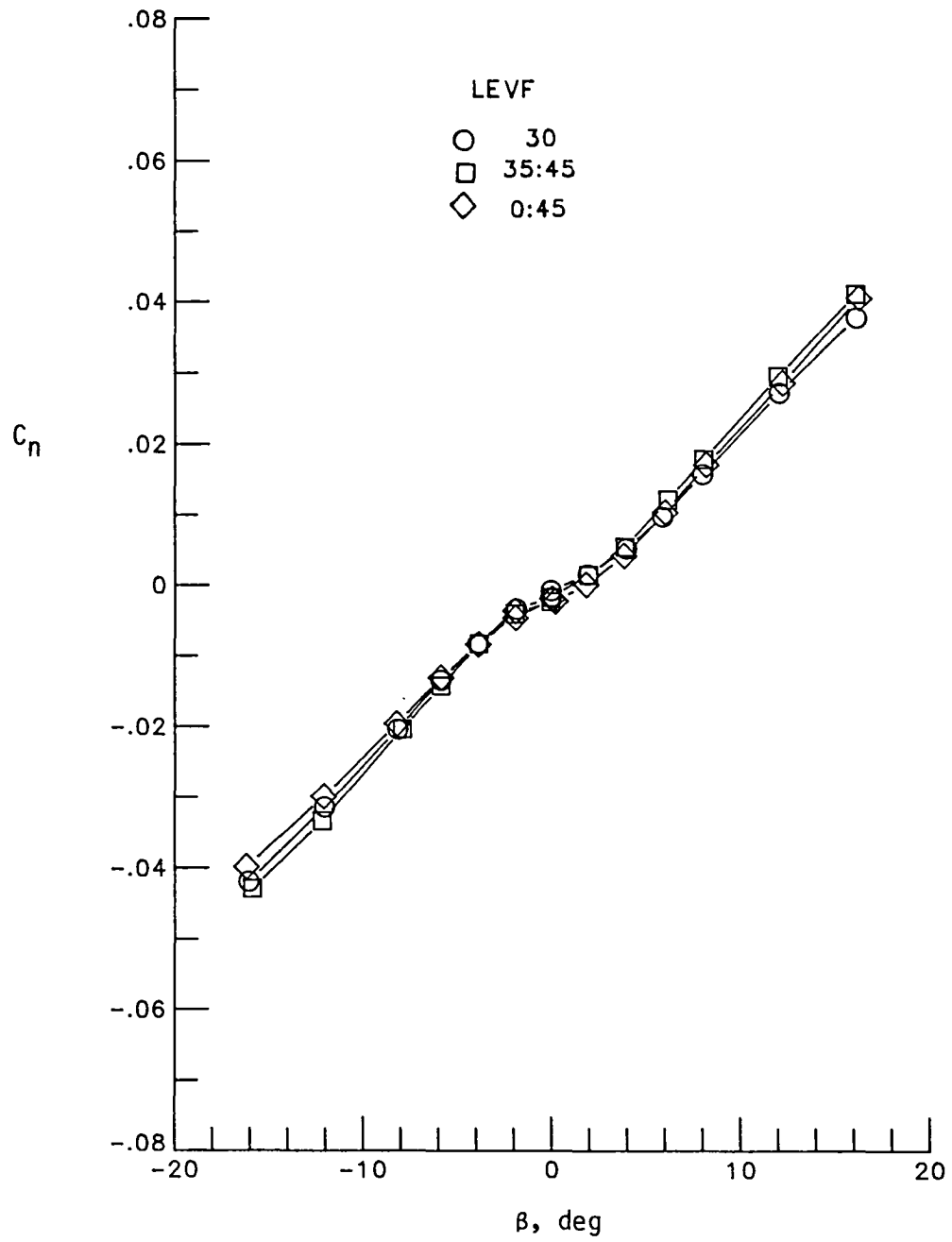
Figure 22.- Effect of asymmetrical LEVF deflection on yawing moment.

(b) $\alpha = 15^0$
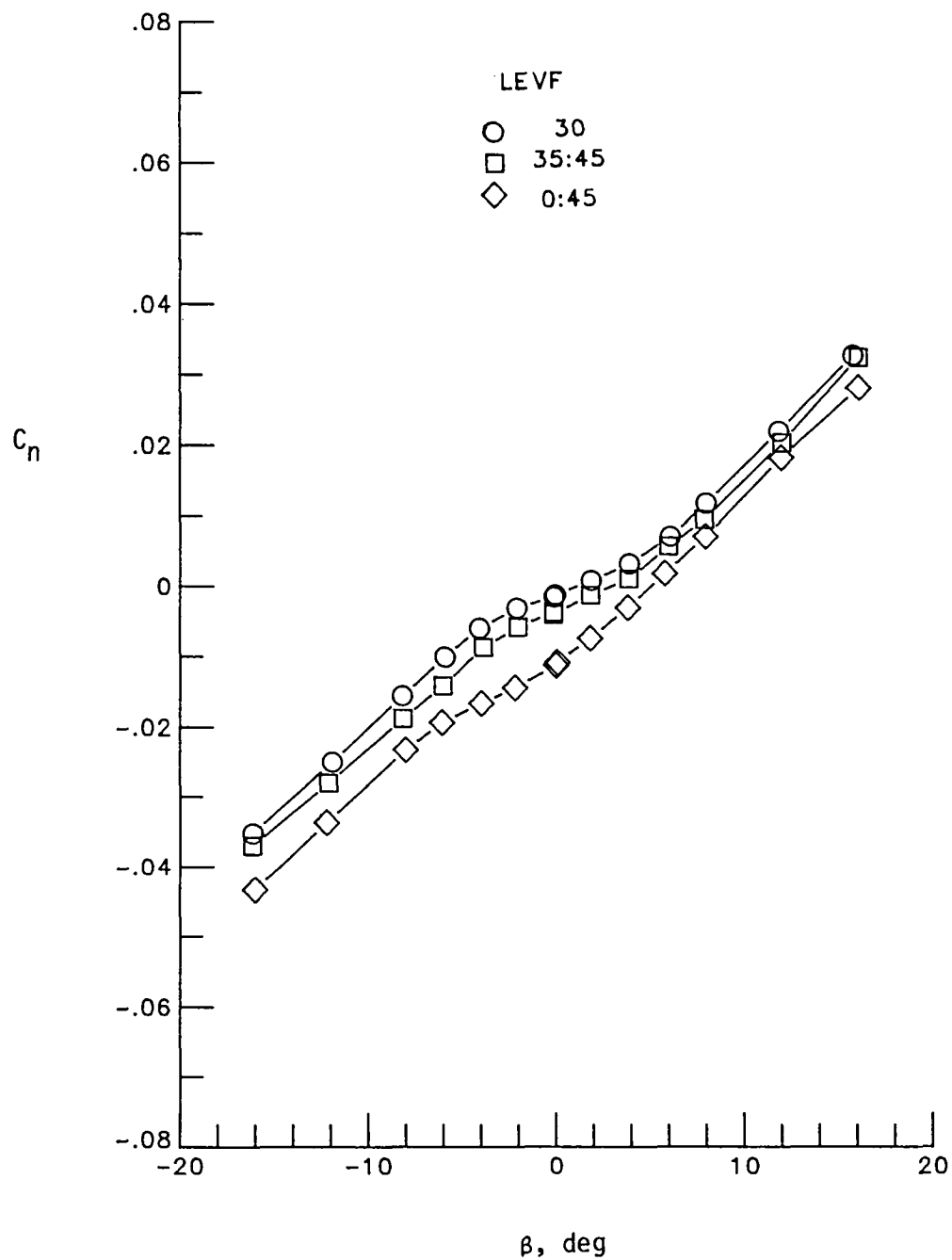
Figure 22.- Continued

(c) $\alpha = 25^0$
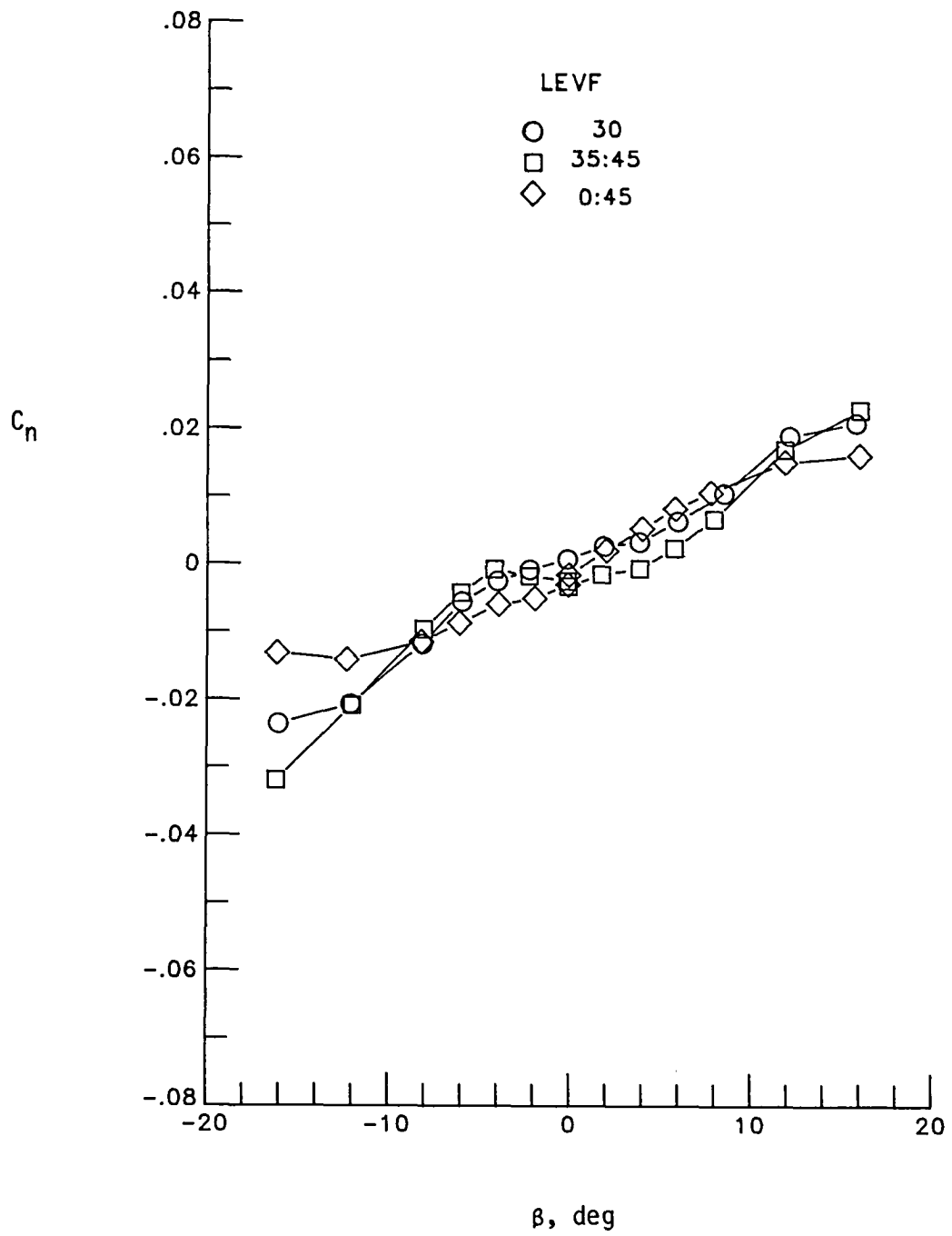
Figure 22.- Continued

(d) $\alpha = 30^0$
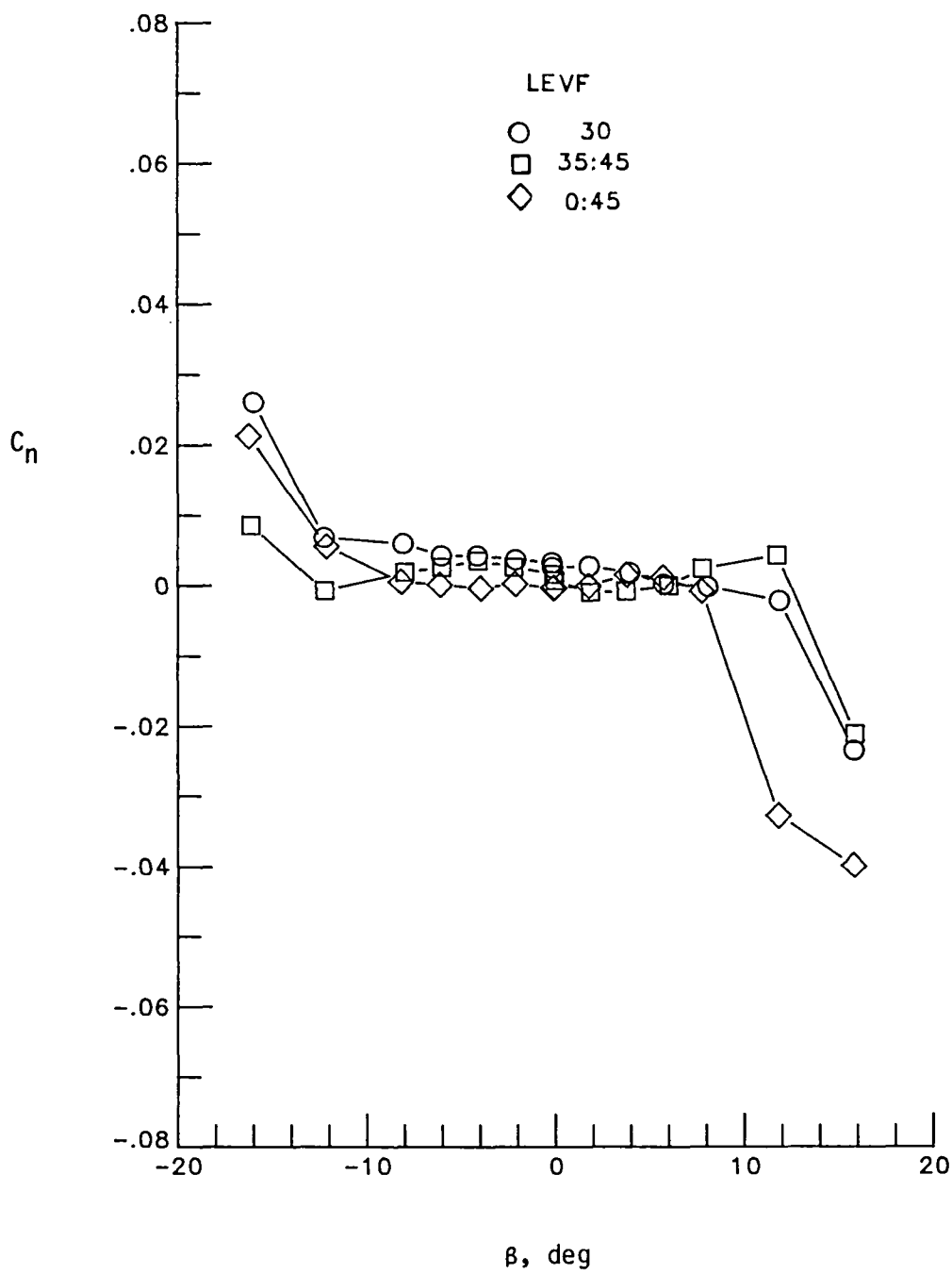
Figure 22.- Continued

(e) $\alpha = 35^0$
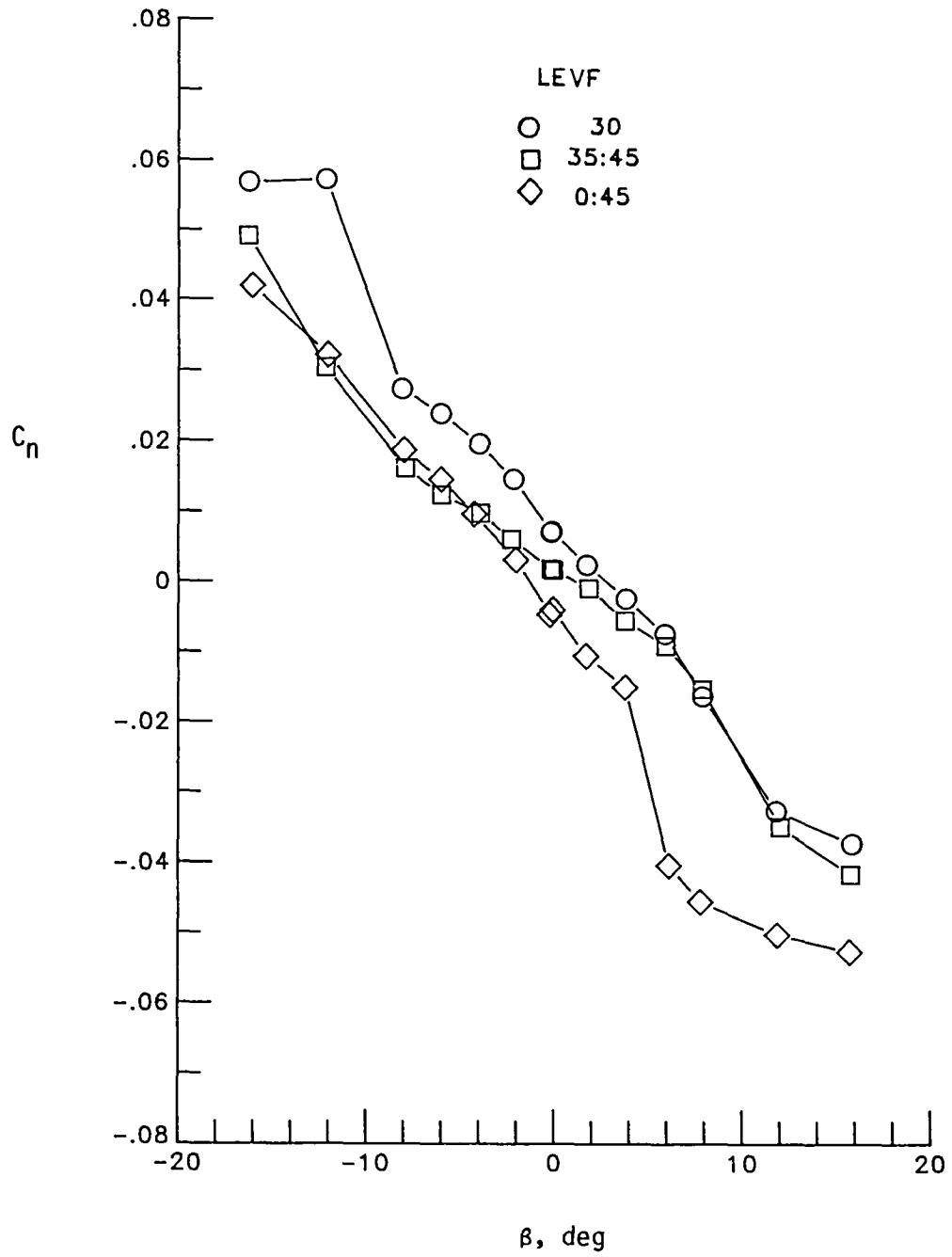
Figure 22.- Concluded.

(a) $\alpha = 5^0$
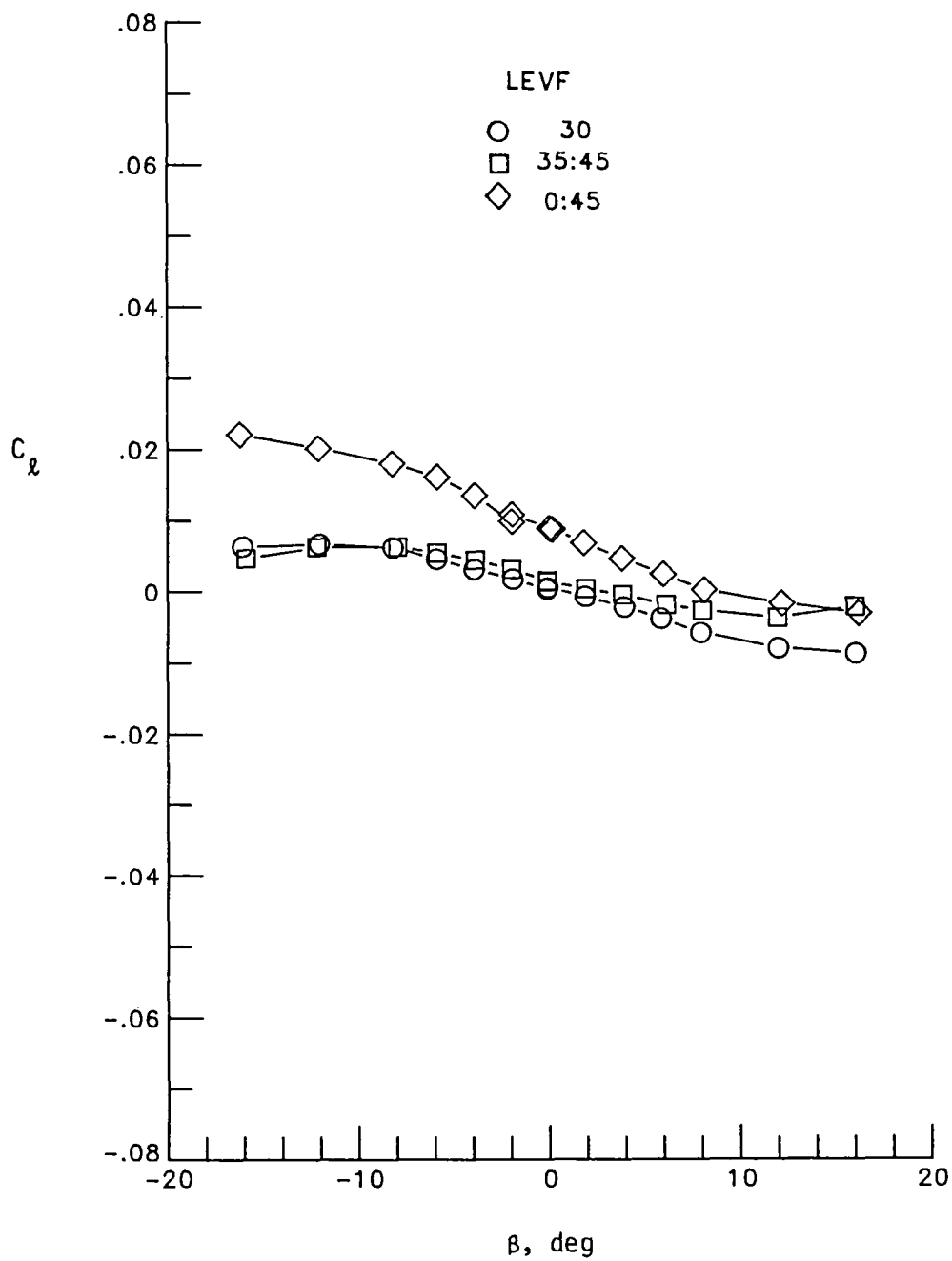
Figure 23.- Effect of asymmetrical LEVF deflection on rolling moment.

(b) $\alpha = 15^0$
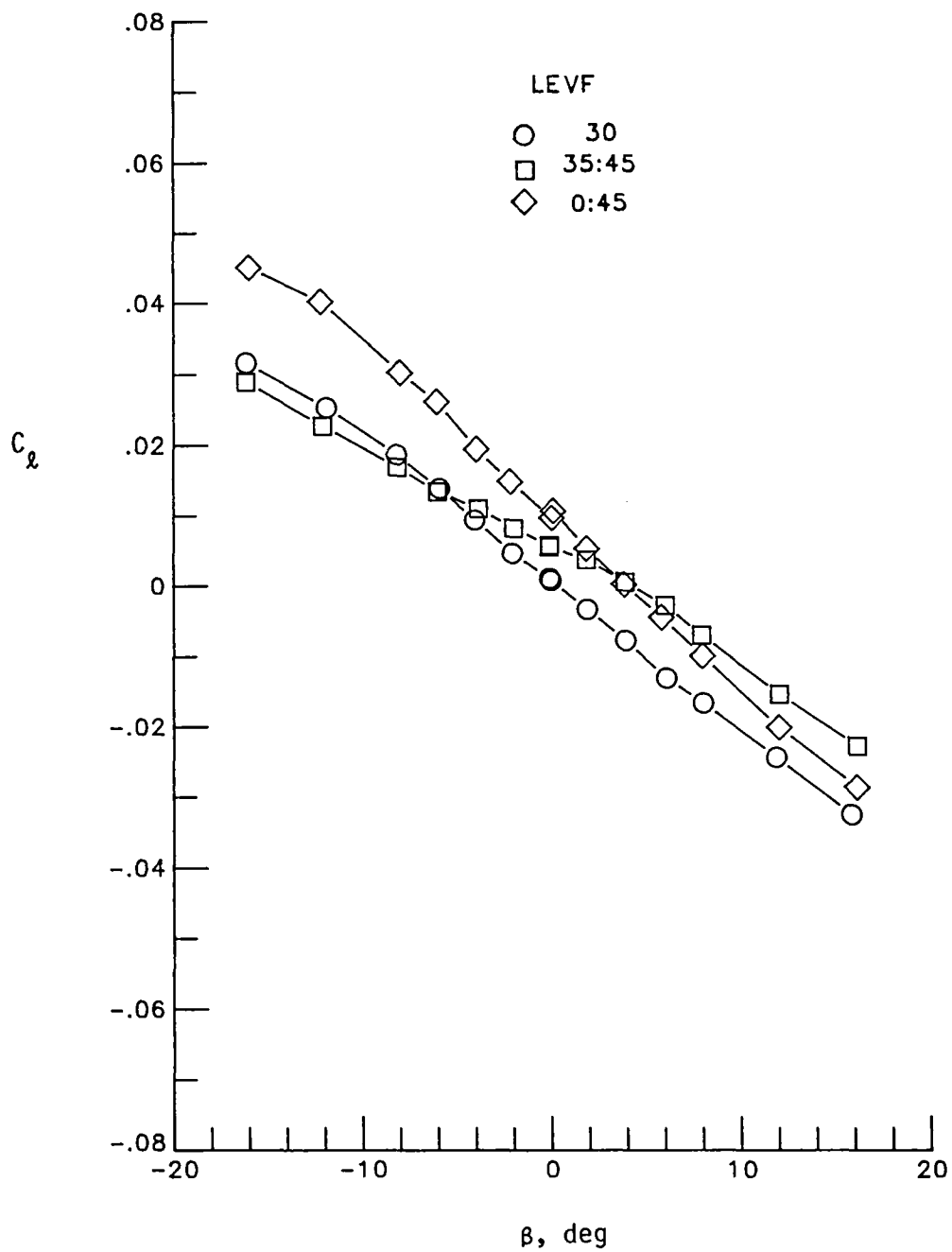
Figure 23.- Continued

(c) $\alpha = 25^0$
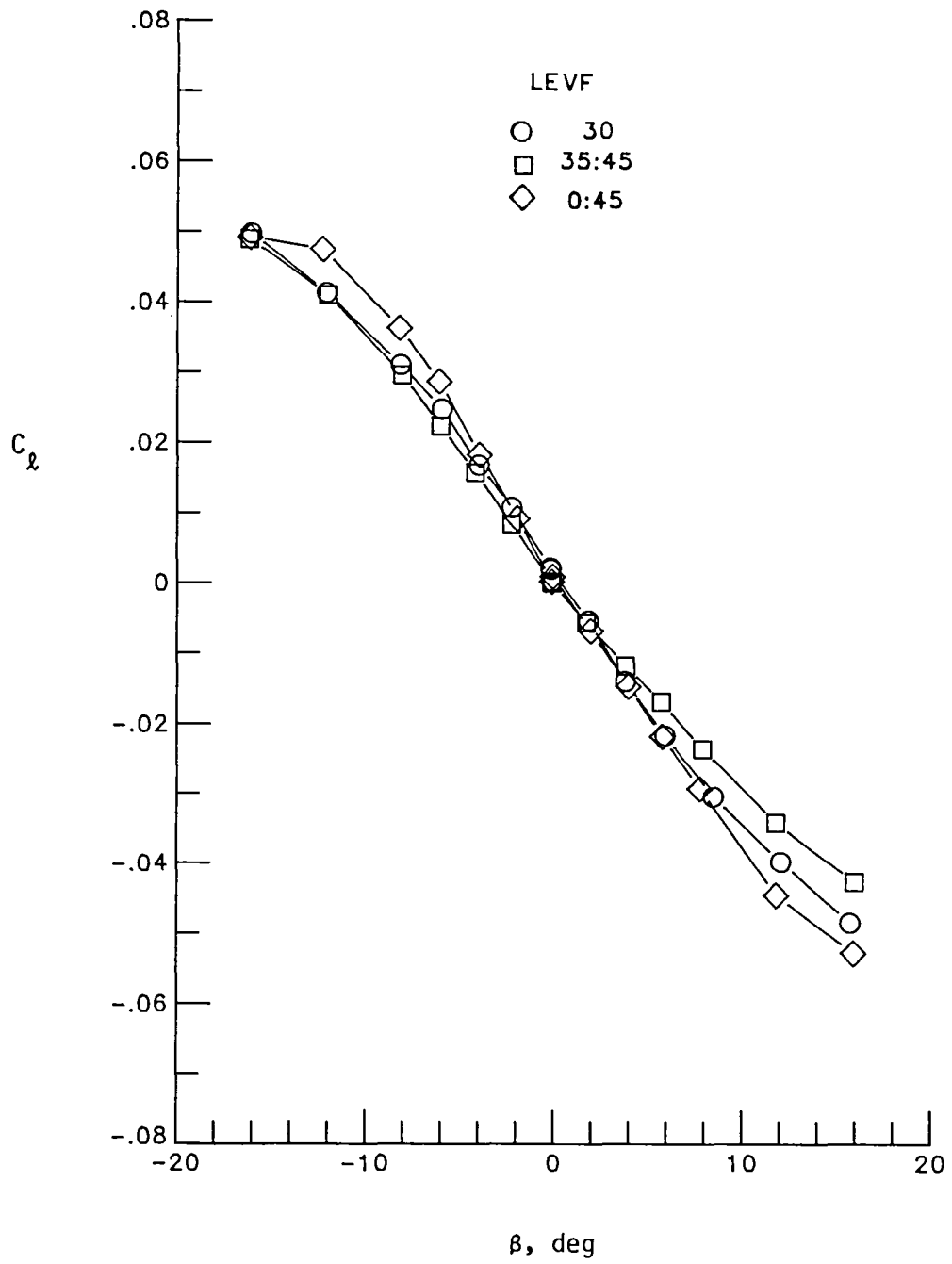
Figure 23.- Continued

(d) $\alpha = 30^0$
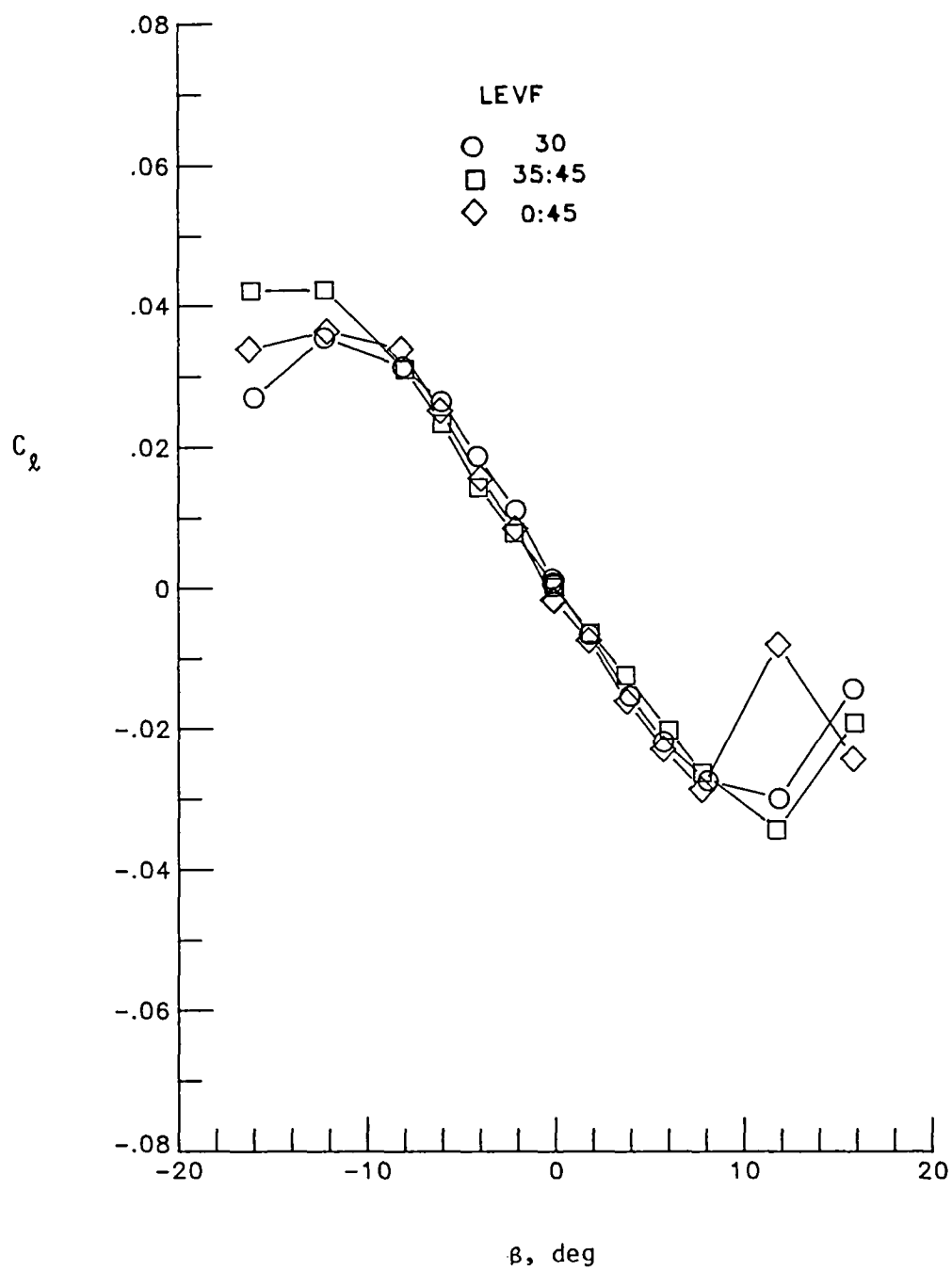
Figure 23.- Continued

(e) $\alpha = 35^0$
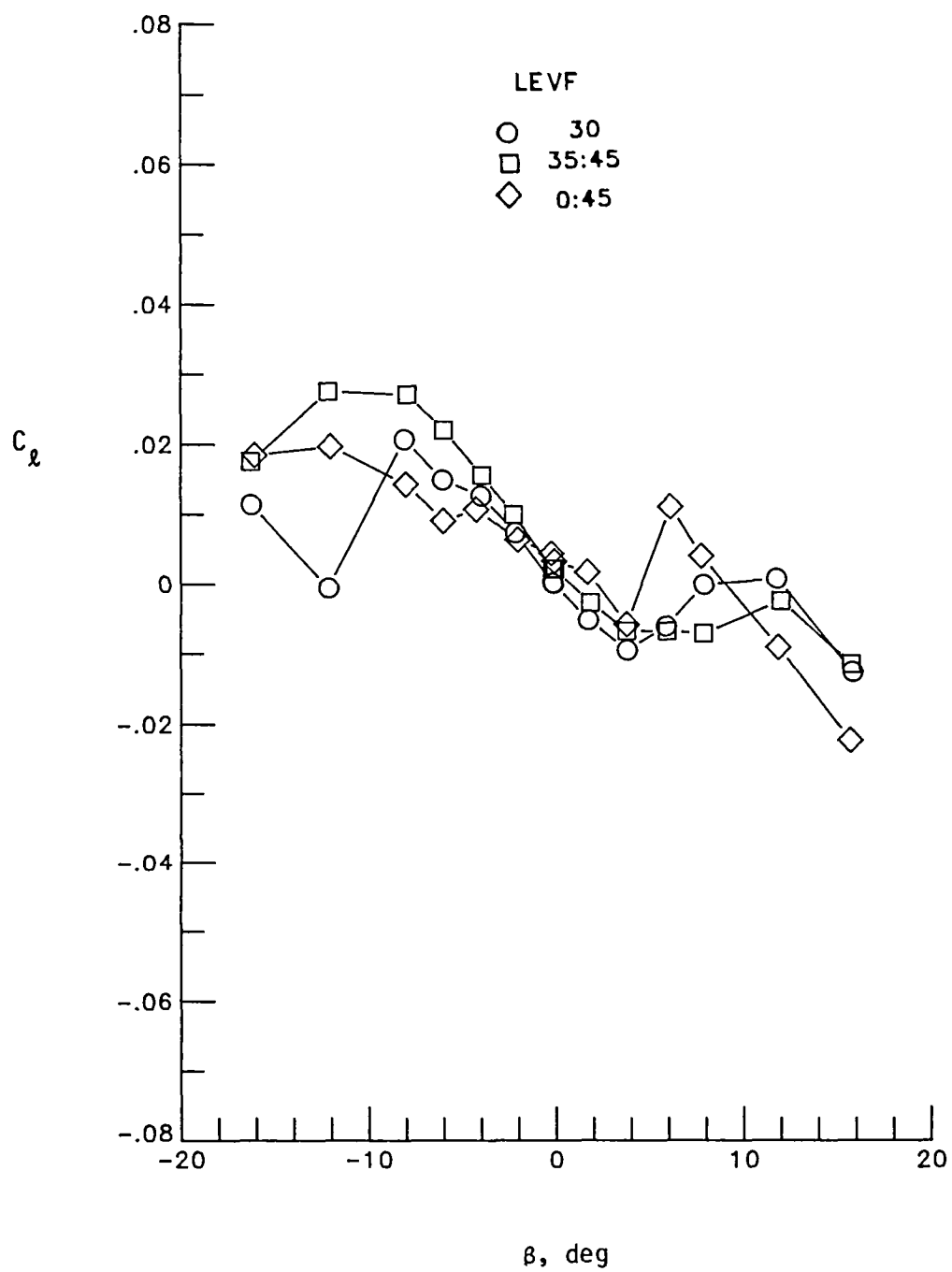
Figure 23.- Concluded.

(a) α = 5⁰
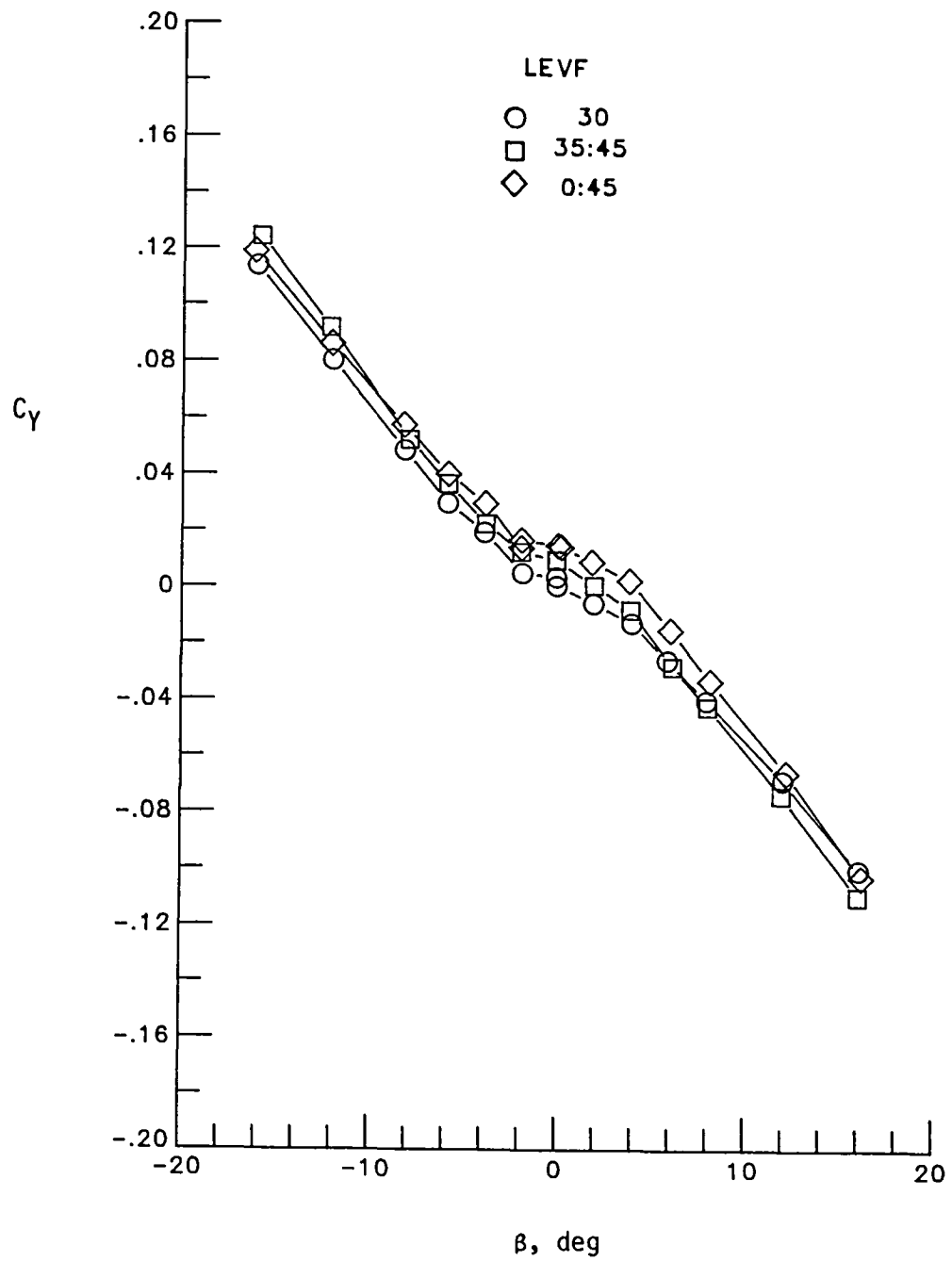
Figure 24.- Effect of asymmetrical LEVF deflection on side force.

(b) $\alpha = 15^0$

Figure 24.- Continued

(c) $\alpha = 25^0$

Figure 24.- Continued

(d) $\alpha = 30^0$

Figure 24.- Continued

C_Y

LEVF

○   30
□   35:45
◇   0:45

β, deg

(e) α = 35⁰

Figure 24.- Concluded.
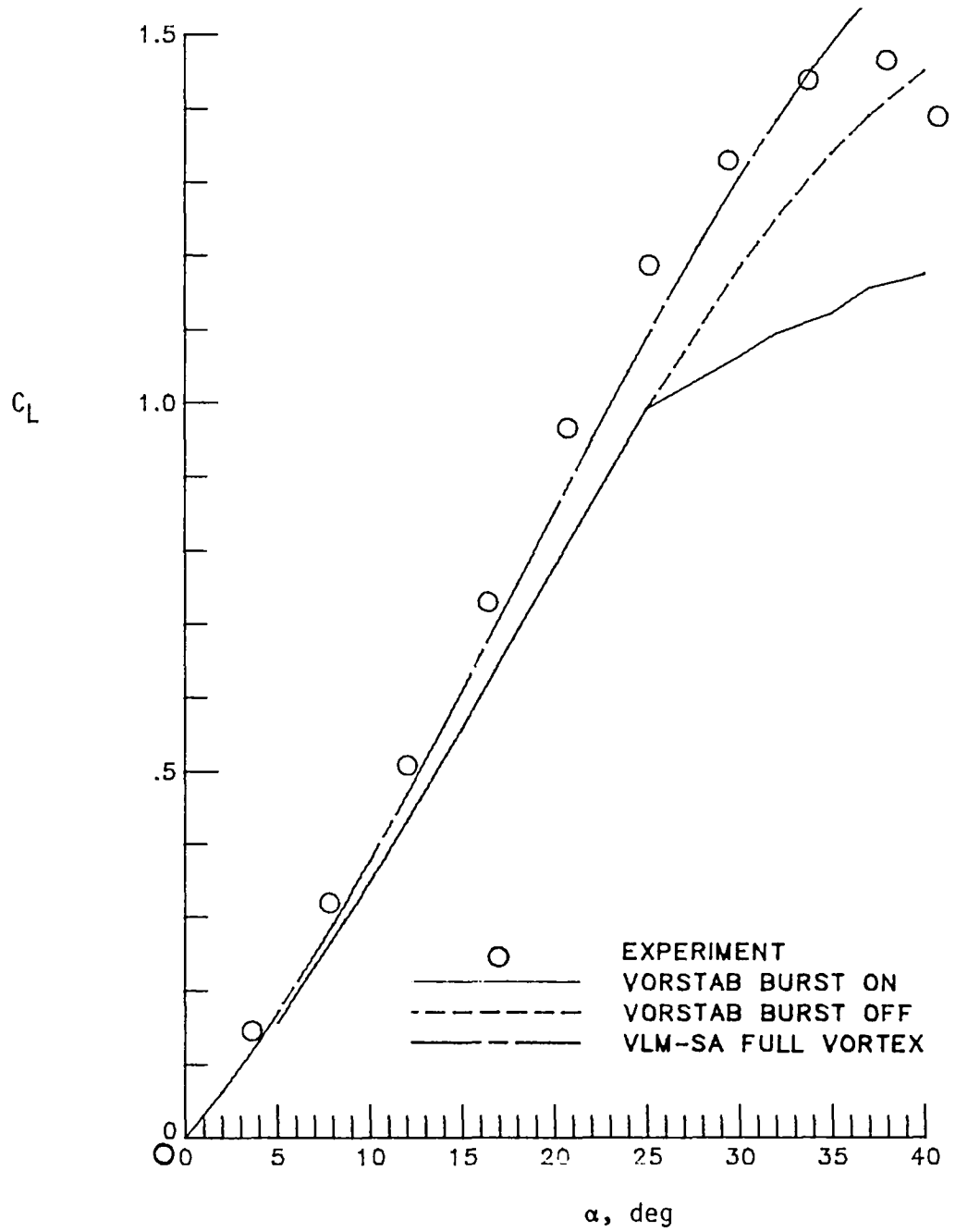
Figure 25.- Comparison of theoretical and experimental longitudinal aerodynamic characteristics with $\delta_{LE} = 0°$.
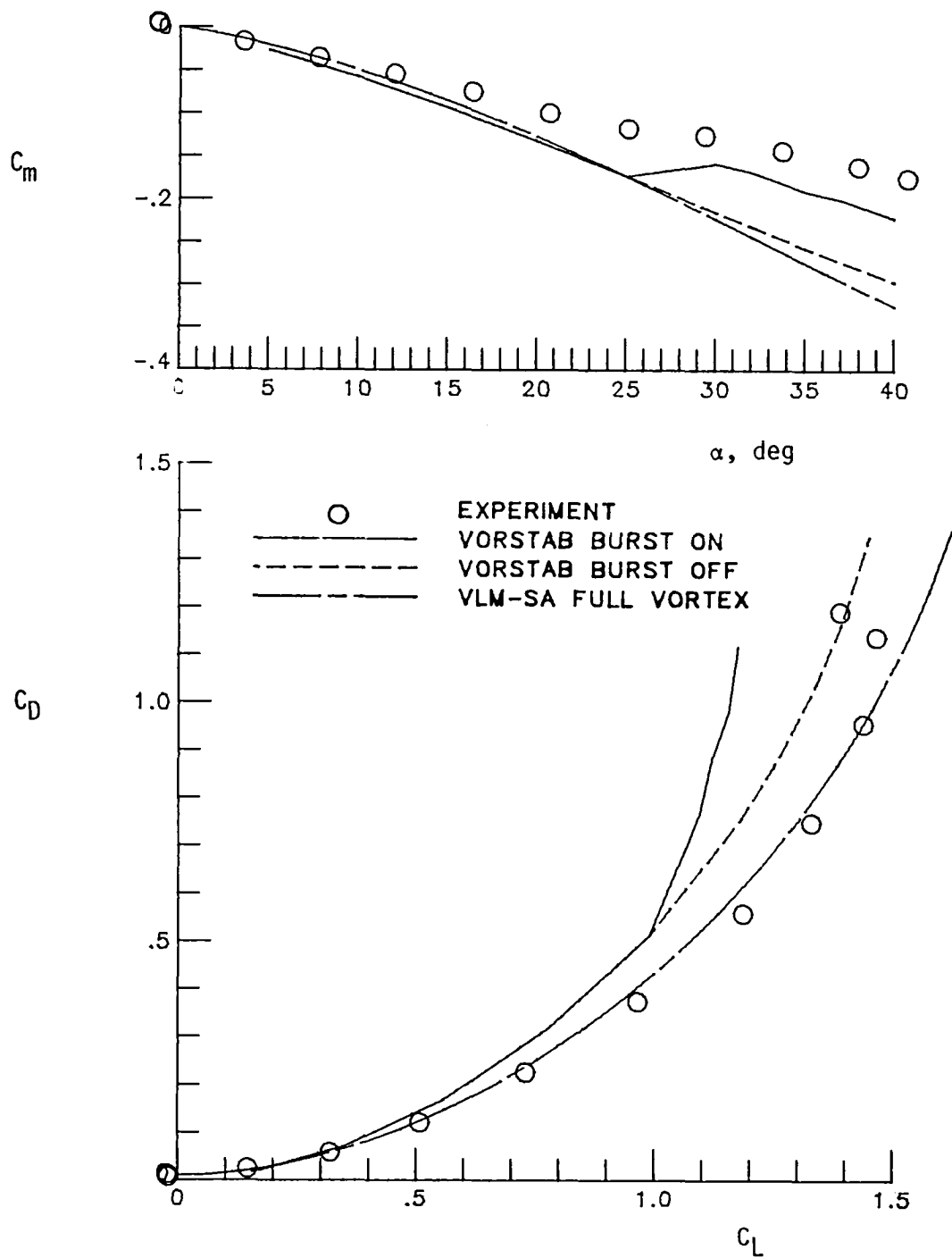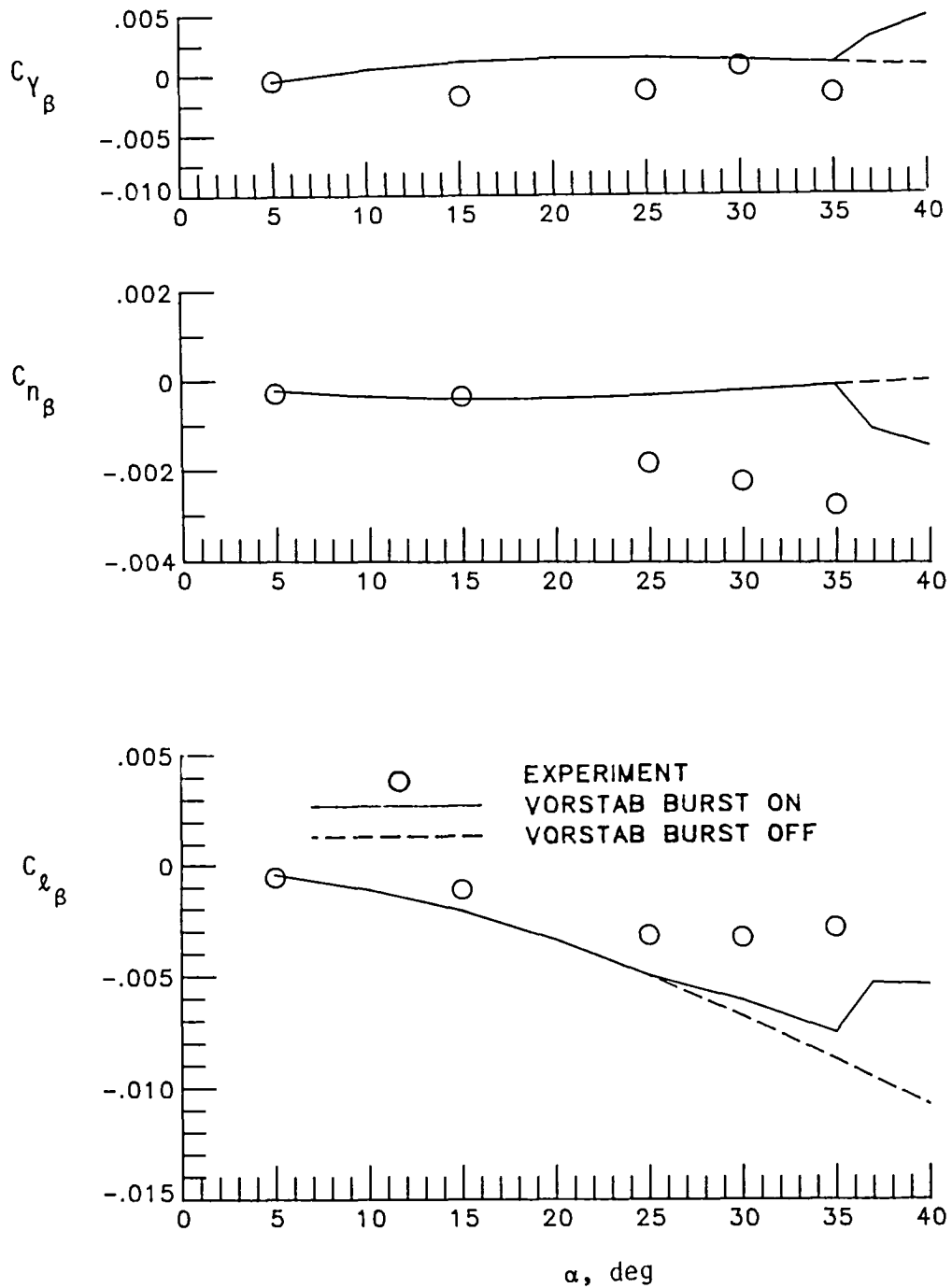
Figure 25.- Concluded.
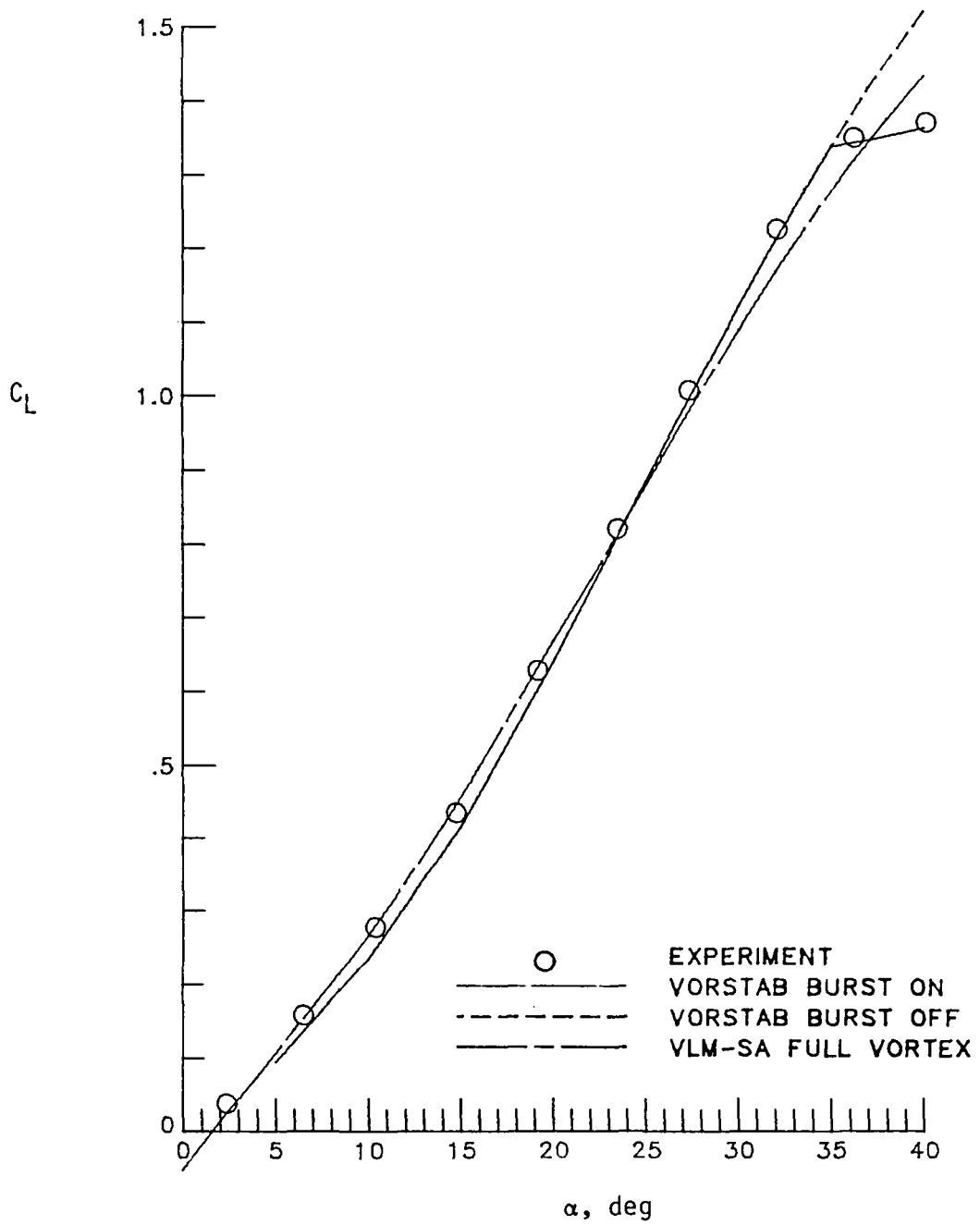
Figure 26.- Comparison of theoretical and experimental longitudinal aerodynamic characteristics with δ_{LE} = 40°.
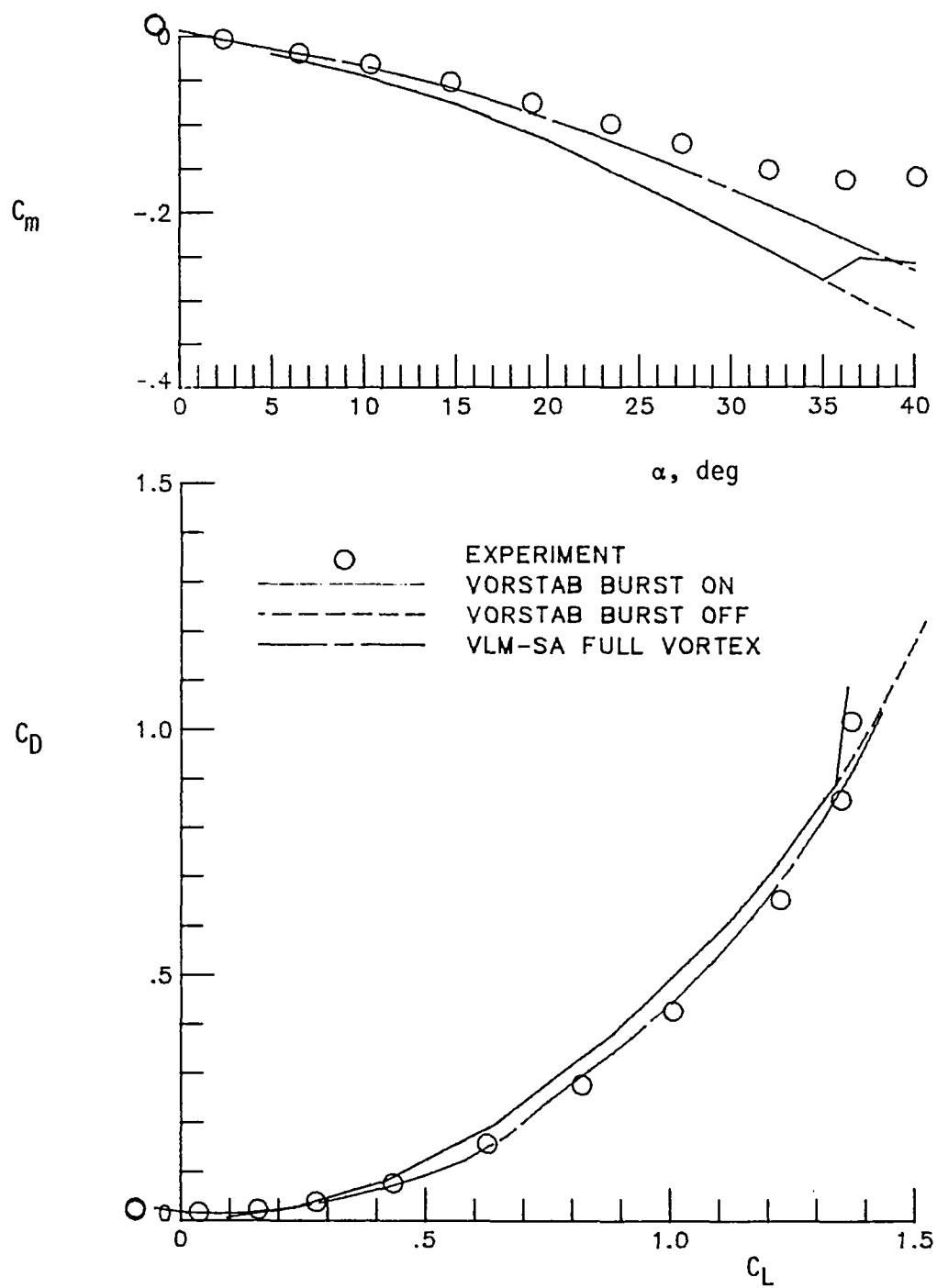
Figure 26.- Concluded.
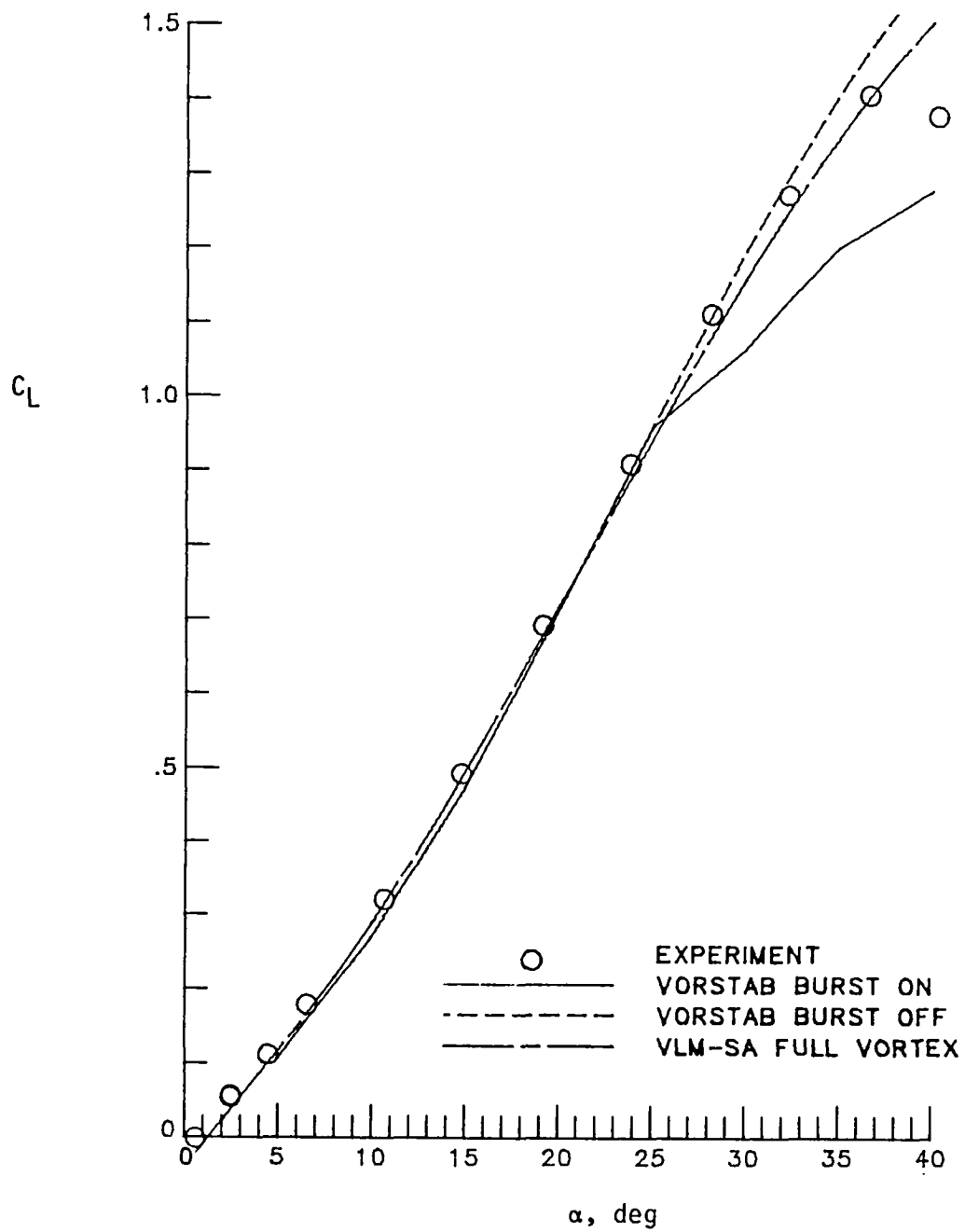
Figure 27.- Comparison of theoretical and experimental longitudinal aerodynamic characteristics with δ_{LE} = 30°.
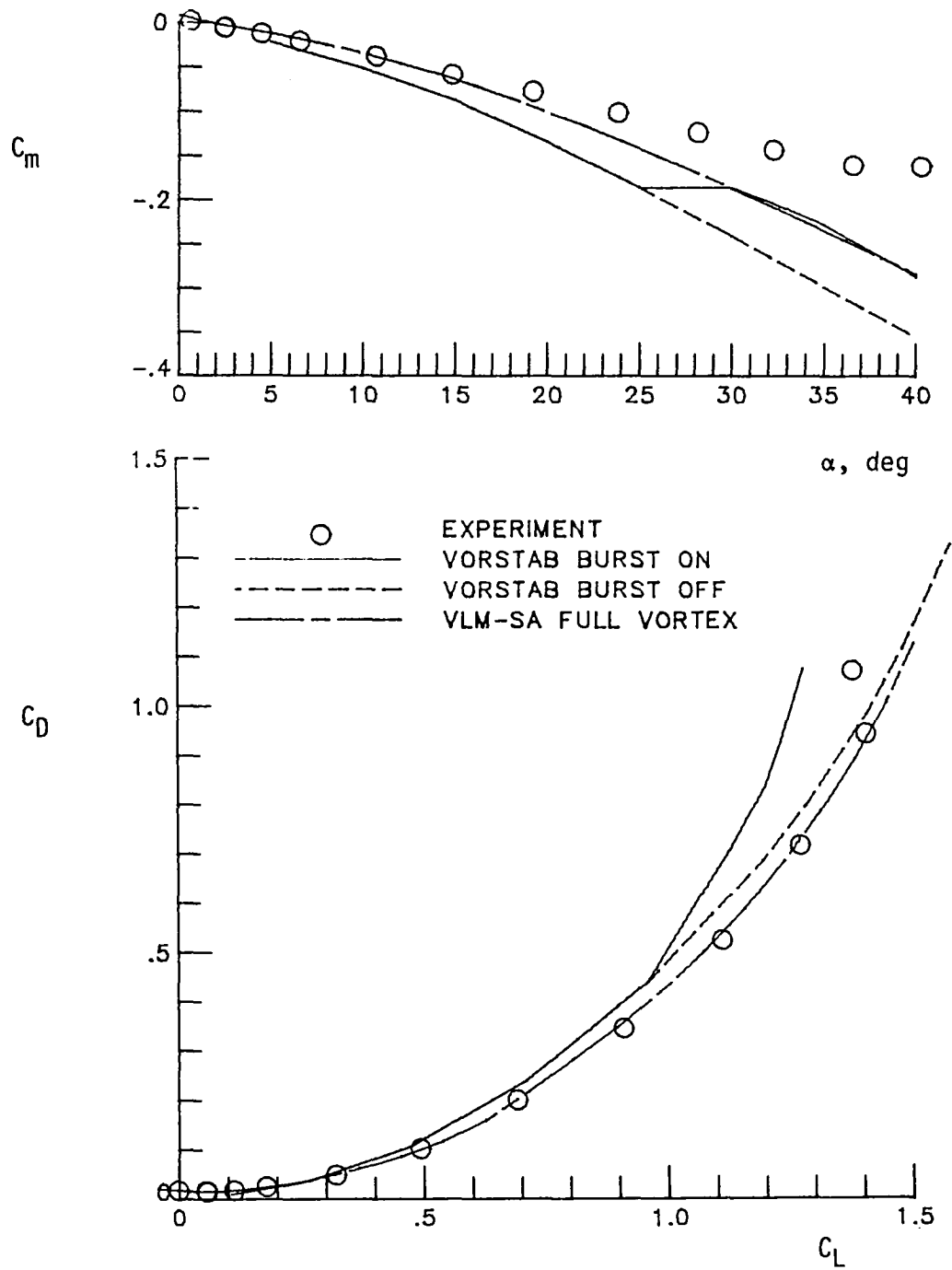
Figure 27.- Concluded.
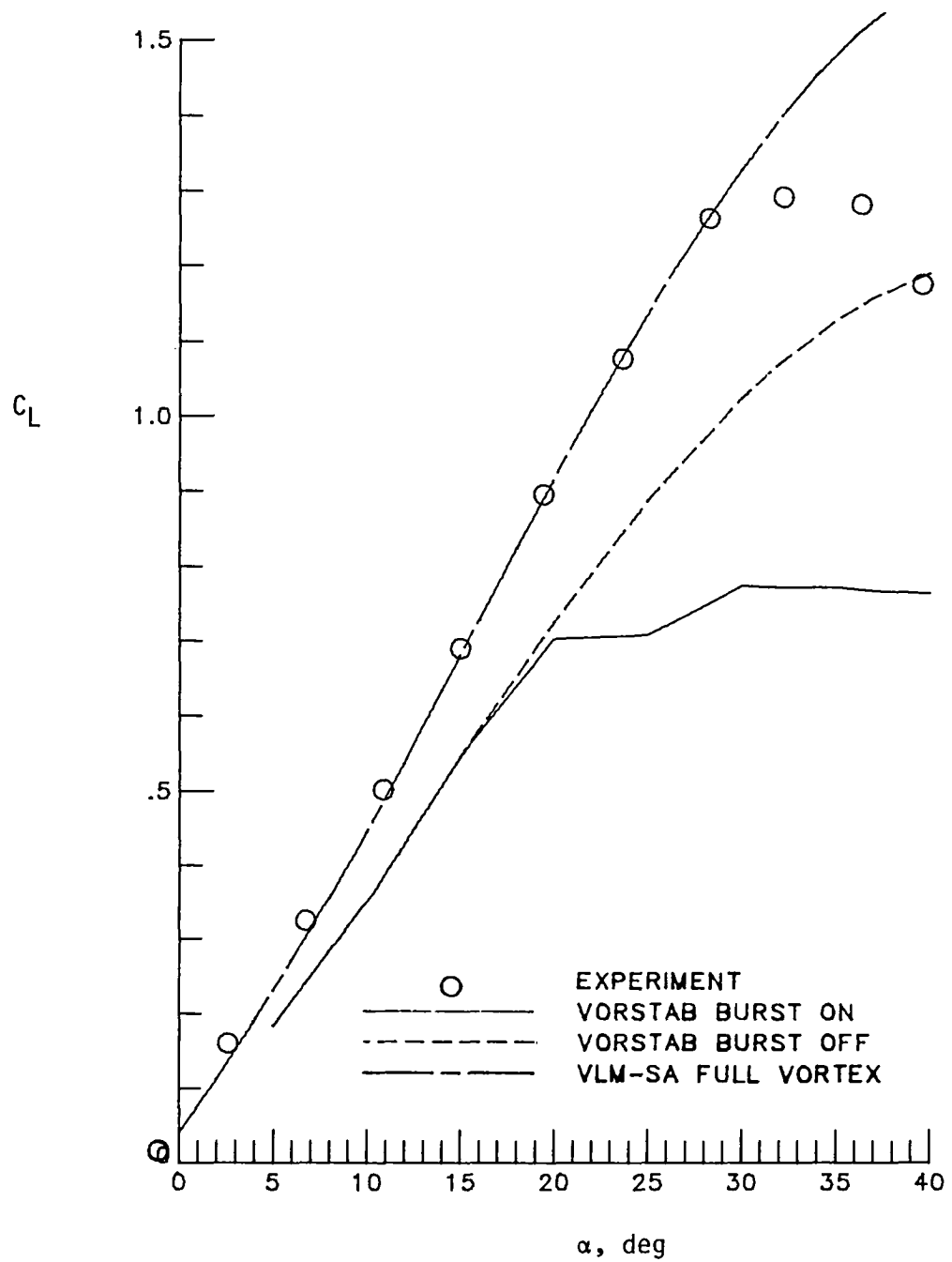
Figure 28.- Comparison of theoretical and experimental longitudinal aerodynamic characteristics with δ_{LE} = -30°.
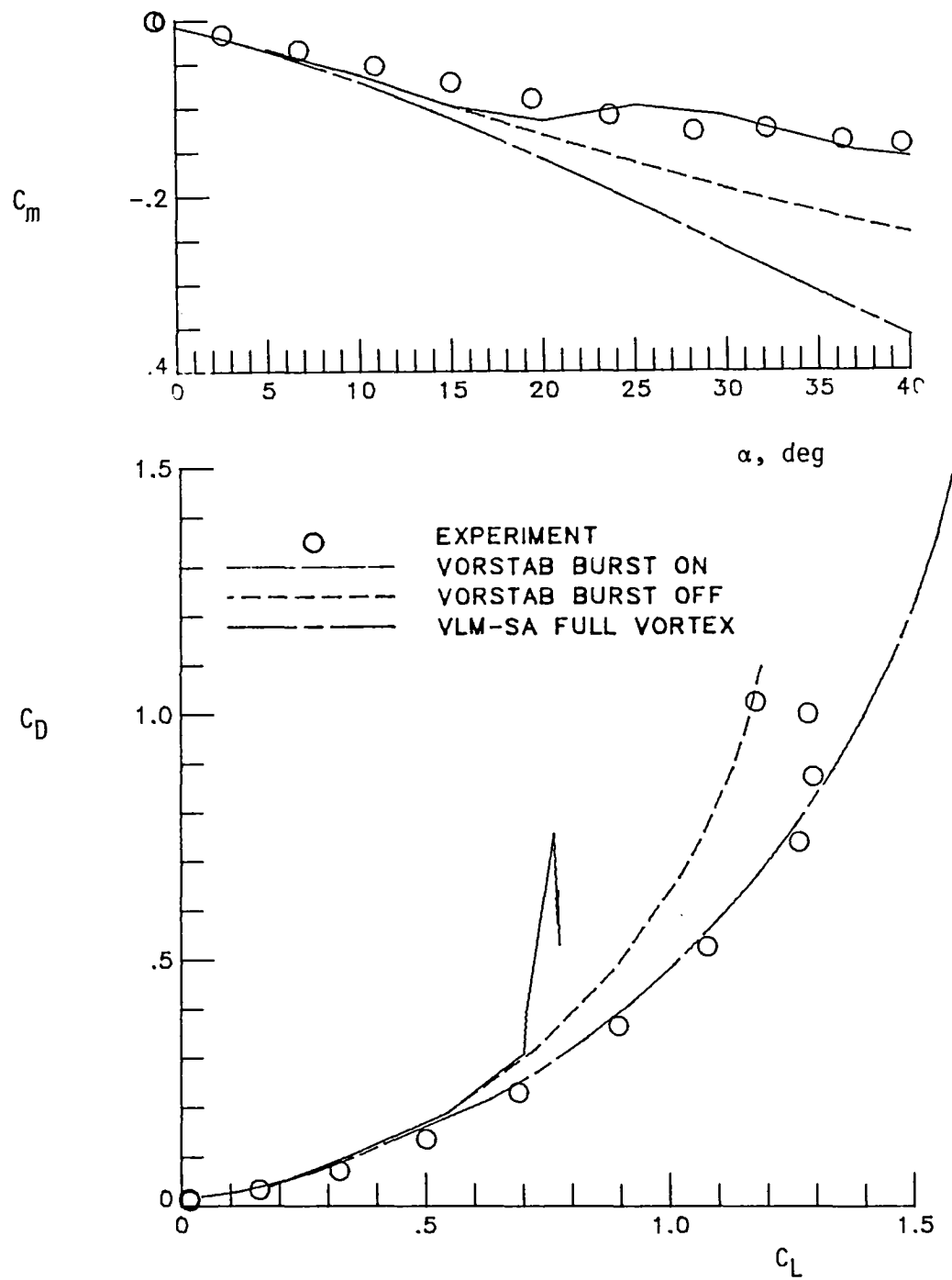
Figure 28.- Concluded.
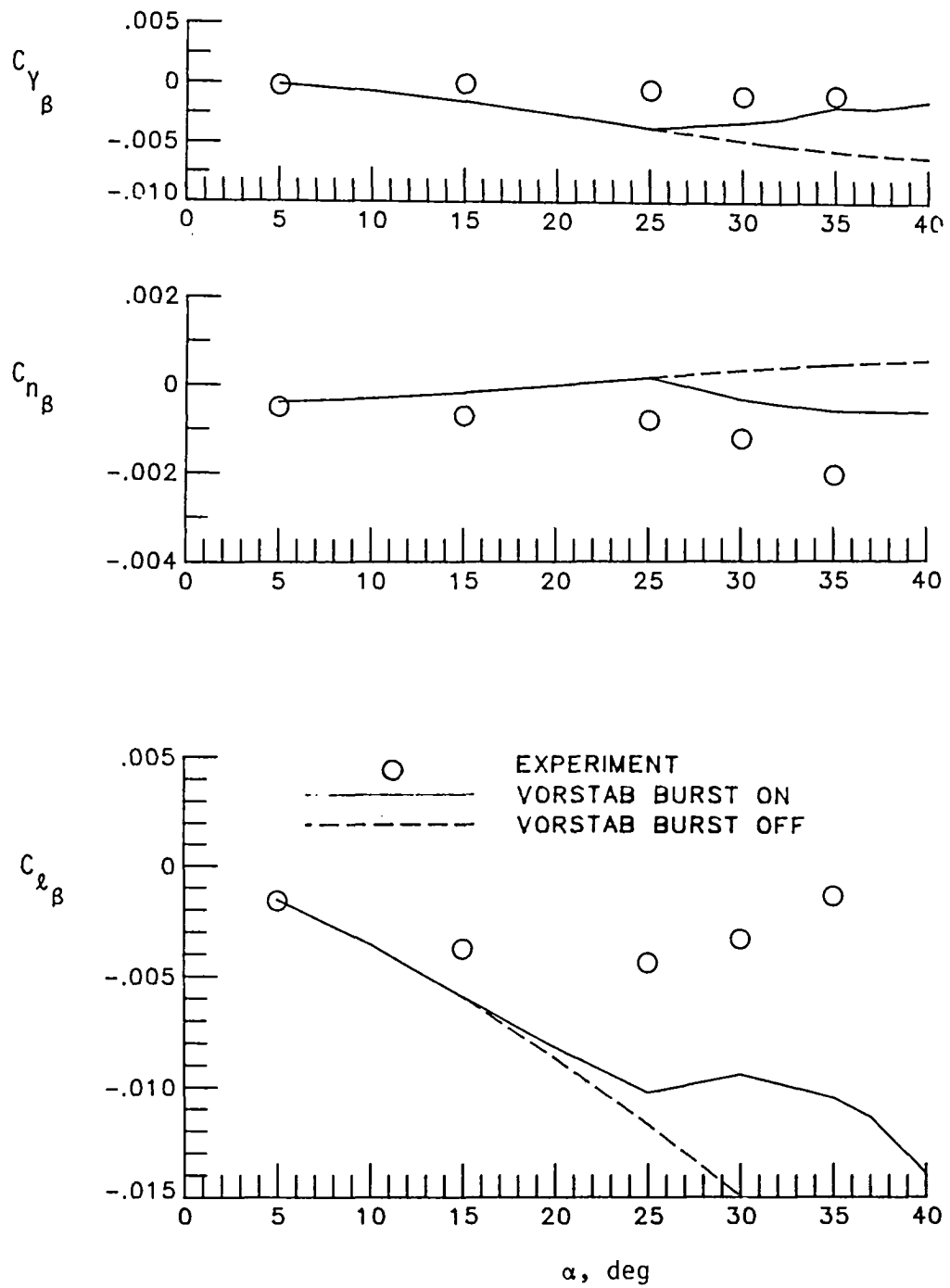
(a) Tail off

Figure 29.- Comparison of theoretical and experimental lateral-directional stability characteristics with $\delta_{LE} = 0°$.
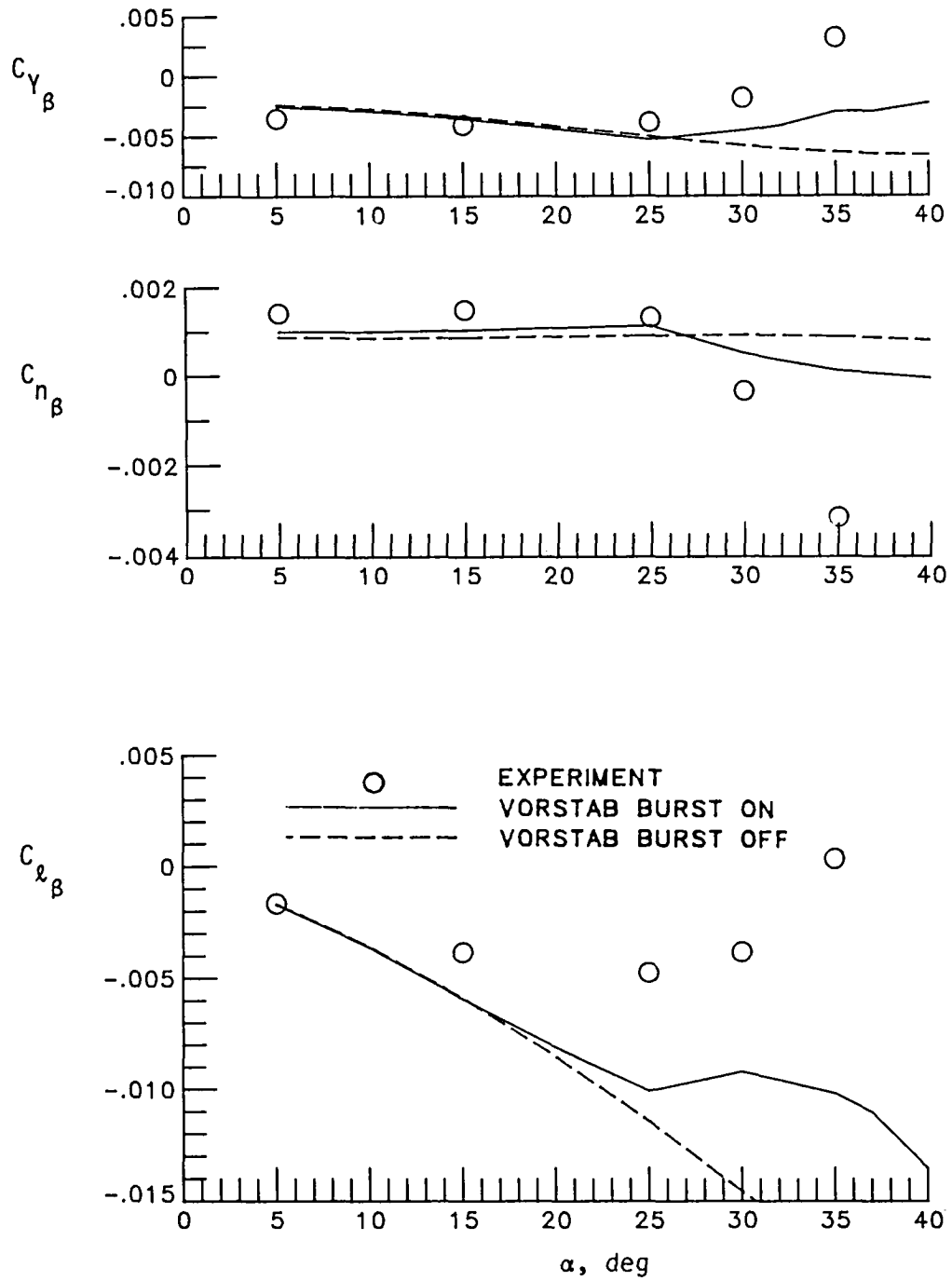
(b) Tail on

Figure 29.- Concluded.

(a) Tail off

Figure 30.- Comparison of theoretical and experimental lateral-directional stability derivatives with $\delta_{LE} = 40°$.
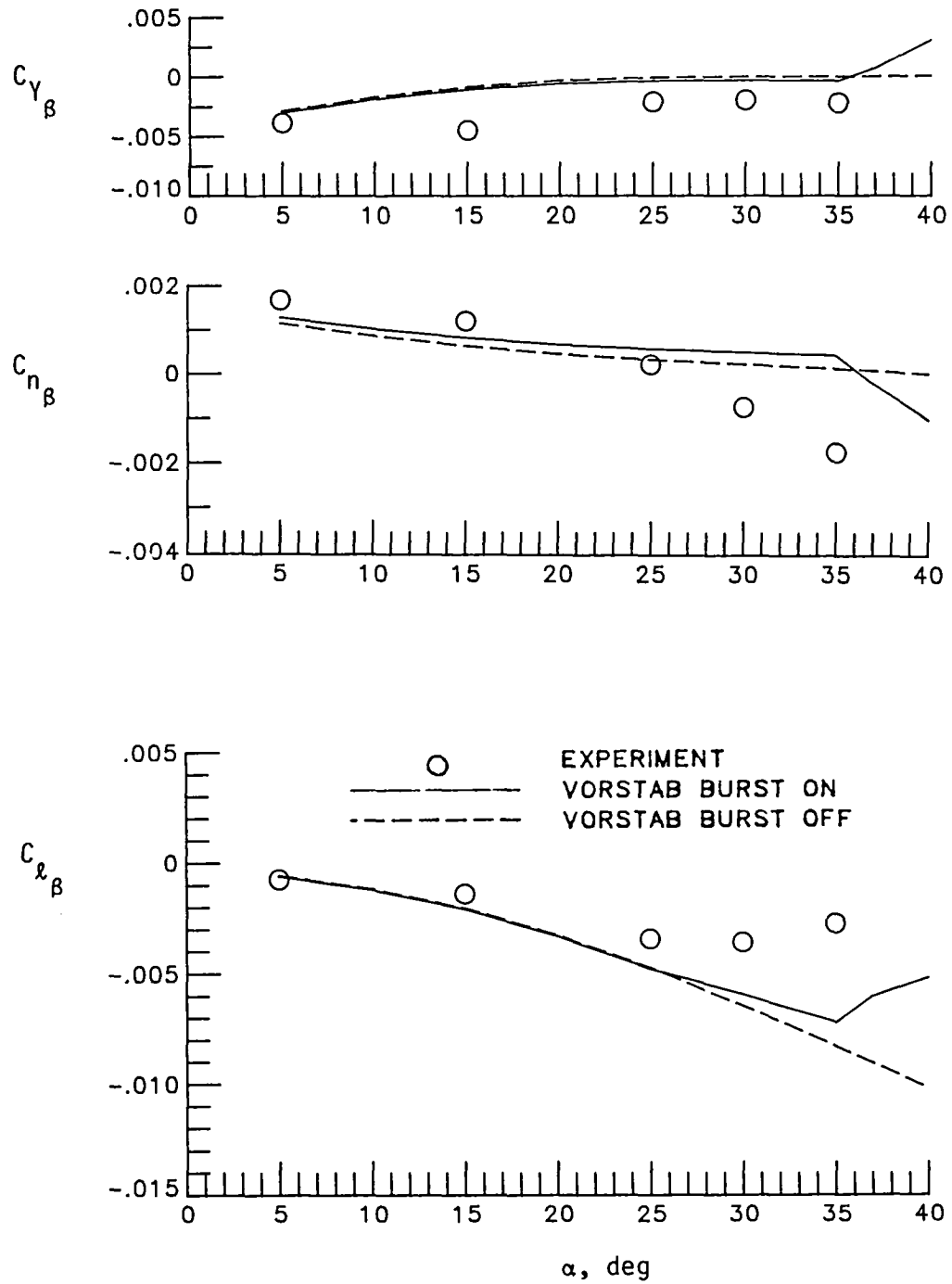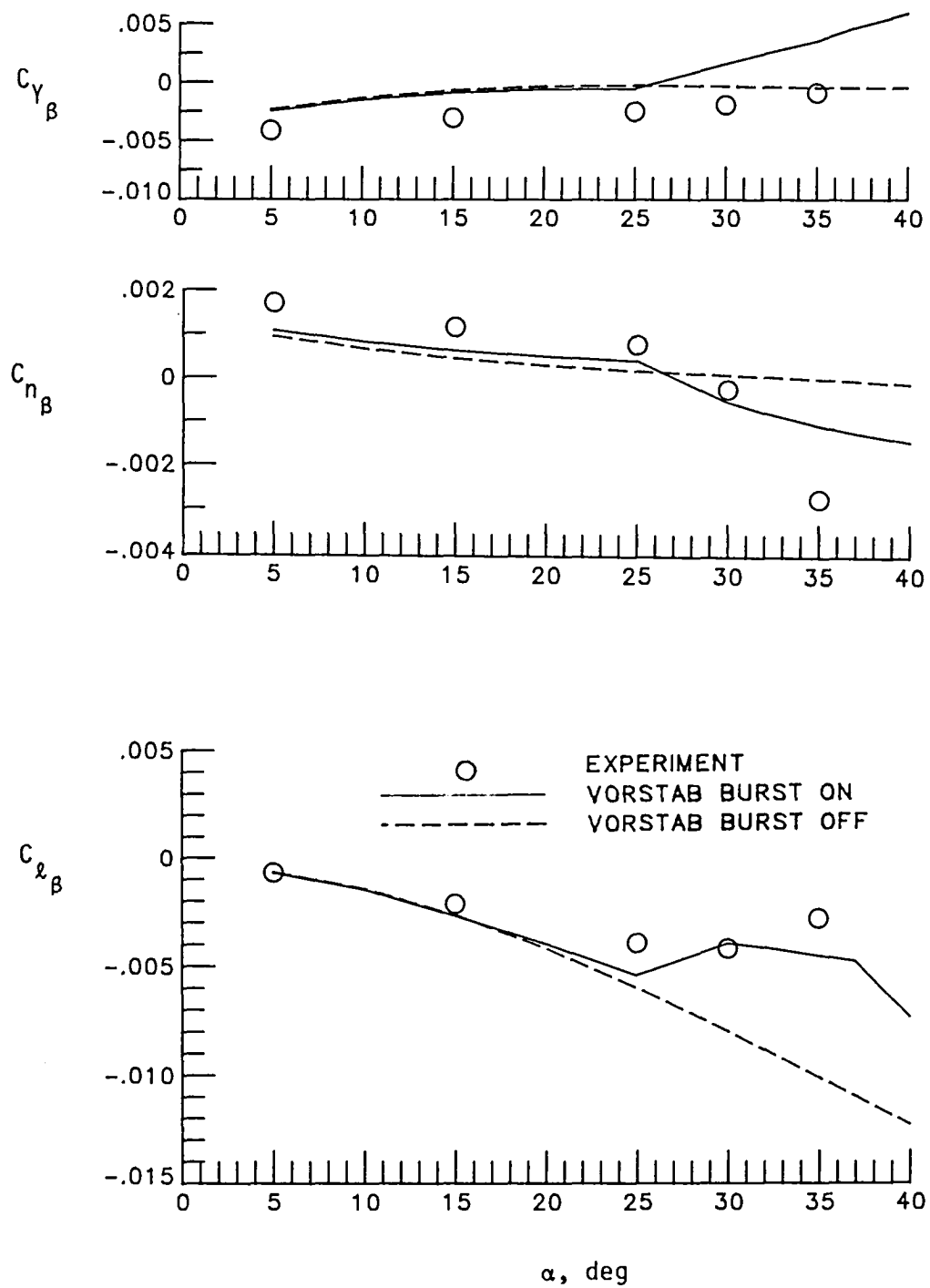
(b) Tail on

Figure 30.- Concluded.

Figure 31.- Comparison of theoretical and experimental lateral-directional stability derivatives with $\delta_{LE} = 30°$.
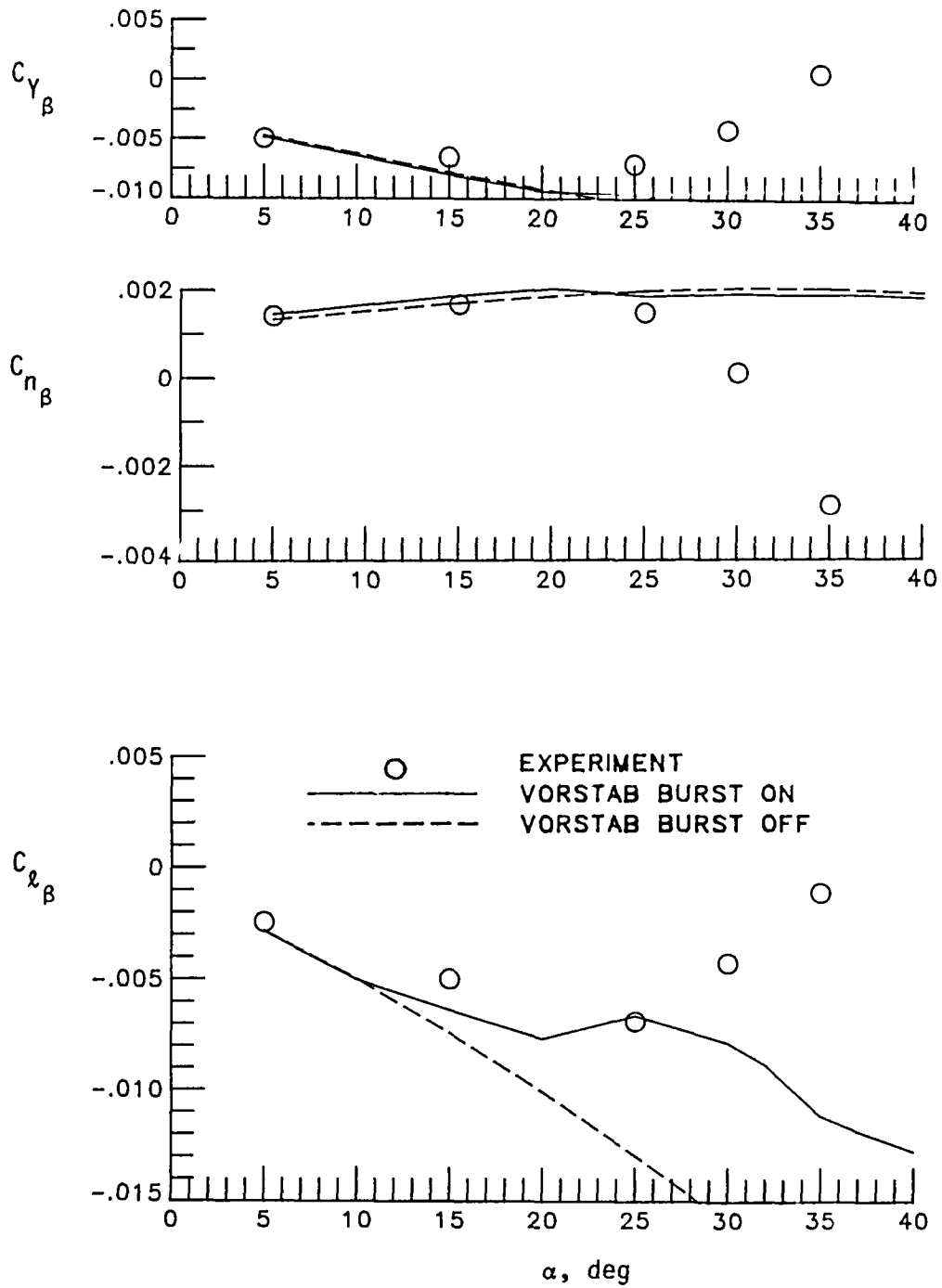
Figure 32.- Comparison of theoretical and experimental lateral-directional stability derivatives with $\delta_{LE} = -30°$.

.

1. Report No. NASA CR-3848	2. Government Accession No.	3. Recipient's Catalog No.
4. Title and Subtitle The Lateral-Directional Characteristics of a 74-Degree Delta Wing Employing Gothic Planform Vortex Flaps		5. Report Date November 1984
		6. Performing Organization Code
7. Author(s) Arthur C. Grantz		8. Performing Organization Report No.
		10. Work Unit No.
9. Performing Organization Name and Address Virginia Polytechnic Institute and State University Aerospace and Ocean Engineering Department Blacksburg, Virginia 24061		11. Contract or Grant No. NGT 47-004-802
		13. Type of Report and Period Covered Contractor Report
12. Sponsoring Agency Name and Address National Aeronautics and Space Administration Washington, DC 20546		
		14. Sponsoring Agency Code 505-31-23-07

15. Supplementary Notes

Langley Technical Monitor: James M. Luckring

16. Abstract

An experimental investigation to determine the low-speed lateral-directional characteristics of a generic 74-degree delta wing-body configuration employing the latest generation, gothic planform vortex flaps has been conducted. Longitudinal effects are also presented. The data are compared with theoretical estimates from VORSTAB, an extension of the Quasi-Vortex-Lattice Method of Lan which empirically accounts for vortex breakdown effects in the calculation of longitudinal and lateral-directional aerodynamic characteristics.

The experimental results indicate that leading-edge deflections of 30 and 40 degrees significantly reduce the magnitude of the wing effective dihedral relative to the baseline for a specified angle of attack or lift coefficient. For angles of attack greater than 15 degrees, these flap deflections reduce the configuration directional stability despite improved vertical tail effectiveness. Asymmetric leading-edge deflections are shown to be inferior to conventional ailerons in generating rolling moments.

VORSTAB calculations provide coarse lateral-directional estimates at low to moderate angles of attack. The theory does not account for vortex flow induced, vertical tail effects. The empirical formulae for predicting vortex burst effects proved to be inaccurate for the present configuration.

17. Key Words (Suggested by Author(s)) Vortex flaps VORSTAB Delta wings Lateral-directional Low-speed aerodynamics	18. Distribution Statement Unclassified - Unlimited Subject Category 02

19. Security Classif. (of this report) Unclassified	20. Security Classif. (of this page) Unclassified	21. No. of Pages 145	22. Price A07

National Aeronautics and
Space Administration

Washington, D.C.
20546

THIRD-CLASS BULK RATE

U.S.MAIL

NASA

POSTMASTER: If Undeliverable (Section 158
Postal Manual) Do Not Return